Politecnico di Bari

ROMA TRE
UNIVERSITÀ DEGLI STUDI

Consortium *Argonauti*

Ph.D. in Architecture: Innovation and Heritage
XXIX Cycle

Ph.D. Thesis in

Rehabilitation of the RC structures of the Brazilian heritage buildings with innovative techniques and materials

Ph.D. Student

Jeferson Azeredo da Rosa

Professor Advisor

Prof. Camillo Nuti

Ph.D. Coordinator

Prof. Elisabetta Pallottino

University of *Roma Tre*

Ph.D. Curriculum

Curriculum 1 - Culture of the Construction

Ph.D. research in Structural Rehabilitation

Professors Evaluators

Prof. Angelo Tarantino

(University of Modena)

Prof. Fernando R. Stucchi

(Unversity of São Paulo USP)

Rome, January 2017

Dedication

In memory of my great-grandfather Francesco,
by gratitude for this opportunity.

Acknowledgements

I would like to express my gratitude to Professor Camillo Nuti for his guidance in this research and for the valuable teachings and advice throughout the Ph.D.

To the Brazilian federal government, I thank it for granting the doctoral scholarship, through the Ministry of Education, the Ministry of Science and Technology, Innovation and Telecommunications and the CAPES agency.
I am very grateful to my former employer, Company *Pedreira Engenharia*, for its support during my preparation for joining the Ph.D. and during the study period abroad, also for the supply of technical material for the research and the structural software TQS. In particular, the directors Augusto G. Pedreira de Freitas and Mauricio Martins Pires.
I would like to thank the Brazilian Association of Engineering and Structural Consulting (ABECE), for the availability and supply of updated technical documents, and the Italian Association of Prestressed and Reinforced Concrete (AICAP) for the didactic contribution.

Throughout the Ph.D. research, three professors were of fundamental importance. Without their collaboration it would not be possible to arrive at the quality of this work:
To Dr. Davide Lavorato (University of *Roma Tre*), I thank him for the teachings, support in the research and collaboration in the numerical investigation.

To Prof. José Américo A. Salvador Filho (Federal Institute of São Paulo - IFSP), I thank him for the advice, the support in the research and collaboration in the experimental investigation.
To Prof. José S. de Belmont Pessôa (Fluminense Federal University - UFF), I thank him for the support in the Ph.D. studies mission, in Rio de Janeiro, and for the collaboration in the research related to the conservation of buildings in Brazil.

I would like to thank Professors Francesco Cellini and Claudio D'Amato for their knowledge, advice and inspiration. I also thank Prof. Elisabetta Pallottino for the valuable teaching in the Ph.D. and in the Master in Restoration. To Prof. Giorgio Piccinato, I thank him for the valuable advice and the support concerning the building conservation.
I would also like to thank Prof. Silvia Santini for collaboration in the structures laboratory and Prof. Lorena Sguerri for the support and collaboration in the accomplishment of the experimental tests.

It was a great privilege to work with the Ph.D. colleagues, Gabriele Fiorentino, Angelo Forte and Enrico Pagano on the inspections of the structures of the buildings struck by the Central-Italy earthquake (2016), in the technical inspection team led by Prof. Camillo Nuti. I thank them for the collaboration and their friendship.

I would like to thank *NAR Engenharia*, especially director Antônio Querido Junior, for his support during the Ph.D. And also to thank the National Institute of Industrial Property (INPI), for the technical visit in the *A Noite* building (Rio de Janeiro) during the study mission, and for supplying documents and designs of the building.
During the Ph.D. study mission, many organizations had the generosity to provide materials, documents and designs of Brazilian historical buildings, and gave permission to use them in this thesis. I would like to thank them for this courtesy.

They are the following organs: IPHAN, Engineering Club, National Library, Municipal Secretary of Cultural Heritage of Rio de Janeiro, Municipal Secretary of Urbanism, Rio Municipality, Pereira Passos Institute, CREA RJ, Banco do Brasil Cultural Association, Archive General of the City of Rio de Janeiro, National Archives, INEPAC, Getulio Vargas Foundation, and the administrations of the buildings *A Noite*, ABI and MES.
I wish to express my gratitude to Buzzi Unicem Spa, Addiment Spa, Honeywell Inc., Bekaert Spa, HG Inc, Kerakoll and Sika for supplying the materials used in the experimental investigation. To Concrete S.l.r., I thank it doubly for providing the SismiCad structural software, during the master and now also during the Ph.D.

I would like to thank my colleagues of Bristol for their friendship during my stay in England and the University of Bristol for their readiness and kind reception, my friend Sergio Ballesteros for the support in the elaboration of mathematical formulations, Drs. Silvia Alessandri and Zhihao Zhou, for their friendship and support in the research for the use of the structural software OpenSees.

I thank my dear friend and colleague Fabiana Riparbelli for the company, for the support in the Ph.D. and for the help in the texts and presentations in Italian language. I thank my Ph.D. colleagues for their support, friendship and good times shared.

I would like to thank Francesca Porcari and her family for their hospitality, exchange of culture and experience and valuable friendship. I would also like to thank my friends of the Anshin Temple, for their knowledge, support and sincere friendship.
And lastly, but not least, I would like to thank my family for their patience in waiting for this long time. I thank my parents for always providing me encouragement, support and trust.

Contents

Dedication III
Acknowledgements IV
Abstract 13

Chapter I
Introduction
1.1 General presentation and significance of the research 15
1.2 Purpose of the thesis..... 20
1.3 Structure of the work 20
1.4 Organization of the work..... 21

Chapter II
The Brazilian heritage RC buildings with particular reference to the historic buildings of the city of *Rio de Janeiro*
2.1 Introduction on the evolution of building in reinforced concrete
in Rio de Janeiro 27
2.1.1 Description of the case study's three buildings..... 35
2.1.1.1 *A Noite* building 35
2.1.1.2 ABI building 43
2.1.1.3 MES building 48
2.1.2 Comparison of general characteristics of the
three buildings studied 55

2.2 Brief panoramic on the conservation culture
of historic RC buildings in Brazil 57
2.2.1 The main conservation criteria that could be considered
on structural interventions of historic RC buildings 59
2.3 References 61

Chapter III
The manifestation of structural deterioration
3.1 General considerations 64
3.2 The deterioration of reinforced concrete structures in Brazil 66
3.3 Environmental aggressiveness on the structures 69
3.4 Considerations on the durability of reinforced concrete structures 78
3.5 Deterioration mechanisms of the structures 81
3.6 Main causes of RC structures' deterioration in Brazil 82
3.7 The reinforcement corrosion 88
3.7.1 Carbonation-induced corrosion 90
3.7.2 Chloride-induced corrosion 91
3.8 References 92

Chapter IV
Structural safety assessment for heritage RC buildings that present deterioration
4.1 General approach 96
4.2 Model proposal of assessment hierarchy for rehabilitation
of deteriorated heritage structures 97
4.3 Condition assessment of deteriorated RC structures 100
4.3.1 Deterioration evolution 102
4.3.1.1 Limit states for reinforcement corrosion 103
4.3.2 Evaluation of steel depassivation by carbonation 104

4.3.3 Evaluation of steel depassivation by chloride attack 107
4.3.4 Evaluation of reinforcement corrosion in concrete..... 110
4.3.4.1 Propagation of corrosion 110
4.3.4.2 Residual capacity of corroded reinforcing bars..... 112
4.3.4.3 Evaluation of yield strength in tension and compression
for non-uniform cross-section loss of corroded bars..... 116
4.4 References 118

Chapter V

The main techniques and materials for structural rehabilitation

5.1 Scope 121
5.2 Interventions in heritage RC structures 121
5.3 Normative reference to interventions in existing buildings..... 122
5.4 The main conventional techniques and materials
for structural rehabilitation 123
5.4.1 General approach..... 123
5.4.2 Section increase in reinforced concrete..... 124
5.4.3 Strengthening in steel structure..... 126
5.5 The main innovative techniques and materials
for structural rehabilitation 127
5.5.1 General approach..... 127
5.5.2 Strengthening by CAM system 128
5.5.3 Structural rehabilitation by FRP and FRCM systems 129
5.5.3.1 General approach..... 129
5.5.3.2 Normative references 130
5.5.3.3 Mechanical characteristics 131
5.5.3.3.1 FRP system..... 131
5.5.3.3.2 FRCM system..... 133
5.5.3.4 Strengthening for RC structures 135

5.5.3.4.1 General criteria 135
5.5.3.4.2 Debonding mechanisms 136
5.5.3.4.3 Flexural strengthening 137
5.5.3.4.4 Shear strengthening 139
5.5.3.4.5 Confinement 143
5.6 References 148

Chapter VI

Experimental investigation of the mechanical properties of High Performance Fiber Reinforced Cementitious Composites (HPFRCC)

6.1 Scope 150
6.2 General approach 151
6.3 Experimental procedure 154
6.3.1 Materials 154
6.3.2 Mix design and preparation 157
6.3.3 Specimens preparation 159
6.3.4 Test setup 160
6.3.5 Results and discussion 162
6.3.5.1 Compressive strength 164
6.3.5.2 Flexural strength 165
6.3.5.3 Uniaxial direct tensile strength 166
6.4 References 171

Chapter VII

Numerical investigation for RC structures rehabilitation with HPFRCC and FRCM techniques

7.1 Purpose 174
7.2 *A Noite* Building: Case study for numerical investigation 174
7.2.1 Scope 174

7.2.2 Description of the *A Noite* building 176
7.2.3 Preliminary inspection 177
7.2.4 Reference element for numerical investigation..... 178
7.2.5 Evaluation of residual capacity of the corroded bars 180
7.2.6 Numerical model 181
7.2.6.1 Numerical modeling details 182
7.2.7 Numerical tests..... 182
7.2.7.1 Push-Over analysis 184
7.2.7.2 Tests results comparison..... 185
7.2.8 Rehabilitation of the beam with HPFRCC technique 186
7.2.8.1 Multilinear-hysteretic simplified model for HPFRCC..... 186
7.2.9 Rehabilitation with FRCM technique 193
7.2.10 Rehabilitation combining HPFRCC and FRCM techniques..... 201
7.3 RC Bridge: Case study for numerical investigation 204
7.3.1 General approach..... 204
7.3.2 Reference element..... 205
7.3.3 Current condition and remaining service life assessment..... 207
7.3.3.1 Evaluation of the remaining service life concerning to steel reinforcement depassivation by carbonation (initiation period) 208
7.3.3.2 Evaluation of the remaining service life concerning to steel reinforcement corrosion (propagation period) 209
7.3.3.3 Evaluation of residual capacity of corroded bars..... 212
7.3.4 Structural performance assessment..... 213
7.3.4.1 Numerical model 214
7.3.4.1.1 Numerical modeling details 215
7.3.4.2 Confinement model for concrete 216
7.3.4.2.1 Mander model 216
7.3.4.2.2 Kawashima model..... 219
7.3.4.3 Numerical tests..... 221

7.3.4.3.1 Push-Over analysis 224
7.3.4.3.1.1 Tests results comparison..... 225
7.3.4.3.2 Cyclic analysis..... 227
7.3.4.3.2.1 Tests results comparison..... 227
7.3.5 Rehabilitation with HPFRCC technique..... 231
7.3.6 Rehabilitation with FRCM technique 238
7.3.7 Rehabilitation combining HPFRCC and FRCM techniques..... 248
7.4 References..... 253

Chapter VIII
Conclusions..... 257

List of Tables..... 273
List of Figures..... 275

Appendices
Numerical modeling..... 285

Abstract

The research deals with the processes and techniques related to the preservation of reinforced concrete structures of the Brazilian heritage buildings, which include constructions of significant historical and architectural importance that present implications for both conservation and safety, which are deteriorated and need structural rehabilitation interventions.

The main objectives of the research are to develop evaluation criteria of the current condition of the buildings, in terms of safety, and to assess through theoretical and experimental analyses the effects resulting from the use of structural reinforcements constituted of high performance cementitious composites mixed with micro-fibers or short fibers (HPFRCC) and fiber reinforced cementitious matrix (FRCM system), applied in rehabilitation of damaged heritage structures in reinforced concrete, both in terms of structural performance and the conservation of the buildings.

Essential aspects are the assessment of conservation requirements of the original characteristics of the buildings and the impact of the analyzed intervention systems. The durability requirements for structural recovery and the criteria relating to minimum intervention are also considered.

Sommario

La ricerca riguarda i processi e le tecniche connessi alla salvaguardia degli edifici in calcestruzzo armato del patrimonio storico edilizio Brasiliano, di cui fanno parte le costruzioni di rilevante importanza storica ed architettonica che presentano implicazioni sia di conservazione che di sicurezza, che sono degradate e necessitano di interventi di riabilitazione strutturale.

Gli obiettivi principali della ricerca sono quelli di mettere a punto criteri di valutazione dello stato di fatto degli edifici, in termini di sicurezza, e valutare mediante analisi teorica e sperimentale gli effetti conseguenti l´utilizzo di rinforzi strutturali costituiti da compositi cementizi ad alta prestazione miscelati con micro-fibre o fibre corte HPFRCC (High Performance Fiber Reinforced Cementitious Composite) e da sistemi di compositi fibrorinforzati con matrice a base cementizia FRCM (Fiber Reinforced Cementitious Matrix), applicati in interventi di riabilitazione di strutture del patrimonio storico in calcestruzzo armato, sia da un punto di vista prestazionale, sia da un punto di vista conservativo.

Aspetti essenziali sono la valutazione delle esigenze di conservazione delle caratteristiche originali della costruzione e l´impatto dei sistemi di intervento analizzati. Sono inoltre considerati i requisiti di durabilità per il recupero strutturale e i criteri relativi al minimo intervento.

Chapter I
Introduction

1.1 General presentation and significance of the research

Brazil is a country that possesses several important heritage buildings in reinforced concrete, of exceptional historical, architectural and cultural value. They were designed by great architects and engineers, and deserve to be considered and preserved. Many of these buildings that were built in the last century present deterioration problems, both for the phenomena related to maintenance, and for the effects linked to aggressive agents of the environment.

The lack of proper maintenance of the structure during its service life can originate pathological phenomena such as deterioration of concrete and steel, which manifest before the limit time defined in the design, often with serious consequences and significant damage. Many cases of deterioration of the buildings, mostly the older ones, are neglected until an important problem related to the structural safety happens.

On the other hand, old structures were designed in such a way that they could satisfy the prescriptions of structural performance, in accordance with the recommendations for designs and standards existing at the time they were built. Thus, the requirements prescribed in current standards naturally bring about differences that could compromise the reliability of structures. As an example, the mechanical properties of materials, the minimum dimensions of the elements and their respective minimum concrete covers, in addition to the prescriptions regarding the durability of the materials. Furthermore, existing structures are often requested

to sustain greater variable loads than they used to do in the past, thus requiring an increase of their bearing capacity. An increase of their bearing capacity is not always simple to obtain, though it is one of the most crucial aspects in rehabilitating such structures.

Because great part of the construction work in the next years will concern existing buildings, the need to recovery old structures with degradation problems, and the possibility of extending its service life, becomes of paramount importance.

However, the conceptual issues related to the conservation of RC (reinforced concrete) buildings are rarely discussed in the context of the Brazilian structural engineering, which does not have clear criteria and methodologies of intervention for heritage structures. This could be one of the main factors explaining why many operators in the structural design field, construction and maintenance, still do not have an understanding of necesssary preservation culture to make the most appropriate decisions in their interventions. The absence of specific national standards for interventions in existing structures may be one of the main causes responsible for inadequate, low quality rehabilitation works carried out in the country. That, besides being a factor that can compromise the security of the users, may also neglect essential aspects related to the maintenance of the building's original characteristics. In this perspective, errors and uncertainties are not uncommon in the definition of models for analysis and structural evaluation.

An intervention of historic building rehabilitation is a complex work that involves a series of specialized disciplines that are independent, but at the same time correlated. It also requires accurate historical-documental, ichnographical and bibliographic research. An ample understanding of structure behaviour and material properties is essential for structural conservation and recovery designs.

An adequate choice of intervention type with techniques and materials compatible with the formal and documentary aspects of the construction is essential in the rehabilitation of heritage buildings. It is important to respect its configurations and develop a feasible project in accordance with the building's genuine features. The

architectural impact of the intervention technique and the durability of the chosen materials could be taken into account during the evaluation work, in addition to the aspects related to the structural safety in order to reach the requirements of resistance. At the evaluation stage it is normal that there are doubts and uncertainties in the definition of an analysis models and their respective parameters, not always being possible to apply to cultural goods the design procedures established for ordinary buildings. Thereby, a need to assess the adequacy of structures arises, either from a functional point of view, but also conservative, with theoretical methodologies and appropriate intervention technologies.

Recovery and strengthening of reinforced concrete structure have always been carried out through traditional design, with interventions that inevitably foresee the integration of the elements' geometry, with significant increases of sections or through the insertion of metallic elements, such as, for example, the conventional technique of *béton plaqué*. These methods, if on the one hand guarantee an increase in the resistance of the elements, in most cases may represent contradictory points to the principles of heritage structures conservation. The application of section increase in the elements could not, however, be excluded, as it may be indispensable for a rehabilitation of the structure as a whole (provided that this solution is adequately evaluated by the designers). In this case, it could represent an increase of mass and consequently an improvement in the overall stiffness.

In the field of structural rehabilitation the use of innovative technologies and materials for interventions in historic buildings is confronted with the need to preserve the structure and the possibility to change, aiming to recover or improve its resistance capacity. However, one of the main factors that come into play is related to how and how much to preserve the characteristics that interest the architectural quality, the cultural values and the construction memory. In addition to

factors related to structural reliability, are the requisitions of the architectural identity protection, not only the aesthetic aspect, but also the constructive integrity.

The modern approach of recovery and strengthening with innovative techniques, treated in this thesis, could be used in heritage structures, not only for increasing the mechanical structural performance, but mainly with the purpose of contributing to the conservation of the geometry of elements and their features. Of course, this new concept of intervention in existing buildings puts us in a broader perspective that covers the different areas of expertise involved in the process. On the other side, it is through careful study of the mechanics of recovery and reinforcement systems, through the knowledge of the structural behaviour of each material and its interaction with the existing structure, that any conservation design could be realized.

It is in this line of studies that the present thesis proposes the use of high performance cementitious composites reinforced with micro-fibers or short fibers, for rehabilitation of reinforced concrete elements. The HPFRCC technique (High Performance Fiber Reinforced Cementitious Composites)[1] could be used also combined with other techniques, such as the FRCM systems (Fiber Reinforced Cementitious Matrix), to improve the bearing capacity of the elements subjected to compressive stresses, shear, bending and flexo-compression. This purpose requires use of finite element software with fiber modeling, capable of analyzing the non-linear behaviour of the structure, presenting its performance level and the resistance points exceeded by each limit provided by the standard. The use of this technique may request a more refined work in the analysis and elaboration of the

[1] High Performance Fiber Reinforced Cementitious Composites (HPFRCC) is a class of materials studied extensively for the applications in new structures design and, currently in structural rehabilitation of existing structures. These materials have high mechanical strength, pseudo strain-hardening behaviour and low porosity due to a highly dense microstructure of the cementitious matrix. Furthermore, they guarantee great durability by adding micro fibers in proper ratio, which limit the crack opening.

rehabilitation design, but, consequently, it is able to provide a high quality in the final result of the intervention works.

Italy is a pioneer country in the area of structural rehabilitation that occupies a representative position worldwide, both for its important building patrimony with exceptional historical and architectural value, and for its millennial tradition in the area of restoration and recovery of structures. Italian standards and recommendations for design and execution of intervention in existing constructions, updated and taking into account the results of the latest research, are made available and used in several countries around the world, serving as a base of studies and research not only for researchers, but also for professionals in the field of rehabilitation.

The research group of the engineering and architecture departments of *Roma Tre University* has a long tradition of research and experimentation on the structural behaviour of existing constructions. Furthermore, it is active in the scope of experimentation of innovative materials and in the development of technologies of sustainable reinforcements for the rehabilitation of structures of the historical-architectural patrimony. Due to the seismic events that have occurred in the last decades with large-scale destruction, *Roma Tre University* has developed important works in the field of structural rehabilitation technology, both in the research area and in the reinforcement works for seismic adjustment and improvement, presenting important contributions of technical-scientific knowledge to the international scientific community.

Considering the exposed scenario, it is known that the resources of innovative technologies available for recovery interventions and structural strengthening, associated with an appropriate intervention type choices could benefit the principles of historic buildings preservation. The lack of knowledge about how to design and execute rehabilitation works, as well as the lack of knowledge of the existing innovative materials and techniques, could no longer be a justification for the continuous use of conventional solutions that are easily accessible. But in most

cases they do not satisfy the conservation criteria, erasing the values that could be transmitted to the present and future generations, so that people could take benefit of the cultural goods and identify the values that have been conserved and preserved.

1.2 Purpose of the thesis

The purpose of the thesis is to develop evaluation criteria of the real state of RC buildings that have problems of structural degradation, in terms of safety, and to assess through theoretical and experimental analyses the effects resulting from the use of structural reinforcements constituted of high performance cementitious composites mixed with micro-fibers or short fibers (HPFRCC) and with fiber reinforced cementitious matrix (FRCM systems), applied in rehabilitation interventions of reinforced concrete structures, both from a mechanical performance and a conservative point of view with regard to the historical heritage.
As object of study, historic buildings of the city of *Rio de Janeiro* are selected (including constructions of historical relevance and architectural importance), which serve as a basis for the development of the research. Essential aspects are the assessment of the preservation needs of the building's original characteristics and the impact of the analyzed intervention systems. The durability requirements for structural recovery and the criteria relating to minimum intervention are also considered.

1.3 Structure of the work

An intervention design on heritage buildings involves several stages of evaluation, ranging from the identification of the cultural good's values to the choice of the most appropriate techniques and rehabilitation materials, in order to preserve these values. Hence, the development of the research resulted in the division of the thesis into six parts, which are organized according to the research purpose:

- Chapter II deals with the identity of the historic RC buildings of Rio de Janeiro and the preservation culture of RC buildings in Brazil.
- Chapter III discusses the problematic of deterioration of the heritage structures and the main types of degradation of reinforced concrete in Brazil.
- Chapter IV refers to the evaluation of the performance of heritage RC structures that presents problems of deterioration, considering the original condition of the structure, the current condition with presence of damage and the prediction of the residual service life.
- Chapter V deals with the main conventional and innovative techniques and materials of structural rehabilitation used in Brazil and Italy, and the reference standards.
- Chapter VI presents the main results of the experimental investigation in laboratory on the mechanical properties and characterization of high performance composite reinforced with fibers (HPFRCC using different types of fibers with different volumes), to evaluate the behaviour of these materials under tensile, flexural and compressive forces.
- Chapter VII deals with the numerical investigation, considering the results obtained during experimental research to evaluate the applicability of the HPFRCC technique (also combined with other techniques, such as the FRCM system), in the rehabilitation of heritage RC structures. As a case study, degraded structural elements belonging to the *A Noite* building (Rio de Janeiro) and a RC bridge located in seismic zone in Italy were used.

1.4 Organization of the work

1.4.1 Chapter II: The identity of the historic RC building, concerning the architectural heritage of the city of Rio de Janeiro (from the beginning of the twentieth century until the 40s) and the preservation culture of the RC buildings in Brazil

As for the identification of the heritage buildings it has been fulfilled a study mission to Rio de Janeiro, to know the development of the reinforced concrete technique in Brazil, at the beginning of the last century, as well as the impact of this technology in the architecture of Rio de Janeiro. Visits were made in some representative RC buildings to make photographic surveys, to know about their history and their current state of conservation, based on the direct experience of a site visit. Visits were also made to libraries, public archives and to the organisms responsible for the artistic and historical-architectural heritage, to collect documents and designs concerning the visited buildings. In addition, interviews were carried out with professors and experienced professionals of the areas of structures and restoration, in order to establish a collaborative relationship with the purpose of acquiring and exchanging knowledge and experience.

On the first part of the research, the thesis presents an introduction with a brief history about the evolution of the reinforced concrete technique in Brazil (at the beginning of the last century) and its influence on the *Carioca* architecture, identifying a part of the heritage buildings of the city of Rio de Janeiro and taking as example three buildings as case studies, considered representative and important for the history of the Brazilian architecture and engineering. In this first part, the question related to the culture of the buildings preservation in Brazil, which has historical and cultural values in itself, is discussed, with particular reference to the preservation of these values and the conservation of the original characteristics of the RC structures.

1.4.2 Chapter III: The main causes of RC structures' deterioration in Brazil

In the theoretical analysis, investigation criteria of the pathologies that cause major damage and deterioration in reinforced concrete structures, methods for determining the residual service life of the structures, as well as the assessment of the performance of damaged elements were examined.

Regarding this stage of the research, the thesis exposes the problem of the degradation of buildings in reinforced concrete in the different regions of Brazil, the main types and mechanisms of deterioration, as well as their causes. In this chapter the standards we have at our disposal are also discussed and questions are raised as to the lack of clear criteria for rehabilitation interventions in heritage structures with deterioration problems.

1.4.3 Chapter IV: Structural safety assessment for heritage RC buildings that present deterioration

Under this chapter parameters of evaluation of existing RC structures have been identified and the mechanical properties of materials have been investigated. In addition, methods of analysis and safety assessment of the structures (complies with standards) have been studied.

This part of the thesis is related to the evaluation of the heritage structures that present degradation. The main purpose of this chapter is to provide additional considerations on assessment of damaged heritage structures, based on the premise that a structure may have cultural and heritage value in itself.

The evaluation procedures, according to Italian and European standards, are explained and exemplified through case studies presented in Chapter VII. In the case studies, evaluations of the current state of deterioration, the original condition (initial period in the past) and prediction of the residual service life were carried out, identifying the possible ultimate and serviceability limit states of the structure. Evaluations of the capability of structural strength and the performance loss of the degraded structure were also carried out, in the current condition and forecast for the future (if the structure does not receive any type of structural rehabilitation intervention). Pushover analyses and cyclic analyses (also simulating seismic actions) were performed for the evaluation of structural performance levels.

1.4.4 Chapter V: The main techniques and materials for structural rehabilitation

For this phase the most used conventional and innovative techniques of structural rehabilitation were compared, through theoretical calculation methods for strengthening of RC structure of the Italian and European standards. Calculation models for flexural strengthening of beams, beam shear, compression (confinement) of columns and flexo-compression of columns were applied, through use of the innovative techniques FRP (Fiber Reinforced Polymer) and FRCM (Fiber Reinforced Cementitious Matrix). In addition, the use of systems FRCM and HPFRCC for repair and strengthening of reinforced concrete elements were evaluated.

This chapter presents the main techniques and materials for intervention in RC structures, in the area of structural rehabilitation, most currently used in Brazil and Italy. The objective of this chapter is to expose innovative technologies for recovery and strengthening of elements in reinforced concrete, in an integrative way, as an option of use, beyond the conventional techniques. The main attributes taken into consideration are high performance in terms of mechanical capacity, ductility, light weight, support adaptability (existing structure) and durability of materials (prolongation of service life).

1.4.5 Chapter VI: Experimental investigation of the mechanical properties of High Performance Fiber Reinforced Cementitious Composites (HPFRCC)

Regarding the experimental investigations on HPFRCC materials, compression tests, direct tensile, bending and modulus of elasticity tests were carried out for analyzing the mechanical properties and the behaviour of the materials up to rupture, the performance increase, the improvement in terms of resistance and deformability (tenacity), of each individual specimen of HPFRCC.

This chapter presents the main results obtained by an experimental campaign carried out on HPFRCC, at the Laboratory of Structures of the *Roma Tre* University,

and deals with the mechanical properties assessment of HPFRCC mixtures designed with locally available materials. In particular, different HPFRCC mix designs were considered with a very compact cementitious matrix reinforced with three different types of microfibers: basalt fibers, high density polyethylene fibers and hooked stainless-steel fibers, considering 1% or 2% of the volume contents.

1.4.6 Chapter VII: Numerical investigation for RC structures rehabilitation with HPFRCC and FRCM techniques

This part of the thesis deals with the assessment of a degraded heritage structure pertaining to the *A Noite* building (explained in Chapter II) and to a RC bridge located in seismic zone (in Italy), based on the procedures described in the present thesis. The purpose of this part of the research is to apply the knowledge acquired during the PhD studies to conduct evaluations of structural performance of the case studies' elements, relating to its current condition (state of structural deterioration), residual service life, as well as its bearing capacity and its rehabilitation with innovative techniques and materials.

In the last part of the research, the main results obtained from the experimental investigation on HPFRCC materials and the numerical models purpose-built in FEM software (Finite Element Method) with fiber modeling, programming language Tcl (Tool Command Language), have been applied to the case studies to assess the results of the experimental and theoretical analyses of the studied models, both in terms of mechanical performance (increase in resistance), and taking into account the identity of the object of intervention that may be preserved within the recovery of the structure.

Chapter VII also presents the results from the numerical investigation to evaluate the structural behaviour of the RC elements, their damage due to deterioration (or to seismic actions) of concrete and steel materials, repaired and strengthened by high performance fiber reinforced cementitious composites (HPFRCC) and fiber reinforced cementitious matrix (FRCM). In the numerical tests, different HPFRCC

mix designs were considered to repair the case studies' structural elements (column and beam), assuming different fiber types. The HPFRCCs used as repair material were developed and tested experimentally in the laboratory of structures and materials of *Roma Tre* University (explained in Chapter VI), whereas the FRCM properties were assumed by commercial products specifications.

The proposed solutions, based on the repair of corrosion-damaged RC elements without increasing of section, aims to enhance the performance capability, both bending and flexo-compression on the reinforced elements, besides contributing with a significant increase in the durability of the materials and, consequently, in the service life of the recovered structure.

Chapter II

The Brazilian heritage RC buildings with particular reference to the historic buildings of the city of Rio de Janeiro

2.1 Introduction on the evolution of building in reinforced concrete in Rio de Janeiro

The first constructions and technicians

The use of reinforced concrete technique started in Brazil in the early of the twentieth century, around 1904 in Rio de Janeiro, at some residences of *Copacabana* neighborhood (Fig. 2.01)[1], to build foundations, walls, stairs, and retaining walls[2].

Figure 2.01 *Copacabana, Rio de Janeiro,* 1906

[1] Source: Available in <http://copacabana.com/fotos-classicas-1900-1950/ye80zdeu637s05rx5yjxyph1xjcjta>, accessed on March 24, 2016.

[2] Vasconcelos, Augusto Carlos. *O concreto no Brasil: recordes, realizações, história (1985).*

Subsequently the reinforced concrete was used in other types of constructions, such as bridges, overpasses and reservoirs (Fig. 2.02)[1]. The application of the new technique began to be used in buildings only after a few years, with the expansion of the city and as a result of the high cost of land, mainly in the central area. The use of reinforced concrete technique has definitely started around 1911 with the arrival of German engineers, in particular Lambert Riedlinger[2].

Companhia Construtora de Cimento Armado[3] was the first Brazilian company specialized in design and construction works in reinforced concrete. It was founded in 1912 by Riedlinger. He also brought from Germany master builders and technicians who were already quite familiar with the new material and the use of calculation rules, which along with the reinforced concrete began to be disseminated in Brazil.

Figure 2.02 Water reservoir of the *Engenho de Dentro* (built in reinforced concrete, circa 1908)

[1] Source: Photographic reproduction of the book *"A aventura do concreto armado no Rio de Janeiro 1900 – 1936"*, by Gabriela Carvalho, Claudia Lacombe Rocha, Rio de Janeiro, 2003.

[2] Silva, Fernando Nascimento; Dos Santos, Sidney Gomes. *Rio de Janeiro em seus quatrocentos anos: formação e desenvolvimento da cidade (1965).*

[3] Carvalho, Gabriela; Rocha, Claudia Lacombe. *A aventura do concreto armado no Rio de Janeiro 1900 – 1936 (*2003).

This company was fundamental to the propagation of this new construction technique in Rio. The first Brazilian specialists in the area were trained there and soon replaced the foreign ones. Among them, stands out the Engineer Emílio Henrique Baumgart (Fig. 2.03)[1], son of German immigrants, who years later became known as the father of reinforced concrete in Brazil. Interning with Riedlinger soon he dominated the technique, developing it later at his own technical office in a quite original way. This gave to Rio and Brazil a unique role in the history of reinforced concrete.

Figure 2.03 Eng. Emílio Henrique Baumgart

Construction materials

In the early twentieth century, both natural and industrialized materials to build reinforced concrete were easily accessible in Rio de Janeiro. The basaltic stone and sand for making concrete were available in the region. The wood to build formworks came from the south of Brazil and the steel produced in the form of bars, which depended on the industry for their preparation, was imported from Europe[2].

[1] Source: Available in < http://1.bp.blogspot.com/-kSIRfFoSqDQ/Uf_n00jKyaI/AAAAAAAABaU/3vjdJGptrCM/s1600/emilio.png >, accessed on March 24, 2016.

[2] As England was a major producer and exporter of iron and steel in the late nineteenth century, there is a tendency that most of the steel used in the construction of reinforced concrete in Brazil was imported from

The cement, which was initially also imported, came to be replaced by a national factory called *Cimento Rodovalho,* established in 1897 (current *Votorantim*)[1]. It was evident the relationship between the construction technique and the available resources.

First design procedures

At first, Brazilian constructions in reinforced concrete were designed considering only the material's mechanical properties. As the reinforced concrete technique was developed, its application gradually changed from empiricism to rational use. This development was based on dosage tests and material strength studies, as well as, on the elasticity theory, mathematical analysis and mechanics of structures. The first studies of concrete dosages were carried out in 1927 by the former Strength of Materials Office of the Polytechnic School of São Paulo[2], in São Paulo, now known as the Institute for Technological Research - IPT. In January 1930 the first Brazilian technical magazine specializing in reinforced concrete was founded and in 1936 in Rio de Janeiro the Brazilian Portland Cement Association ABCP was established, creating for the first time a definition of standard (Fig. 2.04) which would be used nationwide[3]. Four years later it was created by the Brazilian

England. Source: *História da metalurgia*. Available in < http://www.pmt.usp.br/notas/notas.htm >, accessed in Jun 07, 2016.

[1] ABCP *Associação Brasileira de Cimento Portland. Uma breve história do Cimento Portland*. Available in < http://www.abcp.org.br/cms/basico-sobre-cimento/historia/uma-breve-historia-do-cimento-portland/ >, access ed in May 05, 2016.

[2] Around this institution, the ties between European engineers, promoters of the use of reinforced concrete in construction and technological applied research in Brazil would be formed. (Vasconcellos, Carlos Augusto de. "History of reinforced concrete in Brazil")

[3] Vasconcellos, Juliano caldas de. "The maturity of the reinforced concrete in the field of Brazilian engineering in the 1930 And 1940". In: *11° Seminário Nacional Do Docomomo Brasil*. Recife: Docomomo_Br, 2016. P. 1-12.

Association of Technical Standards (ABNT) the first official Brazilian standard for design and execution of reinforced concrete works, called NB-1[1].

Table 2.01: Minimum thickness of reinforcement cover*

Constructive elements	(cm)
Internal slabs	1.0
External slabs	1.5
Internal beams	1.5
External beams	2.0
Internal columns	1.5
External columns	2.0
Concrete in contact with the ground	2.0

*NB-1 The first Brasilian Standard for calculation and reinforced concrete execution (November 11, 1940)


CIMENTO E CONCRETO
BOLETIM DE INFORMAÇÕES
ASSOCIAÇÃO BRASILEIRA DE CIMENTO PORTLAND
ESPECIAL
1937

NORMAS PARA EXECUÇÃO E CALCULO DE CONCRETO ARMADO

APRESENTAÇÃO

ASSOCIAÇÃO BRASILEIRA DE CIMENTO PORTLAND

Figure 2.04 Standard ABCP for execution and calculation of reinforced concrete in 1937

The influence of reinforced concrete in the transformation of the city

Concrete was the main modern material which was viable to prepare at the construction site, and did not require a relatively skilled labor. It also had the advantage of being a relatively economic material, adapted to the needs of an underdeveloped country. In addition to these factors, the ease at low cost transport of this material and the customers' financial possibilities, which depend largely on the economic situation of the country also influenced the implementation of the reinforced concrete technique in the Brazilian capital[2], which gradually was giving

[1] ABNT *Associação Brasileira de Normas Técnicas*, History of the Brazilian Standards, São Paulo (2011).

[2] Rio de Janeiro was the Brazilian capital until 1960, from that date the capital became the city of Brasília.

space for increasingly thinner and higher buildings, and consequently changing the morphology of the city (Fig. 2.05)[1].

Figure 2.05 Evolution of construction in Rio de Janeiro. View of the port zone (*Mauá* square)

1608

1710

[1] Source: SEDREPAHC of the city of Rio de Janeiro (Extraordinary Secretariat for the Promotion, Defense, Development and Revitalization of Heritage and Historical-Cultural Memory).

1817

1930

2004

Rio is a city with little land available to build; this is a factor that could also explain its urban appearance and vertical growth. Perhaps it would be preferable that Rio´s buildings never rised above 4 or 6 floors. Thus, it would be possible to preserve the landscape and a better circulation of the sea breeze. We would have a better provision of public services and a lower traffic density.

Baumgart's significant designs

In the technical office of Baumgart, structures were designed in reinforced concrete. They represented a challenge for the Brazilian engineering structures, by overcoming some common standards at the time for structural designs. Among those structural projects of greater expressiveness is *A Noite* building, considered in 1929 the world's tallest building in reinforced concrete[1]. The building, despite having great importance in the structural engineering field, was for decades a controversial subject of critics to the Brazilian architecture. Baumgart is also author of the *MES* building (Ministry of Education and Health – Fig. 2.30) structural designs, with participation on the architecture designs of Le Corbusier, Lucio Costa and Oscar Niemeyer. Among other buildings which are important and representative to the history of the *Carioca* architecture stand the *Copacabana Palace* Hotel and *Gloria* Hotel, both designed by architect Joseph André Gire and Baumgart (Figures 2.06 and 2.07) [2].

Figure 2.06 Gloria Hotel, built in 1922

Figure 2.07 Copacabana Palace Hotel, built in 1923

[1] *Da Costa, Terezinha. Engenharia da Transparência, Vida e Obra de Lobo Carneiro (2005).*

[2] Source: Photographs of archive of the National Institute of Historical and Artistic Heritage IPHAN, Rio de Janeiro, July 2014.

2.1.1 Description of the case study's three buildings

2.1.1.1 *A Noite* building

Architecture

The *A Noite* building was built between 1926 and 1929 in *Mauá* square[1] (port zone in the city center of Rio) and was designed by Joseph André Gire (former student of the School of Fine Arts in Paris) together with Elisário da Cunha Bahiana, who had won the public competition of the architectural design. Gire designed the building suiting up to the new technology of reinforced concrete and following the architectural style *Art Deco*, with a simple composition of straight lines, articulated geometric shapes and absence of decorative elements. The model used was based by on commercial multi-storey buildings of Chicago.

Construction of the building

The construction of the building was carried out by the construction company *Gusmão, Dourado & Baldassini* under a request of the journalist Geraldo da Rocha, who at the time was the owner of the newspaper *A Noite*. With 24 floors[2] and 102.8 meters high (comparable to 30 floors in today's times, due to its high ceiling), the building in its inauguration was the tallest in Latin America and the world's tallest in concrete (Figures 2.08[3] and 2.09[4]).

[1] At the north end of Avenida Rio Branco (one of the main avenues of Rio).

[2] Initially planned with 22 floors, then it had an increase of over 2 floors, but not served by lifts.

[3] Source: Photographic reproduction of the book *"A aventura do concreto armado no Rio de Janeiro 1900 – 1936"*, by Gabriela Carvalho, Claudia Lacombe Rocha, Rio de Janeiro, 2003.

[4] Source: Photographic reproduction of the book *"A Praça Mauá na memória do Rio de Janeiro"*, by João Fortes Engenharia. Publisher Ex Libris, Rio de Janeiro, 1989.

Figure 2.08 Brazilian newspapers called *A Noite* of July 18, 1928, with some photos of the construction of the *A Noite* building

Figure 2.09 Building construction in 1928

On the ground there was the building of the Portuguese Literary Lyceum (Figures 2.10[1] and 2.11[2]), which was demolished to make way for the *A Noite* building, beginning the process of transformation and disfigurement of the Rio's port area.

Figure 2.10 *Mauá* square in the 20s, before the construction of the building *A Noite*

[1] Photographic reproduction of the book "*História dos Bairros - Zona Portuária"*, by João Fortes Engenharia. Publisher Ex Libris, Rio de Janeiro, 1987.

[2] Photographic reproduction of the book "*A Praça Mauá na memória do Rio de Janeiro"*, by João Fortes Engenharia. Publisher Ex Libris, Rio de Janeiro, 1989.

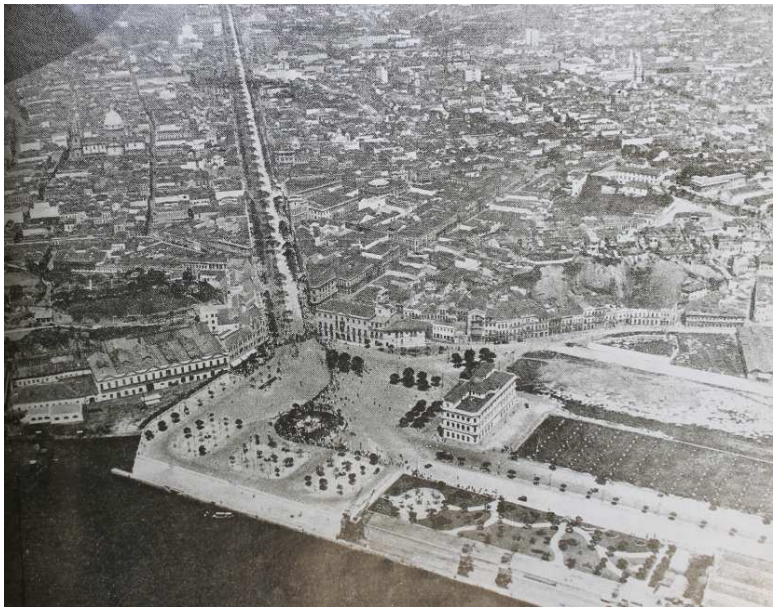

Figure 2.11 Aerial view of the port area of Rio, in 1920

During construction, Baumgart faced some questions about the structural safety of the work. The thicknesses of the designed slabs did not fit into construction standards[1]. To solve the deformation problem of the thin slabs (only 7cm thick), Baumgart created corbels of 10.4cm x 42cm (Figures 2.13, 2.14, 2.15) along the beams, with two steps, also serving as a decorative element.

[1] In the absence of national standard, Baumgart used German standards as the DIN-1045, 1925, to calculate the reinforced concrete. This may have been one of the main factors that explain the tradition of influence of European standards in Brazil.

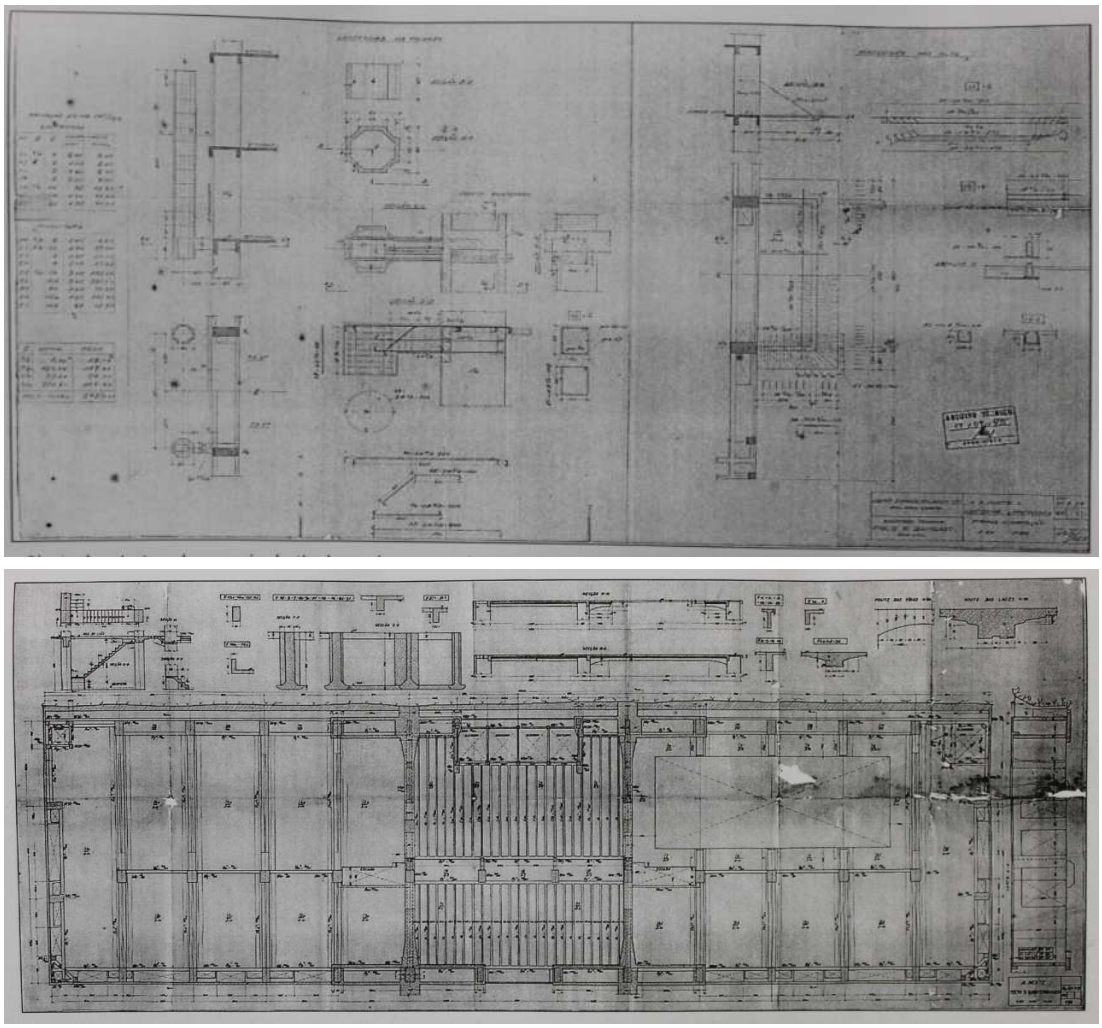

Figure 2.12 Copy of the original structural plans made by Baumgart

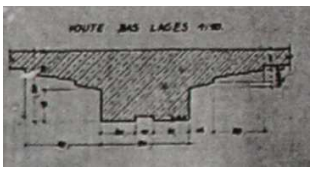

Figure 2.13 Beam section detail made by Baumgart

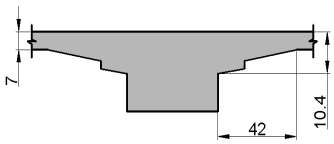

Figure 2.14 Reproduction of the beam section (dimensions in cm)

Figure 2.15 Internal building photos showing a beam with corbels. Photograph taken in July 2014

Also during the construction of the building, under a request supported by the supervising engineer Octávio Carneiro about the consideration of horizontal forces from the wind, Baumgart provided reinforcement in the structure up to the 14th floor (Fig. 2.12[1]), inserting wall-pillars in the central part of the building in the most requested direction[2]. According to a scholar of the history of concrete in Brazil, Eng. Augusto Carlos de Vasconcelos, this type of activity was not common from the professional responsible for the work supervision. Usually the supervisor work remains passive in the conceptual design issues, just checking if the project is being followed, and the construction is being well executed.

Five years after its construction, the management of the building proposed the construction of a restaurant with a dance floor on the roof slab (Fig. 2.16). In carrying out this expansion work, Baumgart designed a structural reinforcement using the elements that integrated the architectural plan; a new pergola was dimensioned to be part of the supporting structure of the roof slab, which entailed a significant load increase.

Figure 2.16 View of the pergola after completion of the structural reinforcement works. [Concreto Magazine n. 75 June 1945]:183

Figure 2.17 Current photo of the building's roof, taken in July 2014

[1] Source: Collected in the archive National Institute of Historical and Artistic Heritage IPHAN, Rio de Janeiro, July 2014.

[2] Vasconcelos, Augusto Carlos de. *O Concreto no Brasil*. São Paulo, Pini (1992).

Considering that the slabs had little thickness and the actions reached values that the structure could not stand without reinforcement, Baumgart decided to create a pergola with a beam placed in the center of the slab and three columns working under tension (as a chain) to support the loads of the new beam and of the existing slab (Fig. 2.19). The moment diagram reproduced in figure 2.18 shows an idea of the new distribution of the bending moments of the slab, it may be noted that the new diagram calculated after the creation of the center beam does not reach a negative moment in the center of the slab.

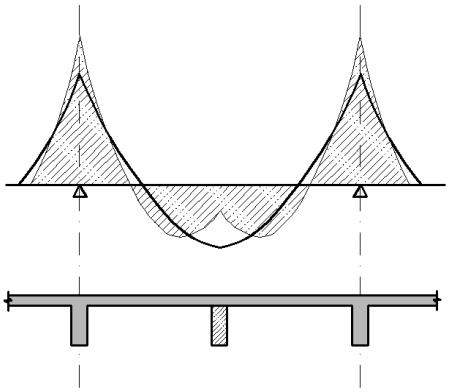

Figure 2.18 Reproduction of bending moment diagram of the reinforced slab. The strongest line represents the unreinforced slab moments. The crosshatch diagram represents the final moments. [Adapted from Concreto Magazine n. 75 June 1945]:186

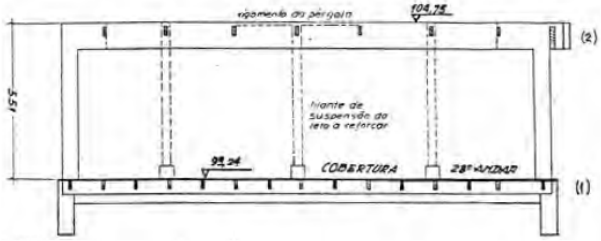

Figure 2.19 Representative section of the new structure (pergola). [Concreto Magazine n. 75 June 1945]:185

Increasing the bearing capacity of a structural element requires a careful evaluation and an accurate analysis on the possible change of static scheme of the structure. It is known that a structural reinforcement done with redistribution of loads can cause deformations and even the appearance of cracks in the reinforced element. The reinforced structure however showed no defects and accepted the new elements designed and executed under the guidance of Baumgart.

Cultural value

The building was located by the port, the main gateway to Rio de Janeiro and Brazil, and it was a symbol of the city. Together with the monument to *Cristo Redentor* and *Pão de Açúcar*, it began to be visited by large number of travelers who came to Rio[1].

Some authors mention that the building was a landmark that initiated the verticalization process of the city of Rio de Janeiro; since then the profile of the city becomes less European and more American. The value of the building was associated with the economic power of large companies that settled there[2], as the newspaper *A Noite* and the radio *Radio Nacional* that at the time was the most powerful means of communication in Brazil. In consequence, several sophisticated companies settled in the neighborhood (Fig. 2.20)[3].

Figure 2.20 Aerial view of the *Mauá* square, in 1930

[1] Tourists visiting the city paid a fee to visit the building's roof.

[2] It is also installed in the building architecture offices, including the office of structural designs Emílio Baumgart.

[3] Source: Photographic reproduction of the book *"A Praça Mauá na memória do Rio de Janeiro"*, by João Fortes Engenharia. Publisher Ex Libris, Rio de Janeiro, 1989.

Degradation and protection of the building

In the late 50s, the buildings around the *Mauá* square began to be demolished and replaced by other high-profile buildings, and in a way taking a part of the view of the *A Noite* building off. For several times the building resisted the demolition proposals (Fig. 2.21). In the 60s, offices and large companies which were in the building and neighboring buildings were moving to other areas of the city. The increasingly empty point was occupied by unattractive activities, leaving a degraded aspect in the place.


O GLOBO

Serão demolidos o edifício 'A Noite' e prédio do MIS

O edifício "A Noite", uma tradição na Praça Mauá

O prédio do Museu da Imagem e do Som, perto da Praça 15

DESAGRADO

Figure 2.21 Headline in the *O Globo* newspaper, about the supposed demolition of the building on September 27, 1978

Figure 2.22 Building photograph taken in July 2014

On October 5, 2012, the 83 years-old building joined the list of Historical and Artistic Heritage[1], being inscribed in the Historical and Fine Arts books of the National Institute of the Historical and Artistic Heritage IPHAN (Decree n.18.995 – Process n.1648). Among the main reasons why the *A Noite* building was protected

[1] Available in < http://portal.iphan.gov.br/uploads/ckfinder/arquivos/Lista_Bens_Tombados_marco_2016.pdf >, accessed in May 09, 2016.

is its significance to the history of the Brazilian media, its architectural value associated with the city verticalization process of Rio de Janeiro, and the importance the building has to engineering structures in Brazil and in the world.

Current condition

During the visit to the building, in July 2014[1], it was possible to identify points of deterioration at the reinforced concrete structure, inside and outside of the building. In figure 3.09, Chapter III, it is possible to visualize advanced deterioration points at the concrete and steel bars with cross-section loss caused by steel corrosion.

Currently, the building belongs to the National Institute of Industrial Property INPI[2]; it is inactive and awaiting restoration work as well as adequacy of the structure to the safety standards.

2.1.1.2 ABI building

Architecture

The choice of reinforced concrete in the *Carioca* architecture[3], besides being explicable by economic factors, also represented a manifestation of freedom. *Le Cobusier's* architecture influenced the use of the columns with the adoption of *Pilotis* and the principle of the columns retreating in buildings (Fig. 2.23)[4], in order to release the façade and all structural servitude, but mainly on the exploration of the material plasticity. Moreover, its use as a building material has brought numerous advantages for civil construction, in terms of safety and structural durability.

[1] In July and August 2014, during the PhD study mission were conducted visits and visual inspections in some buildings located in the center of Rio de Janeiro.

[2] In fact the building belongs to the INPI, Brazilian Federal Government (Union) and Brazil Communications Company (EBC).

[3] Architecture of the city of Rio de Janeiro.

[4] Source: Collected in the archive National Institute of Historical and Artistic Heritage IPHAN, Rio de Janeiro, August 2014.

The structures of Rio's buildings, which started from a simpler design formed by columns, beams and slabs, gradually evolved to the various presentations, both in functional and formal aspect.

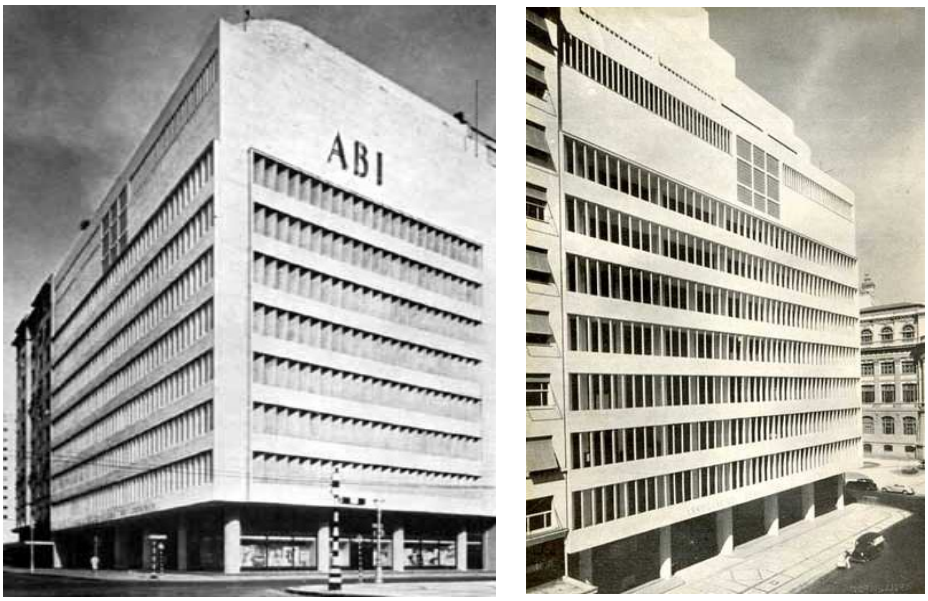

Figure 2.23 ABI Building (Brazilian Press Association), built between 1936 and 1938. Photograph taken in the 40s, after the inauguration of the building

The ABI building was one of the first modern buildings in the city center of Rio de Janeiro[1]. It was built in two years between 1936 and 1938 (Figures 2.24[2] and 2.25[3]) and designed by the Brazilian architects Marcelo Roberto and Milton Roberto (Fig. 2.26)[4]. The two brothers also designed other important buildings in Rio, but this was the first large-scale building (big massive volume) with the concepts of modern

[1] Located in 71 Araújo Porto Alegre Street, center of Rio de Janeiro.

[2] Source: Photograph of the archives of the ABI, Rio de Janeiro, August 2014.

[3] Source: Collected in the archive National Institute of Historical and Artistic Heritage IPHAN, Rio de Janeiro, August 2014.

[4] Source: Collected in the archive National Institute of Historical and Artistic Heritage IPHAN, Rio de Janeiro, August 2014.

architecture in Brazil. It was also heavily criticized for not having visible windows. The building was designed for a suitable architecture to the tropical climate: on the façades there are vertical *brise-soleils* in reinforced concrete in place of windows.

Figure 2.24 ABI Building during construction

Figure 2.25 View of the building. Photograph taken in the 40s

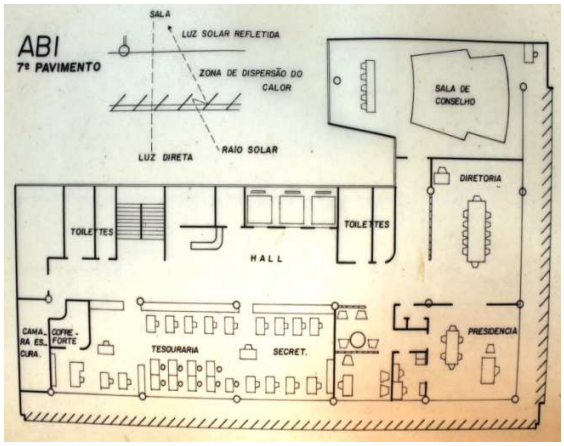

Figure 2.26 Reproduction of the original architecture plans (façades and 7th floor)

Construction of the building

The building was built in 71 *Araújo de Porto Alegre* Street (in the city center of Rio), by the construction company *Duarte e CIA*[1] to host the *Associação Brasileira de Imprensa* (ABI). The structural design (Fig. 2.27) [2] was elaborated on the responsibility of the Engineer Paulo da Rocha Fragoso, who was also author of other important building designs in Rio and had the opportunity to work at Baumgart's structural design office. The engineer used the ribbed slab technology in the design, when this type of slab was a technological novelty in Brazil.

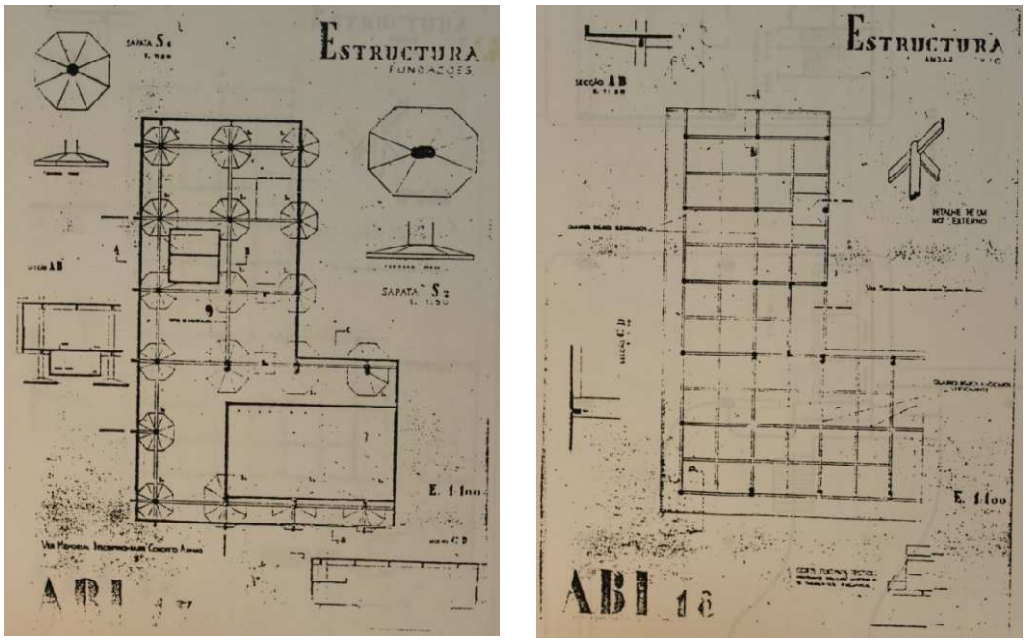

Figure 2.27 Reproduction of the original structural plans

With 15 floors, it was considered a high building at the time. For the structure to withstand the horizontal actions resulting from the wind, the engineer used wide

[1] Guide of the *Carioca* Modern Architecture. *Guia da Arquitetura moderna no Rio de Janeiro, pg. 28. Secretaria Municipal de Urbanismo, Prefeitura Municipal da Cidade do Rio de Janeiro.*

[2] Source: Collected in the archive National Institute of Historical and Artistic Heritage IPHAN, Rio de Janeiro, August 2014.

reinforced concrete beams with small heights, embedded in slab and armed to contribute in the bracing of the building. These beams, in addition to increase the overall stiffness of the structure, also served to reduce the slabs' deformations caused by vertical loads. This solution is very similar to that used by Baumgart for the structure of MES building.

Current condition and protection

In July 2014[1] the ABI went through restoration works on the façades (Fig. 2.28). Apparently, the building structure was in good condition, with few points of the concrete in deterioration process in initial stage and without presence of corrosion in the exposed steel bars (Fig. 2.29).

Figure 2.28 Photographs taken in July 2014, during the restoration works of the facades

[1] In July and August 2014, during the PhD study mission visits and visual inspections were conducted in some buildings located in the city center of Rio de Janeiro.

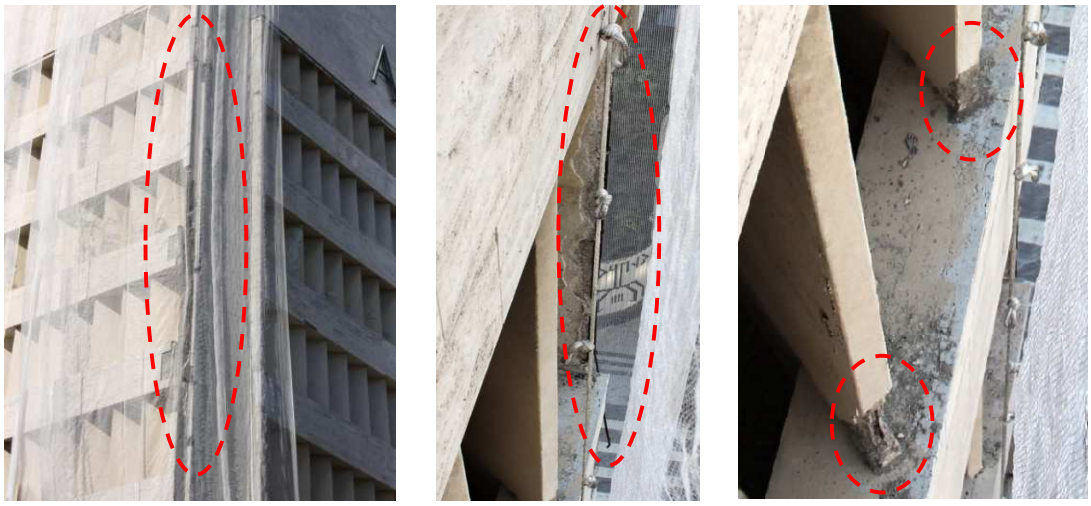

Figure 2.29 Structure in initial deterioration process. Photographs taken in July 2014

Currently, ABI building is protected by the Brazilian government agencies. On May 29, 1984 it was inscribed in the *Belas Artes* book (Book II, Rg. 559) of the IPHAN[1]. The building was protected not only by its architectural value, but also due to the meaning that the ABI (*Associação Brasileira de Imprensa*[2]) has for the country's history.

2.1.1.3 MES building

Architecture

The MES building (Figures 2.30[3], 2.31 and 2.32), also known as *Palácio Capanema*, is a representative reinforced concrete building of the twentieth century due to its exceptional quality and also for being one of the first applications of the basic principles of modern architecture adopted by Le Corbusier.

[1] National Institute of Historical and Artistic Heritage.

[2] Brazilian Press Association.

[3] Source: Photograph of archive of the National Institute of Historical and Artistic Heritage IPHAN, Rio de Janeiro, July 2014.

Figure 2.30 MES (Ministry of Education and Health), inaugurated in 1943. Photograph taken in the 40s, after its inauguration

Figure 2.31 Double *Pilotis*. Photograph taken in July 2014

Figure 2.32 Glass façade. Photograph taken in July 2014

The building is located at 16 Imprensa Street, center of Rio de Janeiro, and was built between 1937 and 1943 to host the Ministry of Education and Health. It was designed by a team of architects, which included Lucio Costa and Oscar Niemeyer, starting from the studies of Le Corbusier (Figures 2.33, 2.34 and 2.35)[1]. The building is considered a landmark of the modern architecture in Brazil, highlighting the structure on double *pilotis*, the *brise-soleil* on the façade, the gardens of Burle Marx, the panels of Candido Portinari and the sculptures of Bruno Giorgi and Antonio Celso Menezes.

[1] Source: Collected in the archive National Institute of Historical and Artistic Heritage IPHAN, Rio de Janeiro, July 2014.

Figure 2.33 Le Corbusier and Oscar Niemeyer with the committee responsible for building construction, in 1936

Figure 2.35 Le Corbusier on the ship returning from Brazil to France, in 1929 (his first trip in Brazil)

Figure 2.34 Second trip of Le Corbusier in Rio de Janeiro, in 1936 (in the background the hill *Pão de Açucar*)

The architectural design

Le Corbusier arrived in Rio de Janeiro aboard a *Hindenburg* dirigible, on June 12, 1936, to join the design team as a consultant of the young architects led by Lucio Costa and composed by Oscar Niemeyer, Affonso Reidy, Carlos Leão, Jorge Moreira and Ernani Vasconcelos.

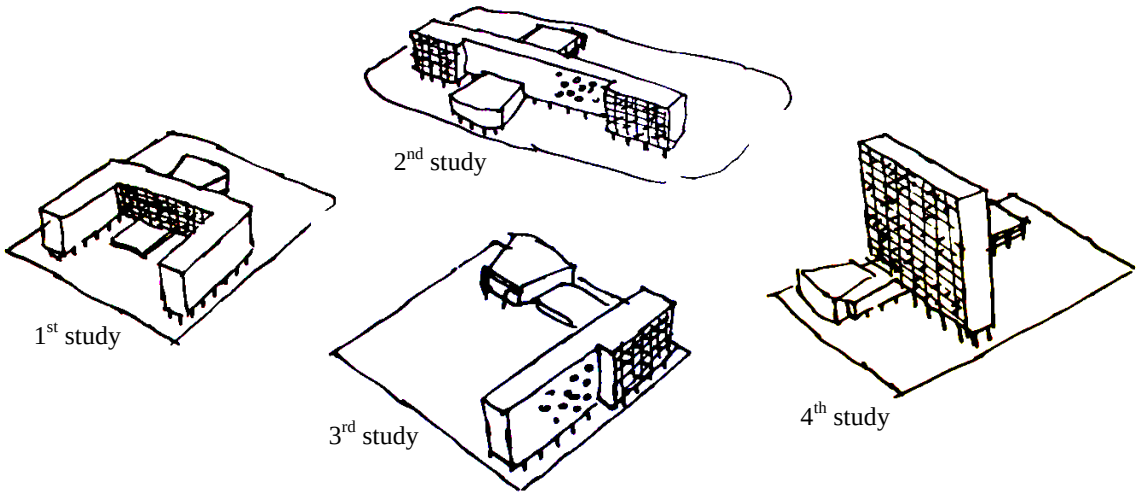

Figure 2.36 Preliminary studies made by Le Corbusier

The design of the MES was subject of careful and long studies. To contemplate the importance of the building, several initial studies were made by Le Corbusier (Figures from 2.36 at 2.40)[1].

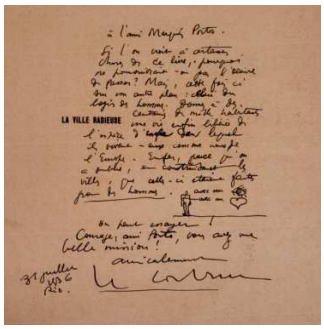

Figure 2.37 Photographic reproduction of the letter from Le Corbusier to engineer Marques Porto. Rio de Janeiro, July 31, 1936

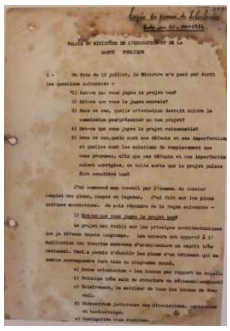

Figure 2.38 Photographic reproduction of the front page of Le Corbusier report about the MES design, Rio de Janeiro, August 10, 1936

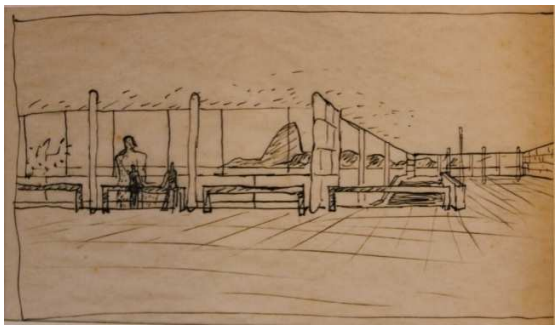

Figure 2.39 Photographic reproduction of the original design of Le Corbusier for the MES, Rio de Janeiro, 1936

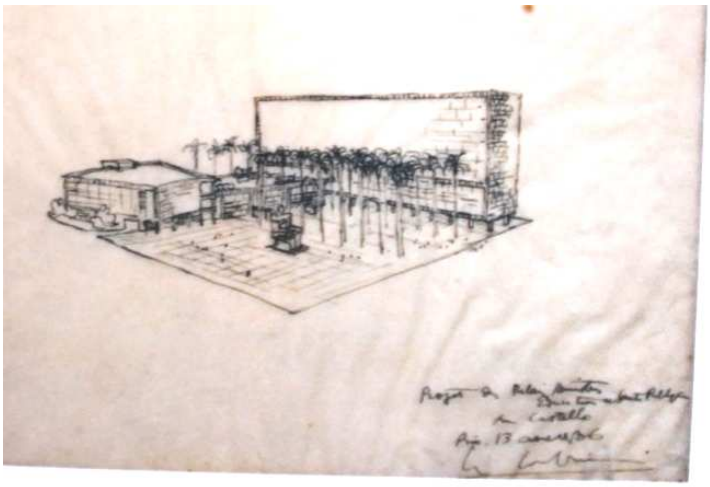

Figure 2.40 Photographic reproduction of the original volumetric design made by Le Corbusier, Rio de Janeiro, 1936

[1] Source: Collected in the archive National Institute of Historical and Artistic Heritage IPHAN, Rio de Janeiro, July 2014.

The volumetric composition of the building is composed of three interconnected blocks: administrative offices, auditorium and showroom. The main block has 14 floors on 10 meters high *pilotis* (Fig. 2.31) and the two main façades are different from each other in accordance with the solar incidence: the north with mobile horizontal *brise-soleil* (Fig. 2.30) and the south treated with a glass façade (Fig. 2.32).

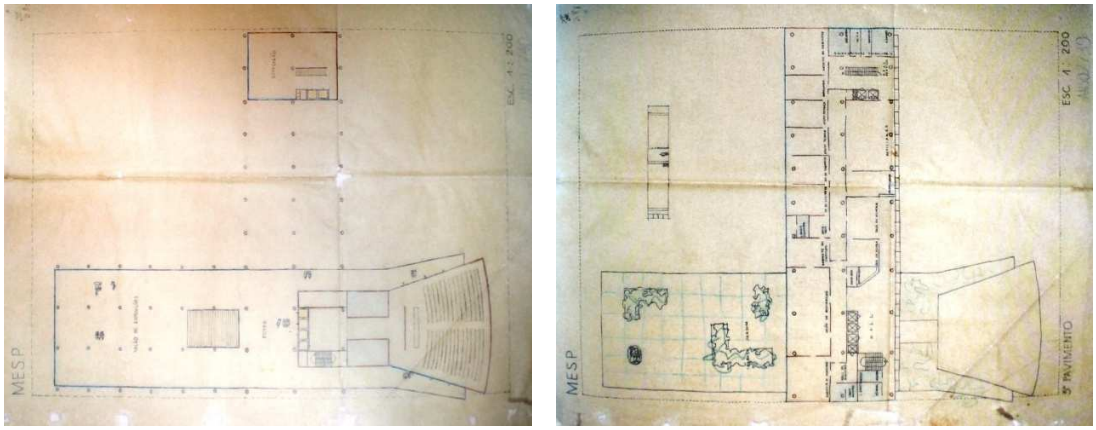

Figure 2.41 Photographic reproduction of the original architecture plans (2nd and 3rd floors)
Rio de Janeiro, 1936

Structural design

The structural design (Figures 2.42 and 2.43)[1] was made by Emílio Baumgart, who used the technology of reinforced concrete structure with flat plate slab (Fig. 2.44)[2]. For the building to resist the horizontal loads from the wind, the engineer used wide reinforced concrete beams with small heights embedded in slab, armed to contribute on the bracing of the building (Fig. 2.44). These beams along with the pillars form frames that help to increase the overall stiffness of the structure.

[1] Source: Collected in the archive National Institute of Historical and Artistic Heritage IPHAN, Rio de Janeiro, July 2014.

[2] Source: Collected in the archive National Institute of Historical and Artistic Heritage IPHAN, Rio de Janeiro, July 2014.

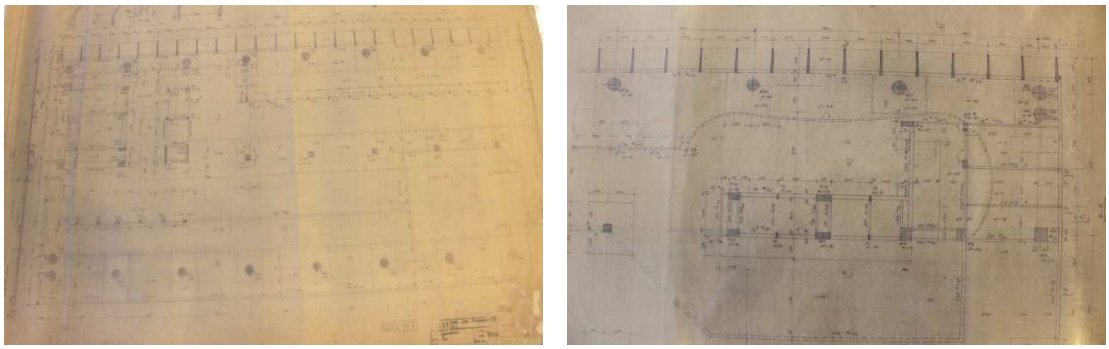

Figure 2.42 Photographic reproductions of the original structural plans made by Baumgart Rio de Janeiro, 1937

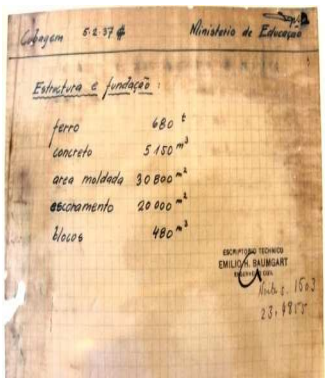

Figure 2.43 Quantitative of materials for the building structure made by Baumgart in 1937

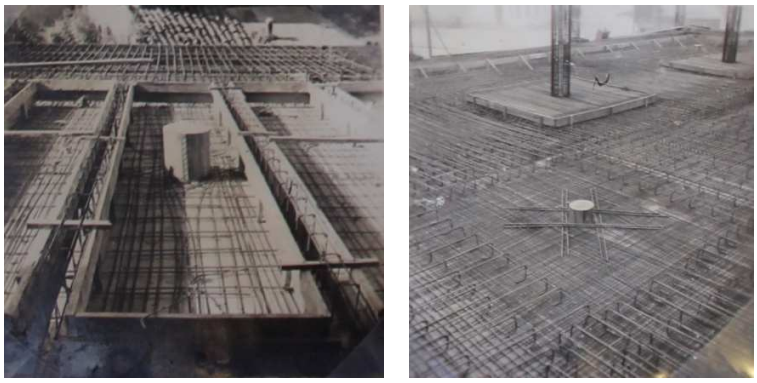

Figure 2.44 Photographs of the slab reinforcements, taken in 1939. On the right, reinforcement of the capitals and on the left, the reinforcement of the merged beams in the slab

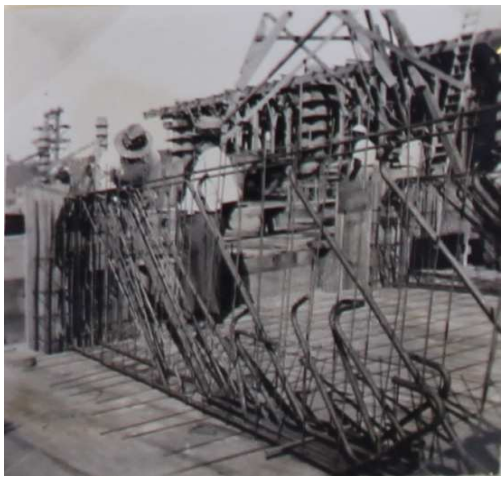

Figure 2.45 On the left, the structure of the building under construction and above a reinforcement cage of a beam. Photographs taken in 1939

Protection

On March 18, 1948, the building joined the list of Historical and Artistic Heritage[1], being inscribed in the *Belas-Artes* book of the National Secretariat of Historical and Artistic Heritage SPHAN (Process n.375). Among the main reasons why the building was protected, in addition to its cultural value, is its value of being a public building associated with the national political power and its importance for the history of Brazilian and world architecture.

Current condition

In July 2014[2] the MES went through restoration works on the façades (Fig. 2.47). Apparently the building structure was in good conditions, with few points of deterioration that presented concrete spalling and steel bars corrosion (Fig. 2.46).

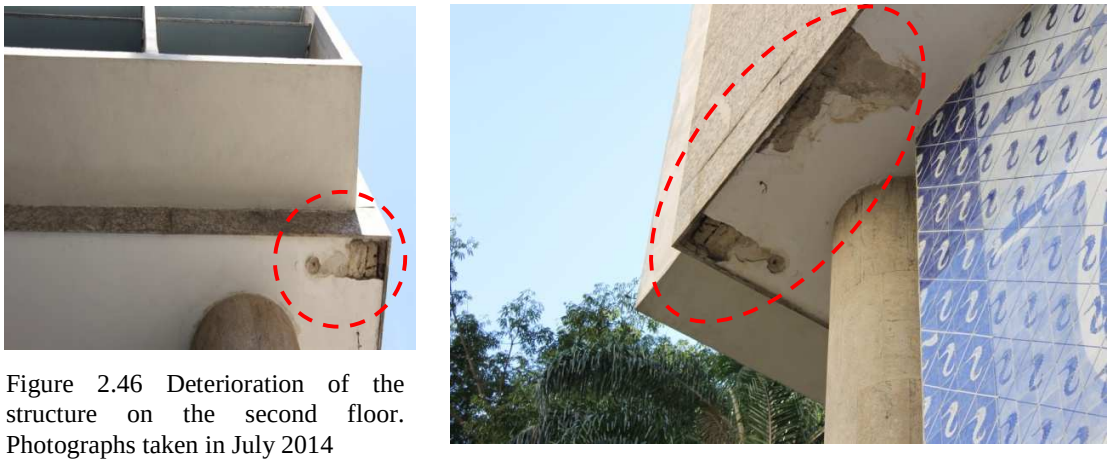

Figure 2.46 Deterioration of the structure on the second floor. Photographs taken in July 2014

[1] Available in < http://portal.iphan.gov.br/uploads/ckfinder/arquivos/Lista_Bens_Tombados_marco_2016.pdf >, accessed in August 10, 2016.

[2] In July and August 2014, during the PhD study mission visits and visual inspections were conducted in some buildings located in the center of Rio de Janeiro.

Figure 2.47 Restoration works on the façades. Photographs taken in July 2014

2.1.2 Comparison of general characteristics of the three buildings studied

Source: Google maps

Figure 2.48 Center of Rio de Janeiro:

1. *A Noite* building
2. *ABI* building
3. *MES* building

Table 2.02: Comparison of general characteristics of the buildings

	1. *A Noite* (1929)	2. ABI (1938)	3. MES (1943)
Architectural design	Joseph André Gire and Elisário Bahiana	Marcelo Roberto and Milton Roberto	Le Corbusier, Lucio Costa, Oscar Niemeyer, Carlos Leão, Jorge M. Moreira, Affonso E. Reidy and Ernany Vasconcelos
Structural design	Emílio H. Baumgart (first use of concrete technological control in Brazil)	Paulo da Rocha Fragoso	Emílio H. Baumgart
Architectural style	Art *Deco* architecture (tallest in the world, in reinforced concrete in 1929)	*Carioca* Modern Architecture (first use of *brise-soleil* in Brazil)	*Carioca* Modern Architecture
Features	24 floors (102.8m) Simple composition without decorative elements A regular layout in plan	15 floors Great massive volume No windows, with use of *brise-soleil* in the façades	16 floors Building on double *pilotis* *Brise-soleil* and glass on the façades
Intended use	Business offices	Business offices (press)	Administrative offices Public activity
Type of structure and constructive elements	Conventional structure frame and some wall-pillars Bricks masonry walls	Conventional structure with ribbed slabs Prefabricated external RC elements, fixed vertical *brise-soleil*	Conventional structure with flat plate slab (first use in Brazil) Prefabricated external RC elements, movable horizontal *brise-soleil*
Columns	Rectangular pillars Modules 5 x 7 and 10 meters Central wall-pillars	Circular columns Modules 7 x 7 meters	Circular columns in the periphery and square columns the center Modules 8 x 8.4 meters

Other characteristics	Symmetry in plan Centered core lifts	Lack of symmetry in plan Centered core lifts	Lack of symmetry in plan Two not centered cores lifts
Protection[1] (Safeguard)	On October 5, 2012 the *A Noite* building was protected by IPHAN (Decree 18,995)	On May 29, 1984 the ABI building was protected by IPHAN (*Belas-Artes* book II, Rg. 559)	On March 18, 1948 the MES building was protected by SPHAN (*Belas-Artes* book, Process 375)
Current[2] condition	Lack of maintenance The structure of the ground floor and roof in deterioration process Building currently out of use	Building in maintenance (restoration works) Presence of deterioration in a few points of the structure	Building in maintenance (restoration works) Presence of deterioration in a few points of the structure

2.2 Brief panoramic on the conservation culture of historic RC buildings in Brazil

Brazilian problematic

Brazil is a country that has a large amount of heritage buildings in reinforced concrete, designed by great architects and engineers, located in the cities of Rio de Janeiro, Brasília, São Paulo, and other large Brazilian cities which have a cultural heritage of exceptional value from the point of view of the history, art, science and culture; this makes them worthy of being considered and maintained. However, the conceptual issues related to the conservation of reinforced concrete buildings are rarely discussed in the context of the structural engineering in Brazil, this could explain why the country does not have clear criteria and methodologies of intervention in historic reinforced concrete buildings.

[1] Available in <http://portal.iphan.gov.br/uploads/ckfinder/arquivos/Lista_Bens_Tombados_marco_2016.pdf >, accessed in August 10, 2016.

[2] Current condition in July 2014 during the study visits in the buildings.

Many professionals of the structural design field still do not have an understanding of the required conservation culture to make the most appropriate decisions in rehabilitation interventions. It is known that when not working adequately in the maintenance of the structures, deterioration occurs before the expected time, often with serious consequences. Thereby, many cases of deterioration of the buildings, mostly the older ones, are neglected until an important problem related to the structural safety happens. On the other hand, short-sighted interventions on the recovery of reinforced concrete can result in poorly performed works that do not respect certain principles of preservation of the historical and architectural value of the heritage goods.

Protection of heritage buildings in Brazil

In Brazil, the protection of heritage buildings began to be organized in a meaningful way after the creation of the Legislative Decree no. 25 (November 30, 1937). Its text constitutes the historical and artistic heritage and creates the four books of *Tombo*[1]. Thus, the heritage buildings that are recognized as cultural goods, whether in local, state and federal instances, are inscribed on the *Tombo* books. The Department of Historical and Artistic Heritage (SPHAN), first agency at national level responsible for ensuring the conservation of the Brazilian cultural heritage, was founded on January 13, 1937[2]. Currently called National Institute of Historical and Artistic Heritage (IPHAN), it has the function of protecting and promoting the country's cultural heritage, ensuring its permanence and usufruct for the present and future generations.

[1] Archaeological, Ethnographic and Landscape *Tombo* book; Historical *Tombo* book; Fine Arts *Tombo* book; and Applied Arts *Tombo* book.

[2] IPHAN, Publication number 31: *Proteção e Revitalização do Patrimônio Cultural no Brasil: uma trajetória.* By Secretary of the National Institute of Historical and Artistic Heritage.

2.2.1 The main conservation criteria that could be considered on structural interventions of historic RC buildings

The heritage buildings that have been or are representative and important for a culture should be preserved in order their values (Fig. 2.49) could be conveyed to the people, be they historical and architectural, memorial and symbolic. The structure of a building could be preserved, for example, through the choice of type of intervention compatible with its documental and formal aspects, keeping its configuration and developing a possible design according to their original characteristics.

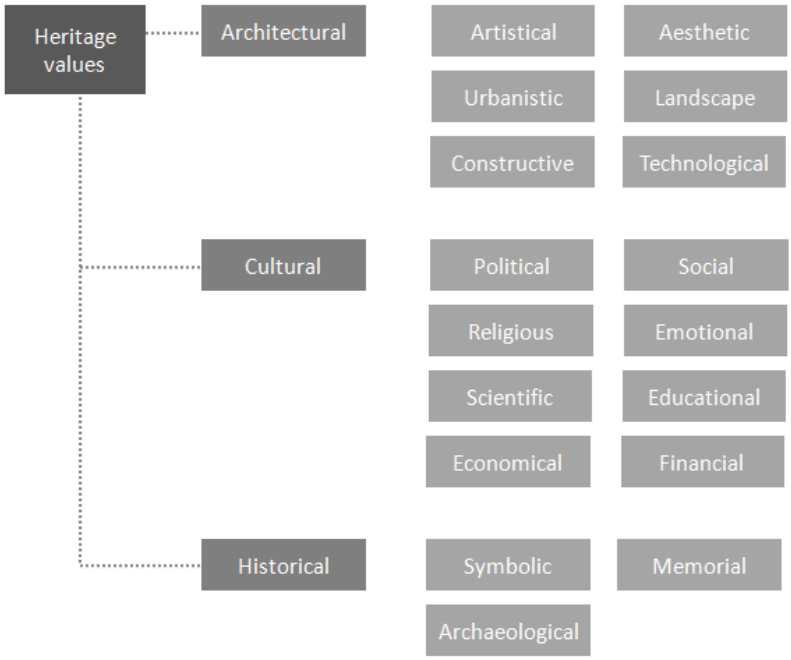

Figure 2.49 The main values of heritage buildings

By identifying heritage goods with cultural interest, their values should be regarded and protected as interest for the community as a whole. Changing the elements of a building without careful connotation and methodology to conserve its values

could be considered as a destruction of historical data that interrupts the transmission of knowledge and memory of a culture.

The preservation of the structure of a historic building could mean to understand and to value the whole and its parts, respecting the elements that compose it, which are closely connected. Therefore, it would be necessary to understand the architecture and its relationship with the structure, the original use of materials and construction techniques, the interventions over time and the various phases it passed until reaching the current setting, as well as understanding the uses that followed and its history.

The conservation of heritage structures was clearly addressed in the letter approved by the 14th General Assembly of ICOMOS (International Council of Monuments and Sites) in Zimbabwe in 2003[1]. The letter refers to the principles of the *Carta di Venezia*[2] and applies to the preservation of the structures of buildings. Among its general criteria, there are:

2.2 A full understanding of the structural and material characteristics is required in conservation practice. Information is essential on the structure in its original and earlier states, on the techniques that were used in the construction, on the alterations and their effects, on the phenomena that have occurred, and, finally, on its present state.

2.7 The safety evaluation, which is the last step in the diagnosis, where the need for treatment measures is determined, should reconcile qualitative with quantitative analysis: direct observation, historical research, structural analysis and, if it is the case, experiments and tests.

[1] ICOMOS charter. Principles for the analysis, conservation and Structural Restoration of Architectural Heritage. Ratified by the ICOMOS 14th General Assembly, in Vicoria Falls, Zimbabwe, October 2003.

[2] Venice Charter, 1964. International Charter for the Conservation and Restoration of Monuments and Sites.

An intervention of historic building rehabilitation could be considered an important work that involves a series of specialized disciplines which are independent, but at the same time correlated. It is necessary to conduct studies[1] of architecture and structure, as well as to perform topographical and metrical surveys. Eventual experimental tests on site and in laboratory are required to know the mechanical characteristics and the current condition of the structure and its materials. An ample understanding of structural behaviour and the materials properties should be considered essential for conservation and structural recovery designs.

2.3 References

1. Bruand, Yves. L´architecture contemporaine au Brésil, 2010.
2. Carta di Venezia. Carta internazionale sulla conservazione e il restauro di monumenti e insiemi architettonici, 1964.
3. Carta Italiana del Restauro, Circolare N°117 del 6 aprile 1972, Ministero Della Pubblica Istruzione.
4. Decree-Law no. 25, November 30, 1937, organizes the protection of national historical and artistic heritage (Decreto-Lei n. 25, de 30 de novembro de 1937. Organiza a proteção do patrimônio histórico e artístico nacional).
5. Feilden, Bernard M.; Conservation of Historic Buildings (third edition). Architectural Press, 2003.
6. Gabriela Carvalho, Claudia Lacombe Rocha. *A aventura do concreto armado no Rio de Janeiro 1900* – 1936. Rio de Janeiro, 2003.
7. Garré, Fabián. Patrimonio arquitectónico urbano, preservación y rescate: bases conceptuales e instrumentos de salvaguarda. Rosario, Argentina, Conserva N.05, 2001.
8. História da Normalização Brasileira, Associação Brasileira de Normas Técnicas ABNT, São Paulo, 2011.

[1] This requires an accurate research: historical-documental, ichnographical and bibliographic.

9. ICOMOS charter Principles for the analysis, conservation and Structural Restoration of Architectural Heritage. Ratified by the ICOMOS 14th General Assembly, in Vicoria Falls, Zimbabwe, October 2003
10. João Fortes Engenharia. A Praça Mauá na memória do Rio de Janeiro de. Editora Ex Libris, Rio de Janeiro, 1989.
11. João Fortes Engenharia. História dos Bairros – Zona Portuária. Editora Index, Rio de Janeiro, 1987.
12. Kuhl, Beatriz Mugayar. Preservação do Patrimônio Arquitetônico da Industrialização, São Paulo, 2009.
13. Mindlin, Henrique E., "Arquitetura Moderna no Brasil", Aeroplano Editora, 1999.
14. Prefeitura da Cidade do Rio de Janeiro, "Guia do Patrimônio Cultural Carioca – Bens tombados" – 2014.
15. Secretaria do Estado do Rio de Janeiro, "Patrimônio Cultural – Guia dos bens tombados pelo Estado do Rio de Janeiro" – 2012.
16. Secretaria Municipal de Urbanismo, Prefeitura Municipal da Cidade do Rio de Janeiro. Guia da Arquitetura moderna no Rio de Janeiro. Ed. Casa da Palavra, 2000.
17. Silva, Fernando Nascimento; Dos Santos, Sidney Gomes. *Rio de Janeiro em seus quatrocentos anos: formação e desenvolvimento da cidade. Editora Récord, São Paulo (1965).*
18. *Terezinha da Costa. Engenharia da Transparência, Vida e Obra de Lobo Carneiro (2005).*
19. Vasconcelos, Augusto Carlos. O concreto no Brasil: recordes, realizações, história. São Paulo: Copiare, 1985.
20. Vasconcellos, Juliano Caldas de; Concreto Armado, Arquitetura Moderna, Escola Carioca: levantamentos e notas. Dissertação (Mestrado em Arquitetura) - Universidade Federal do Rio Grande do Sul (PROPAR), 2004 313p.

21. Vasconcellos, Juliano caldas de. The maturity of the reinforced concrete in the field of Brazilian engineering in the 1930 And 1940. In: 11° Seminário Nacional do Docomomo Brasil. Anais. Recife: Docomomo_Br, 2016. Pg. 7.
22. Xavier A.; Britto A.; Nobre A.; “Arquitetura Moderna no Rio de Janeiro”, Rioarte, Pini, Vilanova Artigas, Rio de Janeiro e São Paulo – 1991.

Chapter III

The manifestation of structural deterioration

3.1 General considerations

The Brazilian issue concerning to deterioration of heritage buildings

Many reinforced concrete structures built in Brazil in the beginning of last century present deterioration problems, both for the phenomena related to the maintenance of buildings and for the effects linked to aggressive agents of the atmosphere. The lack of proper maintenance of the structure during its service life can originate pathological phenomena such as deterioration of concrete and steel, which manifest before the time provided in the structural design, often with serious consequences and great damage. The corrosion phenomenon is one of the first direct consequences of the deterioration of reinforced concrete, which can cause a reduction of the structures' performance. The intervention of rehabilitation of these structures in order to recover or increase their load-bearing capacity is not always simple to obtain (though it is one of the most crucial aspects in rehabilitating such structures), especially when it intervenes in historic buildings that have cultural and heritage value in itself.

Nonetheless, the problematic related to the conservation of RC structures are little treated in the area of Brazilian structural design. In the case of architectural works in reinforced concrete belonging to the Brazilian cultural heritage, because of their typological varieties and constructive singularities (also due to the changes made during the building´s history), there are difficulties in defining analysis criteria and to identify the most appropriate intervention procedures inherent to the

conservation of heritage buildings. At the evaluation step, it is normal to face uncertainties in defining a model of analysis and its respective parameters. Not always being possible to apply to the cultural goods the design procedures established for common buildings. Thereby, a need to assess the adequacy of the structures arises, not only from a point of view linked to security, but also a conservative one, with methodologies and appropriate intervention technologies.

Standards for intervention in existing structures

The lack of clear criteria and a specific national standard for intervention in existing buildings[1] could be considered the major cause for most of the uncertainties and inadequate interventions in structural recovery works in Brazil.

In Italy, the standard NTC 2008 (*Norme Tecniche per le Costruzioni*)[2] defines in Chapter 8, the general criteria for the safety assessment and for designs of existing buildings. In chapter 2, concerning the structural safety and the expected performance, the standard deals with the consideration of structural deterioration in the design phase, as follows:

2.5.4 The structure must be designed so that the degradation throughout its service life, adopting a normal routine maintenance, does not harm their performance in terms of strength, stability and workability, taking the structure below the levels of performance required by the standard. The security measures of the structure against excessive degradation must be established with reference to specific environmental conditions, and must be obtained through an appropriate choice of construction details, materials and structural dimensions, with the

[1] In Brazil, in the absence of a specific standard for intervention in existing structures, is used the Brazilian standard procedure for concrete structures design, the ABNT NBR 6118, concerning the new construction design.

[2] Italian standard NTC 2008, *Norme Tecniche per le Costruzioni*, Ministerial Decree January 14, 2008. This standard is currently being reviewed and a new version will be released soon.

possible application of substances or coverings protectors, and the adoption of other active or passive protection measures.

According to the NTC 2008, deterioration of structures can be classified as endogenous deterioration, which is the natural change of material that comprises the structure, and exogenous deterioration, which is the change in the characteristics of the materials constituting the structure, followed by external agents. The *fib*[1] Model Code for Concrete Structures 2010 defines structural damage as a physical disruption or change in the condition of a structure or its components, caused by external actions, so that the current or future performance of the structure is damaged.

3.2 The deterioration of reinforced concrete structures in Brazil

Corrosion costs

The expenses with deterioration of structures (especially when the cause is reinforcement corrosion) are generally very high. The annual cost of corrosion worldwide is 2.2 trillion USD, over 3% of the world's GDP[2]. In Brazil it is estimated that the costs are relatively higher, around 3.5% of GDP[3]. Among other factors, this can be explained by the fact that in Brazil the practice of inspecting and periodic monitoring of concrete structures is not very common (in relation to countries where the practice of maintaining structures is well-established). Thereby, interventions are carried out when the structure presents an advanced deterioration process, raising the rehabilitation costs.

[1] Fédération internationale du béton / International Federation for Structural Concrete (fib).

[2] World Corrosion Organization. George F. Hays, PE. "Now is the Time". Available in < http://corrosion.org/wco_media/nowisthetime.pdf >, accessed in May 26, 2016.

[3] Instituto de Tecnologia para o Desenvolvimento and Manaus Energia S.A. Physicochemical performance of metals and concrete structures used in electricity distribution networks: case study in Manaus Region. Brzil, 2 006. Available in < http://quimicanova.sbq.org.br/imagebank/pdf/Vol29No4_724_17-AR05251.pdf >, access ed in May 26, 2016.

The influence of the environment on the deterioration of structures

Brazil has one of the most extensive coastal areas in the world: 9198 km (considering the geographical clippings)[1], divided into 17 of the 26 Brazilian states[2] and facing the Atlantic Ocean. It has different climates among equatorial, humid, tropical and tropical coastal, subtropical and temperate, with constant winds and sea salinity above the average of ocean water on the planet.

Figure 3.01 Brazilian coast: considered aggressive environment for reinforced concrete structures

The environment has a significant influence on the type and intensity of structural deterioration. As a result of climate variety, various manifestations of structural deterioration are found in different regions in Brazil. Among them, the more frequent one is the reinforcement corrosion. For example, in the South, in the state of Rio Grande do Sul, where the climate is temperate/humid subtropical, it is

[1] Data available in < http://www.coladaweb.com/geografia-do-brasil/zonas-litoraneas-do-brasil >, accessed in May 25, 2016.

[2] Most of the 17 coastal states have their capital near the coast.

observed that the incidence of reinforcement corrosion is in the order of 30%[1]. In the Midwest, where the climate is semi-humid tropical, it is estimated that incidence of reinforcement corrosion is in the order of 30.1%[2], and in the North where the predominant climate is humid equatorial, in the order of 43%[2]. In the regions located on the sea coast (with humid tropical climate prevailing), where there is a higher incidence of chloride attack, in particular in the state of Pernambuco, it is estimated that reinforcement corrosion accounts for the majority of the structural pathologies of the order of 64%[3].

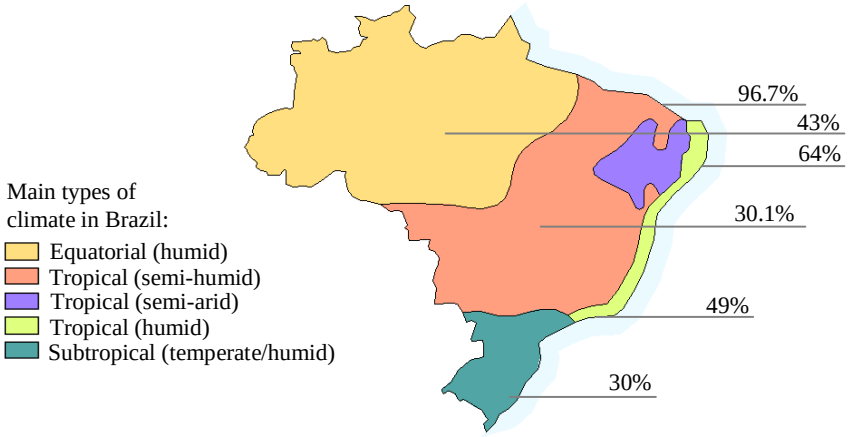

Figure 3.02 Studies on the incidence of reinforcement corrosion in buildings that present structural deterioration in Brazil

[1] Cinpar – VI Congresso Internacional sobre Patología y Recuperación de Estructuras. Assessment of contami nation by chloride ions in concrete samples subjected to aggressive conditions. Mota, J.M. de Freitas et al. Jul y 2010. Data available in < http://www.edutecne.utn.edu.ar/cinpar_2010/Topico%203/CINPAR%20120.pdf > accessed in August 17, 2016.

[2] XV National Meeting of the Built Environment Technology. ENTAC 2014. Maceió-Brasil. Survey of pathological manifestations in reinforced concrete structures in the State of Ceará.

[3] Durability of reinforced concrete structures: Analysis of the structure deterioration in Pernambuco State. By Andrade and Dal Molin, 1997. Data available in < http://www.lume.ufrgs.br/bitstream/handle/10183/122441/000215709.pdf?sequence=1 > accessed in August 17, 2016.

Chloride attack

The cities grow faster in Brazilian coastal regions, as is the case of the big cities such as Rio de Janeiro, Florianópolis, Salvador, Fortaleza, Recife, Maceió, Natal, São Luís, João Pessoa, Aracajú, among others. Whereas reinforced concrete is the most widely used building material in Brazil, the reinforced concrete structures located in these regions, are subject to the aggressive actions of the marine environment. Therefore, the number of structural deterioration problems in these areas increases substantially.

In the marine environment, there is a lower performance of the structures to resist the harmful agents. Thus, manifestations of deterioration due to corrosion caused by chloride attack may occur (Fig. 3.11).

Concrete carbonation

The buildings located in the inner cities of the country also suffer from structural deterioration problems. Especially in large population centers with high pollution index, which have an environment with a higher concentration of CO_2, such as São Paulo, Brasília, Belo Horizonte, Curitiba, Porto Alegre, among others (some cities suffer from acid rain, as is the case of the industrial city of Cubatão in the state of São Paulo). The incidence of reinforcement corrosion in these cities is quite significant, and is usually caused by the carbonation process of concrete, especially in micro-climates as garage buildings where the CO_2 concentration is much higher. In these cases, accented signs of corrosion may appear in a few years after the construction of the building, compromising the safety of the structure (Fig. 3.10).

3.3 Environmental aggressiveness on the structures

The aggressiveness of the environment is related to physical and chemical processes that act on the reinforced concrete structures, independent of mechanical actions, volumetric variations of thermal origin, hydraulic retraction and

other actions provided in structural design. Environmental aggression must be assessed and considered in the design of new structures and intervention design of existing structures, according to classifications of the environment types and aggression intensity, and also according to the exposure conditions of the entire structure or its parts.

Brazilian standard for environmental aggressiveness

The Brazilian standard procedure for concrete structures design (NBR 6118), classifies the risk of deterioration of the structure according to the type and environmental aggression, as the table below:

Table 3.01: Environmental aggressiveness classes (ABNT NBR 6118:2014 - Brazilian standard)

Environmental aggressiveness class	Aggressiveness	Environment type classification for project	Risk of structure deterioration
I	Low	Rural	Insignificant
		Submerged	
II	Moderate	Urban	Low
III	High	Marine	High
		Industrial	
IV	Very high	Industrial	Elevated
		Spatter tide	

Due to a large correspondence of environmental aggressiveness class with the concrete water-cement[1] ratio, its compression strength and the thickness of the reinforcement cover, the following minimum requirements are expressed in the standard ABNT NBR 6118:

[1] Important factor for definition of voids index of the concrete and, consequently, on the durability of the structure.

Table 3.02: Correspondence between the aggression class and the quality of concrete (ABNT NBR 6118:2014 - Brazilian standard)

Concrete	Type	Environmental aggressiveness class (Table 3.01)			
		I	II	III	IV
Water-cement ratio in mass	CA	≤ 0.65	≤ 0.60	≤ 0.55	≤ 0.45
	CP	≤ 0.60	≤ 0.55	≤ 0.50	≤ 0.45
Concrete class	CA	≥ C20	≥ C25	≥ C30	≥ C40
	CP	≥ C25	≥ C30	≥ C35	≥ C40

CA It corresponds to the components and structural elements of reinforced concrete
CP It corresponds to the components and structural elements of prestressed concrete

Table 3.03: Correspondence between the aggression class and the nominal concrete cover (ABNT NBR 6118:2014 - Brazilian standard)

Type of structure	Component or element	Environmental aggressiveness class (Table 3.01)			
		I	II	III	IV
		Nominal concrete cover (mm)			
Reinforced concrete	Slab	20	25	35	45
	Beam/Column	25	30	40	50
	Structural elements in contact with the ground	30		40	50
Prestressed concrete	Slab	25	30	40	50
	Beam/Column	30	35	45	55

European standard for environmental aggressiveness

The European standard EN 206 (Concrete - Specification, performance, production and conformity) specifies that the structural designer should study the local environment where the construction will take place characterizing it qualitatively and quantitatively, relating it to potential typologies structural deterioration (classified according to the intensity of the damage action), and making it a key task for the designer even before choosing the type of concrete and the structure design.

Table 3.04: Exposure classes (UNI 11104:2004 - Italian standard. Harmonized with the European standard EN 206)

Class designation	Class description	Informative examples applicable in Italy
1 No risk of corrosion or attack (X0 class)		
X0	For concrete without reinforcement or embedded metal: all exposures except where there is freeze-thaw, abrasion or chemical attack For concrete with reinforcement or embedded metal: very dry	Inside of buildings with very low air humidity. Unreinforced concrete surfaces inside structures. Unreinforced concrete buried in non-aggressive soil. Unreinforced concrete submerged in non-aggressive water. Unreinforced concrete surfaces in cyclic wet and dry, in conditions not subject to abrasion, freezing or chemical attack.
2 Corrosion induced by carbonation		
Note: The moisture condition relates to that in the concrete cover to reinforcement or other embedded metal, but in many cases, conditions in the concrete cover can be taken as reflecting that in the surrounding environment. In these cases classification of		

the surrounding environment may be adequate. This may not be the case if there is a barrier between the concrete and its environment.		
XC1	Dry or permanently wet	Concrete inside buildings with low air humidity. Ordinary reinforced concrete or pre-stressed concrete with surfaces within structures with the exception of parts exposed to condensation, or immersed in water.
XC2	Wet, rarely dry	Concrete surfaces subject to long-term water Contact, many foundations. Ordinary reinforced concrete or pre-stressed prevalently set in water or not aggressive terrain.
XC3	Moderate humidity	Ordinary reinforced concrete or pre-stressed outdoors on exterior surfaces sheltered from the rain, or in indoor with humidity moderate to high.
XC4	Cyclic wet and dry	Ordinary reinforced concrete or pre-stressed outdoors on surfaces subject to alternating dry and wet. Exposed concrete in urban environment. Concrete surfaces subject to water contact, not within exposure Class XC2.
3 Corrosion induced by chlorides other than from sea water		
XD1	Moderate humidity	Ordinary reinforced concrete or pre-stressed on the surface or parts of bridges and viaducts exposed to water spray

		containing chlorides.
XD2	Wet, rarely dry	Ordinary reinforced concrete or pre-stressed structural elements totally immersed in water (e.g. swimming pools) and industrial environment containing chlorides.
XD3	Cyclic wet and dry	Ordinary reinforced concrete or pre-stressed, structural elements directly subject to the de-icing agents or spray containing de-icing agents. ordinary reinforced concrete or pre-stressed elements with a surface immersed in water containing chlorides and the other surface exposed to air. Parts of bridges exposed to spray containing Chlorides, pavements and car park slabs.
4 Corrosion induced by chlorides from sea water		
XS1	Exposed to airborne salt but not in direct contact with sea water	Ordinary reinforced concrete or pre-stressed structural elements on the coasts or in proximity.
XS2	Permanently submerged	Ordinary reinforced concrete or pre-stressed marine structures completely immersed in water.
XS3	Tidal, splash and spray zones	Ordinary reinforced concrete or pre-stressed structural elements exposed to the shoreline or areas subject to the splashes and waves of the sea.
5 Freeze/thaw attack with or without de-icing agents		

XF1	Moderate water saturation, without de-icing agent	Vertical concrete surfaces exposed to rain and Freezing. No vertical surfaces and not subject to the full saturation but exposed to freezing, rain or water.
XF2	Moderate water saturation, with de-icing agent	Vertical concrete surfaces of road structures exposed to freezing and airborne de-icing agents
XF3	High water saturation, without de-icing agent	Horizontal concrete surfaces exposed to rain and freezing
XF4	High water saturation, with de-icing agent or sea water	Horizontal surfaces such as roads or pavements exposed to freezing and de-icing salts, directly or indirectly, elements exposed to freezing and prone to frequent wetting in the presence of de-icing agents or sea water.
6 Chemical attack		
XA1	Slightly aggressive chemical environment according to Table 2 of the UNI EN 206-1	Containers of sludge and settling tanks. Containers and tanks for waste water.
XA2	Moderately aggressive chemical environment according to Table 2 of the UNI EN 206-1	Structural elements or walls in contact with aggressive soils.
XA3	Highly aggressive chemical	Structural elements or walls in contact with highly aggressive industrial water.

	environment according to Table 2 of the UNI EN 206-1	Containers of fodder, animal feed and slurry coming from breeding animal. Cooling towers of industrial fumes and exhaust gas.

UNI-EN 206 presents for each environmental exposure class of the structure, a prescription in terms of limits that must be respected in the concrete properties so that the structure durability requirements are met. As the maximum water-cement ratio, the minimum amount of cement per cubic meter of conglomerate and the minimum characteristic strength (Table 3.05).

Table 3.05: Exposure classes (UNI 11104:2004 - Italian standard. Harmonized with the European standard EN 206)

	Exposure classes																
	No risk of corrosion or attack	Corrosion induced by carbonation				Corrosion induced by chlorides						Freeze/thaw attack with or without de-icing agents				Chemical attack		
						Chlorides from sea water			Chlorides other than from sea water									
	X0	XC1	XC2	XC3	XC4	XS1	XS2	XS3	XD1	XD2	XD3	XF1	XF2	XF3	XF4	XA1	XA2	XA3
Maximum w/c ratio	-	0.60		0.55	0.50	0.50	0.45		0.55	0.50	0.45	0.50	0.50		0.45	0.55	0.50	0.45
Minimum strength class	C12/15	C25/30		C28/35	C32/40	C32/40	C35/45		C28/35	C32/40	C35/45	C32/40	C25/30		C28/35	C28/35	C32/40	C35/45
Minimum cement content (kg/m³)	-	300		320	340	340	360		320	340	360	320	340		360	320	340	360
Minimum air content													3.0					
Other requirements												Aggregates conforming to EN 12620 of adequate resistance to freeze / thaw				It required the use of cements resistant to sulphates		

3.4 Considerations on the durability of reinforced concrete structures

Concept and definition of structural durability

It is understood by structural durability the ability of a structure to resist in time (for the period to which it was designed) and retain its physical and mechanical properties throughout its service life, defined at the beginning of the design process[1]. The structure's durability mainly depends on the quality of concrete with respect to the materials that compose it, its mechanical characteristics, dimensions of concrete cover and its porosity[2] (or void index).

The Italian standard NTC 2008 in Chapter 2, on safety and expected performance, defines durability of the structure as the conservation of the physical and mechanical characteristics of materials and structures, in a way that safety levels are maintained throughout the life of a building. Durability must be ensured through proper choice of materials and the correct dimensioning of the structures including possible measures for protection and maintenance.

Brazilian standard for durability of RC structures

The Brazilian standard procedure for concrete structures design (ABNT NBR 6118) establishes the basic requirements and some criteria aiming the durability of the structure, like the concrete's physical and chemical characteristics, dosage and strength, as well as dimensions and the quality of the reinforcement cover. The Brazilian standard also opens up alternatives for the designer to work with data from performance tests of the structure's durability in relation to the type and

[1] In Brazil, environmental aggressiveness classes are defined by the author of the structural design and the contractor.

[2] The porosity of the concrete is a factor that influences the durability of the structure. The leading causes of reinforcement corrosion, such as carbon dioxide (CO_2) and chloride ions (Cl^-), penetrate more easily when the void index of the concrete is relatively high. To protect the armatures is necessary to control the entry of aggressive agents and also moisture (presence of water), which is an agent that participates in the process of concrete deterioration.

intensity of environmental aggression to establish the minimum standards to be achieved.

According to NBR 6118:2014, concrete structures must be designed and constructed in a way, under the environmental conditions laid down at the design project and when used as recommended in, they maintain their security, stability and serviceability during the period corresponding to its service life. The Brazilian standard means by service life, the period of time during which the characteristics of concrete structures are maintained without significant intervention, provided that they met the use and maintenance requirements prescribed by the designer and the builder, as well as considering the implementation of necessary repairs and accidental damage.

Expected service life according Italian and Brazilian standards

The Italian standard NTC 2008 understands as the service life (nominal life) of a structure, the number of years in which, it can be used for the purpose for which it was intended, provided that ordinary maintenance is made. The nominal life is specified in the design and is classified according to the following table:

Table 3.06: Service life (nominal life) for various types of structures (NTC 2008 – Italian standard)

	Construction type	**Nominal life V_N (in years)**
1	Temporary works; provisional works; structures during construction	$\leq$ 10
2	Ordinary works; bridges; infrastructure works and small dams or normal importance	$\geq$ 50
3	Great works; bridges; infrastructure works and dams of great dimensions or strategic importance	$\geq$ 100

In Brazil, design service life values for reinforced concrete structures are determined by the performance standard for residential buildings NBR 15575:2013. According to the standard, the main structure and elements that are part of the structural system, committed to the security and overall stability of the building must be designed and constructed in a way that, under the environmental conditions laid down, when used as recommended in design and submitted to the periodic interventions of maintenance and conservation, they maintain their functional capacity during all their service life. Given that the design must specify the expected service life for the structure and the absence of service life indication in design, it is assumed that the values adopted correspond to those in the table below[1]:

Table 3.07: Service life for the corresponding performance levels (ABNT NBR 15575:2013 – Brazilian standard)

Part of the construction	Structural elements	Service life for design (in years)		
		Minimum	Intermediate	Superior
Main structure	Foundations, columns, beams, slabs, structural walls, peripheral structures, retaining walls and other structural elements.	$\geq$ 50	$\geq$ 63	$\geq$ 75

The service life criteria, classified as "minimum, intermediate and superior," cited in the table above are related to performance levels that must be met, according to the agreed values between the designer and the contractor at the beginning of the design project. The standard ABNT NBR 15575:2013 sets as obligatory the

[1] The standard procedure for structural design (NBR 6118: 2014) specifies no service life values.

fulfillment of a minimum performance level, corresponding to 50 years, and as optional the fulfillment of the other performance levels.

The concept of service life or nominal life applies to the structure as a whole or its parts, thus certain parts of the structures can receive special considerations on the value of service life. As well as localized structural rehabilitation interventions can receive different treatment in relation to the entire existing structure, adapting to the current standards and aiming a greater durability of the recovered element.

3.5 Deterioration mechanisms of the structures

When reinforced concrete structures are in service, they can be considered, at the beginning, fissured[1]. Proper use of the reinforcement, in the amount, diameter and distribution, contribute to a better crack distribution and smaller openings, but does not eliminate the appearing of cracks. However, the concrete is subject to natural deterioration by physical and chemical attacks, which can reduce the load-bearing capacity of the structural elements, as a consequence of various mechanisms of reinforced concrete deterioration.

In general, the durability of concrete structures depends on the durability of concrete and steel materials (especially of the concrete cover). The bulletin fib 59 (Part II: Procedures for condition assessment) provides a useful identification model of structural damage, classifying the deterioration mechanisms that affect the durability of steel and concrete, as follows:

[1] The standards limit the size of crack openings in reinforced concrete structures, which are calculated and provided in the structural design.

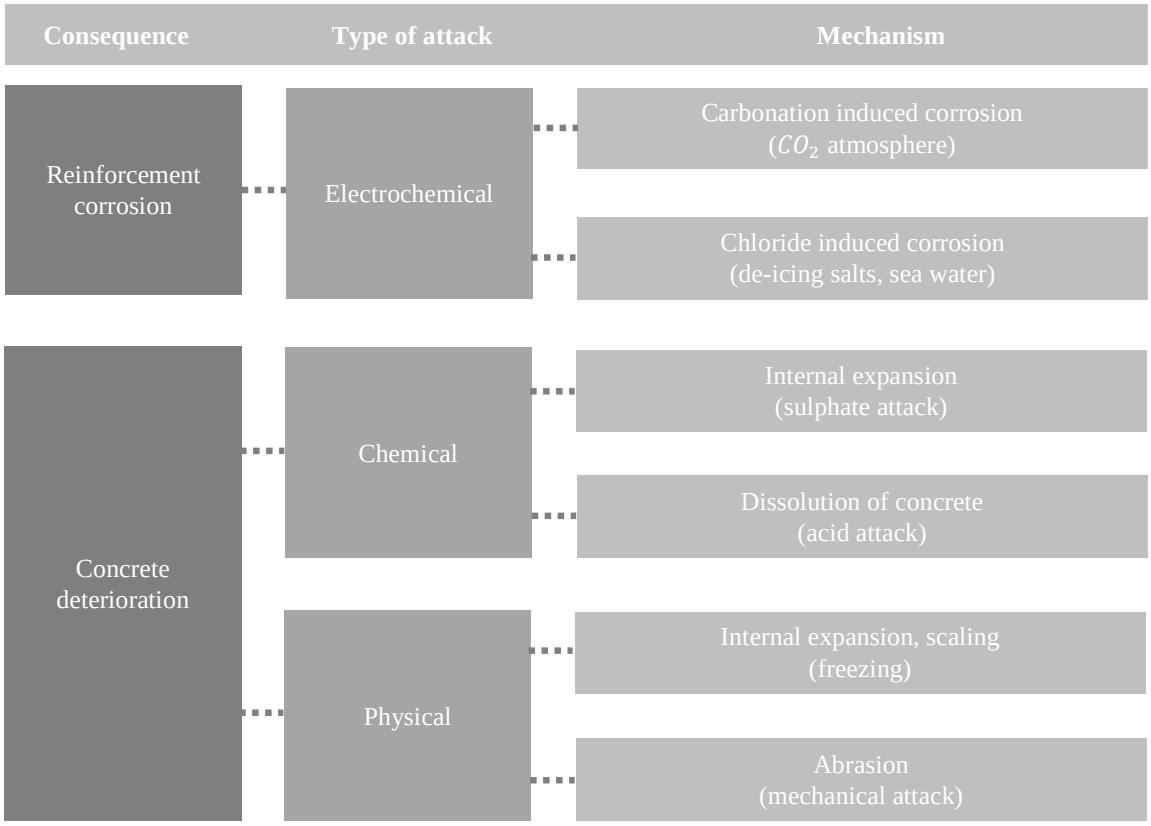

Figure 3.03 Deterioration mechanisms and consequences for reinforced concrete structures

3.6 Main causes of RC structures' deterioration in Brazil

In Brazil, reinforcement corrosion is one of the major causes of reinforced concrete structures' deterioration, not only in buildings but also in industrial works, infrastructure works and monuments. Corrosion may be defined as an electrochemical process that occurs in the steel reinforcement because of the reaction thereof with certain chemical components present in the environment in which it is inserted, causing a spontaneous natural process that occurs with greater or lesser velocity and greater or lesser intensity, depending on the environmental

aggressiveness level. Both carbonation-induced and chloride-induced corrosion are the main mechanisms of reinforcement corrosion on the Brazilian buildings[1].

A study by Andrade and Dal Molin (1997)[2], about the main manifestations of structural damage of 189 buildings located in the State of Pernambuco[3], shows that 64% of the structures presented deterioration problems caused by corrosion of reinforcement (Fig. 3.04).

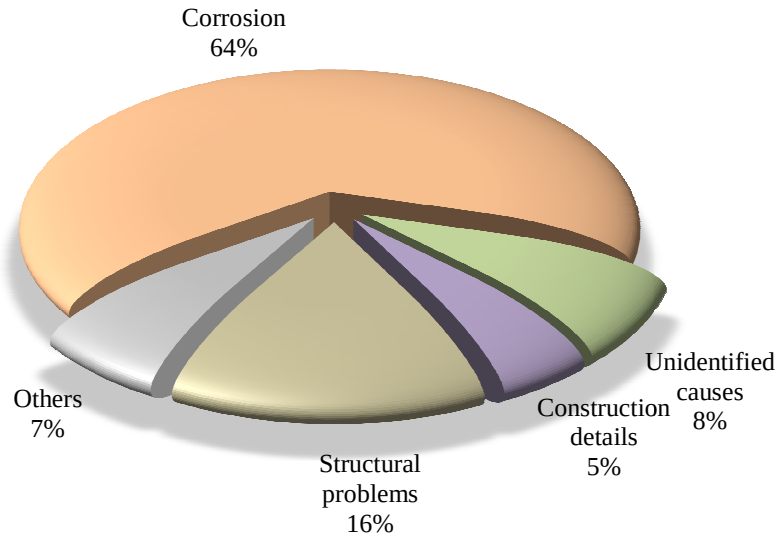

Figure 3.04 Main causes of damage to RC structures
in the State of Pernambuco

[1] The effects of reinforcement corrosion can also induce a phenomenon called hydrogen embrittlement, which may cause a brittle fracture on the bar.

[2] Durability of reinforced concrete structures: Analysis of the structure deterioration in Pernambuco State. By Andrade and Dal Molin, 1997. Data available in < http://www.lume.ufrgs.br/bitstream/handle/10183/122441/000215709.pdf?sequence=1 > accessed in August 17, 2016.

[3] The State of Pernambuco is located in a region of Brazil considered high environmental aggression. According to Brazilian Standard (ABNT NBR 6118) its capital (Recife) is classified as an area of great risk of structural deterioration.

Another study made by De Oliveira A. and De Suoza V.[1], on the types of reinforced concrete structures' deterioration of 541 buildings located in the city of Rio de Janeiro (using data from the municipal archive of the Department of Urban Planning of the Municipality of Rio de Janeiro), shows that 49% of the structures presented deterioration caused by reinforcement corrosion [2] (Fig. 3.05).

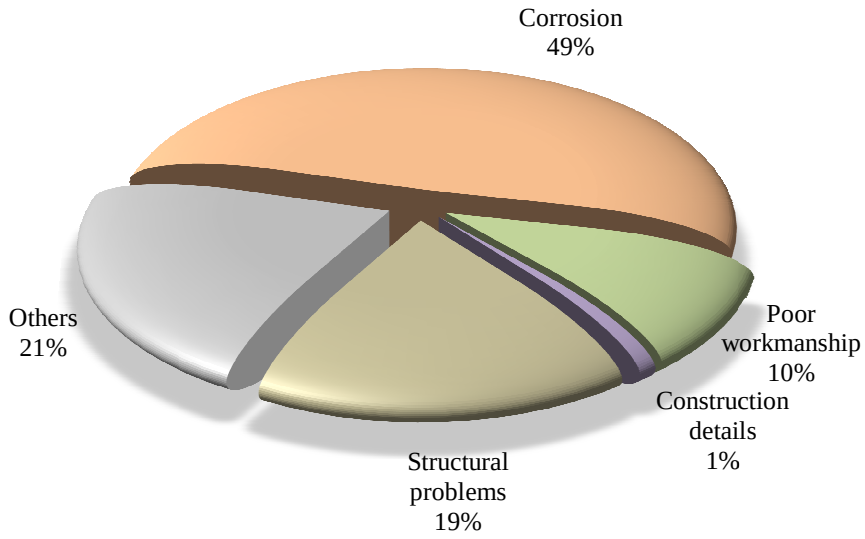

Figure 3.05 Main causes of damage to RC structures
in the city of Rio de Janeiro

The figures below show some examples of structures that present corrosion in the reinforcement, located in the center of the city of Rio de Janeiro[3].

[1] Influence of the micro-climates of Rio de Janeiro on the development of pathological processes in reinforced concrete. Rev. Int. de Desastres Naturales, Accidentes e Infraestructura Civil. Vol. 3. Data available in < http://academic.uprm.edu/laccei/index.php/RIDNAIC/article/viewFile/65/65 > accessed in August 16, 2016.

[2] Among the structures with the presence of reinforcement corrosion, 1.29% were caused by carbonation of concrete.

[3] Photographs were taken in July and August 2014, during the PhD study mission in Rio de Janeiro.

Figure 3.06 Deterioration of the slab of the 1st floor. Reinforcement corrosion and concrete spalling likely caused by chloride attack. Heritage building belonging to Monastery of *São Bento*, located in marine environment, in the center of Rio de Janeiro (photographs taken in July 2014)

Figure 3.07 Deterioration of the columns of the *Rua do Passeio* building, built in the 30s in the center of Rio de Janeiro. Concrete spalling and reinforcement corrosion likely caused by chloride attack. Extreme case of deterioration with breaking of longitudinal and transverse bars of the external columns (photographs taken in July 2014)

Figure 3.08 Steel corrosion and concrete spalling of columns and beams likely caused by carbonation of concrete (most likely occasioned by having a small layer of concrete cover for reinforcement). *Rua Nilo Peçanha* building, built in the 50s in the center of Rio de Janeiro (photographs taken in July 2014)

Figure 3.09 Structural deterioration of the ground floor and roof floor. Concrete spalling and steel corrosion with cross-section loss of the transverse and longitudinal reinforcement, likely caused by chloride attack. *A Noite* building, built in 1929, located in the marine environment, in the center of Rio de Janeiro (photographs taken in July 2014)

Figure 3.10 Extreme case of deterioration of the *Ouro Branco* building, built in 1935, in the center of São Paulo. Steel corrosion and concrete spalling caused by carbonation of concrete, with cross-section loss of reinforcement (photographs taken in January 2014)

A study by Silva, Luiza K. and Cabral, Antonio E. B. (2011)[1], about the main manifestations of structural damage of 30 buildings located in the State of Ceará, shows that 96,7% of the structures presented deterioration problems caused by corrosion of the reinforcement.

[1] XV National Meeting of the Built Environment Technology. ENTAC 2014. Maceió-Brazil. Survey of pathological manifestations in reinforced concrete structures in the State of Ceará.

The figure below shows the advanced state of deterioration of the structure of a building out of use, located in the city of Fortaleza, capital of Ceará State.

Figure 3.11 Structure in terminal state of deterioration caused by chloride attack. Extreme case of steel corrosion and concrete disintegration. Building located in the marine environment in Fortaleza city (photographs taken in May 2015)

3.7 The reinforcement corrosion

Corrosion is considered the main type of steel deterioration of the RC structures, which can cause a substantial reduction in the load-bearing capacity of the elements, consequently compromising the structural safety. The degenerative effects of reinforcement corrosion may manifest in the form of surface blemishes, cracks and detachment (spalling) of the concrete cover [1], loss of bond and reduction of reinforcement cross-section (Fig. 3.12), resulting in reducing of steel strength[2].

[1] The corroded steel produces expansive agents and can increase volume (typically 4 to 5 times), producing reactions that can cause the detachment of the concrete cover.

[2] Residual capacity of corroded reinforcing bars. Magazine of Concrete Research, 2005, 57, N. 3, April, 135-147.

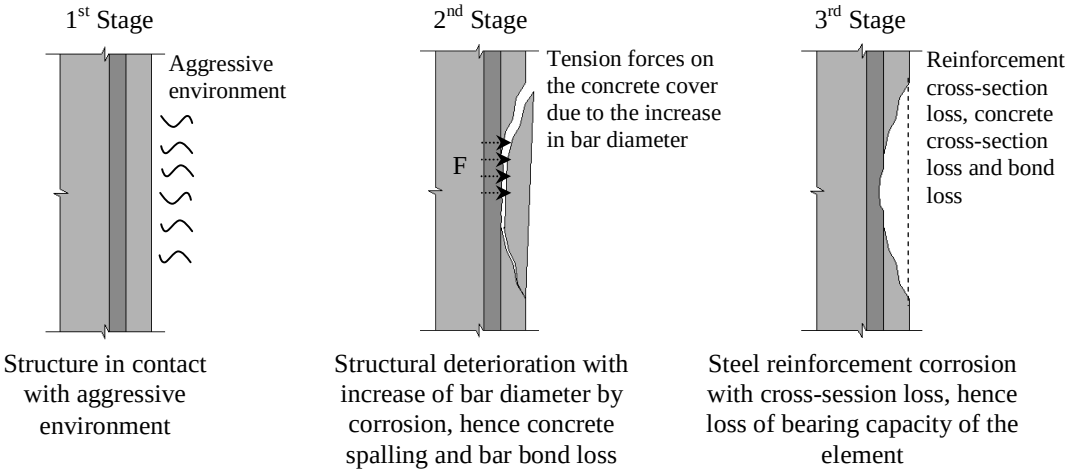

Figure 3.12 General representation of corrosion effects in reinforced concrete structures

Corrosion process

Corrosion is an electrochemical reaction that occurs at the contact surface between the steel reinforcement and the corrosive environment, in this case, the concrete. Metals are produced from ores (e.g. iron ore) existing in nature and this production process consumes energy, so it is natural that the metal alloys when exposed to their environments, reverting to its natural state of lower energy, and donating electrons that are received by oxidizing substance present in its environment. The speed with which this returns to the lower energy state (corrosion) can be known, as well as the progress of corrosion of steel over time[1] can be estimated.

The beginning of the corrosion process occurs after the steel depassivation and is accompanied by a dramatic change in the electrochemical potential at the local anode which may shift to negative (active) values, resulting in a potential difference between anodic and the adjacent passive cathodic surfaces. Anodes and cathodes are usually electrically connected enabling an unhindered transport of the free

[1] This issue is dealt in detail in Chapter IV.

electrons to the cathodes areas. This process causes the decreasing of the steel diameter in the anodic area (Fig. 3.13).

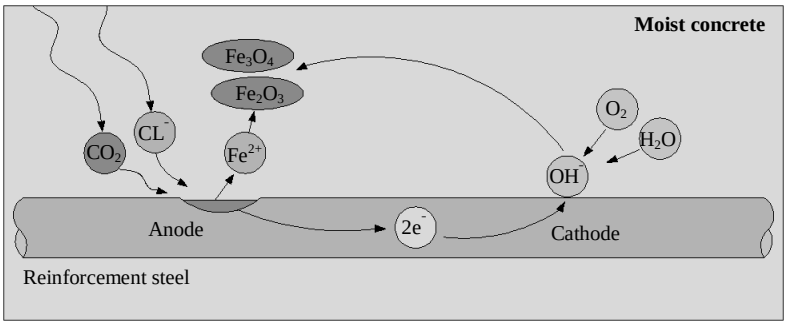

Figure 3.13 Representation of reinforcement corrosion in concrete
(adapted from *fib* Bulletin 59)

3.7.1 Carbonation-induced corrosion

The carbonation of concrete is one of the main causes of reinforcement corrosion, which affects practically all buildings in reinforced concrete exposed to aggressive agents present in the atmosphere, such as carbon dioxide. Carbonation causes no reduction in mechanical characteristics of the concrete, but causes the concrete to lose its ability to maintain the potential of hydrogen in alkaline environment, taking the passivity of the reinforcement surface.

The steel bars of the reinforced concrete structures are in principle protected and passivated against corrosion. This protection is provided by the concrete cover, which forms a physical barrier that prevents the entry of external agents, and especially by a chemical protection provided by the alkalinity of the aqueous solution present in the concrete. This alkaline solution is based on calcium hydroxide, sodium and potassium and have, substantially a pH generally comprised between 13.0 and 13.8[1]. In this environment a reaction between hydroxides (OH^-) and iron ions forms a thin iron oxide layer on the surface of the

[1] La corrosione nel calcestruzzo – Fenomenologia, prevenzione, diagnosi, rimedi. AICAP, Roma - 2006.

steel. When the alkalinity of the concrete is neutralized by CO_2 carbon dioxide[1] present in the atmosphere and a high relatively humidity is present, this alkaline solution reacts by reducing the pH of concrete to values below 9.0[2]. This reaction process is called concrete carbonation (starting from the external face, figure 3.14), which can be written globally using the formula:

$$Ca(OH)_2 + CO_2 \rightarrow CaCO_3 + H_2 \qquad (3.01)$$

When the concrete is carbonated, this so-called passive layer can be destroyed and reinforcement corrosion process can occur.

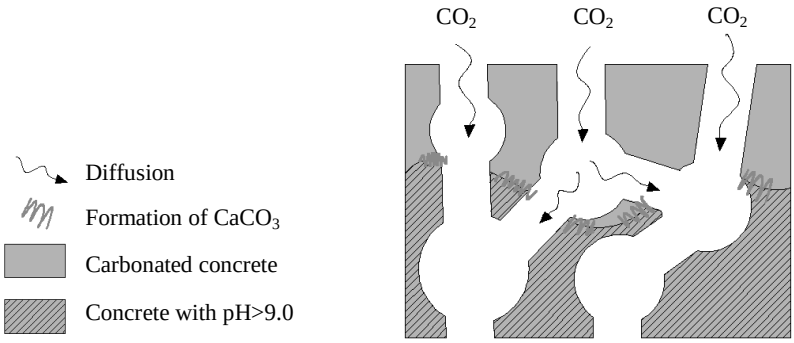

Figure 3.14 Representation of the concrete carbonation process.
Carbon dioxide diffuses through the pore system of the concrete and finally forms calcium carbonate (Tuutti model, adapted from *fib* Bulletin 59)

3.7.2 Chloride-induced corrosion

The contact of the structures with chloride-containing environments (e.g. marine environment) is also a frequent cause of reinforcement corrosion. Chloride ions can penetrate the concrete until they reach the reinforcement, locally drilling the

[1] Other acidic substances in the atmosphere can neutralize the alkalinity of concrete, but their actions are insignificant compared to carbon dioxide.

[2] At these pH values the oxide film (present on the bar surface) and also the conditions of liabilities are destroyed.

protective layer passivation, if its content exceeds a critical limit between 0.4 and 1.0%[1] by mass in relation to the amount of cement (for a chloride content of less than 0.4%, the risk of reinforcement corrosion can be contemptible, provided that there is no presence of carbonation in concrete). And since the surface of the reinforcement loses the passivity condition, with the presence of water and oxygen, the corrosion process starts.

The required time for the chloride content to reach the critical value, known as initiation period, depends on the characteristics of the cement matrix, the thickness of the concrete cover and the concentration of chlorides in the outer surface of the concrete. The transport of chloride through the concrete can occur by mechanisms of capillary absorption, diffusion, permeation and migration, depending on the exposure conditions of the structure.

3.8 References

1. ABNT NBR 6118:2014 (Brazilian standard). Design of concrete structures – Procedure.
2. ABNT NBR 15575:2013 (Brazilian standard). Performance standard for residential buildings.
3. Andrade, Jairo J. O. and Dal Molin. Durability of reinforced concrete structures: Analysis of the structure deterioration in Pernambuco State. Master´s Thesis, 1997.
4. De Oliveira, Armando and De Suoza, Vicente C.M. Influence of the micro-climates of Rio de Janeiro on the development of pathological processes in reinforced concrete. Rev. Int. de Desastres Naturales, Accidentes e Infraestructura Civil. Vol. 3.
5. Fib Model Code for Concrete Structures 2010. Fib, Fédération internationale du béton / International Federation for Structural Concrete, 2013.

[1] Pedeferri P., Bertolini L., et al. “La corrosione nel calcestruzzo – Fenomenologia, prevenzione, diagnosi, rimedi”, AICAP, Roma - 2006.

6. Fib Bulletin 59, Condition control and assessment of reinforced concrete structures. Fib Fédération internationale du béton / International Federation for Structural Concrete, May 2011.
7. Fib Bulletin 34, Model code for service life design. Fib Fédération internationale du béton / International Federation for Structural Concrete, February 2006.
8. Gerdau. Principles of protection of metal structures in situations of corrosion and fire. Sixth edition, 2015.
9. Mota, J.M. de Freitas et al. Assessment of contamination by chloride ions in concrete samples subjected to aggressive conditions. VI Congresso Internacional sobre Patología y Recuperación de Estructuras - Cinpar, July 2010.
10. Mota J. M. F., Pontes R. B., et al. Analysis of the pathologies in concrete structures in coastal town Recife-PE. X Latin American Congress of Pathology and XII Congress of Quality in Construction. CONPAT 2009. Valparaíso, Chile.
11. NTC 2008, Norme Tecniche per le Costruzioni, Decreto Ministeriale 14 gennaio 2008, Italia.
12. Pedeferri P.; Bertolini L.; Biondini F.; Bontempi F.; Collepardi M.; Fratesi R.; Giordano L., “La corrosione nel calcestruzzo – Fenomenologia, prevenzione, diagnosi, rimedi”, AICAP, Roma - 2006.
13. World Corrosion Organization. George F. Hays, PE. “Now is the Time”. Available in < http://corrosion.org/wco_media/nowisthetime.pdf >, accessed in May 26, 2016.
14. UNI 11104 (Italian standard). Calcestruzzo Specificazione, prestazione, produzione e conformità Istruzioni complementari per l’applicazione della EN 206-1.
15. UNI EN 206-1 (European standard). Concrete - Part 1: Specification, performance, production and conformity.

16. Silva, Luiza Kilvia da; Cabral, Antonio Eduardo Bezerra. Survey of pathological manifestations in reinforced concrete structures in the State of Ceará. XV National Meeting of the Built Environment Technology. ENTAC 2014. Maceió, Brazil.
17. Tuutti, K. Corrosion of steel in concrete. Swedish Cement and Concrete Research Institute. Stockholm, 1982.

Chapter IV

Structural safety assessment for heritage RC buildings that present deterioration

Scope

Besides to dealing with evaluation models of the structural performance of elements damaged by corrosion, this chapter also provide additional considerations on assessment of heritage RC structures that present deterioration, based on the premise that a structure may have cultural and heritage value[1] in itself.

Assessment of heritage structures is in many aspects different from the evaluation of common structures, because concerns basically its mechanical performance (familiar to structural engineers) and its value as a cultural resource. These aspects could be dealt together in decisions involving possible rehabilitation interventions.

Reference standards for heritage structures

Currently, in Europe there is a lack of standards for assessment of heritage RC structures[2]. General principles and methodologies for assessment of heritage structures were introduced by international standard ISO 13822:2010 on

[1] The value of a structure could be explained through the aspects that it represents of a culture, its place and its time.

[2] These should be consistent with the Eurocodes.

assessment of existing structures and Italian rules “Guidelines for evaluating and mitigation of seismic risk to cultural heritage (1997)”.

4.1 General approach

Old structures have been designed in such a way that they could satisfy the requirements for safety and serviceability for a defined time period, and the difference between resistance and loads could satisfy prescribed demands regarding structural safety. This means that concrete structures are supposed to deteriorate over time and suffer a decrease in structural performance. If the structure deteriorates its bearing capacity reduces, whereas in the mean time the loading level may also increase considerably.

In order to be sure to make right decisions with regard to rehabilitation interventions, it should be possible to determinate the bearing capacity of the structure as accurately as possible. This requires knowledge about the RC structures deterioration mechanisms and models for assessing structural performance.

As seen in the previous chapter, carbonation-induced corrosion and chloride-induced corrosion are the main types of deterioration of reinforced concrete that may reduce the elements´ mechanical performance, consequently causing a decrease in the structural reliability.

4.2 Model proposal of assessment hierarchy for rehabilitation of deteriorated heritage structures

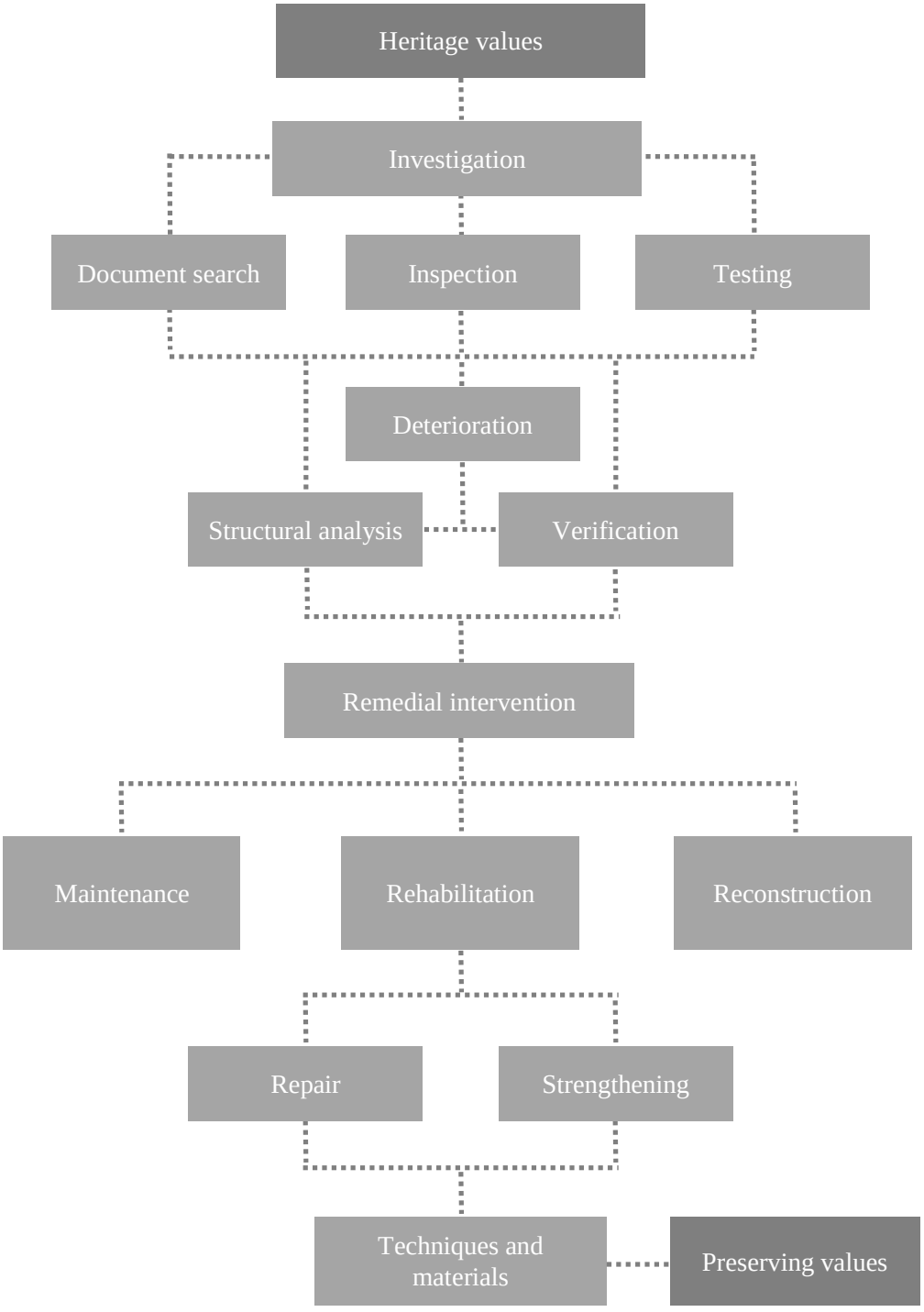

Figure 4.01 Model proposal of assessment hierarchy for the rehabilitation of deteriorated heritage structures

Terms and definitions

Deterioration: Physical disruption or change in the condition of a structure or its components, caused by external actions, such that some aspect of either the current or future performance of the structure or its components will be impaired.

Document search: Collection of all sources of existing information concerning designs, construction and service life of the structure. This refers to the original design documents and standards of the time, all relevant data with regard to the construction techniques and materials, construction records and service history.

Heritage values: Important aspects that a structure itself represents of a culture, its place and its time.

Investigation: Collection and evaluation of information through inspection, document search and testing[1].

Inspection: A primarily visual examination of a structure and its components with the objective of gathering information about their form, deterioration, service environment, and general circumstances to establish the current condition of the structure.

Maintenance: A set of planned activity performed during the service life of a structure, intended to either prevent or correct the effects of minor deterioration of the structure or its components, in order to keep their future serviceability at the level anticipated by the designer[2].

Reconstruction: Reinstating all or part of a structure or component that is in a change, defective or deteriorated state compared to its original or higher level of performance[3].

[1] Adapted from Basic for Assessment of Existing Structures. Milan Holický, Klokner Institute, Czech Technical University in Prague, Czech Republic. 2013.

[2] *fib* Model Code for Concrete Structures 2010.

[3] Adapted from *fib* Model Code for Concrete Structures 2010.

Rehabilitation: Intervention to restore the performance of a structure or its components that are in a changed, defective, degraded or deteriorated state to the original level of performance[2].

Remedial intervention: A conservation activity undertaken after a change in a material property (e.g. that is caused by the influence of carbonation or chlorides) has adversely affected the ability of the structure, or parts thereof, to meet the required performance levels because of deterioration[1].

Repair: Intervention taken to reinstate to an acceptable level the current and future performance of a structure or its components which are either defective, damaged or deteriorated, in order to keep their performance level at the level anticipated by the designer.

Strengthening: An intervention made to increase the strength (load resistance/load capacity) and/or possibly the stiffness of a structure and its components, and/or improve overall structural stability and/or the overall robustness of the structure to a performance level above that adopted by the designer[1].

Structural analysis: Determining the effects of actions on a structure, determining the causes of observed damage and irregular behaviour.

Structural assessment: Set of activities performed in order to verify the reliability of an existing structure for future[2].

Testing: Non-destructive and destructive tests to obtain information on the proprieties of the materials and eventual defects of the structure.

Verification: The establishment of a target level of structural performance for securing acceptable safety and reliability.

[1] *fib* Model Code for Concrete Structures 2010.

[2] Basic for Assessment of Existing Structures. Milan Holický, Klokner Institute, Czech Technical University in Prague, Czech Republic. 2013.

4.3 Condition assessment of deteriorated RC structures

As an integrative part of the current condition assessment of the structure, it is necessary to identify the deterioration mechanisms and its causes, to determinate the present degradation level, the material damage rate and the structural performance loss. It is also essential to use appropriate tools and models (including prediction models), based on information obtained from inspections/surveys and monitoring carried out, design and construction records, information upon previous interventions and the environmental conditions, in order to evaluate the structure real condition to make suitable decision on the rehabilitation intervention.

Deterioration model

Figure 4.02 shows the consequences of the main deterioration kinds in reinforced concrete structures, wherein the reinforcement corrosion acts as an intermediary agent that may cause performance loss of the structure and, in consequence, structural failure.

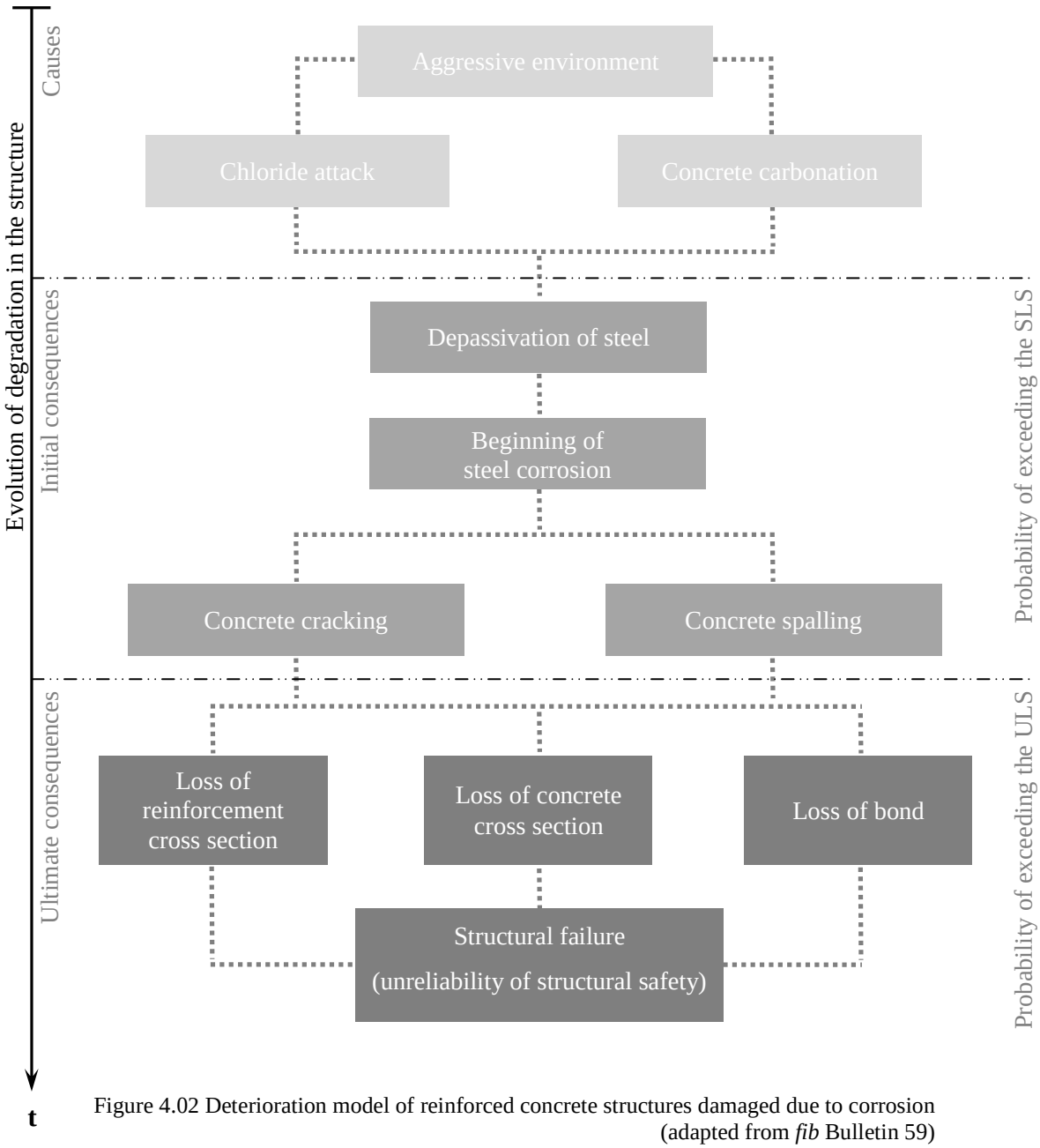

Figure 4.02 Deterioration model of reinforced concrete structures damaged due to corrosion (adapted from *fib* Bulletin 59)

4.3.1 Deterioration evolution

In the corrosion process the lifetime of reinforced concrete structures may be divided into two distinct periods: initiation period, which is produced phenomena that lead to loss of steel passivity condition (destruction of the protective film), and propagation period, which corresponds to the time from when the protective film is destroyed until reaching the maximum acceptable propagation (Fig. 4.03).

The propagation period by chloride-induced corrosion is reduced regarding the propagation period of the carbonation-induced corrosion. In the calculation of the lifetime of structures in contact with environment containing chlorides, the propagation period of corrosion may be neglected and considered equal to initiation period[1].

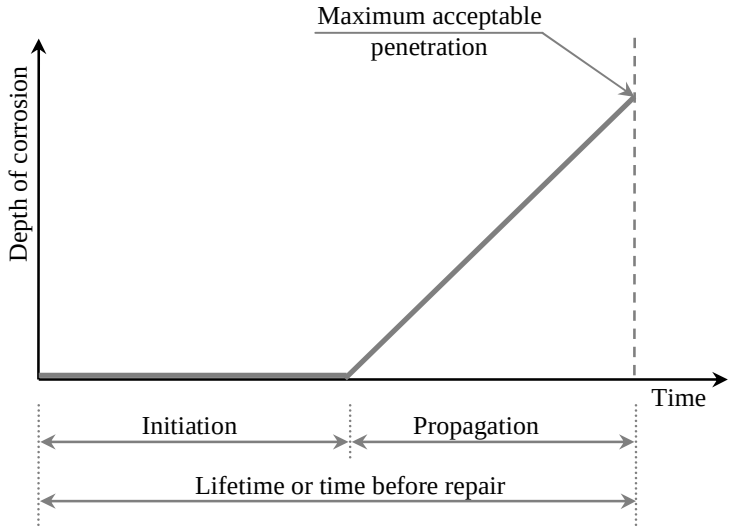

Figure 4.03 Initiation period and propagation period
of corrosion in RC structure (adapted from Tuutti model)

[1] Pedeferri P., Bertolini L., et al. "La corrosione nel calcestruzzo – Fenomenologia, prevenzione, diagnosi, rimedi", AICAP, Roma - 2006.

4.3.1.1 Limit states for reinforcement corrosion

A study by *fib Bulletin 59* presents specific conditions relating the limit states serviceability limit states (SLS) and ultimate limit states (ULS), according to *Euro Code 0 (Basis of structural design)* and the Tuutti model[1] for degree of damage in RC structures due corrosion. This study identifies four consecutive points of marked condition change during the reinforcement corrosion process.

The figure below shows the evolution of deterioration over time of a reinforced concrete structure subject to corrosion.

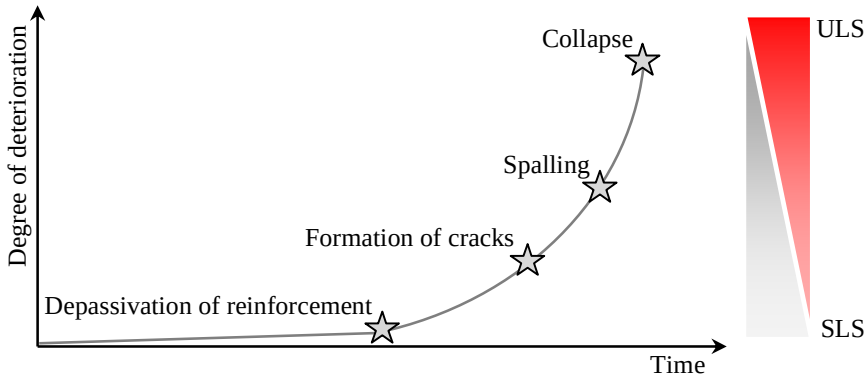

Figure 4.04 Damage of a reinforced concrete structure due to corrosion (adapted from *fib* Bulletin 59)

- Limit state of depassivation: rebar changes from non-corroding (passive) to corroding behaviour;
- Limit state of cracking: initial corrosion induced cracks reach the concrete surface and can be observed;
- Limit state of spalling: concrete cover spalls for the very first time;
- Limit state of collapse: the final point in time reached e.g. by loss of bond or rebar cross section.

[1] Corrosion of steel in concrete. Tuutti, K. Swedish Cement and Concrete Research Institute. Stockholm, 1982.

4.3.2 Evaluation of steel depassivation by carbonation

There are mathematical models which allow us to assess approximately the initiation period (depassivation of reinforcement) of the corrosive phenomena caused by carbonation and chlorides attack. This forecast is more accurate in the evaluations of existing structure[1] because basically depends on the characteristics of the concrete and the environment.

Full-probabilistic design models that meet the requirements for carbonation induced depassivation of steel for uncracked concrete are provided by research project DuraCrete[2]. In formula 4.01 diffusion of CO_2 is considered the dominant transport mechanism. The inverse carbonation resistance of the concrete $R_{ACC,0}^{-1}$ has been introduced as a decisive material parameter.

Therein the carbonation depth is calculated according to Equation below:

$$x_c(t) = \sqrt{2 \cdot k_e \cdot k_c \cdot (k_t \cdot R_{ACC,0}^{-1} + \varepsilon_t) \cdot C_s} \cdot \sqrt{t} \cdot W(t) \qquad (4.01)$$

$x_c(t)$: carbonation depth [m]

k_e: environmental function [-]

k_c: execution transfer parameter [-]

k_t: regression parameter (test method) [-]

$R_{ACC,0}^{-1}$: inverse effective carbonation resistance [(mm^2/year)/(kg/m^3)]

ε_t: error term [(mm^2/year)/(kg/m^3)]

C_s: CO_2 – concentration of the ambient environment [kg/m^3]

W(t): weather function [-]

t: time [year]

[1] This evaluation can also be made for new construction designs, but with a lower level of approach.

[2] Probabilistic performance based durability design of concrete structures. Statistical Quantification of the Variables in the Limit State Functions. DuraCrete. Report No.: BE 95-1347, pp. 62-63, 2000.

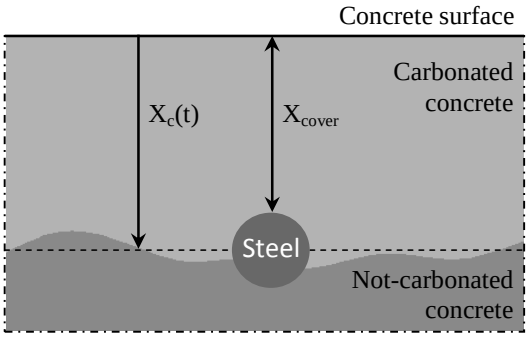

Figure 4.05 Depassivation due to carbonation [$X_c(t) \geq X_{cover}$]
(adapted from *fib* Bulletin 59)

The literature [1] contains some mathematical principles for describing the penetration of the carbonation front in concrete. The oldest theory is based on the square root principle, in formula 4.02. The penetration of carbonation in time follows a law of the type $s = K \cdot t^{\frac{1}{n}}$, where s is the thickness of the layer of carbonated concrete, t the time and K the carbonation coefficient that can be assumed to be a speed index of carbonation penetration. For most of the concretes, the exponent n is about 2, and so one obtains a progress of penetration of the carbonation of parabolic type:

$$s = K\sqrt{t} \qquad (4.02)$$

s: thickness of the layer of carbonated concrete [mm]
K: parameter that depends on concrete and environmental factors [mm/year$^{1/2}$]
t: time [years]

The parameter K depends on environmental factors (moisture, temperature, carbon dioxide content) and factors related to concrete (amount of cement, cement

[1] Corrosion of steel in concrete. Tuutti, K. Swedish Cement and Concrete Research Institute. Stockholm, 1982.

type, porosity). It may be constant or change over time, for example: in the different parts of the structure, protected area from rain and exposed area, when the structure is subjected to wet-dry phenomenon. In existing structures is possible to measure, in different parts of the structure, the penetration of carbonation and experimentally determine the coefficient K (known the age of the structure). In this case it is possible to predict the future progress of carbonation.

According to Pedeferri P., Bertolini L., et al.[1], K values measured in structures exposed to the atmosphere and protected from rain, in the maximum penetration conditions, indicatively vary from 2 to 15 mm/year$^{1/2}$:

- 2 < K < 5: for concrete with high compactness (concrete with low w/c ratio and well matured);
- 5 < K < 8: for concrete with medium compactness;
- K > 8: for low-quality concrete.

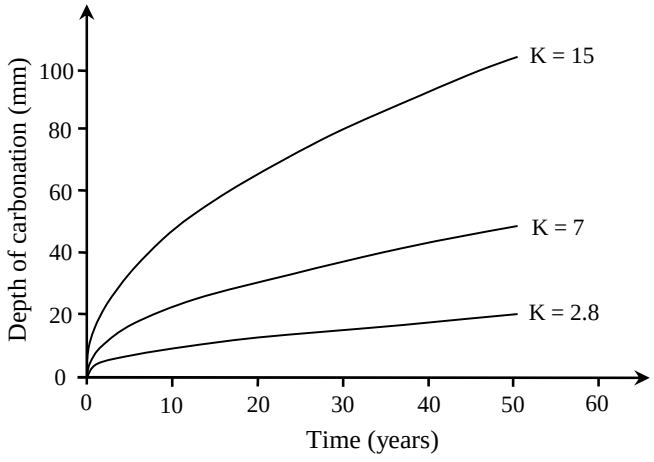

Figure 4.06 Depth of carbonation as a function of time and K[1]

[1] La corrosione nel calcestruzzo – Fenomenologia, prevenzione, diagnosi, rimedi. AICAP. Rome, 2006.

4.3.3 Evaluation of steel depassivation by chloride attack

Transport of chlorides in the concrete is produced by a combination of mechanisms. For example, in a structural element subject to wetting and drying cycles, capillary absorption of the solution is produced, in the wetted phase diffusion of chlorides in contact with water and accumulation of chloride after evaporation of the water.
The chloride ingress model is based on a solution of Fick's second law of diffusion[1] (Formula 4.03) assuming that *diffusion* is the dominant transport mechanism[2].

$$\frac{\partial C}{\partial t} = D\,\frac{\partial^2 C}{\partial x^2} \qquad (4.03)$$

C: total content of chlorides [wt.-%/cem.]
t: time [years]
D: parameter that indicates the chlorides diffusion speed [mm^2/year]
x: distance from the concrete surface [mm]

To quantify the transport of chlorides, through the concrete, by *capillary absorption* can be used a parameter called absorptivity (S). For approximation, the mass of liquid absorbed per unit area may be considered proportional to the square root of time:

$$i = S\sqrt{t} \qquad (4.04)$$

i: mass of liquid absorbed per unit area [g/mm^2]
S: parameter of absorptivity of the concrete [(g/mm^2)/year$^{1/2}$]
t: time [years]

[1] Campbell F.C. Elements of Metallurgy and Engineering Alloys. Fick's second law of diffusion, pg. 67. AMS International. USA, 2008.

[2] Penetration by diffusion occurs, for example, in structural elements operating in immersion in sea water.

The *permeation* is the penetration of a liquid due to a pressure difference. When the water enters in the saturated concrete to pressure, the flow through the pores may be defined by Darcy's law[1], written as:

$$\frac{dq}{dt} = \frac{K \cdot H \cdot A}{L} \tag{4.05}$$

$\frac{dq}{dt}$: water flow [m^3/s]
H: differential height of the water column [m]
K: permeability coefficient [m/s]
A: surface section [m^2]
L: thickness [m]

Both marine structures such as structures exposed to the action of other salts, show that even in presence of different diffusion penetration mechanisms are predicted with good approximation the chlorides concentration profiles over time using the equation of Fick[2]:

$$C(x,t) = C_s \left[1 - erf\left(\frac{x}{2 \cdot \sqrt{D_{ap} \cdot t}}\right)\right] \tag{4.06}$$

$C(x,t)$: chloride content at depth x and time t [wt.-%/cem.]
C_s: concentration of chlorides in the concrete surface [wt.-%/cem.]
D_{ap}: apparent diffusion coefficient [m^2/s]
x: depth of chlorides concentration [mm]
t: time [years]

[1] Introduction to Ground-Water Hydraulics - A programmed text for self-instruction. U.S. Geological Survey, Techniques of Water-Resources Investigations, Book 3, Chapter B2. By Gordon D. Bennett.

[2] La corrosione nel calcestruzzo – Fenomenologia, prevenzione, diagnosi, rimedi. AICAP. Rome, 2006.

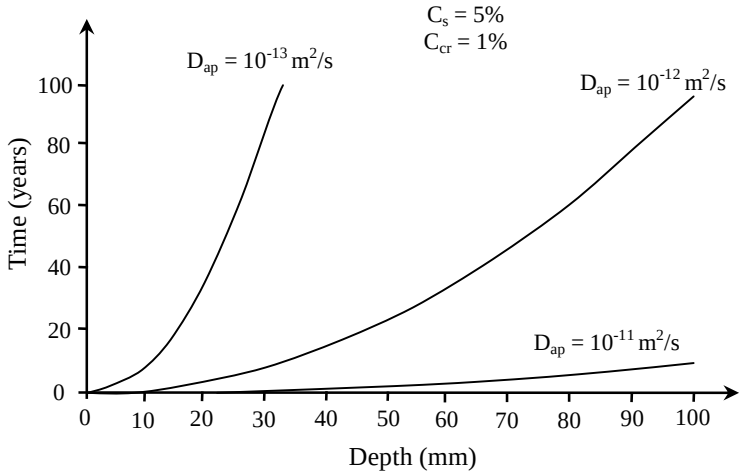

Figure 4.07 Initiation time at different depths in the concrete for several values of diffusion coefficient in the hypothesis of critical chloride content (C_{crit}) equal to 1% and surface concentration of 5% (adapted from *Corrosion in concrete*, *AICAP*)

A recent research by project DuraCrete[1] (funded by the European Union) has developed a full-probabilistic design approach for the modeling of chloride induced corrosion in uncracked concrete (Formula 4.07). In this model, the time and depth dependent chloride content are calculated according to Equation below:

$$C(x,t) = \left\{ C_0 + \left(C_{S,\Delta x} - C_0\right) \cdot \left[1 - erf\left(\frac{x - \Delta x}{2 \cdot \sqrt{K_e \cdot D_{RCM,0} \cdot K_t \cdot \left(\frac{t_0}{t}\right)^{age} \cdot t}} \right) \right] \right\} \qquad (4.07)$$

$C(x,t)$: chloride content at depth x and time t [wt.-%/cem.]

C_0: initial chloride content of concrete [wt.-%/cem.]

$C_{S,\Delta x}$: substitute surface chloride concentration at depth Δx [wt.-%/cem.]

x: depth with a corresponding content of chlorides $C(x,t)$ [mm]

Δx: thickness of the convection zone layer [mm]

K_e: factor for considering temperature impact on $D_{RCM,0}$ [-]

[1] Probabilistic performance based durability design of concrete structures. Statistical Quantification of the Variables in the Limit State Functions. DuraCrete. Report No.: BE 95-1347, pp. 62-63, 2000.

$D_{RCM,0}$: rapid chloride migration coefficient [mm^2/year]

K_t: transfer parameter (test method) [-]

t_0: reference testing time ($t_0 = 28d$) [year]

a_{ge}: ageing exponent [-]

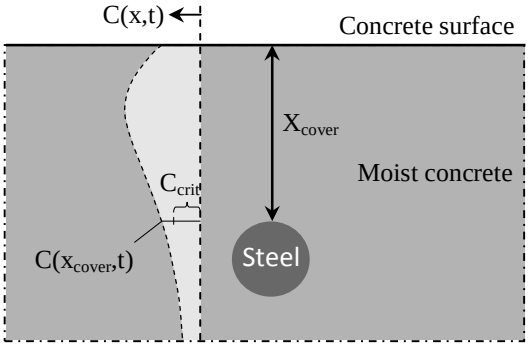

Figure 4.08 Depassivation due to chloride ingress [$C_{crit} \leq C(x_{cover},t)$]
(adapted from *fib* Bulletin 59)

4.3.4 Evaluation of reinforcement corrosion in concrete

4.3.4.1 Corrosion propagation

In the structures that the carbonation of the concrete has reached the reinforcement, depassivating it, corrosion propagates only in the presence of water and oxygen. For this reason, the corrosion propagation speed of the carbonated structures increases when the ambient humidity is high[1]. For example, in concrete saturation condition (wet concrete) it is possible to achieve a corrosion rate on the order of 100 μm/year, whereas the higher values found in most environmental conditions are included between 1 and 20 μm/year. When the ambient relative humidity is below 80%, the corrosion rate is reduced to values less of 1 μm/year.

The humidity of the environment also plays an important role in the case of structures exposed to atmospheres containing chlorides. For example, when the

[1] The corrosion propagation speed increases going from temperate to tropical climates.

located attack is started in structures with chloride content of 3% (relative to cement) and located in environments with relative humidity of 95%, the corrosion rate can pass to 1 mm/year[1]. In practice, in structures contaminated by chlorides and started corrosion process, it may take a short period to unacceptable reductions in the armor section occur.

The propagation of steel corrosion in concrete may be evaluated using the equation proposed by DuraCrete[2]:

$$X_{corr}(t) = \int_{t_{ini}}^{t} V_{corr}(t) \cdot dt \qquad (4.08)$$

$X_{corr}(t)$: loss of steel radius [cm]

$V_{corr}(t)$: degradation rate in radial direction [cm/year]

The loss of cross sectional area can be measured from corroded reinforcing bars in the critical points of a structure. Whereas the degradation rate can be calculated considering the Faradays first law of electrolysis with the mass of iron and its number of liberated electrons, expressed in Equation (4.09).

$$V_{corr} = 1.16 \cdot 10^{-3} \cdot i_{corr} \qquad (4.09)$$

i_{corr}: corrosion current density [μA/cm^2]

A correlation between corrosion rate and degradation of reinforcement cross section, following Faradays 1st law of electrolysis for a rebar with a diameter of 12 mm, is presented in *fib* Bulletin 59:

[1] La corrosione nel calcestruzzo – Fenomenologia, prevenzione, diagnosi, rimedi. AICAP. Rome, 2006.

[2] *fib* Bulletin 59: Condition control and assessment of reinforced concrete structures, 2011.

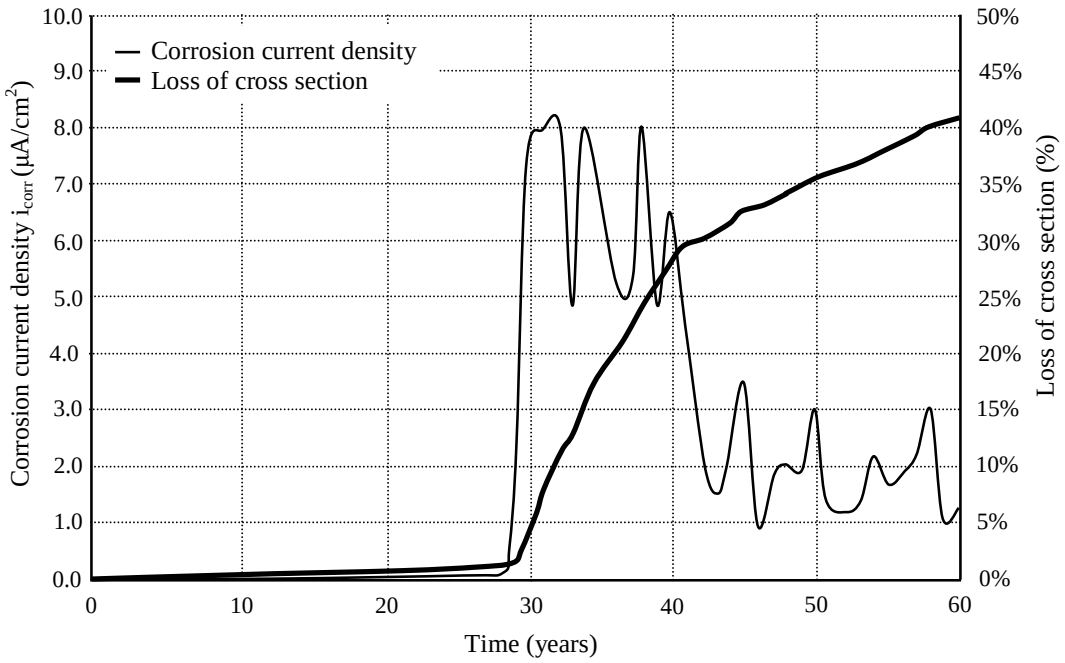

Figure 4.09 Correlation between corrosion rate and degradation of reinforcement cross section (adapted from *fib* Bulletin 59)

It is possible to observe in the graph above that after finishing construction, the mean corrosion current density nearly equals zero and increases when the reinforcement depassivates, after 29 years. Once the corrosion is activated (propagation period) steel starts to lose its cross section.

4.3.4.2 Residual capacity of corroded reinforcing bars

As seen in 4.3.1.1 (Limit states of reinforcement corrosion), the propagation of the steel corrosion can cause various damages to the structure, since the formation of cracks and detachment of concrete until the loss of bars cross-section and therefore over time, to collapse. *Fib* Bulletin 34[1] proposes evaluation models of overcoming forecast of the limit states SLS and ULS, corresponding to the initiation period and propagation period of the corrosion where it is possible to know an

[1] *fib* Bulletin 34. Model code for service life design, 2006.

approximate way the duration of each event listed above. However, the study presented in this thesis is delimited to the loss evaluation of physical and mechanical properties of the reinforcement, which proportionally leads to structural performance loss (ability to resist the actions to which the structure was designed).
The loss of reinforcement cross-section ultimately affects the structural reliability in areas where there is a high and concentrated tensile stress, leading to the last in the series of limit states, the limit state of collapse of the structure. So that the limit state of collapse (Fig. 4.04) is not exceeded, it is necessary that the following condition is met:

$$D_o - X_{corr}(t) \geq D_n \tag{4.10}$$

D_o: original rebar diameter [cm]
D_n: rebar diameter needed for load bearing [cm]
$X_{corr}(t)$: loss of steel radius [cm]

The limit state is reached when the remaining reinforcement cross-section falls below a critical cross-section needed for load bearing. To know the current condition of structural performance is necessary to resort to structural software using FEM (finite element method) models, which are able to analyze the non-linear behaviour of the structure.

Reduction of resistance capacity in corroded reinforcing bars

The steel being a ductile material has a typical plastic behaviour after reaching the yield stress. The reduction of steel resistance capacity is one of the most significant mechanical effects caused by corrosion phenomena in the reinforcing bars.
Experimental analyses on corroded steel bars with local attack penetration show that reduced areas can present relevant stress concentrations and decrease of the

residual forces of corroded reinforcement. Under plain strain distribution hypothesis, the Equation 4.11 gives a simplified expression describing the stress concentration in the reduced area of a corroded steel bar[1].

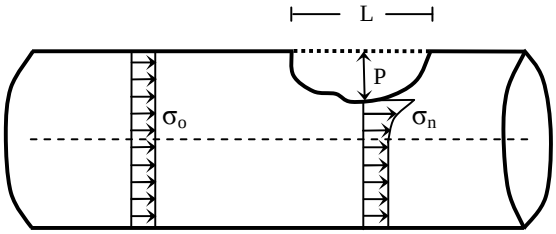

Figure 4.10 Local attack penetration and stress concentrations of corroded reinforcement

$$\sigma_n = \sigma_o \cdot \left(1 + \frac{4P}{L}\right) \tag{4.11}$$

σ_o: initial stress [N/mm^2]

σ_n: stress in the reduced area [N/mm^2]

P: the pit depth [mm]

L: the pit length [mm]

As a result, the residual strength of corroded reinforcement, when measured in terms of stress which can be resisted, also reduces significantly.

Experimental studies by Du et al. (2005)[2], sought to analyze the residual capacity of corroded bars by varying the diameters and types (plain and ribbed), the condition of the bar (single bare bars and bars in concrete), and other factors. The authors explain that corrosion alters the external surface of reinforcement because

[1] Drakakaki Ar., Apostolopoulos Ch., Koulouris K. Mechanical Characteristics of dual-phase steel B500c after shot peening process. Proc. of the Third Intl. Conf. on Advances in Civil, Structural and Construction Engineering – CSCE, 2015.

[2] Du Y.G., Clark L.A., Chan A.H.C. Residual capacity of corroded reinforcing bars. Magazine of Concrete Research, 2005;57(3):135–47.

of very irregular attack penetration and that the residual section of corroded reinforcement[1] is no longer round and varies considerably along its circumference and its length[2].

As a result of the study, Du et al. proposed an empirical equation based on tensile force-extension experimental tests to calculate the regressed tensile yield stress of the corroded rebar, according to the following formula:

$$f = (1.0 - \beta \cdot Q_{corr}) f_0 \qquad (4.12)$$

f: yield or ultimate stress of corroded reinforcement [N/mm^2]
f_0: yield or ultimate stress of non-corroded reinforcement [N/mm^2]
β: strength factor (regression parameter) [-]
Q_{corr}: amount of corrosion of reinforcement [%]

According to Du et al., the values of β are 0.005[3] for mean stress (stress based on average reduced cross section area) and 0.015 for notional stress (stress based on original uncorroded cross section area). The amount of corrosion Q_{corr} used in equation 4.13 may be determined from such measured values by using equations 4.14 and 4.15:

$$Q_{corr} = 1 - (d_s/d)^2 \qquad (4.13)$$

[1] Due to local attack penetration and stress concentrations, the residual forces of corroded reinforcement decrease more rapidly than does their average cross-sectional area.

[2] Although the residual capacity of smaller diameter and/or plain reinforcement decreases more rapidly than that of larger diameter or ribbed reinforcement, the influences of type and diameter of reinforcement are insignificant at the 5% significance level in most cases and can be neglected in practical engineering.

[3] The coefficients for yield strength of ribbed bars obtained by Andrade et al. (1991), Lee et al. (1996) and Saifullah (1994) range from 0.0016 to 0.0045.

$$Q_{corr} = 4\frac{x_{corr}}{d} = 0.046\frac{i_{corr}}{d}t \quad (4.14)$$

$$x_{corr} = 0.0115 i_{corr} t \quad (4.15)$$

d_s: diameter of corroded reinforcement [mm]
d: diameter of non-corroded reinforcement [mm]
x_{corr}: corrosion attack penetration at the reinforcement surface [(μA/cm^2).years]
i_{corr}: corrosion rate of reinforcement (Corrosion current density) [μA/cm^2]
t: time elapsed since the initiation of corrosion [years]

4.3.4.3 Evaluation of yield strength in tension and compression for non-uniform cross-section loss of corroded bars

According to the experimental investigation of corroded bars, the cross section along the length of the rebar may vary. Sometimes it is not possible to identify the position of the pitting corrosion in the real structure, thus the mean cross section of the corroded rebar could be deduced according to the corrosion rate, and calculated by equation used by Kashani M. M. et al. (2013)[1]:

$$D_{corr} = D_0\sqrt{1-\gamma} \quad (4.16)$$

D_{corr}: mean diameter reduced of reinforcement for a specific mass loss [mm]
D_0: initial diameter of uncorroded bar [mm]
γ: mean mass loss ratio [-]

Where the mean mass loss ratio γ used in equation 4.16 can be determined from measured values of the original mass of the rebar (mass per unit length of the

[1] Kashani M.M., Crewe A.J., Alexander N.A.. Nonlinear stress–strain behaviour of corrosion-damaged reinforcing bars including inelastic buckling. Engineering Structures 48 (2013) 417–429.

original steel bar) m_0 and the mass of corroded rebar (mass per unit length of the steel bar after removal of the corrosion products) m by using equation 4.17:

$$\gamma = \frac{m_0 - m}{m_0} \tag{4.17}$$

m_0: original mass of the rebar [kg/m]
m: mass of corroded rebar [kg/m]

Once determined the mean mass loss ratio γ it is possible to calculate the regressed tensile yield strength and the regressed compressive yield strength of the corroded bar (based on the mean mass loss ratio) using the empirical formula proposed by Du et al. (2005) Equation (4.12), mentioned previously, according to the following formulas:

$$f_{yt} = f_y(1 - a_t \cdot \psi) \tag{4.18}$$

$$f_{yc} = f_y(1 - a_c \cdot \psi) \tag{4.19}$$

Where f_{yt} is the notional yield stress in tension and f_{yc} is the notional yield stress in compression corresponding to the corroded rebar based on the original rebar cross section area, f_y is the yield stress of uncorroded rebar, a_t is the regression factor in tension equals 0.005 (stress based on average reduced cross section area) according to Du et al[1] and a_c is the regression factor in compression, considering the effect of non-uniform distribution of pitting corrosion.

[1] The value of "a" obtained by different researchers, ranges from 0.01 to 0.017.

The effect of corrosion on compressive yield strength a_c is defined using the parameters calibrated based on the observed experimental results by Kashani, M. M., Lowes, L. N. et al. (2015)[1]:

$$a_c = \begin{cases} 0.0050 & for\ \lambda_{cr} \leq 6 \\ 0.0065 & for\ 6 < \lambda_{cr} < 10 \\ 0.0125 & for\ \lambda_{cr} \geq 10 \end{cases} \quad (4.20)$$

$$\lambda_{cr} = \frac{L}{D_{corr}} \quad (4.21)$$

Where λ_{cr} is the bar slenderness ratio, L is the length between two adjacent transversal bars and D_{corr} is the diameter of the longitudinal corroded bar by Equation (4.16).

The parameter ψ represents the mass loss due to corrosion, which is defined as:

$$\psi = 100 \cdot \gamma \quad (4.22)$$

4.4 References

1. Basic for Assessment of Existing Structures. Milan Holický, Klokner Institute et al., Czech Technical University in Prague, Czech Republic. 2013.
2. Campbell F.C. Elements of Metallurgy and Engineering Alloys. Fick's second law of diffusion, pg. 67. AMS International. USA, 2008.
3. Darts. Durable and Reliable Tunnel Structures. European Commission, Growths 2000. G1RD-CT-2000-00467.
4. Drakakaki Ar., Apostolopoulos Ch., Koulouris K. Mechanical Characteristics of dual-phase steel B500c after shot peening process. Proc. of the Third Intl.

[1] Kashani, M. M., Lowes, L. N. et al. Phenomenological hysteretic model for corroded reinforcing bars including inelastic buckling and low-cycle fatigue degradation. Computers and Structures 156 (2015) 58–71.

Conf. on Advances in Civil, Structural and Construction Engineering – CSCE, 2015.

5. Du Y.G., Clark L.A., Chan A.H.C. Residual capacity of corroded reinforcing bars. Magazine of Concrete Research, 2005;57(3):135–47.
6. DuraCrete. Probabilistic performance based durability design of concrete structures. Statistical Quantification of the Variables in the Limit State Functions. Report No.: BE 95-1347, pp. 62-63, 2000.
7. Fib Bulletin 34. Model code for service life design. Fib, Fédération internationale du béton / International Federation for Structural Concrete, 2006.
8. Fib Bulletin 59. Condition control and assessment of reinforced concrete structures. Fib, Fédération internationale du béton / International Federation for Structural Concrete, 2011.
9. Fib Model Code for Concrete Structures 2010. Fib, Fédération internationale du béton / International Federation for Structural Concrete, 2013.
10. Fib Model Code for Concrete Structures (Draft - Version 0.1: 15 Sept 2014). Assessment of existing structures. SAG 7 Draft MC Assessment 15 Sept 2014.docx.
11. Giuffrè, A., and Pinto, P. E. (1970). “Il comportamento del cemento armato per sollecitazioni cicliche di forte intensità.” Giornale del Genio Civile, 5(1), 391–408.
12. Gordon D. Bennett. Introduction to Ground-Water Hydraulics - A programmed text for self-instruction. U.S. Geological Survey, Techniques of Water-Resources Investigations, Book 3, Chapter B2.
13. International standard ISO 13822:2010. Bases for design of structures - Assessment of existing structures. Published in Switzerland, 2010.
14. Luechinger P., Fisher J. et al. New European Technical Rules for the Assessment and Retrofitting of Existing Structures. JRC Science and Policy Report. Report EUR 27128 EN. 2015.

15. Milan Holicky, Dimitris Diamantidis et al. Methods for the risk assessment and risk-based management of aging infrastructure. Lifelong Learning Programme. ISBN: 978-80-01-05611-0. 1st Edition by Czech Technical University in Prague, Klokner Institute, 2014.
16. Ministry for Cultural Heritage and Activities, Italian Government. Guidelines for evaluating and mitigation of seismic risk to cultural heritage. Roma, 1997.
17. Pedeferri P., Bertolini L. et al. “La corrosione nel calcestruzzo – Fenomenologia, prevenzione, diagnosi, rimedi”, AICAP, Roma - 2006.
18. Popovics, S. Numerical approach to the complete stress-strain relation for concrete. Cement and concrete research 3, 5 (1973), 583-599.
19. Richart, R. M. and Abbott, B. J. Versatile elasto-plastic stress-strain formula. Journal of engineering mechanics, ASCE 101, 4 (1975), 511-515.
20. Tuutti, K. Corrosion of steel in concrete. Swedish Cement and Concrete Research Institute. Stockholm, 1982.

Chapter V

The main techniques and materials for structural rehabilitation

5.1 Scope

This chapter presents the main techniques and materials for intervention in RC structures most currently used on the area of structural rehabilitation. The objective of this chapter is to expose innovative technologies for recovery and strengthening of reinforced concrete elements, in an integrative way, as an option of use, beyond the conventional techniques. The principal base attributes arise on the high performance of the innovative materials, in terms of: mechanical capacity, ductility or tenacity, light weight, durability, adaptability and compatibility with the existing structure.

5.2 Interventions in heritage RC structures

In the field of structural rehabilitation, the use of innovative technologies and materials for interventions in historic buildings is confronted with the need to preserve the original characteristics of the structures and the possibility of changes aiming to recover or improve its structural performance. Furthermore, the use of available innovative resources, together with appropriate choices could represent an opportunity to integrate an architectural expressiveness, thereby increasing the values of the good.

However, one of the main questions that the designer finds, besides the factors related to structural safety and requirements of architectural identity protection[1], is

[1] Not only the aesthetic aspect, but also the constructive integrity.

relative to how and how much to preserve the features that interest the architectural quality, the cultural values and the building memory.

5.3 Normative reference to interventions in existing buildings

Currently in Europe there is a lack of specific standards covering the entire process of intervention in existing buildings. The European Standard EN 1504 “Products and systems for the repair and protection of concrete structures – definitions, requirements, quality control and evaluation of conformity” defines the procedures and characteristics of products used to repair, maintain and protect concrete structures. General criteria regarding the evaluation of structural safety and procedures for design of existing buildings were addressed in the Italian standard NTC 2008[1] Chapter 8. One of the most important aspects of the Italian standard is on the assessment requirements of structural safety, which concerns not only the isolated structural elements, but also influences, the overall behaviour of the structure. Besides the necessity of determine of the level of security before and after the intervention.

According to NTC 2008, the classification of interventions is divided into three categories:

- *Adjustment interventions to achieve the levels of security provided by the rules;*
- *Improvement measures which will increase the existing structural safety, without necessarily reaching the levels required by the rules;*
- *Repairs or local interventions concerning isolated elements, and that however entail an improvement of pre-existing conditions of safety.*

An adjustment intervention comprises expanding the structure or a considerable load increase, by obligatoriness requiring the evaluation of structural safety. In this

[1] Norme Tecniche per le Costruzioni, Decreto Ministeriale 14 gennaio 2008.

case the design will refer to the analysis and verification of the entire structure after the intervention.

An improvement intervention comprises interventions in order to increase the strength capacity of the structure in accordance with the actions considered. In this case, the design and evaluation of structural safety should include all parts of the structure that have changes in the structural behaviour as well as the structure as a whole. For interventions in limited areas it is considered appropriate to evaluate the overall response of the structure after intervention, in order not to make significant changes in the distribution of stiffness, resistance and masses.

A local intervention or a repair intervention, in general, comprises the isolated structural elements and corresponds to limited parts of the construction. In this case, the design and safety assessment may only refer to the parts or interested structural elements, provided that the intervention does not produce substantial changes in the behaviour of other parts and of the structure as a whole.

The Applicative Circular[1] of the Italian standard NTC 2008 of February 2, 2009, number 617, defines capacity models for rehabilitation interventions of elements in reinforced concrete on conventional reinforcement techniques with metal profiles and reinforced concrete section increase and innovative techniques using composite materials.

5.4 The main conventional techniques and materials for structural rehabilitation

5.4.1 General approach

Currently in Brazil, the techniques of recovery and structural strengthening commonly used are based on the use of traditional materials in the construction industry, such as concrete and steel, through reinforcements with metal profiles and reinforced concrete with increasing section of the elements.

[1] Circolare 2 febbraio 2009, n. 617. Istruzioni per l'applicazione delle nuove Norme Tecniche per le Costruzioni (NTC), di cui al decreto ministeriale 14 gennaio 2008.

Although they are commonly used for structural rehabilitation, the effectiveness of these techniques is still considered questionable and limited. For example, an intervention that provides a section increase of RC elements (considered simple because it does not require a relative skilled labor in their application), when the connection between the existing structure and the new is not well executed can be considered an ineffective solution and useless for the desired purpose. As strengthening in steel structure with use of metal profiles, besides being considered an intervention difficult to perform (which requires the use of heavy equipment for its application) is more susceptible to corrosion phenomenon. This may significantly increase maintenance costs.

However, the main problems found in structural interventions, through the use of the mentioned conventional techniques, are related to the architectural impact due to the change in the elements' geometry and the invasion of the available usable space. As well as to the considerable weight increase in the structure.

5.4.2 Section increase in reinforced concrete

Technique with section increase in reinforced concrete may be used on all elements which comprise the structure (pillars, beams, slabs, nodes between beams and pillars, stairs, walls, and foundation elements). The application of this technique comprises an increase on the elements´ dimensions and its function is to provide a rise of strength and stiffness (also mass), at local and/or global level in the structure. This type of intervention can considerably influence the overall behaviour of the structure in terms of stiffness and also the position of global mass centroid.

Section increase consists of performing a layer in reinforced concrete, around the element (preferably without concrete cover) by inserting longitudinal and transverse reinforcement (Fig. 5.01). This type of intervention can be performed in various settings. For the pillars, even if partial reinforcements are acceptable (in one, two or three sides), the intervention is most effective when the increase in the

dimensions is performed on all sides and symmetrically. The difficulty of concreting can be overcome with the use of self-compacting micro-concrete with shrinkage-compensating.

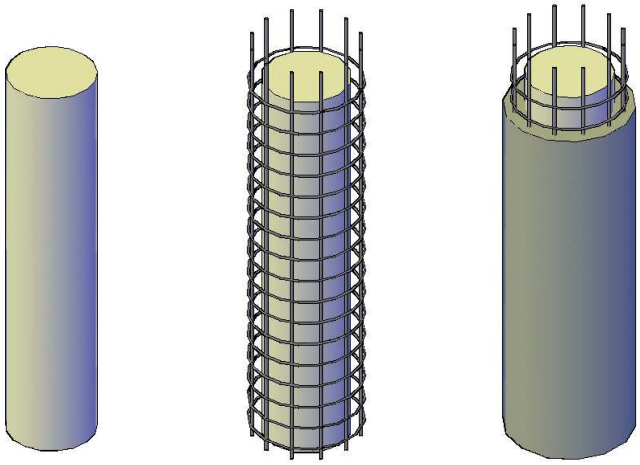

Figure 5.01 Column strengthening details

(a) Original RC column; (b) Reinforcement assembly; (c) Concreting of the new section

This type of intervention is useful for increasing the compressive strength, bending and shear. For the beams it is possible to increase the flexural strength for positive and negative moments.

The evaluation of the resistance increment can be made according to the indications of Applicative Circular 617/2009 of the Italian standard, which defines simplified calculation parameters to be adopted to the capacity values in verifications. With reference to the strengthened reinforced concrete sections, according to the expressions as noted below:

- Shear strength: $\tilde{V}_R = 0.9V_R$ (5.01)
- Bending strength: $\tilde{M}_y = 0.9M_y$ (5.02)
- Steel yield strength: $\tilde{\theta}_y = 0.9\theta_y$ (5.03)
- Ultimate deformation: $\tilde{\theta}_u = \theta_u$ (5.04)

5.4.3 Strengthening in steel structure

The reinforcement of structural elements in steel has characteristics similar to the reinforcement with increase section in reinforced concrete. It consists in applying profiles and/or steel plates that can be fixed to the existing structure with epoxy resin[1] and welded together (Fig. 5.02). This strengthening technique may be used to increase the deformability and resistance to bending stresses and shear of pillars, walls, beams and slabs. When applied steel plates in beams is known as *béton plaqué* technique. To resist the shear stress in beams, profiles are applied with welded steel plates, similar to the solution adopted for the pillars in Figure 5.02.

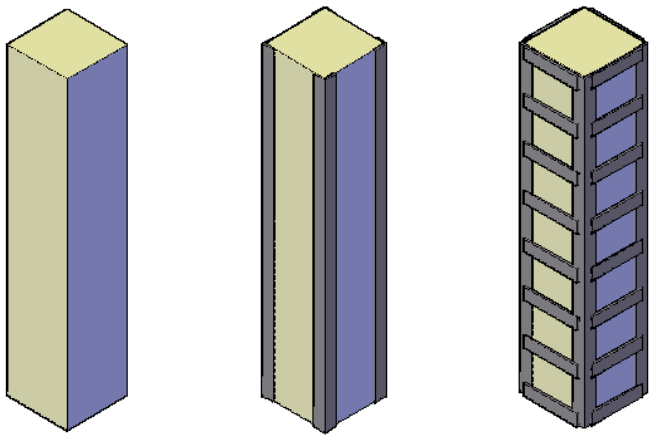

Figure 5.02 Column strengthening details
(a) Original RC column; (b) Fixing of steel profiles; (c) Welding of steel plates

When applied on pillars, there is a notable increase in strength capacity for vertical loads through the confinement effect[2], which can be estimated by Equation (5.05), of the Applicative Circular 617/2009 (Italian standard):

[1] It is common to use the fastening with screws, when applied for the purpose of improving the overlapping steel bars.

[2] Both the beams as for the pillars, the plates can be preheating before welding and pre-stressed the profiles, so as to provide successively a confining pressure. In this case, the reinforcement begins to work as active

$$f_{cc} = f_c \left[1 + 3.7 \left(\frac{0.5\alpha_n \alpha_s \rho_s f_y}{f_c}\right)^{0.86}\right] \quad (5.05)$$

Where ρ_s is the volumetric ratio of transverse reinforcement and, $\alpha_n$and α_s are the confinement efficiency factors in the section and along the member, calculated according to the specific formulations of the Italian standard.

5.5 The main innovative techniques and materials for structural rehabilitation

5.5.1 General approach

It is believed that the main reasons why structural rehabilitation innovative technologies are being increasingly used in countries in development phase (such as Brazil), in addition to high-performance of the materials in terms of mechanical strength capacity, are more related to the low impact of the intervention. This not only corresponds to the architectural aspect of the structure, but also the ease of application in short periods and without major disturbances in the functioning of the building.

Market conditions also may be considered an important factor to understand the innovation level to be used in structural rehabilitation interventions, which could entail a decisive role in the choice of technique. In the application of innovative products and technologies a wide field of attributes, considering all stages of the process, needs to be investigated. The reading of the technology would need to be made from the initial production sector, considering the ecological impacts in all its phases, projectability, adaptability and flexibility of use, achievement, durability of materials and a sustainable end.

confinement mechanism. It can be used to increase the compressive strength capability of pillars and the shear strength capacity of beams.

In developed European countries, such as Italy, there is a significant trend in the analysis of the complete life cycle of a technology, which may comprise from the extraction of the raw material to the final recycling.

5.5.2 Strengthening by CAM system

The resistance of structural elements can be increased using the innovative technique CAM (Cerchiatura or Cucitura Attiva Manufatti) in structural rehabilitation interventions. CAM reinforcement system consists of prestressed strips of high-strength steel (about f_{yk} 850MPa), individual or superimposed with thicknesses ranging from 0.8mm to 1.0mm and widths ranging from 18 to 20 mm, positioned in closed loop actively confining in the RC sections. Strips are supported by steel plates or profiles to provide a confinement state on the structural element (Fig 5.03).

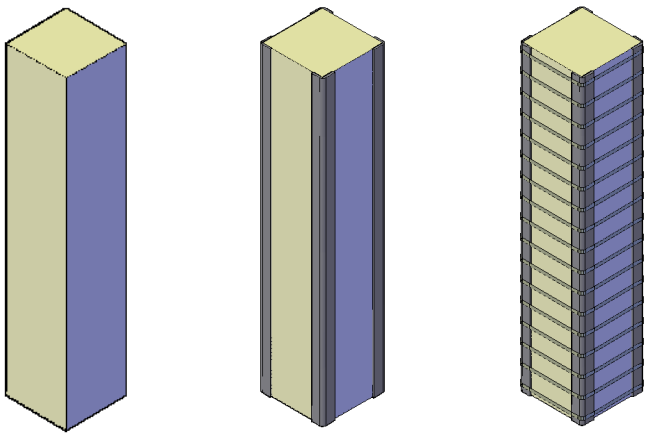

Figure 5.03 Column strengthening details

(a) Original RC column; (b) Fixing of steel profiles; (c) Prestressed steel strips

This system allows increasing the strength of structural elements to compressive stresses through confinement, flexo-compression and shear. It may also be used to resist shear stress and bending of beams, by performing the proper connections

and welds required. The compressive strength of element confined can be calculated according to the formulation of Applicative Circular 617/2009 (Formula 5.05).

The increase of deformation capacity may be evaluated by Equation (5.06) for the ultimate deformations:

$$\varepsilon_{ccu} = 0.004 + 0.5\frac{0.5\alpha_n\alpha_s\rho_s f_y}{f_{cc}} \quad (5.06)$$

While the deformation corresponding to the maximum strength after confinement, can be calculated using the formula reported in Eurocode 8:

$$\varepsilon_{cc2} = \varepsilon_{c2}\left[1 + 5\left(\frac{f_{cc}}{f_c} - 1\right)\right] \quad (5.07)$$

5.5.3 Structural rehabilitation by FRP and FRCM systems[1]

5.5.3.1 General approach

The use of composite materials with use of long fibers began to be used in building sector on the basis of its high performance capabilities (high mechanical strength), combined with the versatility and the ability to fill different functions, not necessarily following standard configurations. Beyond the ability in adapt to the geometric characteristics of the existing structure. These characteristics also contributed to the development of this technique and its preference in relation to convective techniques.

In Brazil, the structural rehabilitation with fiber-reinforced composite material[2] is considered a technological innovation capable of providing structural adjustments

[1] Fiber-reinforced composite systems.

[2] Namely, a material consisting of a matrix reinforced by fibers.

in a simpler and more effective way, making it competitive compared to conventional solutions.

Fiber-reinforced composite system is a technique used to improve the performance capacity of the structural elements subjected to compressive stresses, shear, tension, bending, and flexo-compression. To define the mechanical properties of a fiber-reinforced composite system is necessary to consider not only the properties of the individual fibers, but also, and mainly, the efficiency of the fiber-matrix system and the methodology used in its application. This technology is divided into two systems FRP (Fiber Reinforced Polymer) and FRCM (Fiber Reinforced Matrix Cementitious), with matrix based on epoxy resins (for FRP) and with matrix based on cement (for FRCM), used with different types of fiber: carbon, aramid, glass, steel, basalt[1], PBO[2], among others.

Italy is a country that has an important position at international level in research activities in the structural rehabilitation field on fiber-reinforced composites, for both the value of knowledge contributions and the presence of important heritage buildings. Italian Research Council (CNR) provides a guideline (CNR-DT 200 R1/2013[3]) updated according to the results of the latest research, both theoretical and experimental, which serves as an aid source not only to researchers but also to professionals of the area of rehabilitation.

5.5.3.2 Normative references

At European level, the formulation of documents for structural design of systems that provide for the use of FRP, began in September 1996 with the formation of the Task Group 3.10 CEB (*Comité Euro-International du Béton*). In July 2001 the *fib* Bulletin 14 "Design for Use in Externally Bonded Fibre Reinforced Polymer

[1] Still in experimental stage.

[2] Poliparafenilenbenzobisoxazolo.

[3] Guide for the Design and Construction of Externally Bonded FRP Systems for Strengthening Existing Structures.

Reinforcement (FRP EBR) for Reinforced Concrete Structures" was published by Task Group 9.3 "FRP Reinforcement for Concrete Structures".

In Italy, the CNR (*Consiglio Nacionale delle Ricerche*) through the committee to comment on the technical standards relating to buildings developed the CNR-DT 200/2004 document "Guide for the Design and Construction of Externally Bonded FRP Systems for Strengthening Existing Structures ". In 2013, the document was revised and updated taking into account other international documents such as the 440.2R-08[1] "Guide for the Design and Construction of Externally Bonded FRP Systems for Strengthening Concrete Structures" and the ISIS Design Manual No. 4[2] "FRP Rehabilitation of Reinforced Concrete Structures".

Currently in Italy, it is in preparation an exclusive document for instructions regarding the FRCM systems (strengthening with fiber-reinforced composite materials with cement-base inorganic matrices). In the absence of a specific document for FRCM systems, is used the same adopted for FRP systems.

5.5.3.3 Mechanical characteristics

5.5.3.3.1 FRP system

FRP strengthening is divided into three systems: pre-cured systems, wet lay-up systems and prepreg systems; and is commonly found in the market with different fiber configurations: laminates, bars, meshes and sheets or fabrics. Because they are easily adaptable to the structure, the most common fiber kinds are the bidirectional sheets or fabrics. The family of FRP is formed by the main types of polymers: glass fibers (GFRP), carbon fibers (CFRP) and aramid fibers (AFRP).

According CNR-DT 200 R1/2013, from a mechanical point of view, the FRP strengthening systems are classified based on their values of modulus of elasticity and ultimate capacity. These values are measured under uniaxial tension in the direction of the fibers (pre-cured systems shall be referred to by unit area of the

[1] American Concrete Institute (A.C.I.), committee 440, 2008.

[2] ISIS Canada Corporation, 2008.

FRP, fiber and matrix, and Wet lay-up system only to the area of dry fibers). Values of modulus of elasticity and tensile strength also must be resistant to the environmental degradation induced on the FRP composite (the same bond principle is applies to conventional techniques).

The fibers develop a support function, both in terms of strength and ductility, when they are applied in areas where RC elements are requested to tension. The matrix basically has two functions: to protect the fibers and transfer efforts between fibers and reinforced element. The bond between fibers and the concrete must be considered perfect for an FRP system to be effective.

This reinforcement system with polymeric matrix can be considered composites heterogeneous and anisotropic materials, characterized by a prevalent linear elastic behaviour up to rupture. In Figure 5.04 the constitutive law (stress-strain relationship) for a unidirectional fiber-reinforced material and of its constituent phases (matrix and fibers) is represented.

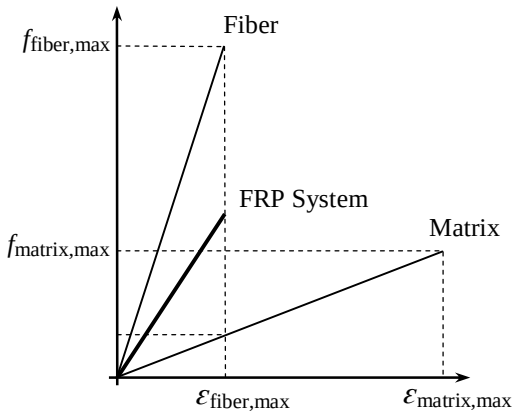

Figure 5.04 Stress-strain relationship of fibers, matrix and FRP System (adapted from *fib* Bulletin 14)

In Table 5.01 and 5.02 are addressed average values of properties and mechanical characteristics of various types of fibers and matrices used in the FRP systems and FRCM.

5.5.3.3.2 FRCM system

The application of FRCM is performed by a wet lay-up system, composed of a cementitious matrix and a very thin bidirectional mesh of fiber in carbon, glass, PBO or steel. Wherein, its mechanical properties are essentially dependent on the constituent materials (fiber and matrix).

The main difference between FRCM and FRP systems is associated to the matrix characteristics. For example, the matrix of a FRCM has high modulus of elasticity and a low tensile strength, compared with a FRP system that has polymer resin based matrix (Table 5.01). In practice, the tensile strength of the cement matrix is higher because their thicknesses in the application are larger, relative to the polymer matrix.

To improve the mechanical properties of FRCM composites in terms of tenacity and mechanical impact resistance, short fibers or micro-fibers dispersed in the cement matrix may be added. Micro-fibers also contribute to minimizing the cracking effect after water evaporation, during thermal hygrometric shrinkage of the conglomerate.

Tables 5.01 and 5.02, show a comparison between the main mechanical characteristics of fibers and matrices for FRP and FRCM systems.

Table 5.01: Comparison between properties of various types of reinforcing matrix (average values)

System	Matrix	Matrices mechanical characteristics				
		Elastic modulus (GPa)	Tensile strength (MPa)	Strain at rupture (%)	Shrinkage (%)	Density (gr/cm³)
FRP (polymeric matrix)	Polyester resin	2.10 – 3.45	34.5 – 103.5	0.5 – 5.0	5 – 12	1.1 – 1.4
	Epoxy resin	2.75 – 4.10	55 – 130	0.5 – 5.0	1 – 5	1.2 – 1.3
	Vinyl Ester resin	3 – 3.5	73 – 81	0.5 – 5.0	5.4 – 10.3	1.12 – 1.32
FRCM (cementitious matrix)	Cement mortar	6 – 15	25 – 35	0.4 – 0.6	a	2.0

Note: a = the commonly used mortars are of type thixotropic with shrinkage compensated; Table adapted from Fiber-reinforced in Architecture. FRP and FRCM technologies in the recovery of RC structures. Naples, 2009.

Table 5.02: Comparison between the properties of the various types of reinforcing fiber (average values)

Fibers	Fibers mechanical characteristics					
	Elastic modulus (GPa)	Tensile strength (GPa)	Strain at rupture (%)	Coefficient of thermal expansion (10-6/°C)	Thermal resistance (°C)	Density (gr/cm³)
Aramid	62 – 179	3.6 – 3.8	1.9 – 5.5	-2	300 – 350	1.45 – 1.47
Glass (E)	70 – 80	2.0 – 3.5	3.5 – 4.5	5.2	400	2.54
Glass (S)	85 – 90	3.5 – 4.8	4.5 – 5.5	1.6 – 2.9	400	2.49
Basalt	90	1.8 – 2.2	1.8 – 2.5	8.6	450 – 650	2.7
Steel	206	0.24 – 0.40[a] 0.35 – 0.60[b]	20 – 30	10.4	700	7.8
Carbon (high strength)	240 – 280	4.1 – 5.1	1.6 – 1.73	-0.75	350 – 400	1.75
PBO[c]	270	5.8	2.1	-6	250 – 315	1.56
Carbon (high modulus)	390 – 760	2.4 – 3.4	0.5 – 0.8	-1.45	350 – 400	1.85 – 1.90

Note: a = yield strength; b = ultimate strength (rupture); c = Poliparafenilenbenzobisoxazolo; Table adapted from Fiber-reinforced in Architecture. FRP and FRCM technologies in the recovery of RC structures. Naples, 2009.

In order to know the values of main mechanical properties of fibers used in the market, in October 2015, three Italian companies of fiber distribution for structural reinforcement were consulted[1]. According to the values reported in Table 5.03:

[1] These companies also operate internationally, two of which have representations in Brazil.

Table 5.03: Comparison between the main characteristics of the existing fibers in the market

Type	Fiber	Fibers mechanical characteristics		
		Elastic modulus (N/mm²)	Tensile strength (N/mm²)	Strain at rupture (%)
Sheets or fabrics	Glass (a)	73,000	2,600	3.5
	Glass (b)	76,000	2,300	2.8
	Basalt (a)	85,000	2,000	2.0
	Steel (a)	190,000	1,900	1.0
	Carbon (b)	230,000	3,800	1.5
	Carbon (b)	230,000	4,510	1.9
	Carbon (a)	230,000	4,800	2.1
	Carbon (c)	240,000	4,800	1.8
	PBO (c)	270,000	5,800	2.15
	Carbon (b)	390,000	4,400	0.8
Laminates	Carbon (c)	165,000	2,200	1.3
	Carbon (a)	170,000	3,100	2.0
	Carbon (a)	200,000	3,300	1.4
	Carbon (c)	210,000	2,500	0.8
	Carbon (a)	250,000	2,500	0.9
Meshes	Carbon (b)	240,000	4,800	1.9

Note: Research performed in three Italian companies (a), (b) and (c) on fibers used in the market (October 2015).

5.5.3.4 Strengthening for RC structures[1]

5.5.3.4.1 General criteria

To carry out structural strengthening with fiber-reinforced composite systems, the reinforced elements must be verified according to the limit states set by current standards. For each limit state must ensure to the following equilibrium condition:

[1] According to *fib* Bulletin 14 (2001) and CNR-DT 200 R1/2013 (Italian standard).

$$E_d \leq \ R_d \tag{5.08}$$

Where, E_d is the design value of the requester actions in the structure, and R_d is the value of the element's ability to resist such actions in terms of deformation and strength.

The resistance capacity R_d is calculated by the following relationship:

$$R_d = \frac{1}{\gamma_{Rd}} \cdot R\{X_{d,i}; a_{d,i}\} \tag{5.09}$$

In the above equation the symbol $R\{\cdot\}$ represents the function related to the specific mechanical model and γ_{Rd} is a partial factor which takes into account the uncertainties of the model. $X_{d,i}$ is the design value of the FRP materials and the existing, and $a_{d,i}$ is the value of the geometric parameters applied to the reinforcement model.

5.5.3.4.2 Debonding mechanisms

The failure mechanisms of FRP system used to strengthen RC members by laminate or tissue is of brittle type and by detachment of the support. Wherein the crisis mechanism cannot precede the collapse by bending or shear of the reinforced element. In this case, the strengthening bond to the existing structure has an important function.

Safety verification for debonding requires an evaluation of the maximum force (tangential and normal) transmitted from the concrete to the strengthening system. The first check is required to meet the ultimate limit state (ULS) and the second to meet the service limit state (SLS).

According to *fib* Bulletin 14, the detachment of an FRP system applied to a beam, occurs primarily through four modes:

Mode 1: peeling-off in an uncracked anchorage zone (the FRP may peel-off in the anchorage zone as a result of bond shear fracture through the concrete);
Mode 2: peeling-off caused at flexural cracks (Flexural (vertical) cracks in the concrete may propagate horizontally and thus cause peeling-off of the FRP in regions far from the anchorage);
Mode 3: peeling-off caused at shear cracks (Shear cracking in the concrete generally results in both horizontal and vertical opening, which may lead to FRP peeling-off. However, in elements with sufficient internal (and external) shear reinforcement (as well as in slabs) the effect of vertical crack opening on peeling-off is negligible;
Mode 4: peeling-off caused by the unevenness of the concrete surface (The unevenness or roughness of the concrete surface may result in localized debonding of the FRP, which may propagate and cause peeling-off).

The Figure 5.05 shows an example of rupture by detachment:

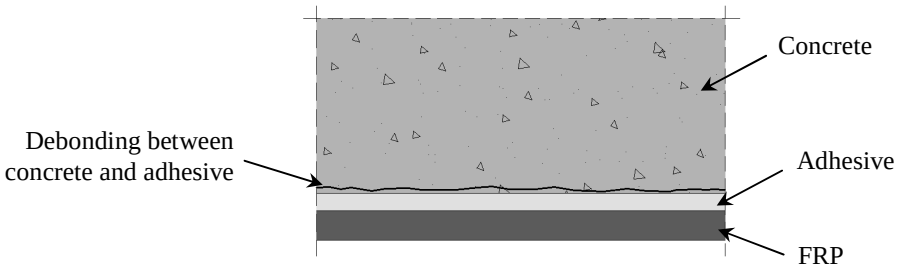

Figure 5.05 Failure mechanism
Debonding between FRP and concrete
(adapted from *fib* Bulletin 14)

5.5.3.4.3 Flexural strengthening

Flexural strengthening design at the ULS, of RC members reinforced with FRP requires that, both bending capacity (M_{Rd}) and factored ultimate moment (M_{Sd}) satisfy the following equation:

$$M_{Sd} \leq M_{Rd} \tag{5.10}$$

The flexural capacity, M_{Rd}, of the strengthened member may be calculated using the following rotational equilibrium equation:

$$M_{Rd} = \frac{1}{\gamma_{Rd}} \cdot \left[\psi \cdot b \cdot x \cdot f_{cd} \cdot (d - \lambda \cdot x) + A_{s2} \cdot \sigma_{s2} \cdot (d - d_2) + A_f \cdot \sigma_f \cdot d_1\right] \tag{5.11}$$

The position of the neutral axis, x (Fig. 5.06) is calculated using the translational equilibrium equation along the beam axis as follows:

$$0 = \psi \cdot b \cdot x \cdot f_{cd} + A_{s2} \cdot \sigma_{s2} - A_{s1} \cdot \sigma_{s1} - A_f \cdot \sigma_f \tag{5.12}$$

Where f_{cd} is the design concrete compressive strength, γ_{Rd} is equal to 1.0, ψ and λ represents the resultant of the compression stresses divided by $b \cdot x \cdot f_{cd}$ and the distance from the extreme compression fiber divide by x.

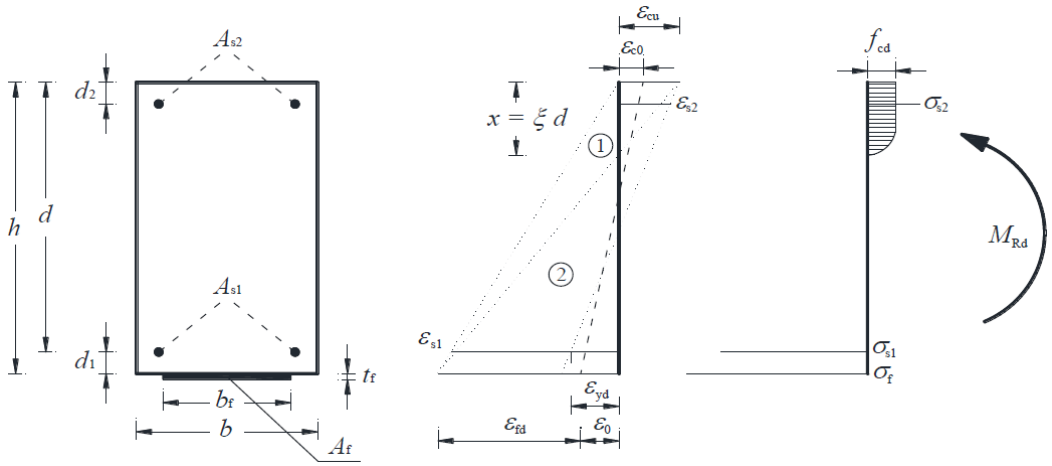

Figure 5.06 Failure mode of a RC member strengthened with FRP
(source CNR-DT 200 R1/2013)

The maximum concrete compressive strain, ε_{cu}, is defined by the current building standard (Eurocode 8), and the maximum FRP tensile strain, ε_{fd}, is calculated as follows:

$$\varepsilon_{fd} = mim\left\{\eta_a \cdot \frac{\varepsilon_{fk}}{\gamma_f}, \varepsilon_{fdd}\right\} \quad (5.13)$$

Where ε_{fk} is the characteristic strain at failure of the adopted strengthening system, γ_f and η_a are the coefficients defined in CNR-DT 200 R1/2013. ε_{fdd} is the maximum strain due to intermediate debonding (generally the minimum value in Equation 5.13 corresponds to ε_{fdd}).

Figure 5.07 represents a beam with flexural strengthening:

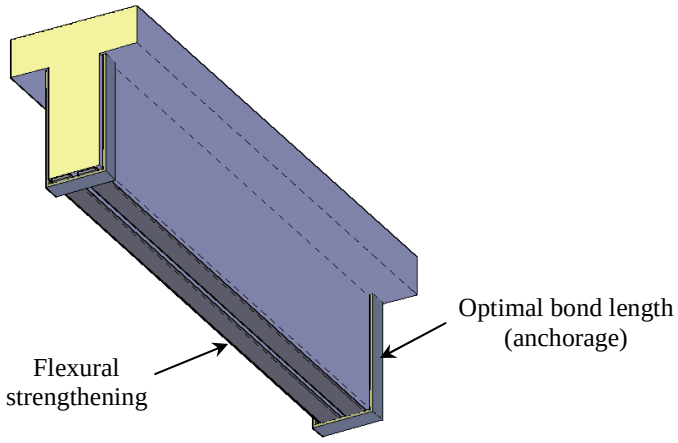

Figure 5.07 Flexural strengthening with laminate FRP

5.5.3.4.4 Shear strengthening

Shear strengthening is necessary when the applied factored shear force is greater than the corresponding shear strength capacity. The shear strength capacity shall

be determined considering contributions of both concrete and transverse reinforcing bars (when available). The shear strength capacity may be evaluated as follow:

$$V_{Rd} = mim\{V_{Rd,s} + V_{Rd,f} + V_{Rd,c}\} \quad (5.14)$$

Where $V_{Rd,s}$ is the steel contribution, $V_{Rd,f}$ is the FRP contribution and $V_{Rd,c}$ is the concrete contribution.

Shear strengthening is achieved by applying one or more layers of FRP material externally bonded on the surface of RC members (Figure 5.08). External monodirectional or bidirectional (e.g. fabric) FRP reinforcement can be applied in a discontinuous way, with gaps between successive strips, or continuously, with strips adjacent each other.

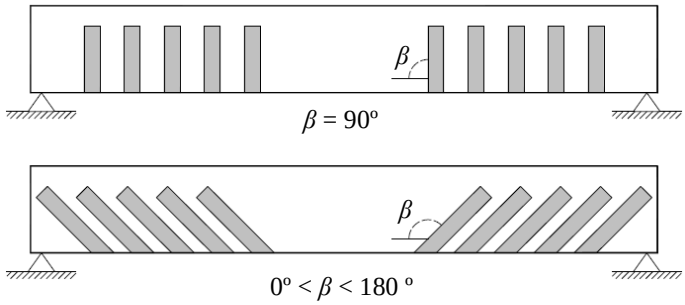

Figure 5.08 Strengthening configurations in lateral view of FRP (source CNR-DT 200 R1/2013)

The arrangement of FRP system around the section can take place in the following ways: U-wrapped or completely wrapped (Figure 5.09).

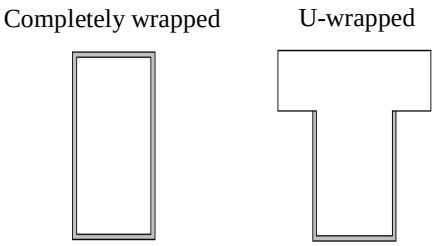

Figure 5.09 Cross section of FRP strengthened members

In the case of available U-wrapped or completely wrapped on a rectangular section, the contribution of the FRP system ($V_{Rd,f}$) can be evaluated according to the Mörsch truss mechanism using the following formula:

$$V_{Rd,f} = \frac{1}{\gamma_{Rd}} \cdot 0.9 \cdot d \cdot f_{fed} \cdot 2 \cdot t_f \cdot (cot\theta + cot\beta) \cdot \frac{b_f}{p_f} \quad (5.15)$$

Where d is the distance from the extreme compression fiber to the centroid of tension steel reinforcement, f_{fed} is the effective design strength of the shear reinforcement FRP, t_f is the thickness of shear reinforcement FRP, γ_{Rd} is the partial factor, b_f and p_f are respectively the width and the spacing of FRP strips, measured orthogonal to the direction of fibers ($\frac{b_f}{p_f} = 1.0$ when FRP strips are placed adjacent to one another or in case of bidirectional FRP elements).

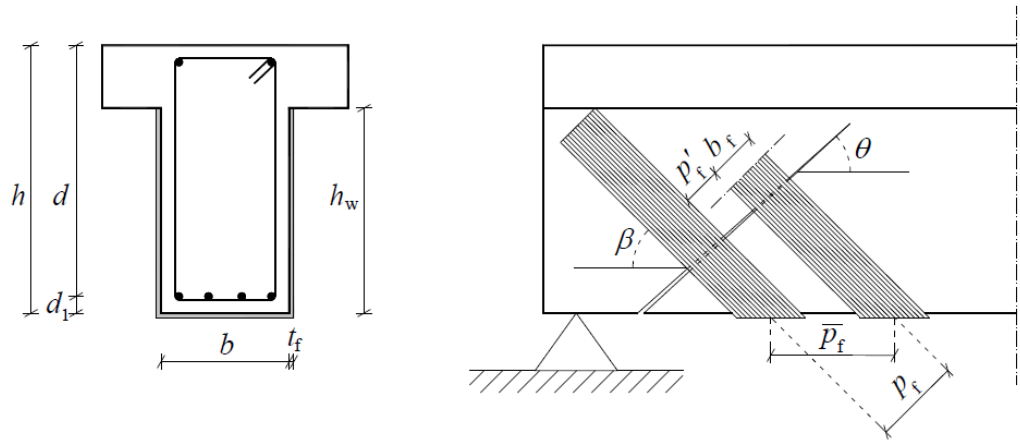

Figure 5.10 Notation for shear strengthening using FRP strips
(source CNR-DT 200 R1/2013)

For completely wrapped members having a circular cross-section with diameter *D* and when fibers are placed orthogonal to the axis of the member (β = 90°), the FRP contribution to shear capacity, $V_{Rd,f}$, shall be calculated as follows:

$$V_{Rd,f} = \frac{1}{\gamma_{Rd}} \cdot D \cdot f_{fed} \cdot \frac{\pi}{2} \cdot t_f \cdot cot\theta \qquad (5.16)$$

Figure 5.11 represents a beam with shear strengthening:

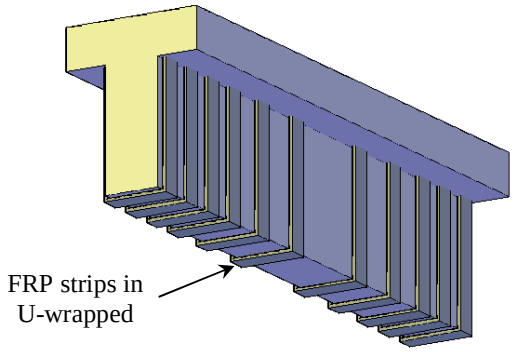

Figure 5.11 Shear strengthening with laminate FRP

5.5.3.4.5 Confinement

Confinement with FRP is usually applied to improve the performance of reinforced concrete elements under axial loads, increasing ultimate compressive strength and ductility. The confinement of elements may be performed in FRP laminate or tissue, applied with continuous or discontinuous external strips, creating a lateral confinement pressure (Fig. 5.12). As a result, the compressive strength and the ultimate deformation of concrete confined with FRP, increase.

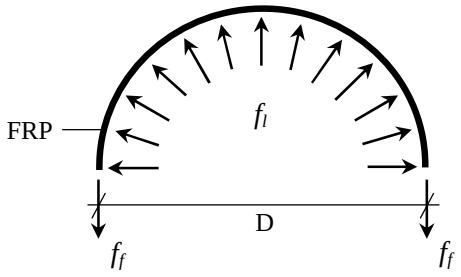

Figure 5.12 Confining pressure exerted by the FRP (adapted from *fib* Bulletin 14)

The confinement lateral pressure shall be evaluated as follows[1]:

$$f_l = \frac{1}{2} \cdot \rho_f \cdot f_f \tag{5.17}$$

$$f_f = E_f \cdot \varepsilon_{fd,rid} \tag{5.18}$$

Where ρ_f is the geometric strengthening ratio as a function of section shape (circular or rectangular) and FRP configuration (continuous or discontinuous wrapping), and E_f is young modulus of elasticity of FRP in the direction of the fibers. The reduced FRP design strain $\varepsilon_{fd,rid}$ shall be calculated as follow:

[1] The effective confinement lateral pressure $f_{l,eff}$, that depends on the shape of the element and of positioning of the FRP strips, shall be estimated in accordance with Italian Standard (CNR-DT 200 R1/2013).

$$\varepsilon_{fd,rid} = min\left\{\eta_a \cdot \frac{\varepsilon_{fk}}{\gamma_f}; 0.004\right\} \quad (5.19)$$

The maximum allowed strain is 0.004, η_a and γ_f represent the environmental conversion factor and partial factor suggested by CNR-DT 200 R1/2013.

The lateral pressure increases by increasing the transverse expansion of the confined element, this lateral pressure is exerted by confinement in FRP that has an elastic behaviour up to the rupture, different from steel confinement that has an elastic-plastic behaviour. For verification of elements confined with FRP, the Italian standard limits the composite ultimate deformation at 0.4%.

Figure 5.13 shows typical stress-strain curves for steel and FRP materials:

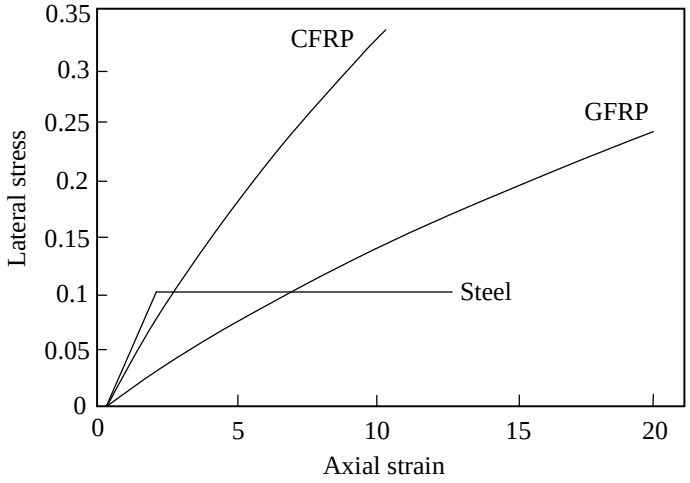

Figure 5.13 Comparison of confinement actions of steel and FRP materials (adapted from *fib* Bulletin 14)

When an initial prestressing is not applied, the reinforcement system operates as a passive confinement mechanism. The action of confinement is significant from the transverse expansion of the reinforced element, which reaches the collapse through of the composite rupture.

Elements confined with FRP are only verified at the ULS, satisfying the following condition:

$$N_{Sd} \leq N_{Rcc,d} \tag{5.20}$$

N_{Sd}, is the design value of the agent axial action and $N_{Rcc,d}$ is the design value of the confined element strength.

In presence of centered compression or small eccentricity of confined elements, the design strength $N_{Rcc,d}$, is provided by the following reaction:

$$N_{Rcc,d} = \frac{1}{\gamma_{Rd}} \cdot A_c \cdot f_{ccd} + A_s \cdot f_{yd} \tag{5.21}$$

Where γ_{Rd} is the partial factor equal to 1.10 (CNR-DT 200 R1/2013), A_c and f_{ccd} represent the member cross-sectional area and design strength of confined concrete, respectively. A_s and f_{yd} represent area and design yield strengths of existing steel reinforcement, respectively.

Design stress, f_{ccd}, of confined concrete may be calculated according the Equation 5.22.

$$\frac{f_{ccd}}{f_{cd}} = 1 + 2.6 \cdot \left(\frac{f_{l,eff}}{f_{cd}}\right)^{\frac{2}{3}} \tag{5.22}$$

Circular sections

For circular sections the geometric strengthening ratio, ρ_f, to be used to evaluate the effective confinement pressure shall be expressed according Equations 5.23 and 5.24.

For continuous wrapping:

$$\rho_f = \frac{4 \cdot t_f}{D} \tag{5.23}$$

For discontinuous wrapping:

$$\rho_f = \frac{4 \cdot t_f \cdot b_f}{D \cdot p_f} \tag{5.24}$$

Where t_f, b_f and p_f represent FRP thickness, width, and spacing, respectively, and D is the diameter of the circular cross section.

Figure 5.14 represents a column strengthened with FRP:

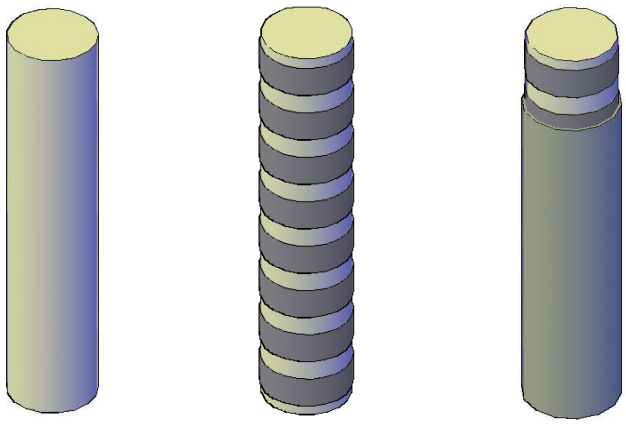

Figure 5.14 Column strengthening details

(a) Original RC column; (b) Confinement with discontinuous FRP strips; (c) Finishing

Rectangular sections

The confinement with FRP of square or rectangular section elements produces only marginal increases of compressive strength. In this case, the confinement of concrete produces an arch effect (Figure 5.15), wherein this effect depends on the rounding radius value of the elements´ corners. It is possible to reach in a confined area value, with good approximation.

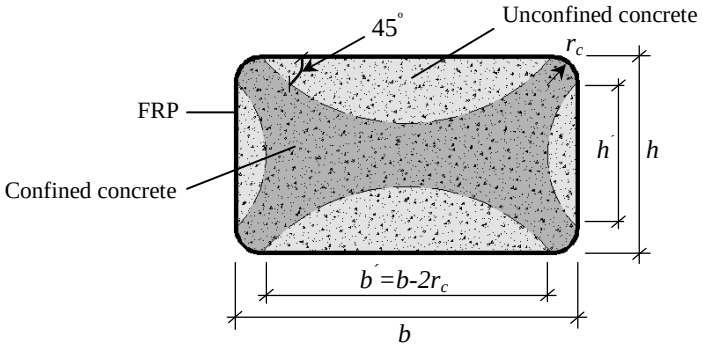

Figure 5.15 Effectively confined core for non-circular sections
(adapted from *fib* Bulletin 14)

For rectangular sections the geometric strengthening ratio, ρ_f, to be used to evaluate the effective confinement pressure may be expressed according Equations 5.25 and 5.26.

For continuous wrapping:

$$\rho_f = \frac{2 \cdot t_f (b+h)}{b \cdot h} \tag{5.25}$$

For discontinuous wrapping:

$$\rho_f = \frac{2 \cdot t_f \cdot (b+h) \cdot b_f}{b \cdot h \cdot p_f} \tag{5.26}$$

Where t_f and b_f are FRP thickness and the width of the strips, respectively. p_f, is the spacing of the strips, b and h are the cross sectional dimensions of the rectangular RC member.

5.6 References

1. ACI 440.2R-08 - Guide for the Design and Construction of Externally Bonded FRP Systems for Strengthening Concrete Structures, American Concrete Institute, 2008.
2. Azeredo, Jeferson da R. Non-Linear Static Analysis (Push-Over) of an existing RC structure and Rehabilitation Intervention. University of *Roma Tre*. Master Thesis (Master in Reinforced Concrete – MICA). Rome, 2010.
3. Bellomo M., D`Ambrosio V., Fibrorinforzati in Architettura. Le Tecnologie FRP e FRCM nel Recupero delle Strutture in C.A. Clean. Napoli, 2010.
4. Circolare 2 febbraio 2009, n. 617. Istruzioni per l'applicazione delle nuove Norme Tecniche per le Costruzioni (NTC), di cui al decreto ministeriale 14 gennaio 2008.
5. CNR-DT 200 R1/2013. Istruzioni per la Progettazione, l'Esecuzione ed il Controllo di Interventi di Consolidamento Statico mediante l'utilizzo di Compositi Fibrorinforzati. Consiglio Nazionale delle Ricerche. Roma, 2013.
6. European Standard EN 1504 "Products and systems for the repair and protection of concrete structures – definitions, requirements, quality control and evaluation of conformity", 2008.
7. Fib Bulletin 14. Externally bonded FRP reinforcement for RC structures. Fib, Fédération internationale du béton / International Federation for Structural Concrete, 2001.
8. Fib Bulletin 24. Seismic assessment and retrofit of reinforced concrete buildings. *Fib, Fédération internationale du béton* / International Federation for Structural Concrete, 2001.

9. NTC 2008, Norme Tecniche per le Costruzioni, Decreto Ministeriale 14 gennaio 2008, Italia.

Chapter VI

Experimental investigation of the mechanical properties of High Performance Fiber Reinforced Cementitious Composites (HPFRCC)

6.1 Scope

This chapter presents the main results obtained by an experimental campaign carried out on HPFRCC, at the Laboratory of Structures of the University of *Roma Tre*.

High Performance Fiber Reinforced Cementitious Composites (HPFRCC) is a class of materials studied extensively for applications in design of new structures and currently in Italy, in structural rehabilitation of existing structures. These materials have high mechanical strength, pseudo strain-hardening behaviour and low porosity due to a highly dense microstructure of the cementitious matrix. Furthermore, they guarantee great durability by adding micro fibers in proper ratio, which limit the crack opening. This means that instead of increasing the width of the cracks, a large deformation with micro-cracks uniformly distributed occurs. This phenomenon makes the use of HPFRCC particularly attractive.

This chapter deals with the mechanical properties assessment of HPFRCC mixtures designed with locally available materials. In particular, different HPFRCC mix designs were considered with a very compact cementitious matrix reinforced with three different types of microfibers: basalt fibers, high density polyethylene fibers and hooked stainless steel fibers (Fig. 6.01), considering 1% or 2% of the volume contents. The influence of the fiber contents on the compressive and tensile strengths, the strain-hardening performance and the fracture energy are discussed.

(a) (b) (c)

Figure 6.01 (a) Basalt micro-fiber; (b) Polyethylene micro-fiber; (c) Hooked Stainless Steel fiber

6.2 General approach

Plain concrete is a brittle material with low tensile strength, to improve these characteristics of the concrete, micro-fibers may be added in the cementitious conglomerate. Besides the contribution in terms of tenacity, the fibers develop an important contribution for a better distribution of cracks in the concrete.

High Performance Fiber Reinforced Cementitious Composites (HPFRCC) is a class of material characterized not only by high strength and low permeability, but also by pseudo-ductility post-cracking behaviour (consequently with high deformability) and development of micro-cracks under tensile stress (Fig. 6.02). These characteristics are achieved due to the highly dense microstructure of cementitious matrix combined with use of micro-fibers that, in adequate proportion can limit the width of the cracks. These materials are obtained by a combination of high strength concrete and short fibers with an improved homogeneity, because traditional coarse aggregates are replaced with fine sand.

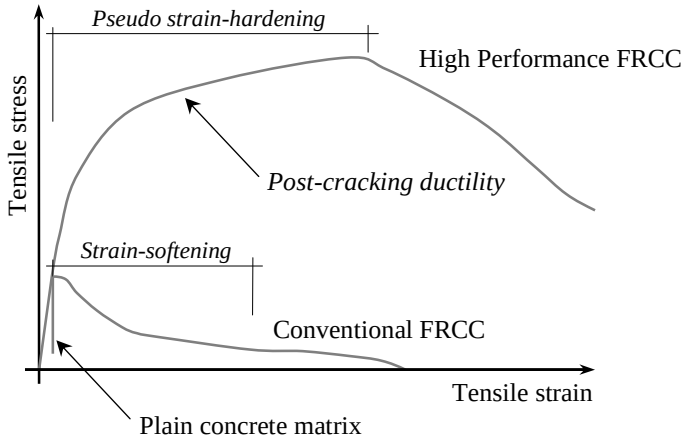

Figure 6.02 Typical stress-strain curves (under tensile stress) for comparison between conventional FRCC and high performance FRCC behaviour

According to "Recommendations for design and construction of HPFRCC with multiple fine cracks (Japan Society of Civil Engineers)[1]", the pseudo strain-hardening behaviour of HPFRCC under direct uniaxial tensile stress is an increase in tensile stress after first cracking (Fig. 6.02). On the other hand, conventional fiber reinforced cementitious composites (FRCC) exhibits a decrease in tensile stress after first cracking that is called strain-softening, as generally seen in cement-based materials such as mortar and concrete.

Other classes of materials with different compositions are studied and developed worldwide, in order to improve the composite's behaviour in relation to mechanical performance and durability.

A comparison of the main mechanical properties of different classes of cementitious composites is presented below:

[1] Concrete Committee, Japan Society of Civil Engineers. Recommendations for design and construction of HPFRCC with multiple fine cracks. Concrete Engineering Series 82, 2008.

Table 6.01: Comparison of mechanical properties of various classes of composites

Material	Composites mechanical properties					
	Compr. Strength (MPa)	First crack strength (MPa)	Ultimate strength (MPa)	Ultimate strain (%)	Elastic modulus (GPa)	Specific energy (kJ/m³)
VHSC	200	8.0	10.0	0.2	50	17
ECC	45	3.5	5.0	3.5	20	148
HSHDC	160	5.7	11.8	3.5	43	305
UHP-FRC	200	6.1	14.9	0.6	53	63
UHP-SHCC	96	6.0	11.0	2.7	32	228

Note: VHSC: Very High Strength Concrete; ECC: Engineered Cementitious Composites; HSHDC: High Strength High Ductility Concrete; UHP-FRC: Ultra High Performance – Fiber Reinforced Composite; UHP-SHCC: Ultra High Performance – Strain Hardening Cementitious Composites; Table adapted from Ranade et al. (2011)[1].

Geometry and mechanical characteristics of fibers and cementitious matrix composition can influence on the behaviour of HPFRCC. The influence of type and amount of fiber on the compressive strength, modulus of elasticity, flexural and tensile strength is presented in this chapter.

Table 6.02 shows the main mechanical properties of the fibers used in cementitious material:

[1] Ranade, R. et al. Development of high strength high ductility concrete. 2nd International RILEM Conference on Strain Hardening Cementitious Composites. Rio de Janeiro, RILEM, 2011.

Table 6.02: Typical mechanical properties of fibers

Fibers	Fibers mechanical characteristics				
	Diameter (μm)	Specific gravity (g/cm^3)	Modulus of elasticity (GPa)	Tensile strength (GPa)	Strain at rupture (%)
Steel	5–500	7.84	200	0.5–2.0	0.5–3.5
Glass	9–15	2.6	70–80	2–4	2–3.5
Asbestos Crocidolite	0.02–0.4	3.4	196	3.5	2.0–3.0
Asbestos Chrysolite	0.02–0.4	2.6	164	3.1	2.0–3.0
Polypropylene	20–400	0.9–0.95	3.5–10	0.45–0.76	15–25
Aramid (kevlar)	10–12	1.44	63–120	2.3–3.5	2–4.5
Carbon (high strength)	8–9	1.6–1.7	230–380	2.5–4.0	0.5–1.5
Nylon	23–400	1.14	4.1–5.2	0.75–1.0	16.0–20.0
Cellulose	—	1.2	10	0.3–0.5	—
Acrylic	18	1.18	14–19.5	0.4–1.0	3
Polyethylene	25–1000	0.92–0.96	5	0.08–0.60	3–100
Wood fibre	—	1.5	71.0	0.9	—
Sisal	10–50	1.5	—	0.8	3.0
Cement matrix (for comparison)	—	1.5–2.5	10–45	0.003–0.007	0.02

Note: Table adapted from Arnon Bentur and Sidney Mindess. Fiber Reinforced Cementitious Composites. 2nd Edition, Canada, 2007.

6.3 Experimental procedure

6.3.1 Materials

Criteria of constituent materials selection used for preparation of HPFRCC, adapted from Nicolaides et al. (2013), are present below:

I. Enhancement of homogeneity by elimination of coarse aggregates;

II. Enhancement of compacted density by utilization of fine granular mixture, i.e. silica fume improves the compacted density of the mix

thereby reducing voids and defects, and Limestone filler improves the plasticity and cohesion of the mixture in fresh state;

III. Low water/cement ratio by inclusion of high range water reducer admixture;

IV. Improvement of thixotropic consistency by inclusion of Thixotropizer admixture;

V. Incorporation of small-sized fibers to enhance ductility (i.e. tenacity);

VI. Although mostly of the HPFRCC in literature has quartz sand in composition due its pozzolanic potential, this material cannot be found in the region of Rome, and in this study it was substituted by limestone sand.

The cement used is Ordinary Portland Cement (OPC) CEM I 52.5 R, provided by Buzzi Unicem Spa. (Italy). This cement contains at least 95% of clinker and up to a maximum of 5% of minor constituents, not considering the additions of calcium sulphate and additives. Silica fume (Addiment Spa., Italy) is used as pozzolanic material, and limestone powder (Buzzi Unicem Spa., Italy) is used as filler. Booth materials were added in volumetric substitution of cement. Limestone sand is used in fraction of 0-1.2mm (Buzzi Unicem Spa., Italy). An acrylic based high-range water reducer (Addiment Spa., Italy) is used to adjust the workability of cementitious composites. A thickener admixture (SIKA) is used to achieve a thixotropic consistency for patching repair. Three different types of small-sized fibers (Fig. 6.03) were used: basalt (HG, China); polyethylene (Honeywell, USA), stainless steel (Bekaert, Italy). The detailed information of used materials is summarized in Tables 6.03 and 6.04.

Table 6.03: List of materials and specific gravity

Material	Specific gravity (g/cm^3)
Portland Cement Type I 52.5	3.16
Silica Fume	2.42
Limestone Filler 0-75 μm	2.76
Limestone Sand 0-1200 μm	2.78
High Range Water Reducing admix.	1.00
Thickener agent	0.96
Shrinkage Reducing admix.	1.10

Table 6.04: Geometry and mechanical properties of the fibers

Fiber	Basalt	Polyethylene	Stainless steel
Notation	B	P	S
Form	Straight	Straight	Hooked
Specific gravity (g/cm^3)	2.63	0.97	7.66
Length (mm)	12	15	30
Diameter (mm)	0.017	0.0042	0.38
Aspect ratio	705.9	3571.4	78.9
Tensile strength (GPa)	3.61	2.57	2
Young's modulus (GPa)	59	73	210

(a) (b) (c)

Figure 6.03 (a) Basalt; (b) Polyethylene; (c) Stainless Steel fibers

6.3.2 Mix design and preparation

For practical and economical feasibility applications[1], it was designed a preliminary mix for a plain cementitious matrix with high volumes of filler substitution with locally available materials. After several trial and error attempts, it was decided to maintain the silica fume and limestone powder proportions in 15% and 20% in volume substitution of cement respectively to reach a minimum water/binder ratio of 0.37. This ratio is likely to have produced a denser and stiffer mix with the desired thixotropic consistency for patching. The derived mixes are presented in Table 6.05 and 6.06.

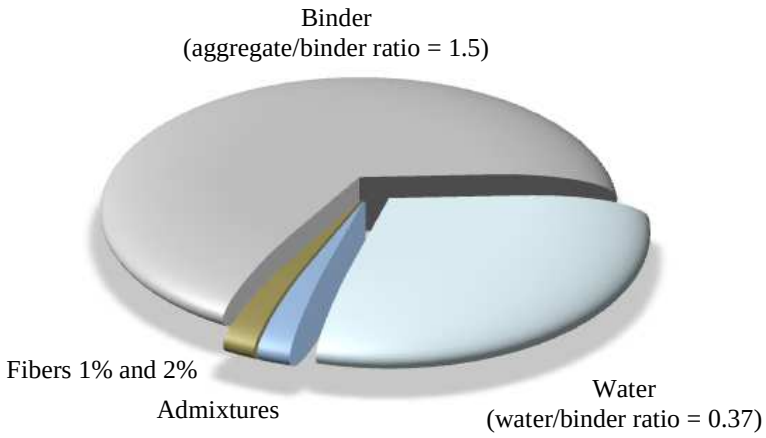

Figure 6.04 General composition of HPFRCC

The mixing procedure was carried out as follows:

1) Cement, Silica Fume and Limestone Filler were dry-mixed for 1 minute, in low velocity;

2) Water pre-mixed with the acrylic-based high range water-reducing admixture was then added, and this paste was mixed for 5 minutes;

3) After a pause of 3 minutes, the mix was resumed for 2 minutes;

4) The sand was added and mixed for 2 minutes;

[1] HPFRCC is considered an expensive material due its high cement content (around 1000 kg/m³).

5) Thickener agent and ant-shrinkage admixture were added and mixed for 2 minutes;

6) For fiber reinforced mixtures, the fibers were added slowly for a good dispersion into the cementitious matrix and then mixed for 2 minutes for a good homogeneity (Fig. 6.05).

To maintain the consistence of the basalt fiber reinforced mixtures, the HRWR admixture was added in 17.4 kg/m³ and 24.5 kg/m³, for basalt fibers incorporation in 1.0 vol.% and 2.0 vol.%, respectively. For others fibers, the HRWR admixture proportion is the same for plain matrix.

(a)

(b)

(c)

Figure 6.05 Preparing of HPFRCC: (a) Composite consistency test; (b) e (c) Molding of the test specimens

Table 6.05: Mixture proportions of binder for HPFRCC (main parameters)

Binder Composition (vol%)		Binder amount	
Portland Cement Type I 52.5	65%	Binder consumption	727.7 kg/m³
Silica Fume	15%	Water/Binder ratio	0.37
Limestone Filler 0-75µm	20%	Aggregate/Binder ratio	1.50

Table 6.06: Mixture proportions of HPFRCC (main parameters)

Mix	R0	B1	B2	P1	P2	S1	S2
Fiber type	-	Basalt		Polyethylene		Stainless Steel	
Fiber volume	0%	1%	2%	1%	2%	1%	2%
Components	**Mass (kg/m^3)**						
Portland Cement Type I 52.5	505.68	498.33	489.93	500.62	495.57	500.62	495.57
Silica Fume	89.32	88.02	86.54	88.43	87.53	88.43	87.53
Limestone Filler 0-75μm	136.07	134.09	131.83	134.70	133.34	134.70	133.34
Limestone Sand 0-1200μm	1279.36	1233.29	1185.12	1239.08	1199.36	1239.08	1199.36
Water	272.29	268.33	263.81	269.57	266.84	269.57	266.84
HRWR admix.	12.64	17.44	24.50	12.52	12.39	12.52	12.39
Thickener agent	5.06	4.98	4.90	5.01	4.96	5.01	4.96
Shrinkage Reducing admix.	5.06	4.98	4.90	5.01	4.96	5.01	4.96
Fiber	0.00	26.30	52.60	9.70	19.40	78.60	157.20

6.3.3 Specimens preparation

The curing was carried out at ambient temperature and humidity and the tests were performed 28 days after preparation of the specimens.

Direct tensile tests on dog-bone specimens (Fig. 6.07), compression tests on cube specimens (Fig. 6.08) and four-point bending tests on small beams (Fig. 6.06) were performed to characterize the material under tension, compression and flexural strength.

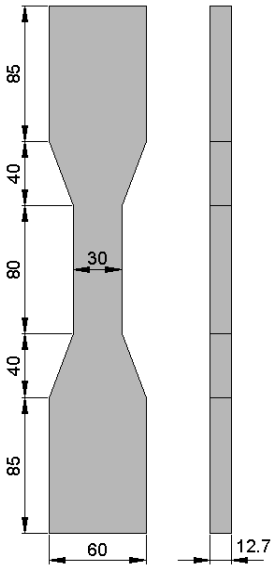

Figure 6.07 Uniaxial tensile test on dog-bone specimen (unit: mm)

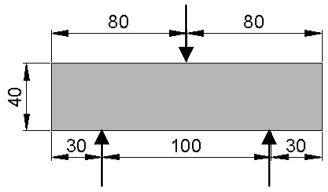

Figure 6.06 Flexural test specimen – thickness = 40 (unit: mm)

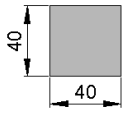

Figure 6.08 Compression test specimen – thickness = 40 (unit: mm)

The specimens were prepared according to standards: EN 12190-3 for compressive strength of 40x40x40mm, cube specimens (Fig. 6.08); EN 1015-11 for flexural strength of 160x40x40mm, quadrangular prism specimens (Fig. 6.06); EN 13412 for evaluation of the longitudinal modulus of elasticity in compression for 160x40x40mm. According to CNR-DT 204/2006[1], the modulus of elasticity just for plain matrix (without fibers addiction) was evaluated.

6.3.4 Test setup

The tests were conducted in the Laboratory of Tests and Experimentations on Structures and Materials of the University of *Roma Tre*, using a universal testing machine MTS (Fig. 6.09) with displacement control. All specimens were tested by

[1] CNR-DT 204/2006. Istruzioni per la Progettazione, l'Esecuzione ed il Controllo di Strutture di Calcestruzzo Fibrorinforzato. Consiglio Nazionale delle Ricerche. Roma, 2006.

adopting the loading system applied by means of a having a load capacity of 500 kN. The tests were carried out at a constant displacement rate of 0.005 mm/s.

Figure 6.09 Universal Testing Machine MTS

The uniaxial tensile test was conducted according to the recommendations of JSCE[1] for the direct displacement-controlled tensile testing of dog-bone samples (Fig. 6.07). The support apparatus[2] for the sample was fixed at both ends according Figure 6.10:

[1] Concrete Committee, Japan Society of Civil Engineers. Recommendations for design and construction of HPFRCC with multiple fine cracks. Concrete Engineering Series 82, 2008.

[2] This support apparatus was manufactured exclusively for carrying out the tensile tests.

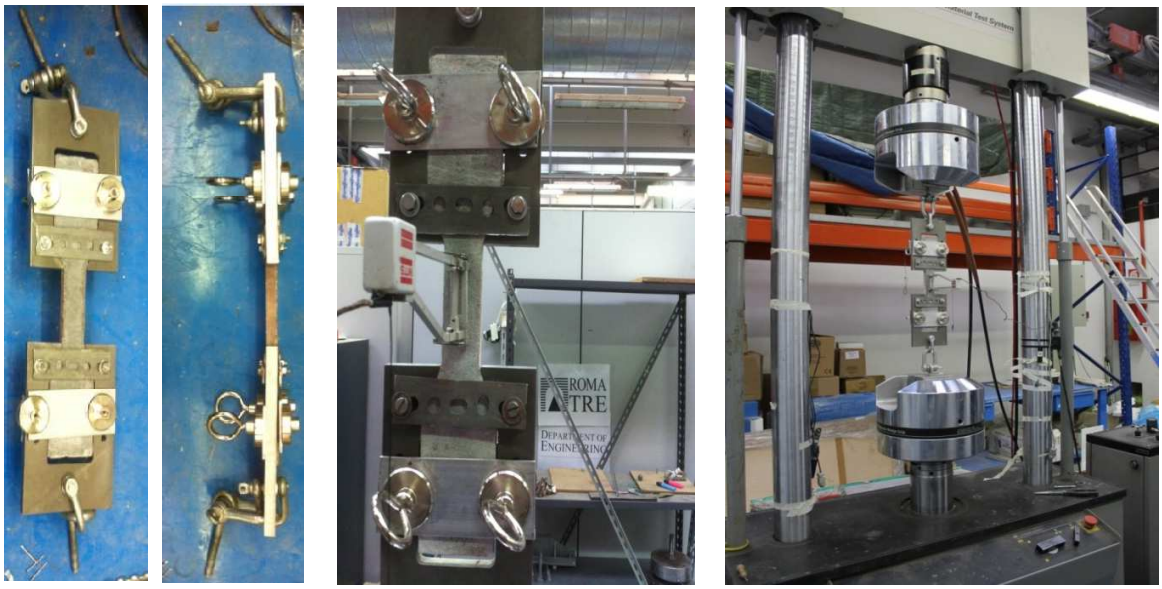

Figure 6.10 Support apparatus for uniaxial tensile test

In the direct tensile tests the dog-bone specimens were tested under quasi-static uniaxial tension loading. The strain in all the dog-bone specimens was computed from the extension of the specimen measured by extensometer mounted parallel to the side edges of the dog-bone specimen (Fig. 6.10).

6.3.5 Results and discussion

The average results of four 40mm cubes under axial compression, three 160x40x40mm prisms under three-point flexure test and six dog-bone specimens tested under direct uniaxial tension for each batch (mix proportions in Table 6.06) are present here. The results are presented following in Table 6.07:

Table 6.07: Tests results: mechanical characteristics of HPFRCCs

Mechanical properties			R0	B1	B2	P1	P2	S1	S2
			Plain cementitious matrix	Basalt (1%)	Basalt (2%)	Polyethylene (1%)	Polyethylene (2%)	Stainless steel (1%)	Stainless steel (2%)
Compressive strength		σ_c (N/mm²)	65.34	60.32	62.73	45.67	45.13	83.60	88.15
Flexural strength		σ_{fl} (N/mm²)	7.64	7.14	10.83	7.65	13.81	25.20	29.37
Uniaxial tensile strength	Yield stress	f_{fy} (N/mm²)	-	-	-	1.89	1.73	3.35	4.40
	Yield strain	ε_{fy} (%)	-	-	-	0.009	0.026	0.015	0.008
	Max. Stress	f_{fm} (N/mm²)	3.04	3.45	6.12	1.98	3.09	4.62	7.26
	Max. strain	ε_{fm} (%)	-	-	-	0.793	0.745	0.357	0.122

The longitudinal elastic modulus of three 160x40x40mm prisms under compression (Fig. 6.11), were determined just for plain cementitious matrix, with the average of the results equal to 26 GPa.

Figure 6.11 Longitudinal elastic modulus test

6.3.5.1 Compressive strength

In Figure 6.13 are presented the results of compressive strength of cubic specimens for each batch of mixtures. The compressive strength of basalt and polyethylene fiber mixtures (B1, B2, P1 and P2) were reduced in 8%, 4%, 30% and 31%, respectively, compared to the plain cementitious matrix (R0). The incorporation of 1 vol.% and 2 vol.% of stainless steel fibers improved the compressive strength in 28% and 35%, respectively.

Figure 6.12 Compressive strength test

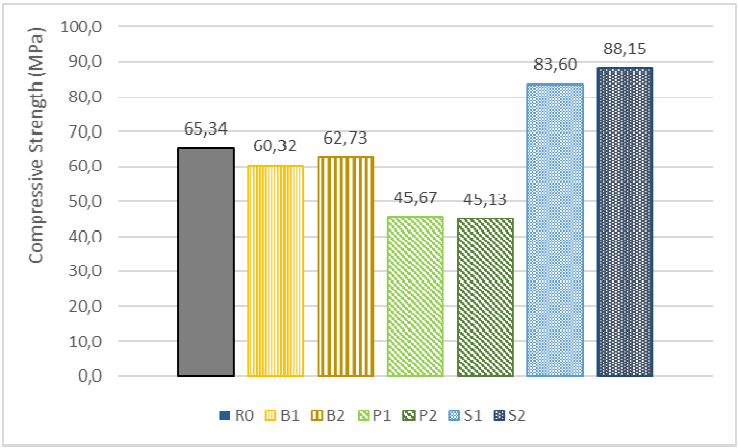

Figure 6.13 Compressive strength results

6.3.5.2 Flexural strength

The incorporation of 1 vol.% of basalt (B1) and polyethylene (P1) fibers maintained the flexural strength close to the results of the plain cementitious matrix (R0). Mixtures with incorporation of 1 vol.% of stainless steel (S1) fibers presented flexural strength 230% higher than plain cementitious matrix (R0). The incorporation of 2 vol.% of basalt (B2), polyethylene (P2) and stainless steel (S2) fibers increased the flexural strength in 42%, 82% and 285%, respectively. These results are presented in Figure 6.14.

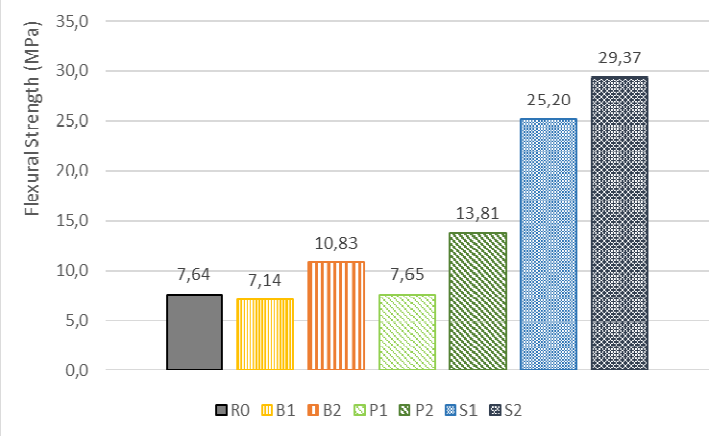

Figure 6.14 Flexural strength results

It was observed the pseudo ductile failure mode (Fig. 6.15) of polyethylene (P1 and P2) and stainless steel (S1 and S2) fiber reinforced mixtures, while the other mixtures presented brittle behaviour in this test.

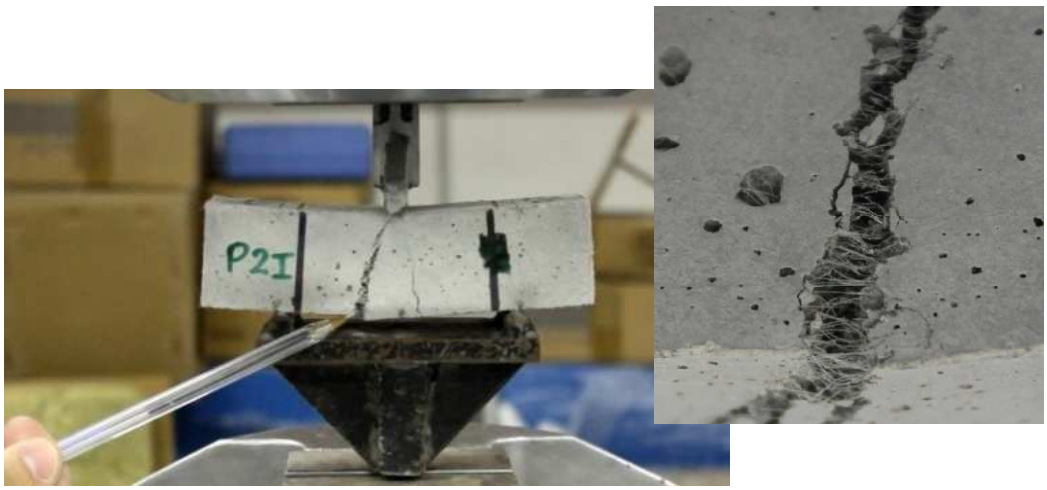

Figure 6.15 Flexural test on HPFRCC with 2 vol.% of polyethylene fiber
Pseudo ductile failure mode

6.3.5.3 Uniaxial direct tensile strength

The uniaxial direct tensile test results of the samples of each fiber reinforced mixture (1 and 2 vol.%) are presented in Figure 6.16. These tests presented strength increases for basalt (B1 and B2) and stainless steel (S1 and S2) fibers mixtures, compared with plain cementitious matrix (R0) results. The higher results were achieved with 2 vol.% incorporation of basalt fibers (6.12 MPa) and stainless steel fibers (7.26 MPa). The incorporation of 1.0 vol.% of polyethylene fibers (P1) reduced the axial tensile strength in 35%, and 2 vol.% (P2) increased 2%, compared with plain cementitious matrix (R0) results.

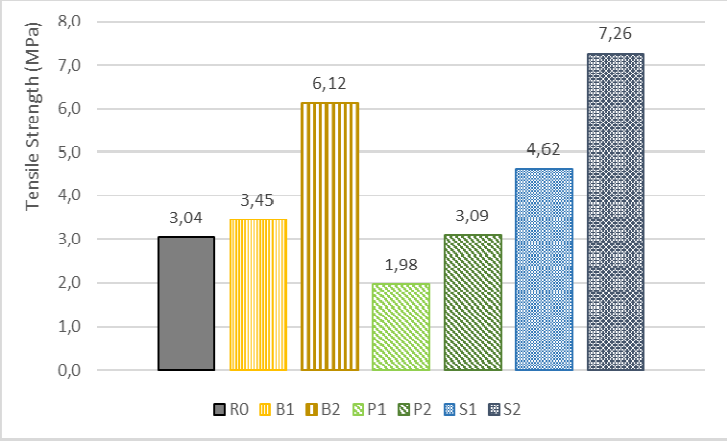

Figure 6.16 Uniaxial direct tensile strength results

Figure 6.17 shows cracks opening of dog-bone specimen (HPFRCC with polyethylene fiber, vol. 1%) under uniaxial tensile test and corresponding force-displacement graph (in real-time during the test). In these test, a large deformation of the specimen with uniformly distributed fine cracks was observed.

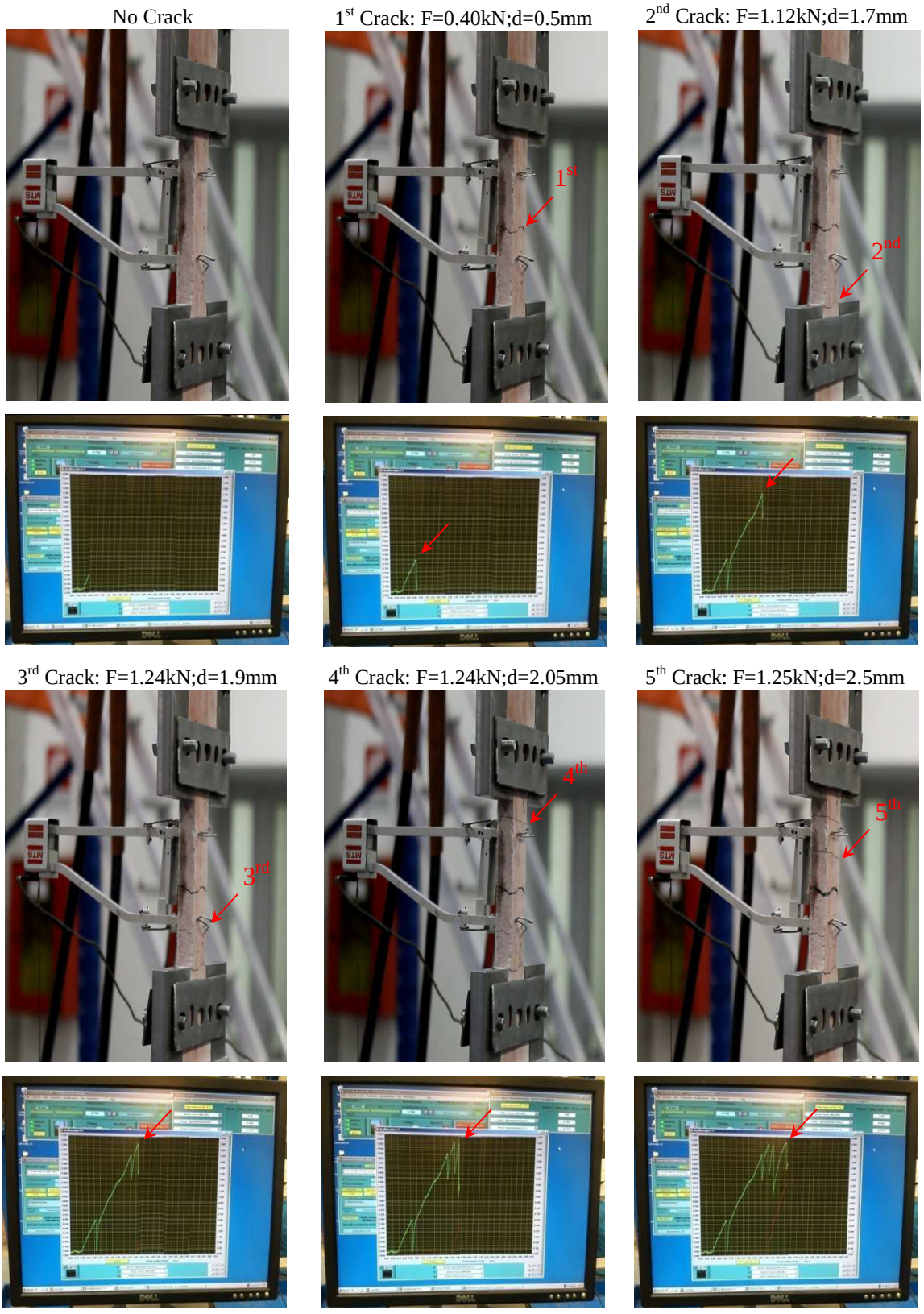

Figure 6.17 Force-displacement graph showing crack opening contemporaneously

The figures below (Fig. 6.18 and 6.19) show the behaviour of three selected samples of HPFRCC with vol.1% of basalt, polyethylene and stainless steel fibers, respectively, subjected to direct tensile test.

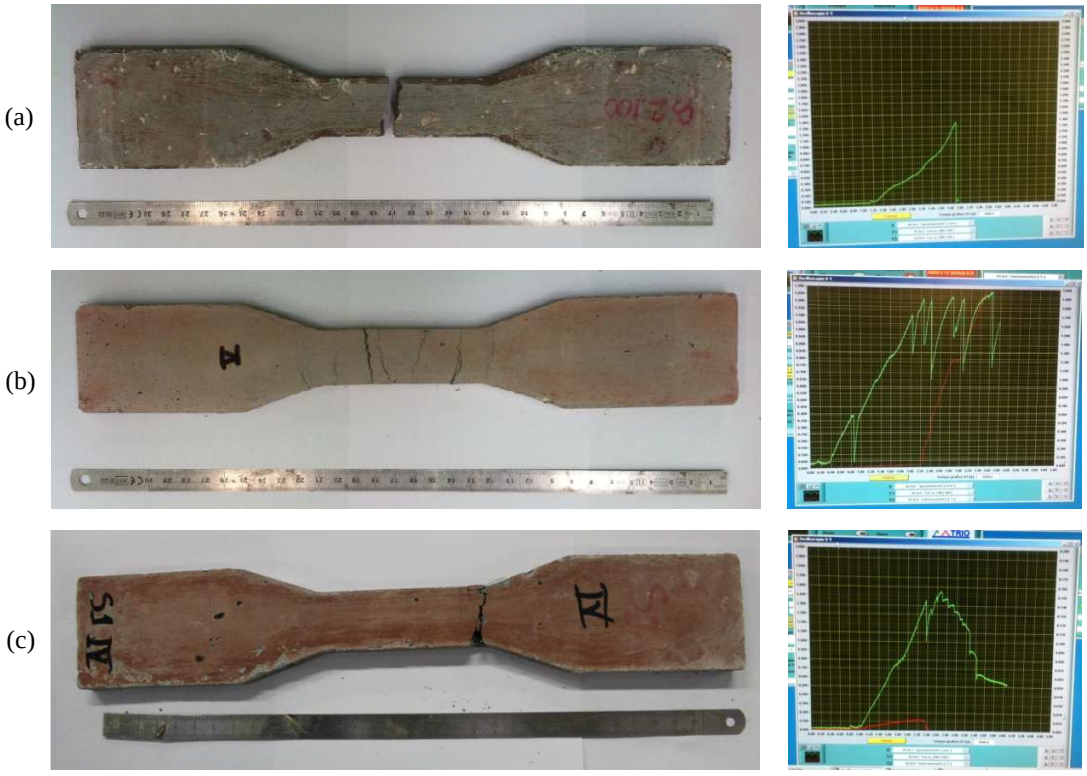

Figure 6.18 Dog-bone specimen after tests and force-displacement graphs from universal testing machine MTS (a) Basalt micro-fiber; (b) Polyethylene micro-fiber; (c) Hooked Stainless Steel fiber

In the first case (a) with basalt micro-fibers, the test was finished with the total rupture of the specimen. Its behaviour was characterized as brittle rupture mechanism in a single point, similar to the behaviour of plain concrete. Universal testing machine MTS recorded a maximum force of 1.40kN and corresponding control displacement of 1.70mm, at the end of the test.

In the second case (b) with polyethylene micro-fibers, the test was interrupted before specimen rupture, with a maximum force of 1.28kN and corresponding control displacement of 3.30mm. This sample showed an increase on the tenacity

of the composite, with a predominantly strain-hardening post-cracking behaviour and evenly distributed fine cracks. In this case it was possible to measure approximately the average crack width (equal to 0.4mm).

The third case (c), reinforced with hooked stainless steel short fibers, showed almost fragile and strain-softening post-cracking behaviours, with cracking concentrated in a single part of the specimen. The test was discontinued prior to the total rupture of the specimen, with a maximum force of 1.57kN and corresponding control displacement of 1.63mm.

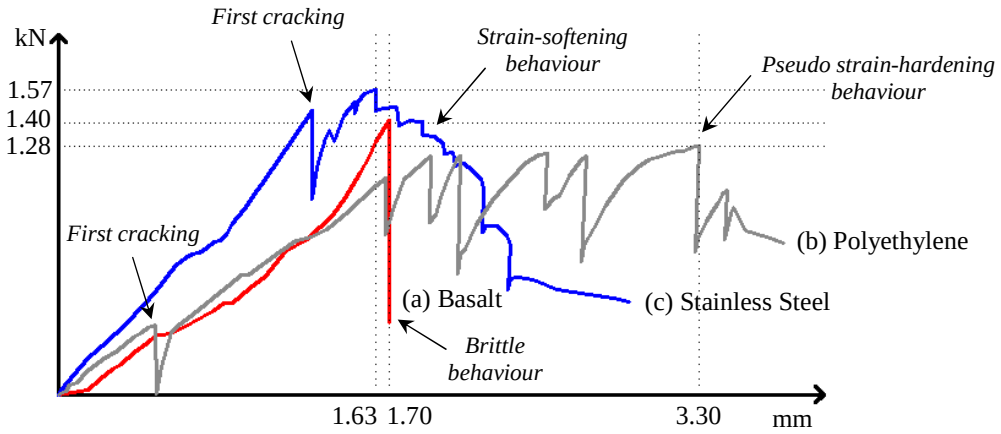

Figure 6.19 Force-displacement curves from uniaxial direct tensile test, for comparison between HPFRCC behaviours (fibers vol. 1%)

Table 6.08: Characteristics of HPFRCC under uniaxial direct tensile test

Characteristics		Fibers (vol. 1%)		
		Basalt	**Polyethylene**	**Stainless steel**
Rupture mechanism		Brittle	Predominantly pseudo ductile	Predominantly brittle
Post-cracking behaviour		-	Pseudo strain-hardening	Strain-softening
Cracking		Rupture	Uniformly distributed fine cracks	Cracks concentrated in a single part
Deformability		-	High	Medium
Tenacity		-	High	Low
Force-displacement First cracking	(kN)	1.40	0.39	1.45
	(mm)	1.70	0.50	1.32
	Stiffn.	0.82	0.78	1.10
Force-displacement Maximum strength	(kN)	1.40	1.28	1.57
	(mm)	1.70	3.30	1.63
	Stiffn.	0.82	0.39	0.96

6.4 References

1. Arnon Bentur and Sidney Mindess. Fiber Reinforced Cementitious Composites. Modern Concrete Technology Series, 2nd Edition, Canada, 2007.
2. CNR-DT 204/2006. National Research Council. Guide for the Design and Construction of Fiber-Reinforced Concrete Structures. Rome, CNR, 2007.
3. Concrete Committee, Japan Society of Civil Engineers. Recommendations for design and construction of HPFRCC with multiple fine cracks. Concrete Engineering Series 82, 2008.
4. EN 13412:2006. Europe Standard. Products and systems for the protection and repair of concrete structures. Test methods. Determination of modulus of elasticity in compression.

5. EN 1015-11:1999. Europe Standard. Methods of test for mortar for masonry. Determination of flexural and compressive strength of hardened mortar.
6. EN 12190-3:1999. Europe Standard. Products and systems for the protection and repair of concrete structures. Test methods. Determination of compressive strength of repair mortar.
7. Kamal, A.; Kunieda, M.; Ueda, N.; Nakamura, H.; Evaluation of crack opening performance of a repair material with strain hardening behaviour. Cement & Concrete Composites, 2008.
8. Kim S.W.; Park W.S.; Jang Y.I.; Feo L.; Yun H.D.; Crack damage mitigation and shear behaviour of shear-dominant reinforced concrete beams repaired with strain-hardening cementbased composite, Composites Part B, 2015.
9. Nicolaides, D.; Kanellopoulos A.; Christou, A.M.P. Development of UHPFRCC with the use of materials available in Cyprus. FIB Symposium. Prague, FIB, 2011.
10. Ranade, R.; Stults, M.D.; Li, V.C.; Rushing, T.S.; Roth, J.; Heard, W.F. Development of high strength high ductility concrete. 2nd International RILEM Conference on Strain Hardening Cementitious Composites. Rio de Janeiro, RILEM, 2011.
11. Ranade, Victor C. Li, Michael D. Stults, William F. Heard, and Todd S. Rushing. Composite Properties of High-Strength, High-Ductility Concrete. ACI Materials Journal/July-August 2013. Title no. 110-M37.
12. Salvador Filho, J. A. A., Nuti, C., Santini, S., Lavorato, D., Azeredo, Jeferson da R. Mechanical properties of hpfrcc reinforced with different types and volumes of fibres. Anais do 58º Congresso Brasileiro do Concreto, CBC2016 – 58CBC2016.
13. Salvador Filho, J. A. A., Nuti, C., Santini, S., Lavorato, D., Azeredo, Jeferson da R. Mechanical properties assessment of High Performance Fibre Reinforced Cementitious Composites with different types and volumes of fibres. Draft for Global Civil Engineering Conference 2017.

14. Salvador Filho, J. A. A., Nuti, C., Santini, S., Lavorato, D., Azeredo, Jeferson da R. Modelling of reinforced concrete circular section column repaired with HPFRCC and confined with FRP. Draft for Global Civil Engineering Conference 2017.
15. Vitek, J.L.; Coufal, R.; Citek, D.; UHPC – Development and Testing on Structural Elements. Procedia Engineering 65, 2013.
16. Wille, K.; El-Tawil, S.; Naaman, A.E.; Properties of strain hardening ultra high performance fiber reinforced concrete (UHP-FRC) under direct tensile loading. Cement & Concrete Composites 48, 2014.
17. Yu, R.; Spiez, P.; Brouwersmh .J.H.; Mix design and properties assessment of Ultra-High Performance Fibre Reinforced Concrete (UHPFRC). Cement and Concrete Research 56, 2014.

Chapter VII

Numerical investigation for RC structures rehabilitation with HPFRCC[1] and FRCM[2] techniques

7.1 Purpose

This Chapter presents a numerical investigation to evaluate the behaviour of reinforced concrete elements, damage due to deterioration (or to seismic actions) of concrete and steel materials, repaired and strengthened by high performance fiber reinforced cementitious composites (HPFRCC) and fiber reinforced cementitious matrix (FRCM).

In the numerical tests, different HPFRCC mix design were considered to repair the elements case studies (column and beam), assuming different fiber types (basalt, polyethylene and stainless steel) and volumes contents 1% or 2%. The HPFRCC used as repair material were developed and tested experimentally in the laboratory of structures and materials of the University of *Roma Tre* (explained in Chapter VI), whereas the FRCM properties were assumed by commercial products specifications.

7.2 *A Noite* Building: Case study for numerical investigation

7.2.1 Scope

This item deals with the assessment of a degraded heritage structure pertaining to the *A Noite* building (explained with more detail in Chapter II) based on the procedures previously described in the present thesis. The purpose of this

[1] High Performance Fiber Reinforced Cementitious Composites.

[2] Fiber Reinforced Cementitious Matrix.

assessment is to apply the knowledge acquired during the PhD studies to conduct a preliminary evaluation of structural performance of the building case study, relating to its current condition, state of structural deterioration and residual life as well as its bearing capacity.

As seen in this thesis the international standard ISO 13822 recommends that the bearing capacity of particular supporting members be specified, taking into account actual loads and material properties including the influence of structural degradation. In this line of study was carried out a preliminary inspection in the *A Noite* building (Figures 7.01 and 7.02) during the PhD study mission (in July and August 2014), for a verification of the real state of the structure and to examine the available data about the building and its structure. The data relating to the others designs, documents on the history of the building, its construction and the changes occurred over time have been also investigated.

Figure 7.01 Front façade of the building (photo taken in July 2014)

Figure 7.02 Lateral façade of the building (photo taken in July 2014)

7.2.2 Description of the *A Noite* building

As described in the Chapter II *A Noite* building was built in *Mauá* square, port zone in the center of Rio de Janeiro between 1926 and 1929. With 24 floors[1] and 102.8 meters high was in its inauguration the tallest in Latin America and the world's tallest in reinforced concrete. The building was a symbol of the city which with the monument to *Cristo Redentor* and *Pão de Açúcar*, was visited by large number of travelers who came to Rio. On October 5, 2012, the 83 years-old building joined the list of Historical and Artistic Heritage[2], being inscribed in the books Historical and Fine Arts of the National Institute of Historical and Artistic Heritage IPHAN (Decree n.18,995 – Process n.1648). Among the main reasons why the *A Noite* building was protected is its significance to the history of the Brazilian media, its architectural value associated with the city verticalization process of Rio de Janeiro, and the importance the building has to engineering structures in Brazil and in the world.

The building was designed for office use, currently the direction of the building belongs to the *Instituto Nacional de Propriedade Industrial* (INPI) and its purpose is suitable for administrative use. In July 2014 the building was inactive and awaiting restoration work as well as adequacy of the structure to the safety standards.

The building itself consists of basement, ground floor, 1st floor, standard floors, roof and attic accessible for people (Figure 7.05).

The structure has symmetry in plan (rectangular floor plan of 67m x 18.5m), is formed by conventional beam-column frames and closing with brick masonry in the interior and exterior. As part of the support system wall-pillars until the 14th floor, in the transversal direction of the building[3], have been inserted (Fig. 7.03).

[1] Initially planned with 22 floors, then it had an increase of over 2 floors, but not served by lifts.

[2] Available in < http://portal.iphan.gov.br/uploads/ckfinder/arquivos/Lista_Bens_Tombados_marco_2016.pdf >, accessed in May 09, 2016.

[3] Vasconcelos, Augusto Carlos de. *O Concreto no Brasil*. São Paulo, Pini (1992).

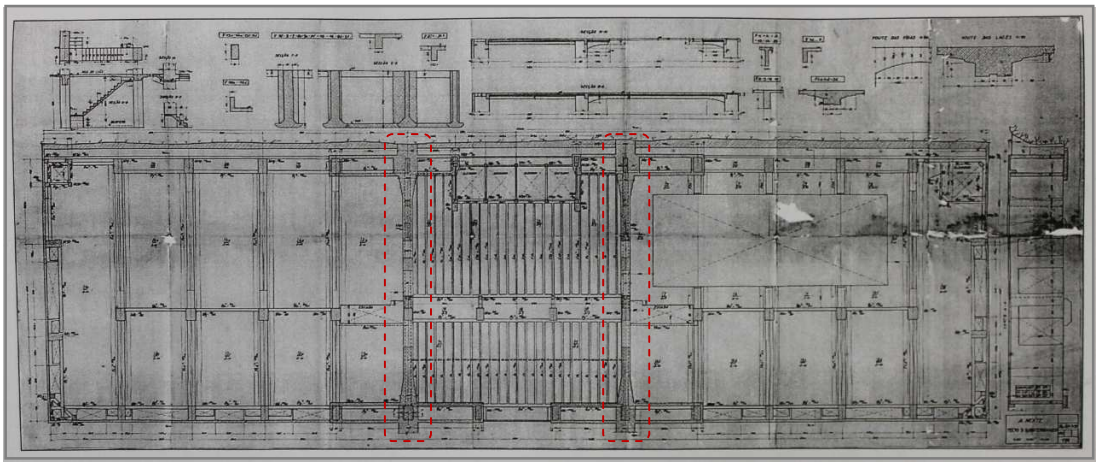

Figure 7.03 Wall-pillars in the most requested direction for wind actions
(copy of the original structural design)

7.2.3 Preliminary inspection

In July 2014 was carried out a preliminary inspection with visual examination, photos of various points of structural degradation, in the interior and exterior of the building, were taken. Figures 7.04 and 7.05 show visible points of concrete spalling and reinforcement corrosion[1], some in advanced process with loss of cross-section probably caused due to presence of moisture in the slab. The nature of the damages does not exclude the possibility of chloride attack (according to the Brazilian standard the building is located in a high environmental aggressiveness zone – marine zone n. III). Inadequate concrete covers in the damaged parts were also identified (at odds with the current standards).

[1] The RC structures may lose its bearing capacity due to reinforcement corrosion.

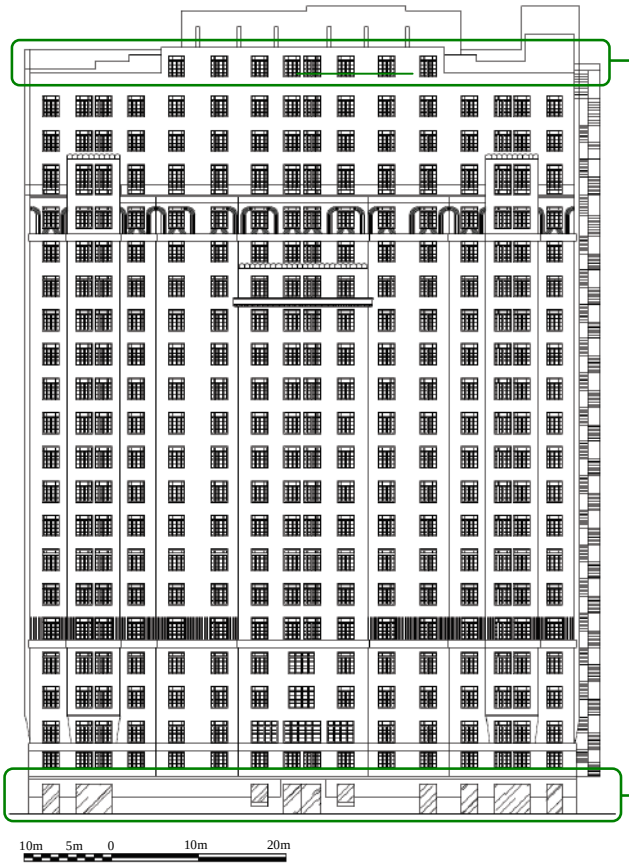

Figure 7.05 Main façade design

Figure 7.04 (a) Roof floor: damaged RC beam by reinforcement corrosion, in advanced state with loss of bars cross-section and concrete spalling

Figure 7.04 (b) Ground floor: damaged RC beam and slab by reinforcement corrosion and concrete spalling

7.2.4 Reference element for numerical investigation

Numerical simulation of reinforced concrete beam damaged by corrosion was performed to evaluate the performance level in terms of bearing capacity. The investigation was carried out by numerical example of a damaged beam located in the roof floor of the *A Noite* building (Fig. 7.06).

Figure 7.06 Damaged RC beam by reinforcement corrosion, in advanced state. With loss of longitudinal bars cross-section, transverse reinforcement broken and loss of concrete cross-section by spalling

To carry out the preliminary inspection inside the building only a visual inspection was allowed, for that reason it was not possible to obtain more details of materials and dimensions of the structural elements, as well as the level of degradation and depth of reinforcement corrosion. Thus, to achieve an approximate preliminary study on the analyses of performance evaluation of the degraded structure, estimated values for the beam section, diameter of longitudinal bars and cross-sectional loss were used. The same applies to material mechanical properties, as shown in Table 7.01.

In the analysis, a rectangular section of 350mm in height and 150mm in width was used, with two longitudinal bars of diameter 12mm ($D_s = 12mm$) provided as the bending rebar (bottom reinforcement), clear cover thickness C = 15mm and transverse reinforcement of diameter D_{st} = 5mm is provided at 200mm spacing. The compressive strength of concrete f_{cm} = 20MPa with modulus of elasticity $E_c = 22.36GPa$ ($E_c = 5{,}000\sqrt{f_{cm}}$) and tensile strength $f_{ctm} = 2.21MPa$ ($f_{ctm} = 0.30 \cdot f_{ck}^{\frac{2}{3}}$). The yield strength of longitudinal reinforcing steel f_{yk} = 500MPa and transverse reinforcing steel f_{yk} = 500MPa, with modulus of elasticity E_s = 200GPa and steel density ρ_s = 7850kg/m^3.

Table 7.01: Key information of the beam section and materials

Concrete						Longitudinal bars				Transverse bars			
W (mm)	*H* (mm)	*C* (mm)	f_{cm} (MPa)	f_{ctm} (MPa)	E_c (GPa)	*Ds* (mm)	*n*	f_{yk} (MPa)	E_s (GPa)	*Dst* (mm)	*s* (mm)	f_{yk} (MPa)	E_s (GPa)
150	350	15	20	2.21	22.36	12	2	500	200	5	200	500	200

Note: W = section width; H = section height C = concrete cover thickness; f_{cm} = concrete cylinder strength; f_{ctm} = concrete tension strength; E_c = elastic modulus of concrete; D_s = diameter of longitudinal bars; n = number of longitudinal steel bars; f_{yk} = yield stress of steel bars; E_s = elastic modulus of steel; D_{st} = diameter of transverse steel bars; s = spacing of transverse steel bars.

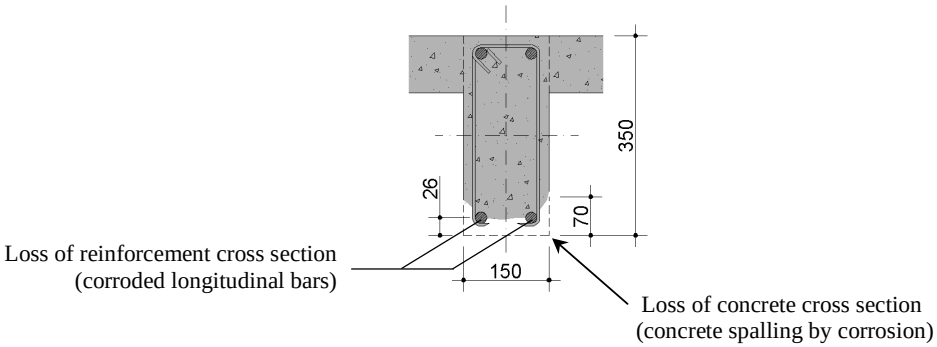

Figure 7.07 Damaged RC beam section by reinforcement corrosion

7.2.5 Evaluation of residual capacity of the corroded bars

Reduction of yield strength by Du et al. model

To evaluate the residual capacity of corroded reinforcement, a cross-section loss of 10% was considered. According Du et al. (2005) the amount of corrosion Q_{corr} can be determined by using Equation (7.01):

$$Q_{corr} = 1 - (d_s/d)^2 = 1 - (10.8/12)^2 = 19\% \quad (7.01)$$

Where, d_s is the diameter of corroded reinforcement and d is the diameter of non-corroded reinforcement. Once the amount of corrosion is known, the residual capacity of corroded reinforcement can be estimated using Equation (7.02):

$$f = (1.0 - \beta \cdot Q_{corr}) f_0 = (1.0 - 0.005 \cdot 19) \cdot 500 = 452.5\ N/mm^2 \qquad (7.02)$$

Where f and f_0 are yield stresses of corroded and non-corroded reinforcement, respectively. The value of β is 0.005 for mean stress (stress based on average reduced cross section area).

7.2.6 Numerical model

The numerical model used to evaluate the structural behaviour of the reference element is based in the theory of finite element method (FEM) where the analysis of the non-linear behaviour of a rectangular reinforced concrete (RC) section is conducted through fiber modeling for steel-concrete composite.

A beam-column fiber section (Fig. 7.08) divided into several parts (fibers) under bending stress was analyzed numerically using *Opensees* software[1] framework. A non-linear static analysis (Push-Over analysis) was carried out considering geometry, efforts and constraints of the rectangular beam section. The damage to the beam due to deterioration of concrete and reinforcement were introduced into the model. The moment-curvature and axial force-deformation characteristics and their interaction are numerically determined, applying vertical load on the section and a deformation history (section rotation) to evaluate the corresponding moment-rotation behaviour.

[1] OpenSees structural software [Computer software]. Berkeley, CA, Pacific Earthquake Engineering Research Center, Univ. of California.

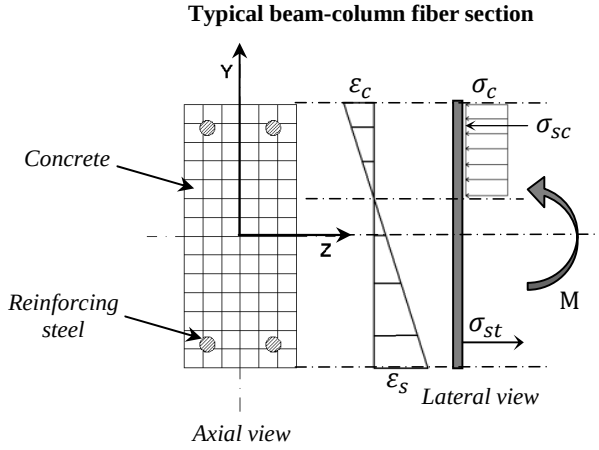

Figure 7.08 FEM model in OpenSees: fiber section model for steel-concrete

7.2.6.1 Numerical modeling details

The UniaxialSection element, which is a fiber section beam-column element available in *OpenSees* that considers both biaxial flexure and axial nonlinear behaviour, was employed in the present numerical simulations. The section is transversely represented using two Uniaxial Materials for concrete and steel. The discretization of section is illustrated in Figure 7.08, where fourteen horizontal and six vertical divisions were employed for the concrete section. This level of discretization is used to lead accurate results based on a convergence study not reported here. The UniaxialMaterial Hysteretic model available in *OpenSees* was used for concrete core and concrete cover. The UniaxialMaterial Hysteretic model was also used to predict the responses of steel reinforcement. For the parts of deteriorated section, the UniaxialMaterial Hysteretic model for steel was used considering the mechanical characteristics obtained from the evaluation of residual capacity of the corroded bars previously calculated.

7.2.7 Numerical tests

Two numerical models are considered in order to assess the performance level of the beam case study: the original condition and the current condition considering

the concrete and reinforcement degradation (Fig. 7.09). In the analyses the transversal reinforcement was neglected, so the concrete core strength was considered equal to the concrete cover. The contribution of the flanges (top of the t-shaped cross-section) in the compressed zone of the beam was not considered. For the reproduction of the mechanical characteristics of the corroded longitudinal reinforcement, the results of the evaluation of residual capacity of the corroded bars were previously calculated according Du et al. model, shown in Table 7.03.

The concrete mechanical characteristics were defined as described in the Table 7.02:

Table 7.02: Concrete mechanics characteristics

	Mechanical characteristics to compression				Mechanical characteristics to Tension			
	f_c (MPa)	f_{cu} (MPa)	ε_c (%)	ε_{cu} (%)	f_{ct} (MPa)	f_{ctu} (MPa)	ε_{ct} (%)	ε_{ctu} (%)
Concrete	20	17	0.20	0.35	2.21	0.00	0.01	0.03

Note: f_c = concrete cylinder strength; f_{cu} = ultimate concrete cylinder strength; ε_c = axial compressive concrete strain; ε_{cu} = ultimate compressive concrete strain; f_{ct} = concrete tension strength; f_{ctu} = ultimate concrete tension strength; ε_{ct} = tension concrete strain; ε_{ctu} = ultimate concrete strain.

The steel mechanical characteristics for uncorroded and corroded bars were defined as described in the Table 7.03:

Table 7.03: Steel mechanical characteristics for longitudinal bars

	Steel mechanical characteristics		
	D (mm)	f_{sy} (MPa)	f_{sm} (MPa)
Uncorroded bars	12.0	500	550
Corroded bars	10.8	452.5	477.6

Note: D = diameter of bar (mean for the corroded bars); f_{sy} = yield stress of steel bars; f_{sm} = steel maximum stress.

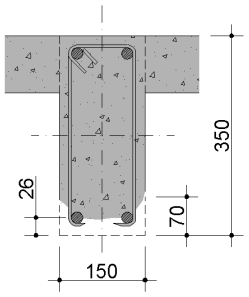

Figure 7.09 Current cross section of the deteriorated beam

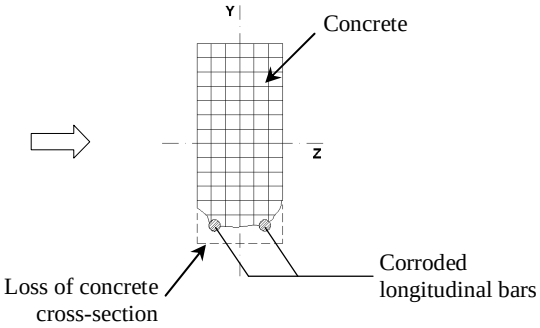

Figure 7.10 FEM model in OpenSees: fiber section model for steel-concrete (considering RC deterioration)

7.2.7.1 Push-Over analysis

Push-over is a common analysis procedure to investigate the non-linear behaviour of a structure and perform a structural design. In the last decades, there has been a growing interest in adaptive pushover analyses from the scientific and professional community. In *OpenSees* software this analysis is being increasingly implemented, even though the user must develop your own code.

The models previously explained were written into the *OpenSees* in a Tcl programming language (Tool Command Language). Then a series of non-linear static analyses (Push-Over) were conducted for the given reinforced concrete sections (damaged and undamaged) applying a vertical load of 22kN on the sections and deformation history (section rotation) with a number of increments equal 100.

The analyses of the section were terminated when the predicted stress-strain for the materials were achieved. In Figure 7.11 the fiber section curves are reported around the axis Z direction.

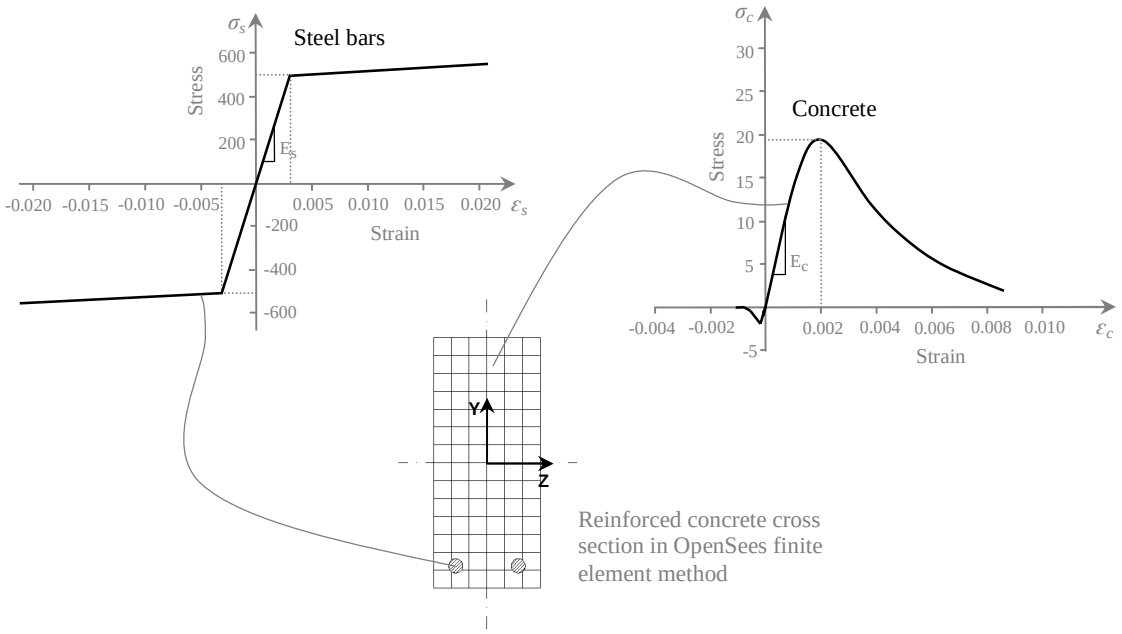

Figure 7.11 Stress-Strain behaviour of the materials under a Push-Over analysis

7.2.7.2 Tests results comparison

In order to assess the performance loss of the analyzed damaged RC section, a comparison to evaluate the corresponding moment-rotation behaviour is reported in Figures 7.12. The moment-rotation consists of four characteristics points: the cracking, yielding, maximum and collapse points. According to the described assumptions, moment-rotation curves for the beam cross-section were obtained considering original condition, current condition (deteriorated) and a future condition (deteriorated in 2 years[1]).

[1] To estimate the remaining service life of the beam, an annual mean of corrosion current density of 10 $\mu A/cm^2$ was considered.

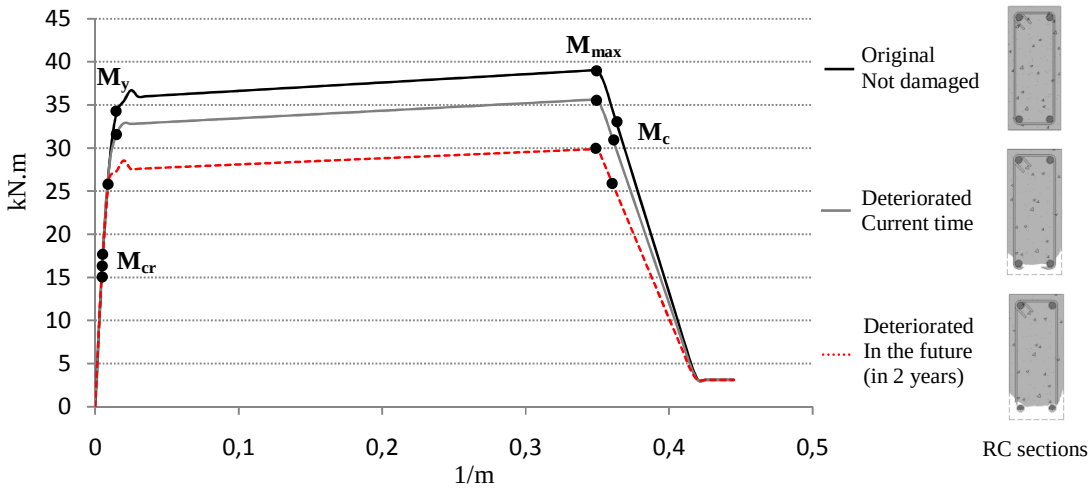

Figure 7.12 Moment-rotation capacity curves of the beam section to assessment of the structural performance level

Table 7.04: Comparison between the three sections

Beam section	Moments of the beam section				
	M_{cr} (kN.m)	M_y (kN.m)	M_{max} (kN.m)	M_c (kN.m)	F_p
Original Not damaged	17	34	39	33	1.00
Deteriorated Current time	16	32	36	31	0.92
Deteriorated in 2 years	15	26	30	26	0.77

Note: M_{cr} = Cracking Moment; M_y = Yielding Moment; M_{max} = Maximum Moment; M_c = Collapse Moment; F_p = Performance Factor (in relation to the Maximum Moment of the original section - not damaged).

7.2.8 Rehabilitation of the beam with HPFRCC technique

7.2.8.1 Multilinear-hysteretic simplified model for HPFRCC

To predict the responses of the strengthened beam with HPFRCC, in terms of flexural strength, on the parts of deteriorated section (Fig. 7.10), UniaxialMaterial Hysteretic model available in OpenSees was used. In order to simplify the numerical analyses performed in finite element software with fiber modeling, the

multilinear-hysteretic model is proposed. The HPFRCC material was used considering the mechanical characteristics obtained from the experimental investigation (explained in Chapter VI) where the values of the force-displacement curves from the test results were written into multilinear-hysteretic simplified models.

This model is basically composed of three straight lines. The first one represents the elastic behaviour of HPFRCC material (which practically maintains the initial stiffness of the original model). The other ones represent different behaviours depending on the fiber type used in the HPFRCC mixtures. For example, polyethylene micro-fibers may represent a pseudo strain-hardening behaviour (Figure 7.14), hooked stainless-steel short fibers a strain-softening behaviour (Figure 7.15) and basalt micro-fibers a linear elastic behaviour until the rupture (similar to the behaviour of plain concrete, Figure 7.16).

The figures below show the construction of the lines representing the hysteretic behaviour of the HPFRCC material under tensile forces, for: basalt, polyethylene and stainless steel fibers (vol. 1%).

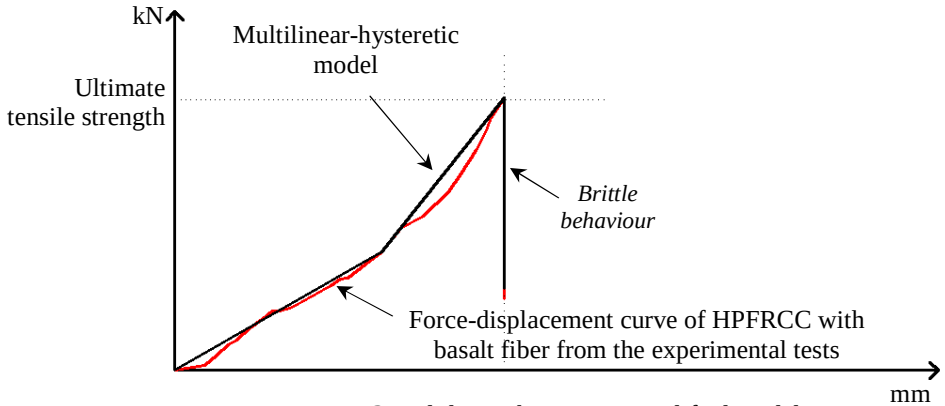

Figure 7.13 Multilinear-hysteretic simplified model for tensile strength of HPFRCC with basalt micro-fiber

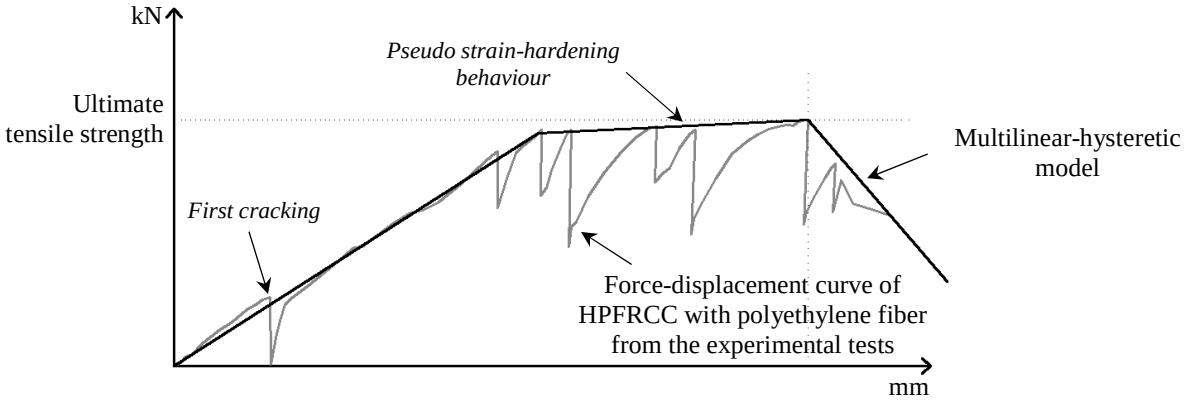

Figure 7.14 Multilinear-hysteretic simplified model
for tensile strength of HPFRCC with polyethylene micro-fiber

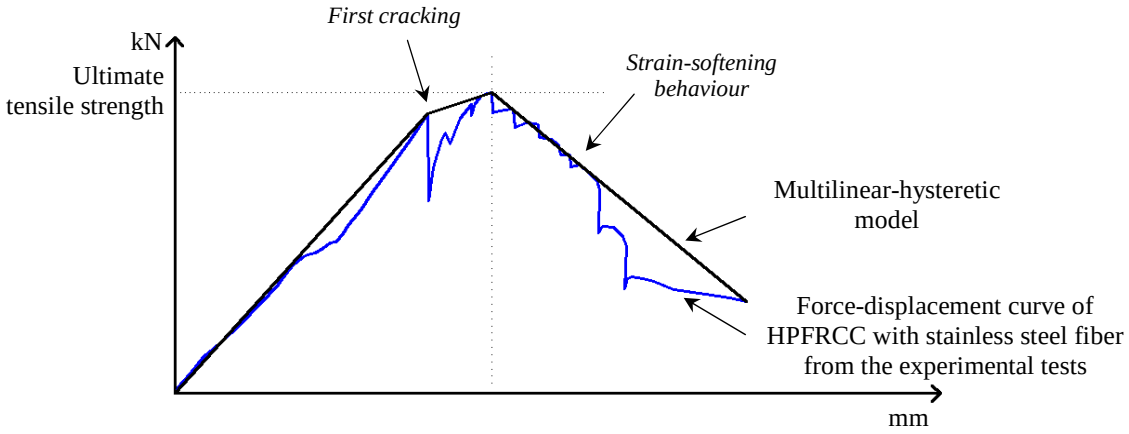

Figure 7.15 Multilinear-hysteretic simplified model for tensile
strength of HPFRCC with hooked stainless-steel short fibers

7.2.8.2 Numerical tests and results comparison

Six numerical models were built in order to assess the performance level of the rehabilitated beam with HPFRCC, considering three cited fiber types in the mixture, with 1% and 2% of volume. Where two strengthening hypotheses were considered:

the first with a HPFRCC layer of 3.5 cm (Fig. 7.16) and the second with 7.0 cm (Fig. 7.20).

The mechanical characteristics for HPFRCC were defined as described in the Table 7.05:

Table 7.05: HPFRCC mechanics characteristics

HPFRCC		Compression mechanical characteristics				Tension mechanical characteristics			
		f_{fci} (MPa)	f_{fcm} (MPa)	ε_{fci} (%)	ε_{fcm} (%)	f_{fty} (MPa)	f_{ftm} (MPa)	ε_{fty} (%)	ε_{ftm} (%)
Basalt	fiber 1%	15.02	50.07	0.0006	0.0034	1.725	3.45	0.0008	0.0016
	fiber 2%	15.62	52.07	0.0006	0.0034	3.06	6.12	0.0014	0.0029
Polyethylene	fiber 1%	11.37	37.91	0.00044	0.0034	1.89	1.98	0.00009	0.0079
	fiber 2%	11.24	37.46	0.00043	0.0034	1.73	3.09	0.00026	0.0074
Stainless Steel	fiber 1%	20.82	69.39	0.0008	0.0034	3.35	4.62	0.00015	0.0036
	fiber 2%	21.95	73.16	0.0008	0.0034	4.40	7.26	0.00008	0.0012

Note: f_{fci} = HPFRCC initial compressive strength; f_{fcm} = HPFRCC maximum compressive strength; ε_{fci} = HPFRCC initial compressive strain; ε_{fcm} = HPFRCC maximum compressive strain; f_{fty} = HPFRCC yield tension strength; f_{ftm} = HPFRCC maximum tension strength; ε_{fty} = HPFRCC yield tension strain; ε_{ftu} = HPFRCC maximum tension strain.

A series of Push-Over analyses for the given sections were conducted and the moment-rotation curves were obtained considering original condition, current condition (deteriorated) and rehabilitated (HPFRCC with basalt, polyethylene and stainless steel fibers, vol. 1% and 2%).

First hypothesis strengthening with HPFRCC layer of 3.5 cm:

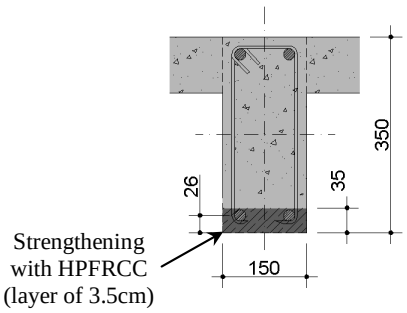

Figure 7.16 Strengthened cross section with 3.5cm of HPFRCC

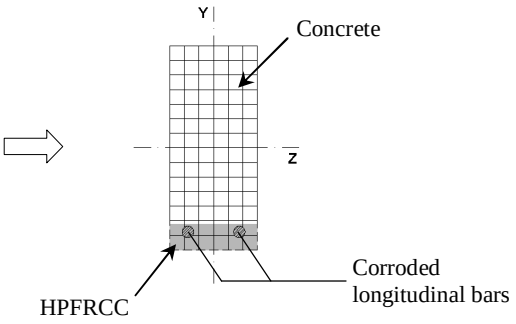

Figure 7.17 FEM model in OpenSees: fiber section model for steel-concrete (considering HPFRCC)

In order to assess the flexural strength increase of the damaged section analyzed, comparisons to evaluate the maximum moment-rotation behaviour are reported in the Figures bellow:

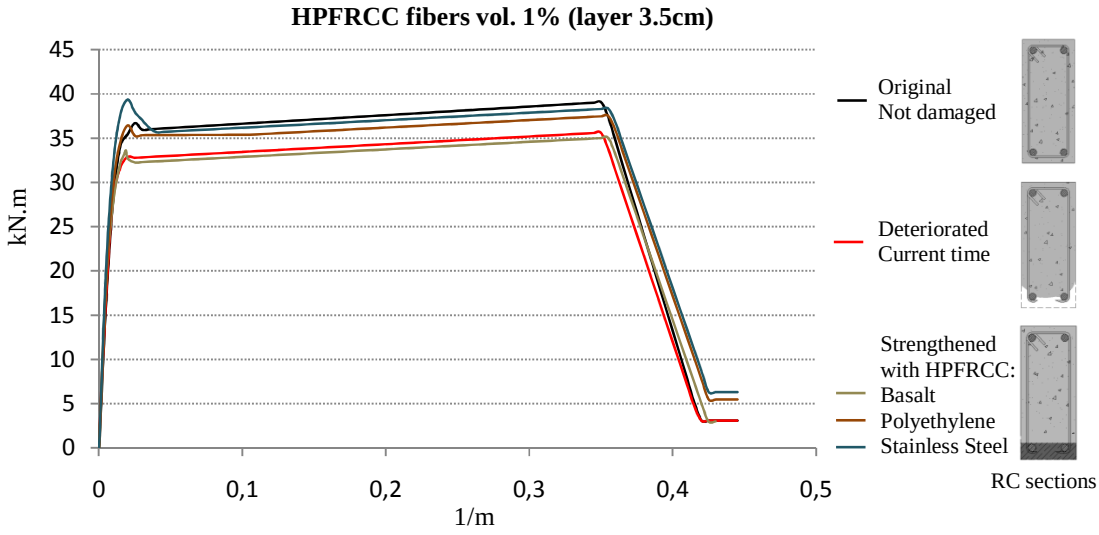

Figure 7.18 Moment-rotation capacity curves of the strengthened beam section for assessment of the structural performance level (HPFRCC fiber vol. 1% - layer 3.5cm)

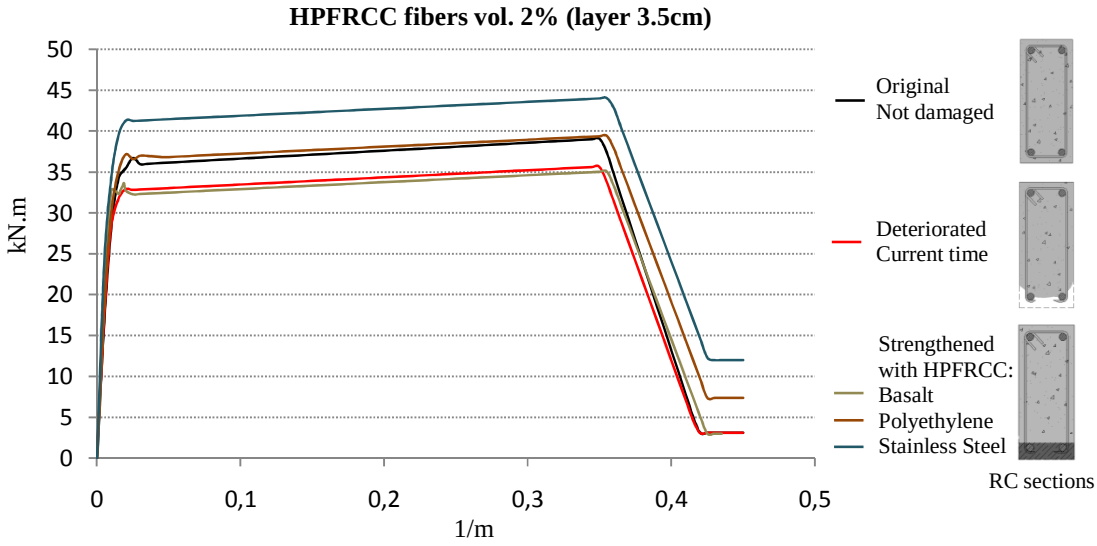

Figure 7.19 Moment-rotation capacity curves of the strengthened beam section for assessment of the structural performance level (HPFRCC fiber vol. 2% - layer 3.5cm)

Second hypothesis strengthening with HPFRCC layer of 7.0 cm:

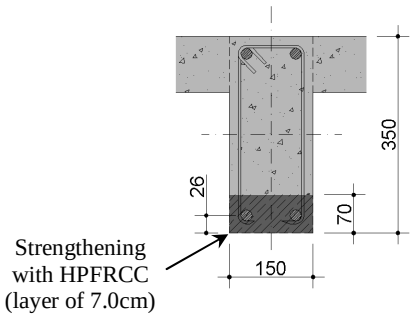

Figure 7.20 Strengthened cross section with 7.0cm of HPFRCC

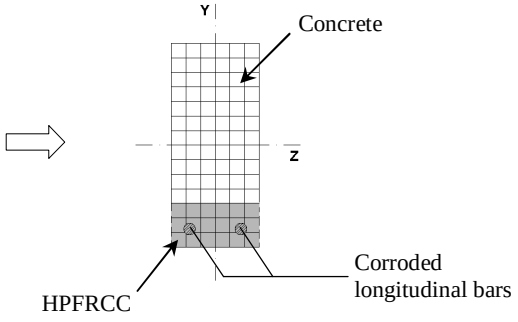

Figure 7.21 FEM model in OpenSees: fiber section model for steel-concrete (considering HPFRCC)

Comparisons to evaluate the maximum moment-rotation behaviour for the second hypothesis are reported in the Figures bellow:

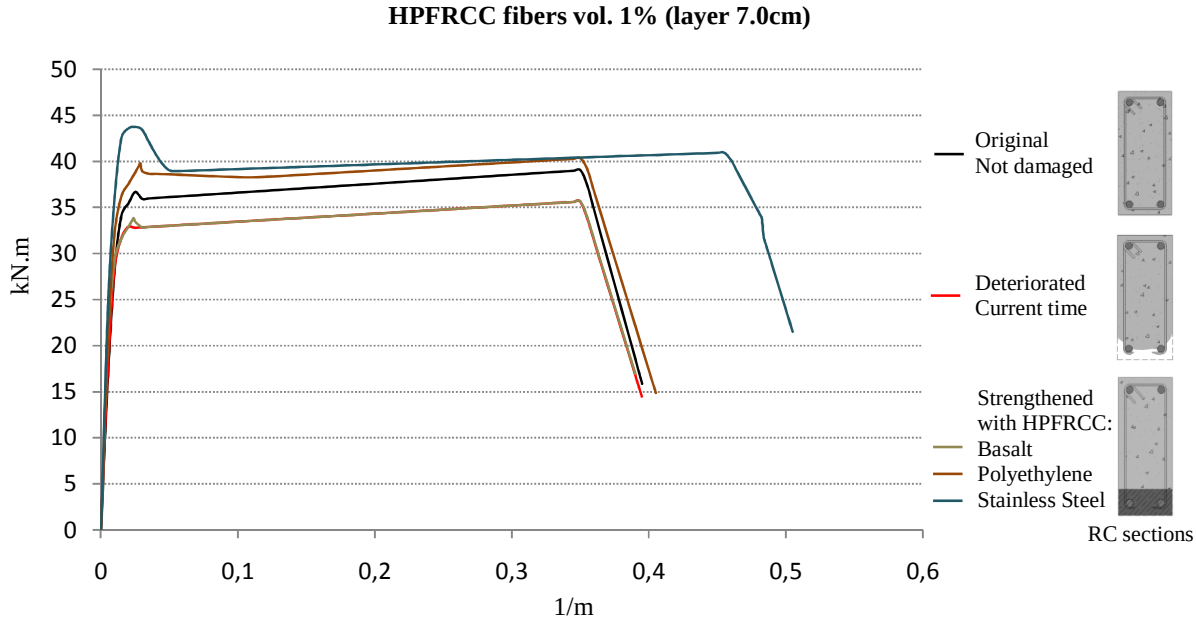

Figure 7.22 Moment-rotation capacity curves of the strengthened beam section for assessment of the structural performance level (HPFRCC fiber vol. 1% - layer 7.0cm)

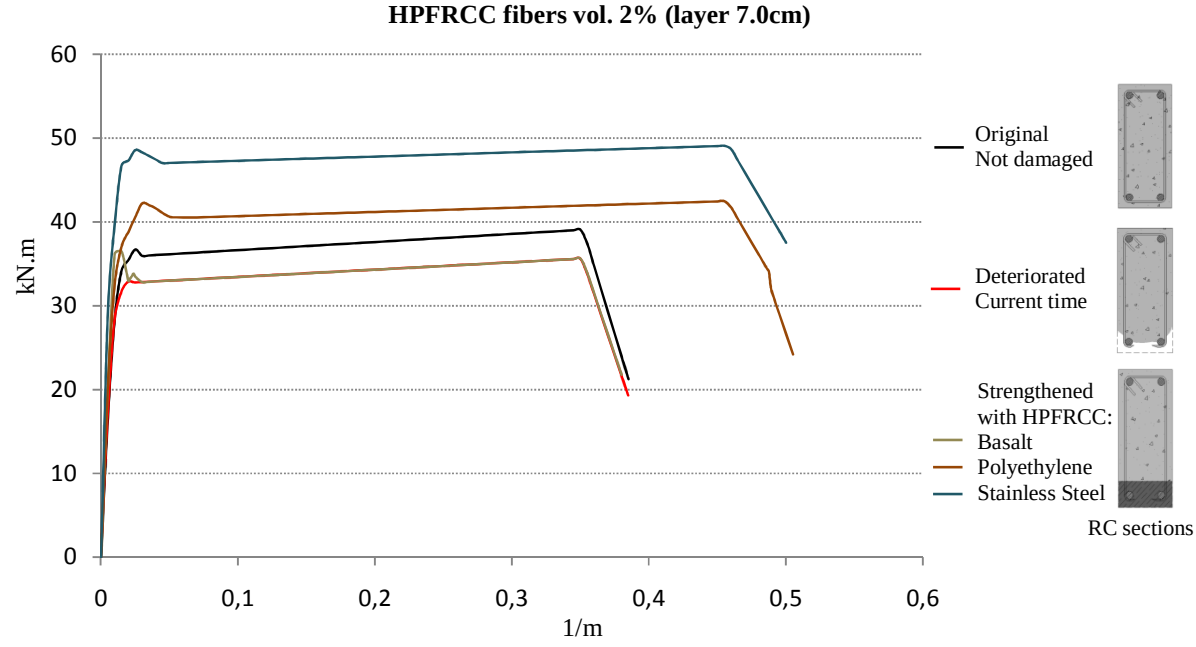

Figure 7.23 Moment-rotation capacity curves of the strengthened beam section for assessment of the structural performance level (HPFRCC fiber vol. 2% - layer 7.0cm)

Table 7.06: Comparison between moment-rotation of the beam section

Beam Section			M_{max} (kN.m)	F_p
Original condition Not damaged			39	1.00
Deteriorated Current time			36	0.92
Strengthened with HPFRCC (layer 3.5cm)	Basalt	(vol. 1%)	35	0.90
		(vol. 2%)	35	0.90
	Polyethylene	(vol. 1%)	37	0.95
		(vol. 2%)	39	1.00
	Stainless Steel	(vol. 1%)	39	1.00
		(vol. 2%)	44	1.13
Strengthened with HPFRCC (layer 7.0cm)	Basalt	(vol. 1%)	36	0.92
		(vol. 2%)	36	0.92
	Polyethylene	(vol. 1%)	40	1.03
		(vol. 2%)	42	1.08
	Stainless Steel	(vol. 1%)	44	1.13
		(vol. 2%)	49	1.26

Note: M_{max} = Maximum Moment; F_p = Performance Factor (in relation to the Maximum Moment of the original section – not damaged).

7.2.9 Rehabilitation with FRCM[1] technique

7.2.9.1 Numerical model and material properties

To evaluate the flexural strength increase of the damaged RC section analyzed, was performed a series of numerical tests with application of internal FRCM by wet lay-up system, composed of cementitious matrix and a very thin mesh of fiber in carbon, stainless steel or glass. Analyses of strengthening of the beam section were carried out at the ULS, according to the current Italian standards, through

[1] Fiber reinforced cementitious matrix.

Opensees software[1] framework and using a calculator (Figure 7.24) for evaluation of RC elements strengthened with FRP and FRCM systems, which was developed during the PhD studies. The FRCM properties were assumed by commercial products specifications available in Italy (Table 7.07).

Table 7.07: FRCM properties used on the numerical tests

Material		FRCM mechanical characteristics			
		Elastic modulus (GPa)	Tensile strength (MPa)	Strain at rupture (%)	Weight (g/m^2)
Fibers (mesh)	Carbon	240	4700	1.80	220
	Stainless Steel	190	2350	1.50	1500
	Glass	73	2600	3.50	300
Matrix	Cement mortar	12.5[(a)]	25 - 35	0.4 - 0.6	[(b)]

Note: (a) = secant elastic module; (b) = specific gravity 1.80; For comparison was used a equivalent dry mesh thickness of 0.167 mm.

Figure 7.24 Calculator for evaluation of RC elements strengthened with FRP and FRCM systems (developed during the PhD studies)
Bending in RC Beam (ULS)

[1] OpenSees structural software [Computer software]. Berkeley, CA, Pacific Earthquake Engineering Research Center, Univ. of California.

7.2.9.2 Numerical modeling details

UniaxialMaterial Hysteretic model available in OpenSees was used to predict the responses of the strengthened beam with FRCM, in terms of flexural strength, on the parts of deteriorated section (Fig. 7.26). The mechanical characteristics obtained from the commercial products specifications available in Italy and the proposed equations from the Italian standard CNR-DT 200 R1/2013 (explained in Chapter V), in the FRCM system were used.

Figure 7.25 shows the FRCM stress-strain[1] behaviour used to build the numerical model in *Opensees* with carbon, stainless steel and glass fibers.

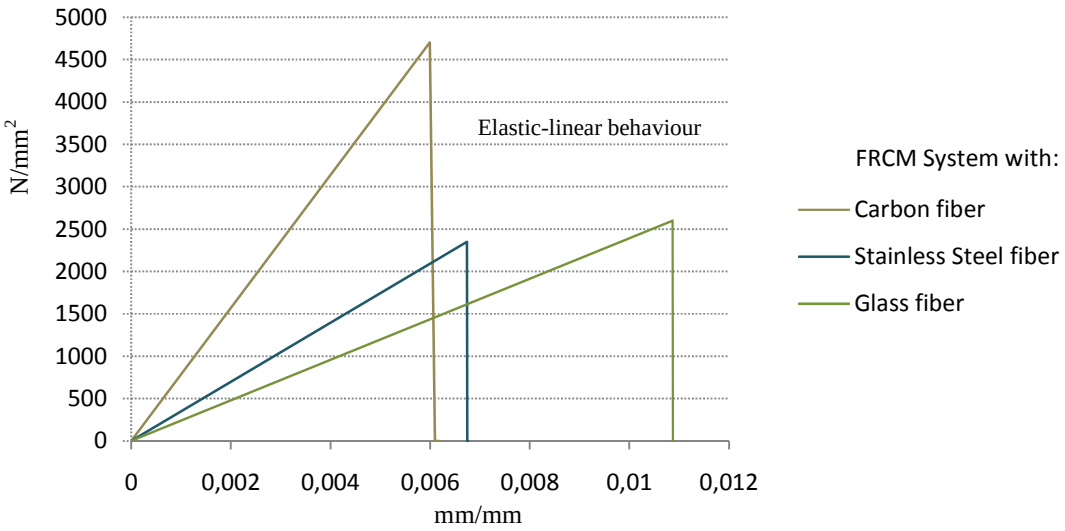

Figure 7.25 FRCM System Stress-Strain curves for analyses with fiber model in *OpenSees* Software (elastic-linear tensile behaviour)

7.2.9.3 Numerical tests and results comparison

The evaluations of the flexural capacity and the equilibrium conditions of the strengthened beam sections were performed using the equations cited in Chapter

[1] Strain limit proposed by CNR-DT 200 R1/2013.

V (item 5.5.3.4.3), where the coefficients and the characteristics of the adopted strengthening system were defined by CNR-DT 200 R1/2013.

Pushover analyses were conducted, where the resistance moments were obtained considering: original condition, current condition (deteriorated) and rehabilitated.

One layer of fiber mesh (shown in Figure 7.28) for the analyses carried out was used and the regularization of the deteriorated beam surface in plain concrete was performed.

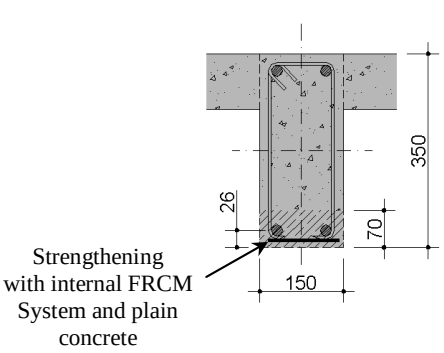

Figure 7.26 Strengthened cross section with FRCM System and plain concrete

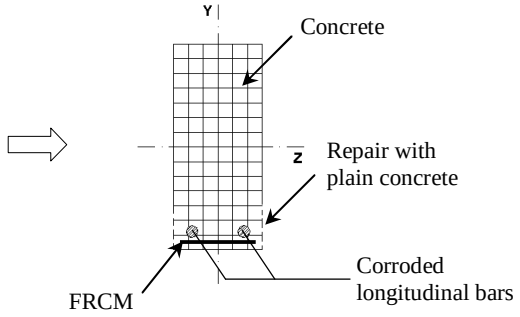

Figure 7.27 FEM model in OpenSees: fiber section model for steel-concrete (considering FRCM)

In order to assess the flexural strength increase of the damaged section analyzed, comparisons to evaluate the maximum moment-rotation behaviour, bellow are reported:

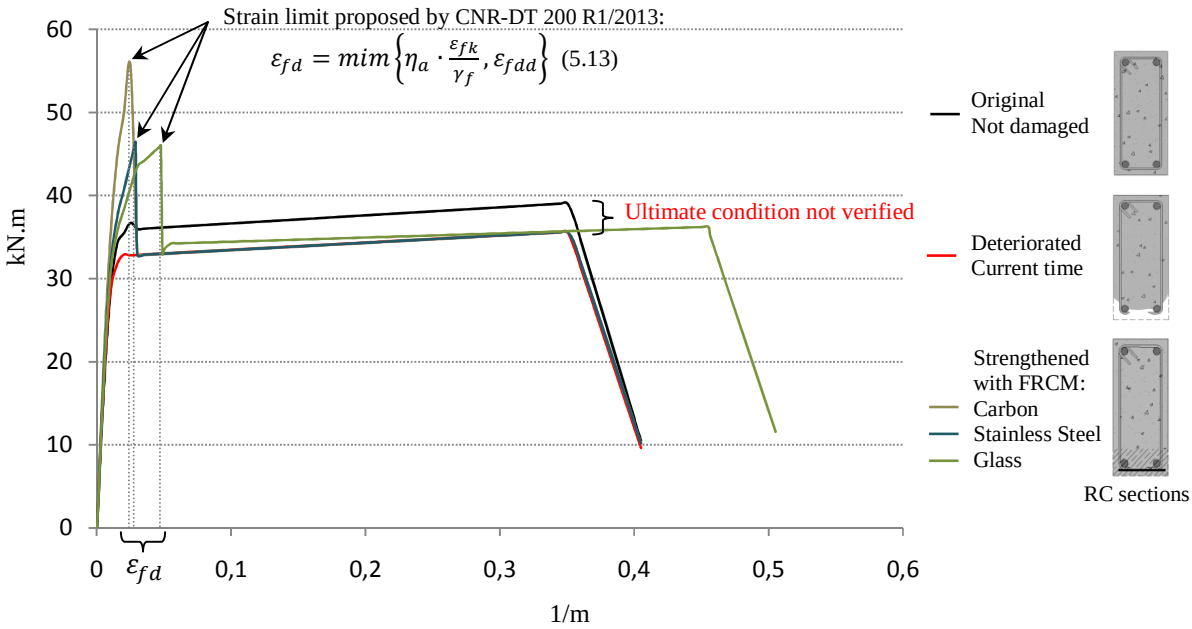

Figure 7.28 Moment-rotation capacity curves of the strengthened beam section for assessment of the structural performance level (FRCM System with fiber mesh)

For verification, input and output data on the calculator for FRCM strengthening with carbon, stainless steel and glass fibers meshes, in Figures 7.30, 7.31 and 7.32 are shown.

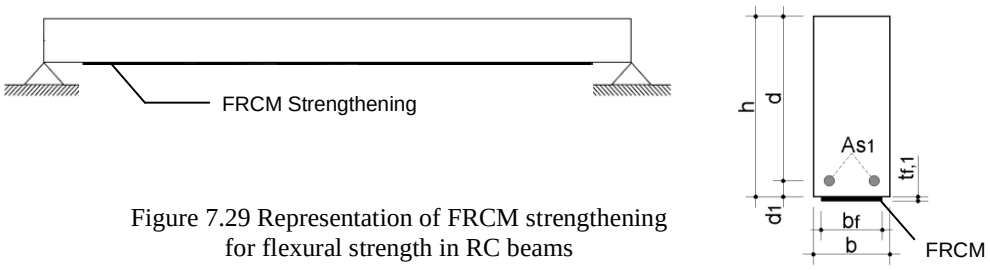

Figure 7.29 Representation of FRCM strengthening for flexural strength in RC beams

Existing Materials Characteristics			
$F_{yk,m}$ (N/mm²)	453	$F_{ck,m}$ (N/mm²)	20
E_s	200000	F_{ctm}	2,21
γ_s	1,00	γ_c	1,00
FC	1,00	$\gamma_{Rd\ (SLU)}$	1,00

Beam Data			
h (mm)	350	d (mm)	329
b (mm)	150	d1 (mm)	21
A_{s1} (mm²)	226	A_{s2} (mm²)	0
$M_{R,Dam}$ (kN.m)	36,00	$M_{R,Orig}$ (kN.m)	39,00

Strengthening System Characteristics			
E_f (N/mm²)	240000	$t_{f,1}$ (mm)	0,167
f_{fk} (N/mm²)	4700	b_f (mm)	120
γ_f	1,10	η_a	0,85
$\gamma_{f,d}$	1,20	η_f	1
$K_{G\ (composite)}$	0,037	K_q	1,25
Su	0,25	γ_{Rd} (led)	1,25

Results			
M_{Rdc} (kN.m)	58,22	x (mm)	96,80
f_{fdd} (N/mm²)	700,71	$f_{fdd,2}$ (N/mm²)	1439,95
f_{bd} (N/mm²)	1,97	led (mm)	200
A_f (mm²)	20,04	Failure Mode	1 (ductile)

Exit

Figure 7.30 Input and output data from the calculator for evaluation of RC elements strengthened with FRP and FRCM systems (Strengthening with Carbon FRCM)

Existing Materials Characteristics			
$F_{yk,m}$ (N/mm²)	453	$F_{ck,m}$ (N/mm²)	20
E_s	200000	F_{ctm}	2,21
γ_s	1,00	γ_c	1,00
FC	1,00	$\gamma_{Rd\ (SLU)}$	1,00

Beam Data			
h (mm)	350	d (mm)	329
b (mm)	150	d1 (mm)	21
A_{s1} (mm²)	226	A_{s2} (mm²)	0
$M_{R,Dam}$ (kN.m)	36,00	$M_{R,Orig}$ (kN.m)	39,00

Strengthening System Characteristics			
E_f (N/mm²)	190000	$t_{f,1}$ (mm)	0,167
f_{fk} (N/mm²)	2350	b_f (mm)	120
γ_f	1,10	η_a	0,85
$\gamma_{f,d}$	1,20	η_f	1
$K_{G\ (composite)}$	0,037	K_q	1,25
Su	0,25	γ_{Rd} (led)	1,25

Results			
M_{Rdc} (kN.m)	45,45	x (mm)	73,61
f_{fdd} (N/mm²)	623,46	$f_{fdd,2}$ (N/mm²)	1281,20
f_{bd} (N/mm²)	1,97	led (mm)	200
A_f (mm²)	20,04	Failure Mode	1 (ductile)

Exit

Figure 7.31 Input and output data from the calculator for evaluation of RC elements strengthened with FRP and FRCM systems (Strengthening with Stainless Steel FRCM)

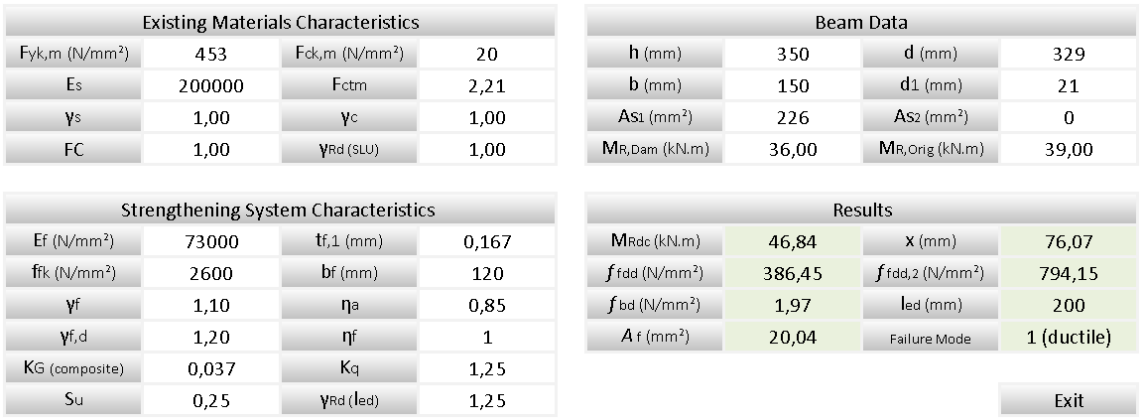

Figure 7.32 Input and output data from the calculator for evaluation of RC elements strengthened with FRP and FRCM systems (Strengthening with Glass FRCM)

Table 7.08: Comparison between maximum moments of the beam section, using OpenSees and FRCM Calculator

Beam Section		M_{max} (kN.m)	F_p
Original condition (Not damaged)		39	1.00
Deteriorated (Current time)		36	0.92
Strengthened with FRCM (1 layer) Using Opensees	Carbon	55	1.41
	Stainless Steel	46	1.18
	Glass	46	1.18
Strengthened with FRCM (1 layer) Using Calculator	Carbon	58	1.49
	Stainless Steel	45	1.15
	Glass	47	1.21

Note: M_{max} = Maximum Moment; F_p = Performance Factor (in relation to the Maximum Moment of the original section – not damaged).

To evaluate the failure modes limits of the reinforced section, three strengthening hypotheses with 1, 2 and 3 layers of mesh in carbon, stainless steel and glass fibers were considered (Fig. 7.33).

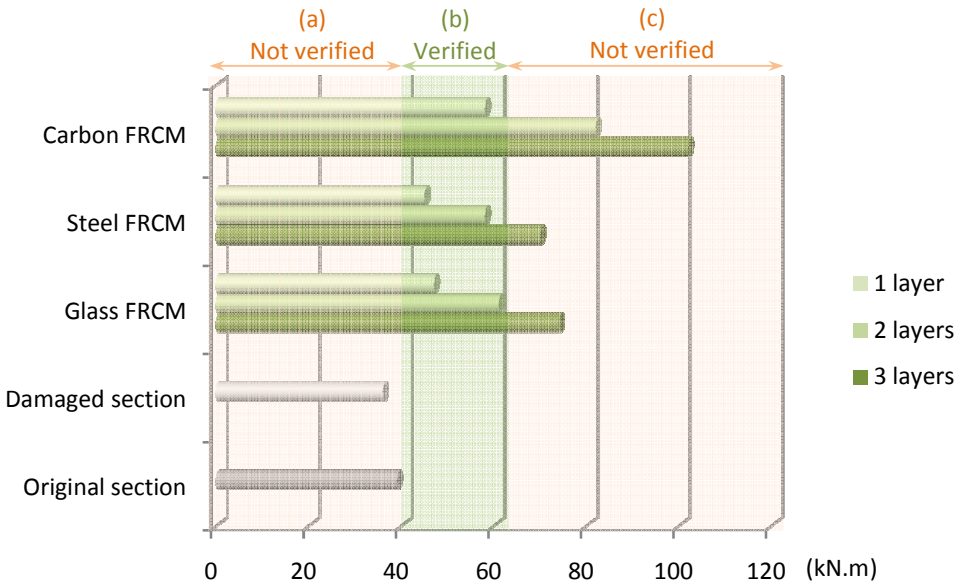

Figure 7.33 Comparison between resistance moments of the RC beam section for assessment of the structural performance level

Figure 7.33 shows that in situation (a) the beam section equilibrium condition is not satisfied because the resistance moment of the reinforced section is less than the moment of the original section ($M_{R,Streg} < M_{R,Orig}$).

In condition (b), with 1 or 2 layers of mesh applied, the equilibrium condition of the section is verified, because $M_{R,Streg} > M_{R,Orig}$ and the distribution of material deformations (concrete, steel and FRCM) is working in region 1 (Fig. 7.34). In region 1, the fail mode of the section occurs through ductile rupture mechanism, with failure of the section tension region (when the FRCM system reaches the limit elastic strain of design, established by the standard).

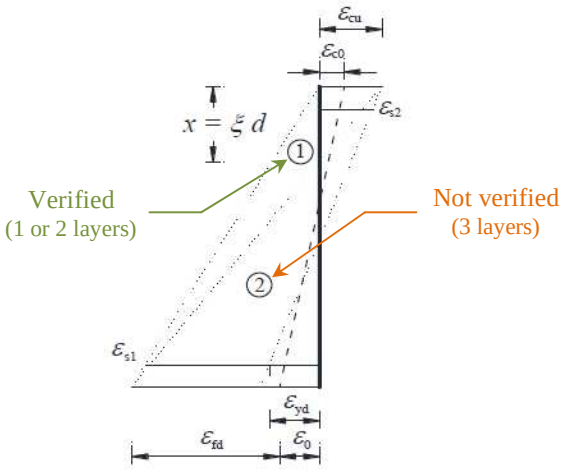

Figure 7.34 Failure mode of a RC member strengthened with FRCM
(source CNR-DT 200 R1/2013)

In condition (c), with 3 layers of FRCM applied, is not verified a situation that satisfies the proper section equilibrium condition, because the distribution of material deformations is working in region 2 (Fig. 7.34), in this region the fail mode of the section occurs through brittle rupture mechanism, with failure of the section compressed region (concrete crushing).

7.2.10 Rehabilitation combining HPFRCC and FRCM techniques

The combination of the two reinforcement techniques HPFRCC and internal FRCM could also be used for rehabilitation of elements in reinforced concrete. The main advantage of using these two techniques together is linked to their physical and chemical compatibility, since they have cement-based matrices.

FRCM has linear elastic stress-strain behaviour until reaching its maximum design limit (Fig. 7.25); On the other hand, HPFRCC technique, when applied with micro-fibers that provide pseudo strain-hardening characteristics, it presents an elasto-plastic non-linear behaviour (with cracking distribution) until rupture. Thereby, the combination of the two techniques could contribute to the minimization or a better

distribution of micro-cracks. In addition to reducing or eliminating cracks commonly caused by shrinkage of the applied cementitious composite.

7.2.10.1 Materials composition and numerical tests

A series of numerical tests for application of HPFRCC combined with internal FRCM system were performed through *Opensees* software framework, to evaluate the flexural strength increase of the damaged RC section.

Four numerical models were built in order to assess the performance level of the rehabilitated beam, considering two types of HPFRCC (with polyethylene and stainless steel fibers, vol. 2%) combined with two types of FRCM System (with stainless steel and glass fiber meshes). In the application of the two techniques, one layer of a very thin fiber mesh combined with a layer of 3.5cm of HPFRCC, were considered (Fig. 7.35).

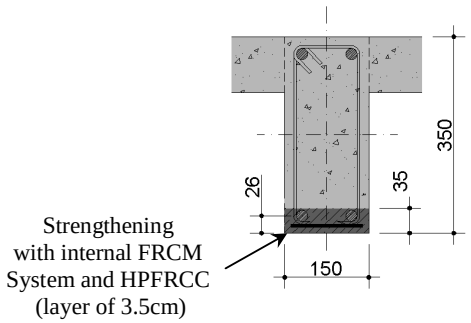

Figure 7.35 Strengthened cross section with FRCM System and 3.5 cm of HPFRCC

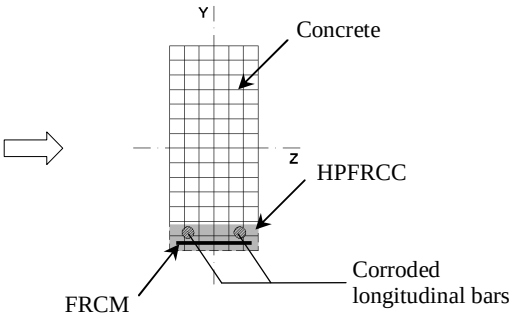

Figure 7.36 FEM model in OpenSees: fiber section model for steel-concrete (considering FRCM + HPFRCC)

A series of analyses (pushover) were conducted, where the moment-rotation capacity curves were obtained considering original condition, current condition (deteriorated) and rehabilitated (Glass FRCM + Polyethylene HPFRCC and Glass FRCM + Steel HPFRCC; Steel FRCM + Polyethylene HPFRCC and Steel FRCM + Steel HPFRCC).

Comparisons to evaluate the maximum moment-rotation behaviour are reported in the Figures and Table below:

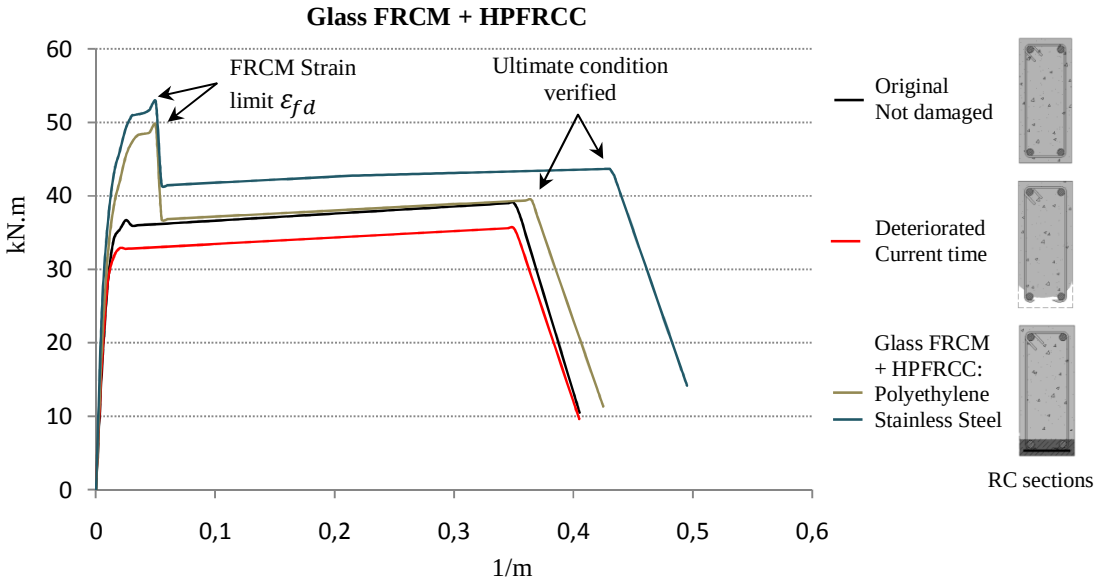

Figure 7.37 Moment-rotation capacity curves of the strengthened beam section for assessment of the structural performance level (Glass FRCM 1 layer + HPFRCC fibers vol. 2% layer 3.5cm)

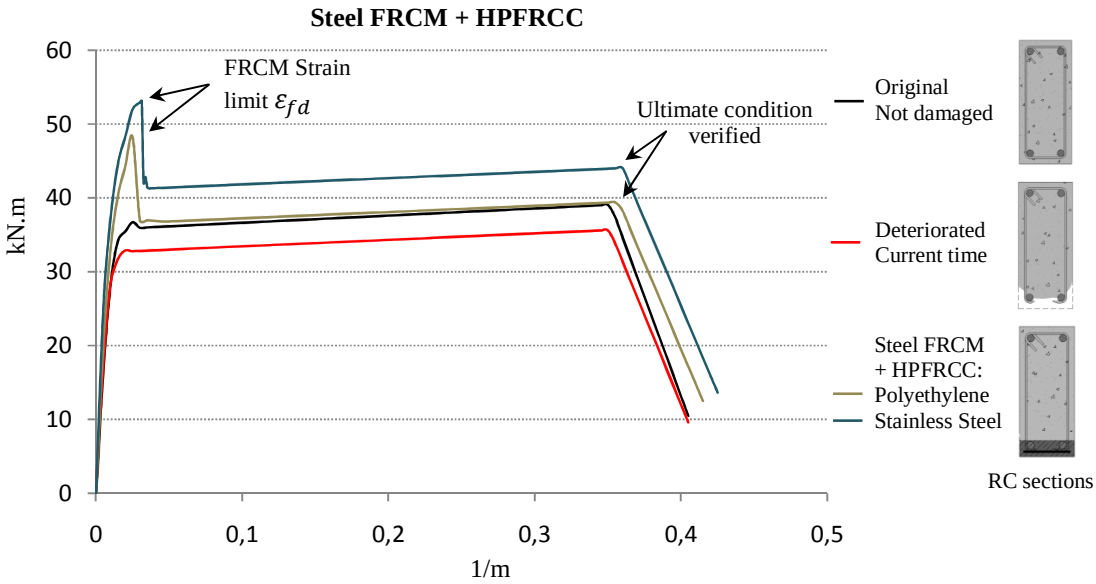

Figure 7.38 Moment-rotation capacity curves of the strengthened beam section for assessment of the structural performance level (Steel FRCM 1 layer + HPFRCC fibers vol. 2% layer 3.5cm)

Table 7.09: Comparison between maximum moments of the strengthened beam section

Beam Section		M_{max} (kN.m)	F_p
Original condition (Not damaged)		39	1.00
Deteriorated (Current time)		36	0.92
Strengthened with Glass FRCM (1 layer) +	Polyethylene HPFRCC	50	1.28
	Stainless Steel HPFRCC	53	1.36
Strengthened with Steel FRCM (1 layer) +	Polyethylene HPFRCC	48	1.23
	Stainless Steel HPFRCC	53	1.36

Note: M_{max} = Maximum Moment; F_p = Performance Factor (in relation to the Maximum Moment of the original section – not damaged).

7.3 RC Bridge: Case study for numerical investigation

7.3.1 General approach

In this item, procedures for the assessment of deteriorated reinforced concrete structures mentioned in the preceding section are applied to a numerical example for a pier of an existing bridge in Italy. The reference element was studied by Davide Lavorato and Camillo Nuti (2015)[1], in an experimental investigation for repair and retrofitting of piers performed in the structural laboratory of University of *Roma Tre*.

The structure prototype, a cantilever pier of an existing reinforced concrete highway bridge (Fig. 7.39) built in Italy in the 70s, have been designed both accordingly to Eurocode 8 Part 1[2] and Eurocode 8 Part 2[3] for the design of bridges

[1] Lavorato D., Nuti C. New Solutions for Rapid Repair and Retrofit of RC Bridge Piers. XII International Conference on Structural Repair and Rehabilitation (Cinpar 2016), 26-29 October, 2016, Porto, Portugal.

[2] Eurocode 8. 1998. "Design of structures for earthquake resistance, Part 2: Bridges. (Draft March 2005)".

[3] Eurocode 8. 1998. "Design of structures of earthquake resistance, Part 3: Assessment and retrofitting of buildings" (Draft November 2004).

in seismic areas, Eurocode 2 for the general rules on concrete structures and Italian Seismic Code D.M. LL.PP. 24.01.86.

The bridge is comprised by a continuous box girder hinged on the circular section piers and on the abutments. It consists of four bridge spans with an equal span length of 50m. The bridge piers have a constant circular full-cross section and structurally they behave as cantilevers, they are of unequal height with the shortest pier 7m in the middle (Fig. 7.39) and two piers with different height, 14m and 21m, on the sides[1].

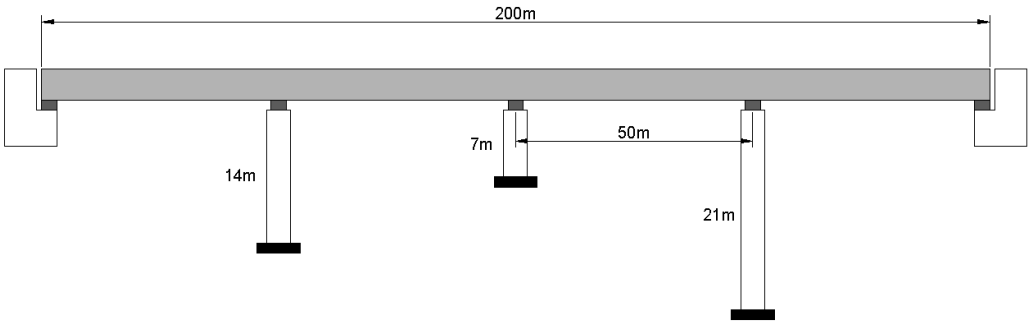

Figure 7.39 Bridge prototype configurations. Case study for numerical example.
(adapted from Lavorato D. and Camillo Nuti, 2015, University of *Roma Tre*)

7.3.2 Reference element

Numerical simulation of reinforced concrete pier damaged by carbonation-induced corrosion it was performed to evaluate the performance level in terms of service life and load bearing (load resistance/load capacity). The investigation was carried out

[1] This bridge is considered irregular by having the shortest pier in the middle, because due to the presence of the central squat pier, under seismic action, the first transverse mode shape of the deck induced very high forces in this central stiff pier.

by numerical example of the cantilever pier based on the experimental investigation for repair and retrofitting of piers by Lavorato D. and Nuti C. (2015)[1].
In this study a RC cantilever pier of 420mm in diameter and 1170mm in effective height, with 1/6 scale factor in relation the original bridge (Fig. 7.40), damaged by carbonation-induced corrosion (hypothesis for numerical simulation) was designed to resist aggressive environment as defined by D.M. NTC 2008, with minimum service life of 100 years. Twelve bars of a diameter D_s = 12mm are provided as the flexo-compression rebar[2] with clear cover thickness of C = 30mm and transverse reinforcement of diameter D_{st} = 6mm is provided at 120mm spacing. The compressive strength of concrete f_{cm} = 20MPa with modulus of elasticity $E_c = 22.36GPa$ ($E_c = 5{,}000\sqrt{f_{cm}}$) and $f_{ctm} = 2.21MPa$ ($f_{ctm} = 0.30 \cdot f_{ck}^{\frac{2}{3}}$, obtained from D.M. NTC 2008). The yield strength of longitudinal reinforcing steel f_{yk} = 574.37MPa, transverse reinforcing steel f_{yk} = 445.46MPa, with modulus of elasticity E_s = 200GPa and steel density ρ_s = 7850kg/m^3.

Table 7.10: Key Information of the section and materials

Concrete					Longitudinal bars				Transverse bars			
D (mm)	C (mm)	f_{cm} (MPa)	f_{ctm} (MPa)	E_c (GPa)	Ds (mm)	n	f_{yk} (MPa)	E_s (GPa)	Dst (mm)	s (mm)	f_{yk} (MPa)	E_s (GPa)
420	30	20	2.21	22.36	12	12	574.37	200	6	120	445.46	200

Note: D = cross-section diameter; C = concrete cover thickness; f_{cm} = concrete cylinder strength; f_{ctm} = concrete tension strength; E_c = elastic modulus of concrete; D_s = diameter of longitudinal bars; n = number of longitudinal steel bars; f_{yk} = yield stress of steel bars; E_s = elastic modulus of steel; D_{st} = diameter of of transverse steel bars; s = spacing of transverse steel bars.

[1] Lavorato D., Nuti C. Pseudo-dynamic tests on reinforced concrete bridges repaired and retrofitted after seismic damage. Engineering Structures 94 (2015) 96–112.

[2] The longitudinal reinforcement ratio of the column is 1.0%, and the volumetric ratio of transverse hoop reinforcement is 0.22%.

Figure 7.40 Pier reference element
(from Lavorato D. and Nuti C., 2015)

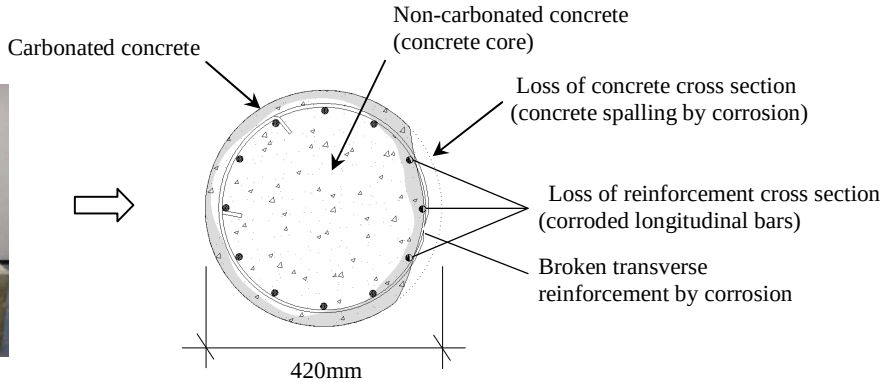

Figure 7.41 Carbonation-induced corrosion effects in the reinforced concrete pier (damaged RC section)

7.3.3 Current condition and remaining service life assessment

This step deals on the assessment of remaining service life of the reference element (RC pier) damaged by carbonation-induced corrosion, with loss of concrete cross section and loss of reinforcement cross section.

The pier is exposed in an aggressive environment with high rate of CO_2 carbon dioxide and high relative humidity. Because one part of the pier is exposed to splash water the depth of concrete carbonation[1] varies in the perimeter of the section (Fig. 7.42) from 10mm to 50mm. For this reason the column section can be subdivided in two zones, moist (subjected to wet-dry phenomenon) and not moist (partially protected). In the moist zone the carbonation depth is higher and the reinforcement steel is depassivate and corroded (some bars). In the not moist zone the reinforcement steel is not yet depassivate. The average loss of cross section measured in the corroded bars is of the order of 14%, approximately 1.7mm per bar, in radial direction.

[1] Depth of concrete carbonation measured by phenolphthalein test.

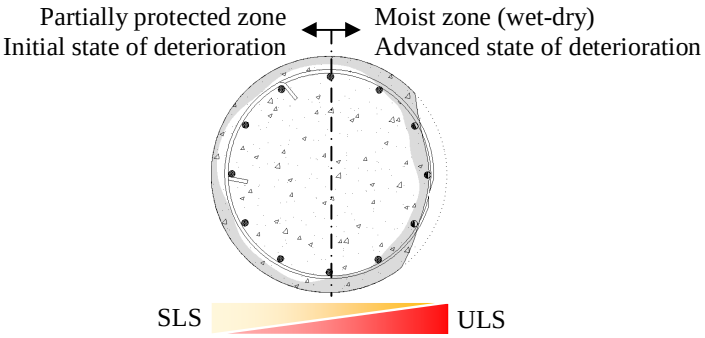

Figure 7.42 Section subdivision:
moist zone and not moist zone

7.3.3.1 Evaluation of the remaining service life concerning to steel reinforcement depassivation by carbonation (initiation period)

To estimate the remaining time to reach the depassivation of reinforcement in serviceability limit state - SLS (initiation period) in the not moist zone, considering current time of 40 years and 24.5mm (mean of the not moist zone) of carbonation depth in the studied section, the carbonation speed factor K [1] (carbonation penetration over time) may be known by Equation 7.03:

$$K = \frac{24.5}{\sqrt{40}} = 3.87 mm/year^{\frac{1}{2}} \quad (7.03)$$

Once found K parameter the remaining time to the carbonation reaches the reinforcement can be calculated as follows:

$$t_i = \left(\frac{5.5}{3.87}\right)^2 = 2\ years \quad (7.04)$$

[1] Constant over time.

So it is likely that the reinforcement depassivation, in the partially protected zone to occur in 2 years.

The initiation period in the moist zone, in the past, may be estimated by the same procedure above. The carbonation speed factor K in the zone with advanced state of deterioration (considering 42.5mm of carbonation depth - mean of the moist zone) may be calculated as follows:

$$K = \frac{42.5}{\sqrt{40}} = 6.72 mm/year^{\frac{1}{2}} \quad (7.05)$$

Whereas the parameter K is constant over time the steel depassivation started 20 years ago. Defined as follows:

$$t_i = \left(\frac{30}{6.71}\right)^2 = 20\ years \quad (7.06)$$

7.3.3.2 Evaluation of the remaining service life concerning to steel reinforcement corrosion (propagation period)

When the corrosion is due to carbonation it is necessary to consider both the initiation period and propagation period. For the studied pier section was assumed a limit of maximum acceptable damage corresponding to a loss of reinforcement cross section of 15%[1]. As limit value for structural collapse was assumed a loss of reinforcement cross section of 40%. These limit values (ultimate limit state - ULS) correspond to a penetration of corrosive attack per bar in radial direction of 1.8mm and 4.8mm (P_{lim}), respectively. Whereas the initiation period previously calculated $t_i = 20\ years$, it was possible to estimate the propagation period (t_p) of reinforcement corrosion and service life of the structure by Equation 7.07:

[1] Average value for the corroded bars.

$$t = t_i + t_p = \left(\frac{x}{K}\right)^2 + \frac{P_{lim}}{V_{corr}} \quad (7.07)$$

Where, t is the service life of the structure, x is the concrete cover thickness and k is the carbonation speed factor which can be known as described previously. Degradation rate in radial direction V_{corr} may be calculated considering the Faradays first law of electrolysis, expressed in Equation (7.08).

$$V_{corr} = 1.16 \cdot 10^{-3} \cdot i_{corr} \quad (7.08)$$

Once measured the mean value of cross section loss of the corroded bars (approximately 1.7mm per bar in radial direction), can be estimated the mean annual corrosion current density (i_{corr}) corresponding from the starting time of the propagation period ($t_i = 20\ years$) to the present time ($t_{present} = 40\ years$), by Equation 7.09 and 7.10:

$$V_{corr} = \frac{P_{measured}}{t_{present} - t_i} = \frac{0.17}{20} = 0.0085\ cm/year \quad (7.09)$$

$$i_{corr} = \frac{V_{corr}}{1.16 \cdot 10^{-3}} = 7.32\ \mu A/cm^2 \quad (7.10)$$

Known the mean annual corrosion current density (i_{corr}) it is possible to estimate the remaining time to reach the ultimate limit states (ULS) of maximum acceptable damage t_{pd} of structural performance (cross section loss of 15%) and the limit state of collapse t_{pc} (cross section loss of 40%), according to the following Equations.

$$t_{pd} = \frac{P_{lim}}{V_{corr}} = \frac{0.18 - 0.17}{1.16 \cdot 10^{-3} \cdot 7.32} = 1.2\ years \quad (7.11)$$

$$t_{pc} = \frac{P_{lim}}{V_{corr}} = \frac{0.48-0.17}{1.16 \cdot 10^{-3} \cdot 7.32} = 36.5\ years \quad (7.12)$$

Results of the analysis conducted previously regarding the evaluation of current condition and remaining service life are given in Table 7.11:

Table 7.11: General framework for current condition and remaining service life assessment

Part of the pier cross section	Lifetime for corrosion	Current condition		Remaining service life				
		Limit State	Mean carbonation depth	Carbonation speed factor K	SLS Steel depassivation	Steel degradation rate V_{corr}	SLU maximum acceptable damage	SLU structural collapse
Not moist zone	Initiation period	SLS Carbonated Concrete	24.5mm	3.87mm /year$^{1/2}$	in 2 years	-	-	-
	Propagation period	-	-	-	-	-	-	-
Moist zone	Initiation period	-	-	-	-	-	-	-
	Propagation period	SLU Concrete spalling and loss of reinf. cross section (14%)	42.5mm	6.72mm /year$^{1/2}$	20 years ago	0.0085cm /year	In 1.2 years	In 36.5 years

To know the historic and current condition of the structure, it was necessary to evaluate its remaining service life and to decide the best time to intervene. Figure 7.43 shows the timeline of the studied structure as a function of the degree of deterioration in the past, present and future.

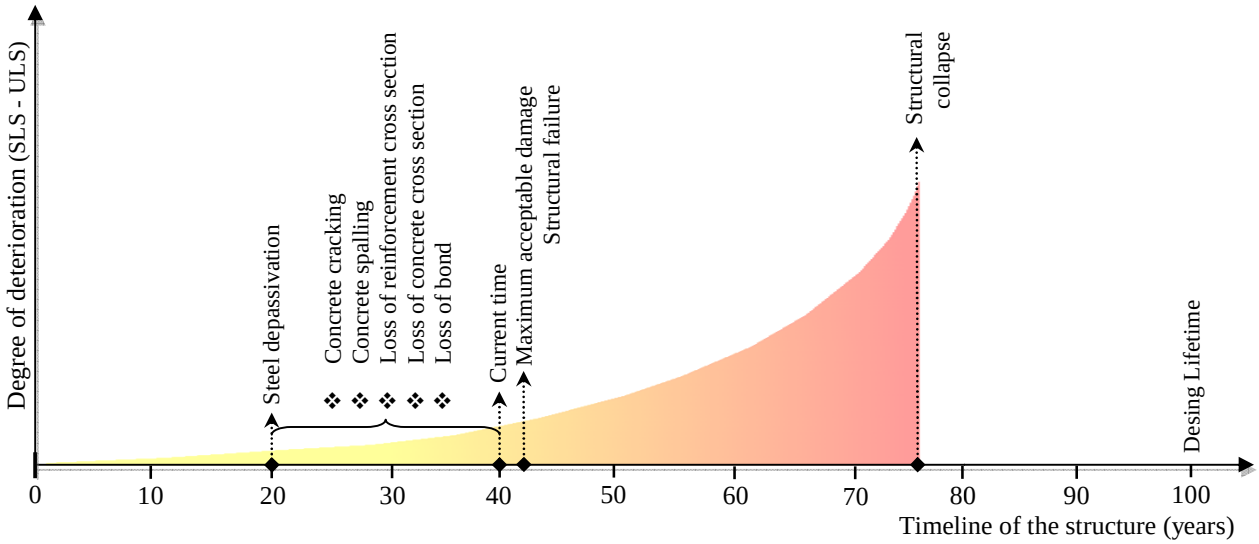

Figure 7.43 Historic of the structure and remaining service time

7.3.3.3 Evaluation of residual capacity of corroded bars

Assessment of yield strength by Du et al. model

A full understanding of reinforcement corrosion in the structure and the determination of the loss of cross-section are needed to assess the residual capacity of the corroded bars. Both residual diameter and corrosion rate need to be measured to evaluate the reinforcement corrosion.

According Du et al. (2005) the amount of corrosion Q_{corr} may be determined from measured values by using Equation (7.13):

$$Q_{corr} = 1 - (d_s/d)^2 = 1 - (10.3/12)^2 = 26.3\% \quad (7.13)$$

Where, d_s is the diameter of corroded reinforcement and d is the diameter of non-corroded reinforcement. Once the amount of corrosion is known, the residual capacity of corroded reinforcement can be estimated using Equation (7.14):

$$f = (1.0 - \beta \cdot Q_{corr}) f_0 = (1.0 - 0.005 \cdot 26.3) \cdot 574.37 = 498.76\ N/mm^2 \quad (7.14)$$

Where f and f_0 are yield strength of corroded and non-corroded reinforcement, respectively. The value of β is 0.005 for mean stress (stress based on average reduced cross section area).

Assessment of yield strength by Kashani et al. model

The residual capacity of the corroded bars was calculated for both in tension stress and in compression stress according Kashani et al. model. To considerate the non-uniform cross-section loss of the corroded bars, the mean mass loss was estimated by formula 7.15:

$$\gamma = \frac{m_0 - m}{m_0} = \frac{0.0089 - 0.0076}{0.0089} = 0.1417\ (14{,}17\%) \tag{7.15}$$

Thus, the mean diameter of corroded bar was calculated by:

$$D_{corr} = D_0\sqrt{1-\gamma} = 12\sqrt{1-0.1417} = 11{,}12\ mm \tag{7.16}$$

The yield strength in tension f_{yt} and in compression f_{yc} corresponding to the corroded rebar, based on the mean cross section area, were deduced by Equations 7.17 and 7.18:

$$f_{yt} = f_y(1 - a_t \cdot \psi) = 574.37(1 - 0.005 \cdot 14.17) = 533.68\ N/mm^2 \tag{7.17}$$

$$f_{yc} = f_y(1 - a_c \cdot \psi) = 574.37(1 - 0.0125 \cdot 14.17) = 472.66\ N/mm^2 \tag{7.18}$$

7.3.4 Structural performance assessment

In order to decide the level of update of the deteriorated structure, it is necessary to know its structural performance level. For the determination of the current

structural resistance and residual structural capacity, it is needed to dispose of realistic numerical models, capable of estimate the original behaviour of the structure (performance level which the structure was designed) and the current behaviour of the damaged structure. On assessment of existing structures is also important to consider that in the past, standard requirements were different than current time and materials with different characteristics have been applied. For example, steel with different ductility of plain bars and lower strength concrete.

7.3.4.1 Numerical model

The numerical model used to evaluate the structural behaviour of the case study (cantilever pier – Figure 7.44) is based in the theory of the finite element method (FEM) where the analysis of the non-linear behaviour of a circular reinforced concrete (RC) section was conducted through fiber modeling for steel-concrete composite.

A traditional beam-column fiber section (Fig. 7.44) divided into several parts (fibers) under flexo-compression was analyzed numerically using *Opensees* software[1] framework. Non-linear static analyses (Push-Over analysis) were carried out considering geometry, solicitations and constraints of the circular section column. Damage in the column, due to deterioration of concrete and reinforcement were introduced into the model. Moment-curvature and axial force-deformation characteristics and their interaction were numerically determined, applying vertical load on the section and a deformation history (section rotation) to evaluate the corresponding moment-rotation behaviour. Where, the balance of the section and the resistance stresses were determined through integration of constitutive laws.

[1] OpenSees structural software [Computer software]. Berkeley, CA, Pacific Earthquake Engineering Research Center, Univ. of California.

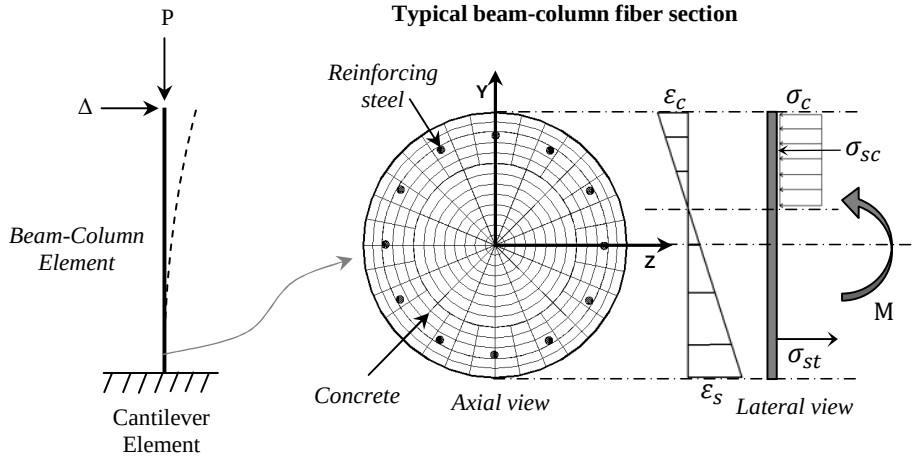

Figure 7.44 FEM model in OpenSees: fiber section model for steel-concrete

7.3.4.1.1 Numerical modeling details

The UniaxialSection element (beam-column fiber section element) available in *OpenSees* was employed in the present numerical simulations. The section was transversely represented using two Uniaxial Materials for concrete and steel. The discretization of the section is illustrated in Figure 7.44. Thirteen radial and sixteen/thirty two tangential divisions were employed for the concrete section. This level of discretization is used to lead accurate results based on a convergence study not reported here. The UniaxialMaterial Hysteretic model available in *OpenSees* was used for confined concrete core and unconfined concrete cover. The UniaxialMaterial Hysteretic model was also used to predict the responses of steel reinforcement. For the parts of deteriorated section, the UniaxialMaterial Hysteretic model for steel was used considering the mechanical characteristics obtained from the evaluation of residual capacity of the corroded bars previously

calculated. To consider the concrete confinement, formulations by Kawashima model[1] were inserted into the FEM model.

7.3.4.2 Confinement model for concrete

In the strengthening of existing RC columns, since there must be the lateral hoops, it is essential to evaluate the confinement effect of the concrete. Several authors have addressed the problem of reinforced concrete confinement featuring some models to explain and quantify the behaviour of concrete confined with reinforcement, subjected to axial compression. Among the published results were selected two models well known in the scientific community, to analyze the confinement effects: Mander and Kawashima models.

7.3.4.2.1 Mander model

Mander model[2] is applicable for different geometric configurations of RC sections and longitudinal and transverse reinforcement. The figure 7.45 shows the concrete behaviour unconfined and confined, with hoop reinforcement proposed by the model:

[1] Hosotani J., Kawashima K. et al. Discussion by A. J. Kappos. Stress-strain model for confined reinforced concrete in bridge piers. J. Struct. Eng., 1998, 124(10): 1228-1230.

[2] Mander, J. B., Priestley, M. J. N., and Park, R. Theoretical stress-strain model for confined concrete. Journal of structural engineering, ASCE 114, 8 (1988), 1804-1826.

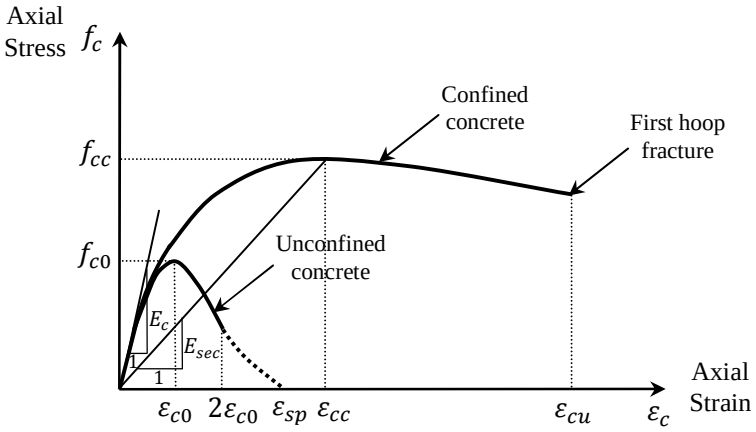

Figure 7.45 Graphic representation of the Mander et al.´s stress-strain model for steel-confined concrete

The maximum stress of confined concrete with steel reinforcement is calculated by equation:

$$f_{cc} = f_{c0}(-1.254 + 2.254\sqrt{1 + \frac{7.94f_l^{'}}{f_{c0}}} - 2\frac{f_l^{'}}{f_{c0}}) \tag{7.19}$$

$f_l^{'}$: effective lateral confinement pressure [N/mm^2]

f_{cc}: strength of confined concrete [N/mm^2]

f_{c0}: strength of unconfined concrete [N/mm^2]

Where the effective lateral confinement pressure $f_l^{'}$ is:

$$f_l^{'} = f_l \cdot k_e \tag{7.20}$$

$$k_e = \frac{A_e}{A_{cc}} \tag{7.21}$$

$$f_l = \frac{2f_{syk}A_{sw}}{d_s s} \tag{7.22}$$

f_l: lateral confinement pressure [N/mm^2]

k_e: effective confinement coefficient [-]

A_e: area effectively confined of concrete core [mm^2]

A_{cc}: area of confined concrete [mm^2]

A_{sw}: total area of the cross section of hoop reinforcement [mm^2]

f_{syk}: yield strength of hoop reinforcement [N/mm^2]

d_s: diameter of A_c [mm]

s: spacing center-to-center of the hoop reinforcement [mm]

A_c: area of concrete core included into circle axis of the hoop [mm^2]

It is assumed 0.2% for strain of unconfined concrete ε_{c0}, corresponding to the maximum compression strength f_{c0}.

The tangent modulus of elasticity in the origin is determined by equation:

$$E_c = 5{,}000\sqrt{f_{c0}} \tag{7.23}$$

While the secant modulus of elasticity E_{sec} is:

$$E_{sec} = \frac{f_{cc}}{\varepsilon_{cc}} \tag{7.24}$$

Where the strain of confined concrete ε_{cc}, corresponding to the maximum compression strength f_{cc} is given by a formulation suggested by Richart[1]:

$$\varepsilon_{cc} = \varepsilon_{c0}\left(1 + 5\left(\frac{f_{cc}}{f_{c0}} - 1\right)\right) \tag{7.25}$$

[1] Richart, R. M. and Abbott, B. J. Versatile elasto-plastic stress-strain formula. Journal of engineering mechanics, ASCE 101, 4 (1975), 511-515.

The relationship between longitudinal compression stress f_c and strain ε_c of concrete is based on equation proposed by Popovics[1]:

$$f_c = \frac{f_{cc} x r}{r - 1 + x^r} \tag{7.26}$$

Where x and r are calculated by:

$$x = \frac{\varepsilon_c}{\varepsilon_{cc}} \tag{7.27}$$

$$r = \frac{E_c}{E_c - E_{sec}} \tag{7.28}$$

7.3.4.2.2 Kawashima model

Hosotani and Kawashima in 1997[2] developed a constitutive model for concrete confined by hoop reinforcement. The model by Kawashima is one of the most widely used models to estimate the axial concrete strength of RC columns confined with transverse steel.

The concrete confined by transverse steel, under monotonic compression has a significant factor for its stress-strain curve (Fig. 7.45) composed of a parabolic first portion and a parabolic second portion with an increase of strength, corresponding to the unconfined concrete and confined concrete respectively. This curve is described using the following equations by Hosotani and Kawashima (1997):

[1] Popovics, S. Numerical approach to the complete stress-strain relation for concrete. Cement and concrete research 3, 5 (1973), 583-599.

[2] Hosotani J., Kawashima K. et al. Stress-strain model for confined reinforced concrete in bridge piers. Member, ASCE. J. Struct. Eng., 1997, 123(5): 624-633.

$$f_c = \begin{cases} E_c\varepsilon_c\left[1-\frac{1}{n}\left(\frac{\varepsilon_c}{\varepsilon_{cc}}\right)^{n-1}\right] \ to \ (0<\varepsilon_c\leq\varepsilon_{cc}) \\ f_{cc}+E_{des}(\varepsilon_c-\varepsilon_{cc}) \ to \ (\varepsilon_{cc}<\varepsilon_c<\varepsilon_{cu}) \end{cases} \quad (7.29)$$

Where n is a coefficient given by:

$$n = \frac{E_c\varepsilon_{cc}}{E_c\varepsilon_{cc}-f_{cc}} \quad (7.30)$$

Where f_{cc} and ε_{cc} are the axial compressive stress and strain of confined concrete; E_c is the modulus of elasticity of unconfined concrete.

$$\varepsilon_{cu} = \varepsilon_{cc} + \frac{f_{cc}}{2E_{des}} \quad (7.31)$$

$$E_{des} = 11.2\frac{f_{c0}^2}{\rho_s \cdot f_{yh}} \quad (7.32)$$

Where ε_{cu} is the ultimate compressive strain of confined concrete; E_{des} is the modulus corresponding to deterioration rate of concrete; f_{yh} is the yield strength of confinement reinforcement; f_{c0} is the strength of unconfined concrete; and ρ_s is the volumetric ratio of hoop reinforcement, which is given by:

$$\rho_s = \frac{4A_h}{s \cdot d} \quad (7.33)$$

Where, s is the spacing center-to-center spiral pitch; d is the diameter of the column section; and A_h is the spiral/hoop bar diameter.

The axial strain of confined concrete (at peak stress of concrete) ε_{cc} may be calculated by Equation (7.34):

$$\varepsilon_{cc} = 0.002 + 0.033 \cdot \beta \frac{\rho_s \cdot f_{yh}}{f_{c0}} \quad (7.34)$$

Where β is a modification factor depending on confined cross section shape: for circular shape $\beta = 1.0$ and for square shape $\beta = 0.4$.

Finally the effective confinement coefficient ($k = \frac{f_{cc}}{f_{c0}}$) can be estimated by using Equation (7.35):

$$\frac{f_{cc}}{f_{c0}} = 1 + 3.8 \cdot \alpha \frac{\rho_s f_{yh}}{f_{c0}} \tag{7.35}$$

Where α is a modification factor depending on confined cross section shape: for circular shape $\alpha = 1.0$ and for square shape $\alpha = 0.2$.

Table 7.12: Comparison between the confinement models applied in the case study

	Concrete mechanical characteristics				
	f_{c0} (MPa)	f_{cc} (MPa)	ε_{c0} (%)	ε_{cc} (%)	k
Mander model	20.0	24.23	0.2	0.41	1.21
Kawashima model	20.0	24.26	0.2	0.39	1.21

Note: f_{c0} = strength of unconfined concrete; f_{cc} = strength of confined concrete; ε_{c0} = strain of unconfined concrete corresponding to the maximum compression strength; ε_{cc} = strain of confined concrete corresponding to the maximum compression strength; k = confinement coefficient.

7.3.4.3 Numerical tests

Two numerical models are considered in order to assess the performance level of the pier: original condition (Fig. 7.46) and current condition considering the degradation of concrete and reinforcement (Fig. 7.48).

In a first case (Figures 7.46 and 7.47) the original physical and mechanical characteristics of materials (concrete and steel) of the reinforced concrete section were considered. To reproduce the strength of the confined concrete (concrete core), its nominal stress-strain law was substituted by a new stress-strain curve obtained from the Kawashima confinement model for concrete, previously

explained and calculated according the Table 7.12. The nominal stress-strain curve for unconfined concrete (concrete cover) is defined as described in the Table 7.13.

Table 7.13: Confined and unconfined concrete mechanical characteristics

	Compression mechanical characteristics				Tension mechanical characteristics			
	f_c (MPa)	f_{cu} (MPa)	ε_c (%)	ε_{cu} (%)	f_{ct} (MPa)	f_{ctu} (MPa)	ε_{ct} (%)	ε_{ctu} (%)
Confined concrete (concrete core)	24.26	19.88	0.39	0.69	2.21	0.00	0.0001	0.0003
Unconfined concrete (concrete cover)	20.00	17.00	0.20	0.35	2.21	0.00	0.0001	0.0003

Note: f_c = concrete cylinder strength; f_{cu} = ultimate concrete cylinder strength; ε_c = axial compressive concrete strain; ε_{cu} = ultimate compressive concrete strain; f_{ct} = concrete tension strength; f_{ctu} = ultimate concrete tension strength; ε_{ct} = tension concrete strain; ε_{ctu} = ultimate concrete strain.

The steel mechanical characteristics for uncorroded bars is defined in Table 7.14 and for corroded bars, reductions of yield strength in tension and compression were considered using the Kashani et al. model by Table 7.15.

Table 7.14: Steel mechanical characteristics for uncorroded reinforcement

	Steel mechanical characteristics				
	$\emptyset$ (mm)	f_{sy} (MPa)	f_{sm} (MPa)	ε_{sh} (%)	ε_{su} (%)
Transverse reinforcing steel	6	445.46	680.40	1.40	16.00
Longitudinal reinforcing steel	12	574.37	666.24	2.25	12.76

Note: $\emptyset$ = bar diameter; f_{sy} = yield stress of steel bars; f_{sm} = steel maximum stress; ε_{sh} = steel strain at hardening initiation; ε_{su} = steel ultimate strain.

Table 7.15: Steel mechanical characteristics for corroded longitudinal bars

	Steel mechanical characteristics			
	D_{corr} (mm)	f_{sy} (MPa)	f_{syt} (MPa)	f_{syc} (MPa)
Mass loss 10%	11.38	574.37	545.65	502.57
Mass loss 14%	11.12	574.37	533.68	472.66

Note: D_{corr} = mean diameter of corroded bar; f_{sy} = yield stress of uncorroded steel bars; f_{syt} = yield strength in tension of corroded bar; f_{syc} = yield strength in compression of corroded bar.

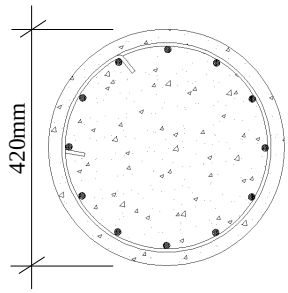

Figure 7.46 Original cross section of non-deteriorated column

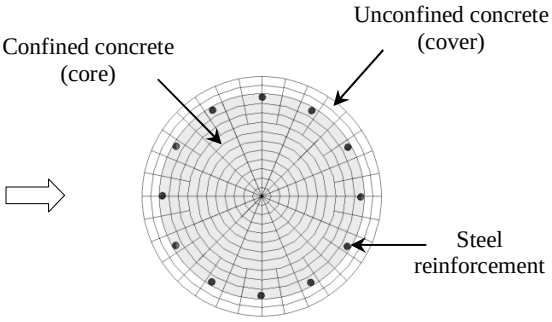

Figure 7.47 FEM model in OpenSees: fiber section model for steel-concrete

In a second case (Figures 7.48 and 7.49) the strength contribution given by the confinement effect of the concrete with hoop reinforcement was neglected as a consequence of the transverse reinforcement breaking by corrosion. In this case, the strength of the concrete core is equal to the concrete cover (Table 7.13). For the reproduction of the mechanical characteristics of the corroded longitudinal reinforcement, the results of the evaluation of residual capacity of the corroded bars previously calculated (Table 7.15) were used in the model.

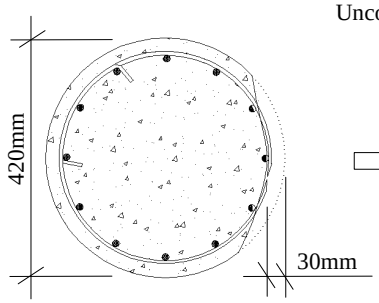

Figure 7.48 Current cross section of deteriorated column

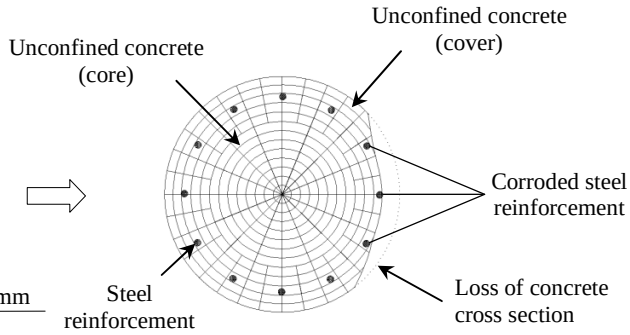

Figure 7.49 FEM model in OpenSees: fiber section model for steel-concrete (considering RC deterioration)

7.3.4.3.1 Push-Over analysis

The models previously explained were written into the *OpenSees* in a Tcl programming language (Tool Command Language). Then a series of non-linear static analyses (Push-Over) were conducted for the given RC sections (damaged and undamaged) applying a vertical load (monotonic axial) of 266kN in the sections and deformation history (section rotation) with a number of increments equal 100.

The analyses of the section were terminated when the predicted stress-strain for the materials were achieved. In Figure 7.50, the fiber section curves are reported around the axis Y direction.

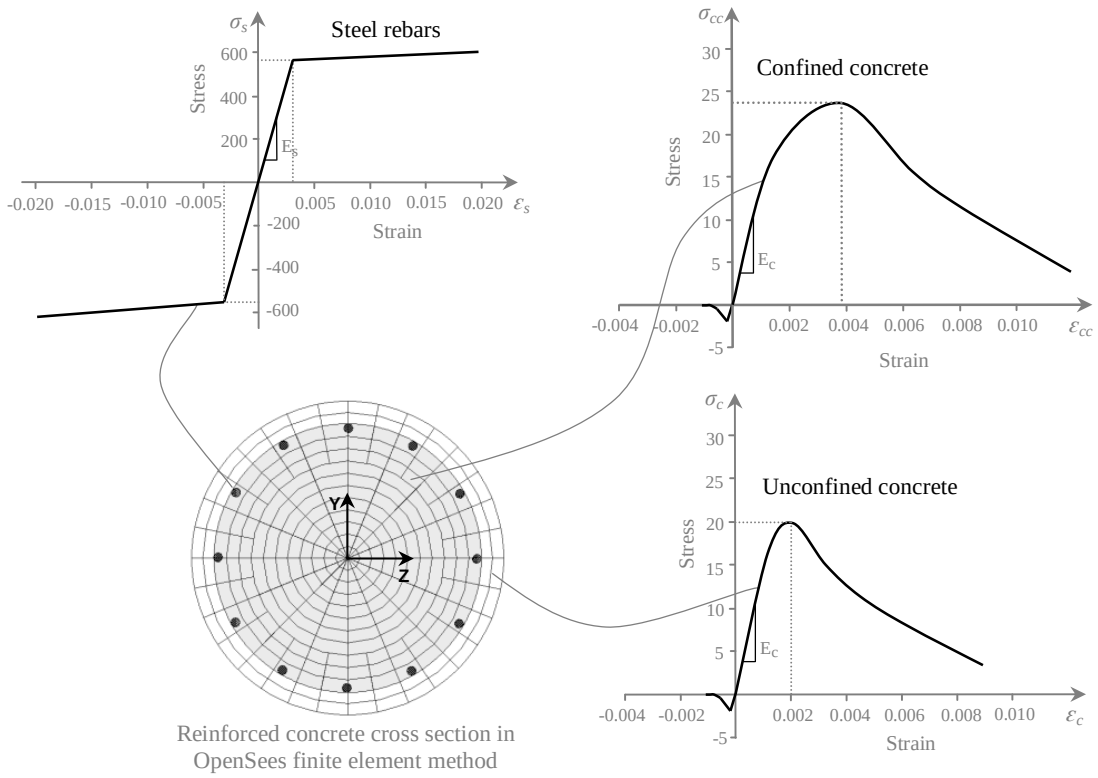

Figure 7.50 Stress-Strain behaviour of the materials under a Push-Over analysis

7.3.4.3.1.1 Tests results comparison

In order to assess the performance loss of the damaged reinforced concrete section analyzed, it is reported in Figures 7.51 a comparison to evaluate the corresponding moment-rotation behaviour. The moment-rotation consists of four characteristics points: cracking, yielding, maximum and collapse points. According to the described assumptions, the moment-rotation curves were obtained for the column cross-sections considering original condition, current condition (deteriorated) and a future condition (deteriorated in 25 years).

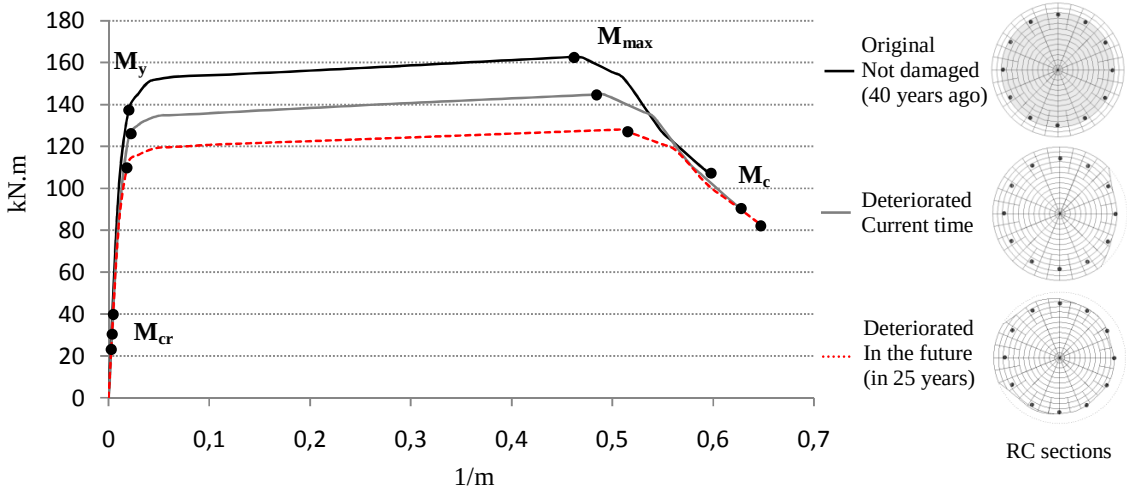

Figure 7.51 Moment-rotation capacity curves of the column section to assessment of the structural performance level

Table 7.16: Comparison between the three sections

Column section	Moments of the column section				
	M_{cr} (kN.m)	M_y (kN.m)	M_{max} (kN.m)	M_c (kN.m)	F_p
Original Not damaged	39	137	163	106	1.00
Deteriorated Current time	30	124	145	89	0.89
Deteriorated in 25 years	24	113	128	81	0.78

Note: M_{cr} = Cracking Moment; M_y = Yielding Moment; M_{max} = Maximum Moment; M_c = Collapse Moment; F_p = Performance Factor (in relation to the Maximum Moment of the original section - not damaged).

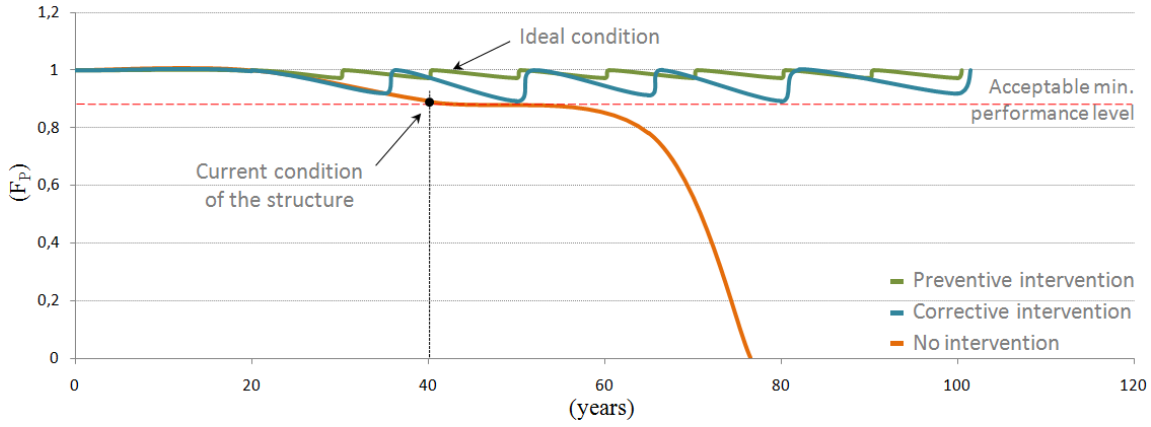

Figure 7.51(a) Comparison between the Performance curves corresponding to the service time of the structure (Fig. 7.43)

7.3.4.3.2 Cyclic analysis

The numerical investigation to evaluate the performance of damaged RC column performed previously by a Push-Over analysis, it was conducted through a series of cyclic tests, with predetermined cyclic history peaks, to know the structural response when the column is subjected to cyclic loading occasioned by seismic actions.

The analyses of the section were carried out for the given sections (damaged and undamaged): original condition, current condition and a future condition (in 25 years). The same section characteristics, previously described were used in these analyses. The UniaxialMaterial Hysteretic model was used to predict the responses of steel reinforcement. For the parts of deteriorated section, the UniaxialMaterial Hysteretic model for steel considering the mechanical characteristics obtained from the evaluation of residual capacity of the corroded bars previously calculated by Kashani et al. model was used.

7.3.4.3.2.1 Tests results comparison

When the predicted cyclic history displacements were reached, the analyses were completed. In Figure 7.54 the cyclic behaviour of the steel under cyclic loading around the axis Y direction are reported.

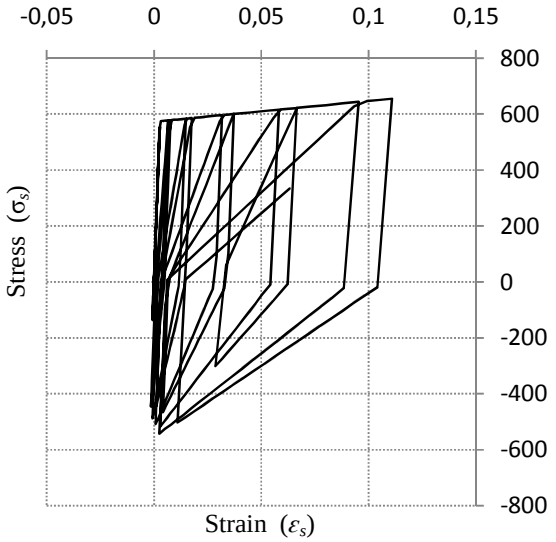

Figure 7.52 Cyclic behaviour (stress-strain) of the Uncorroded Steel

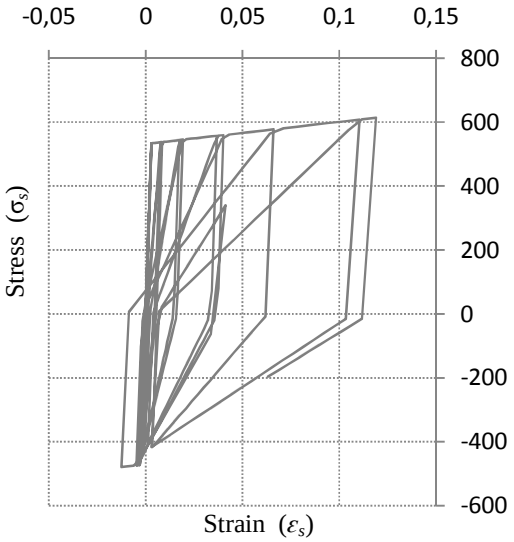

Figure 7.53 Cyclic behaviour (stress-strain) of the Corroded Steel (14%)

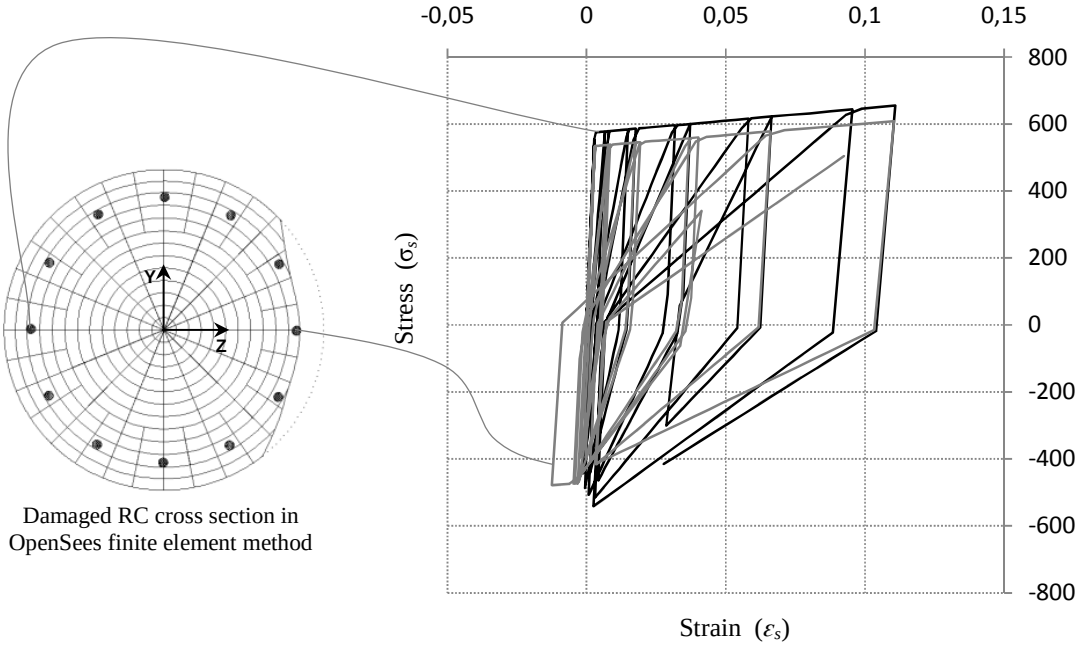

Damaged RC cross section in OpenSees finite element method

Figure 7.54 Cyclic behaviour (stress-strain) of the Corroded Steel (14%) and Uncorroded Steel

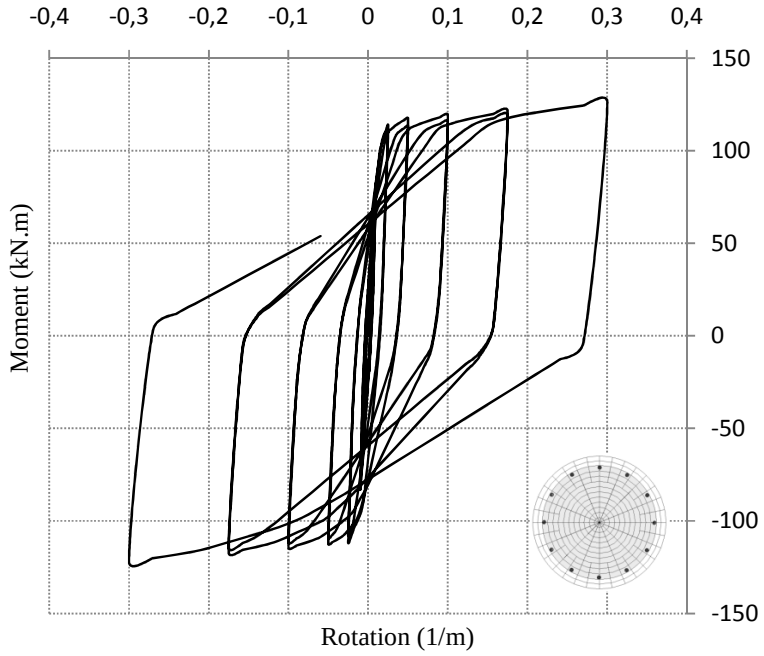

Figure 7.55 Cyclic analysis: Original RC section (no damaged)

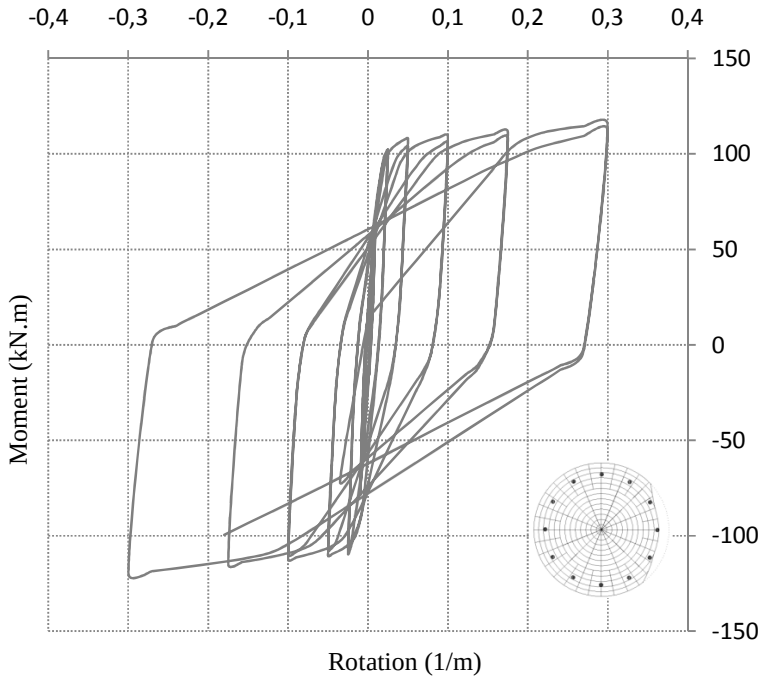

Figure 7.56 Cyclic analysis: Damaged RC section (current time)

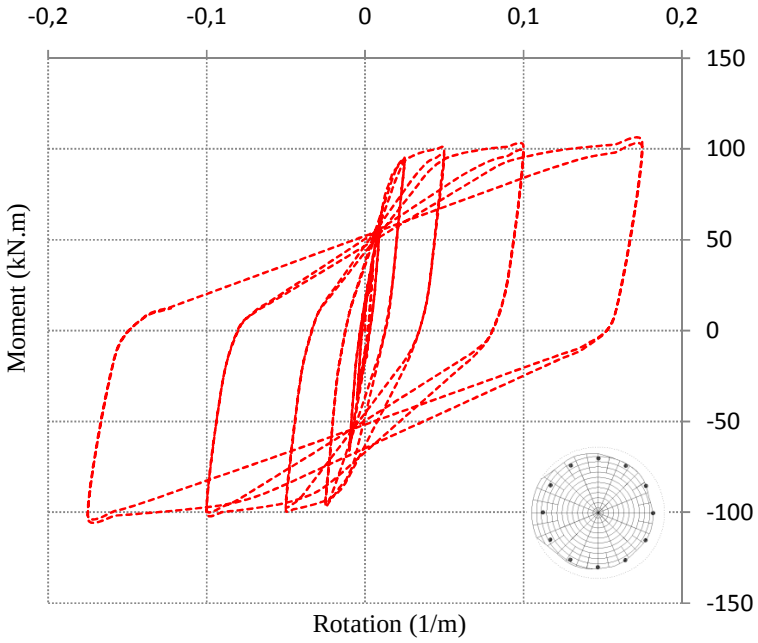

Figure 7.57 Cyclic analysis: Damaged RC section (in 25 years)

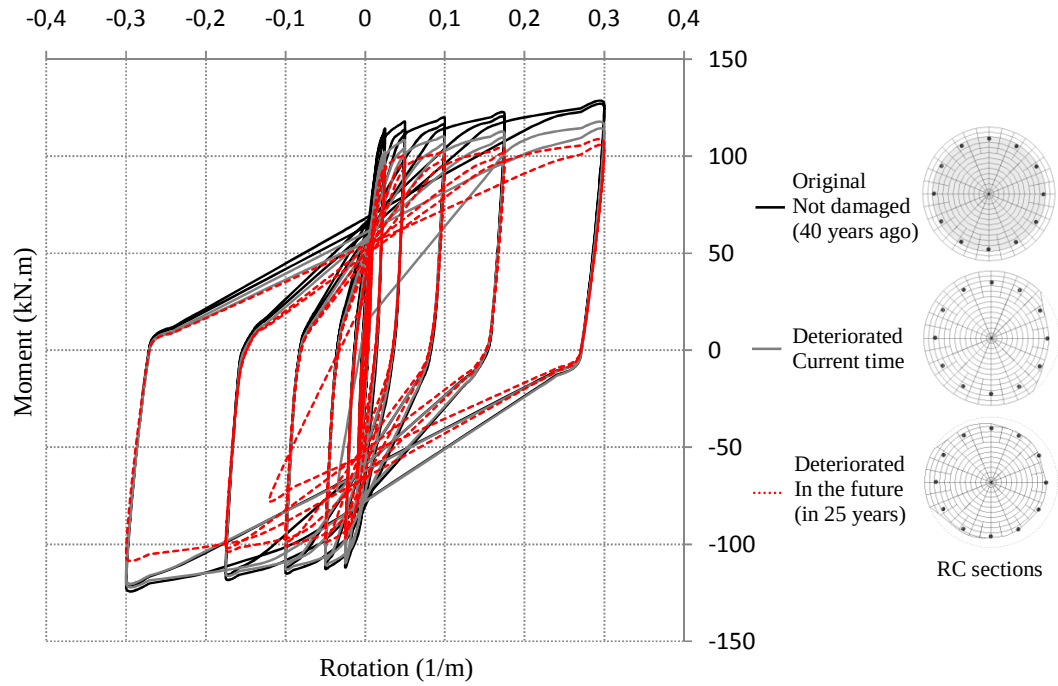

Figure 7.58 Cyclic analysis: Comparison between the three sections

7.3.5 Rehabilitation with HPFRCC technique

7.3.5.1 Numerical modeling

UniaxialMaterial Hysteretic model available in OpenSees was used to predict the responses of the strengthened column with HPFRCC, in terms of flexo-compression strength, on the parts of deteriorated section (Fig. 7.59). HPFRCC material, considering the mechanical characteristics obtained from the experimental tests (explained in Chapter VI) was used, where the values of the force-displacement curves from the test results were transformed into multilinear-hysteretic models. In order to simplify the numerical analyses performed in finite element software with fiber modeling, multilinear-hysteretic model proposed in this Chapter (Figures 7.13, 7.14 and 7.15) was used. The mechanical characteristics for HPFRCC were defined as described in the Table 7.05.

7.3.5.2 Numerical tests

In order to assess the performance level of the rehabilitated column with HPFRCC, six numerical models were built. Where, two strengthening hypotheses with three types of fibers (basalt, polyethylene and stainless steel, 1% and 2% volume) in the mixture were considered. An 8.0cm layer of HPFRCC was considered in the perimeter of the RC section analyzed (Fig. 7.59).

A series of pushover and cyclic analyses for the given RC sections were conducted. Considering original condition, current condition (deteriorated) and rehabilitated, the capacity curves for the column cross-section were obtained.

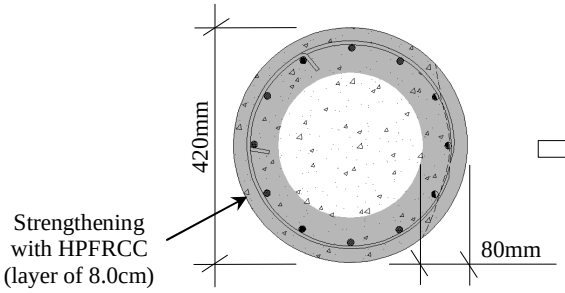

Figure 7.59 Strengthened cross section with 8.0 cm of HPFRCC

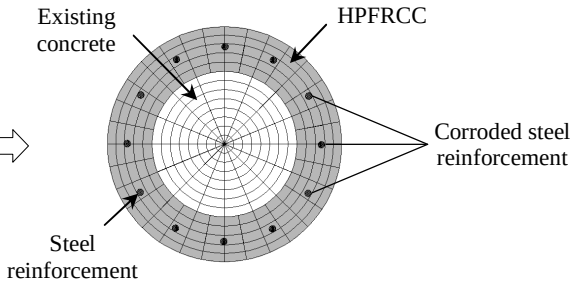

Figure 7.60 FEM model in OpenSees: fiber section model for steel-concrete (considering HPFRCC)

7.3.5.3 Tests results comparison

In order to evaluate the flexo-compression strength increase of the damaged section analyzed, comparisons of maximum moment-rotation behaviour are reported in the Figures below.

7.3.5.3.1 Pushover analysis

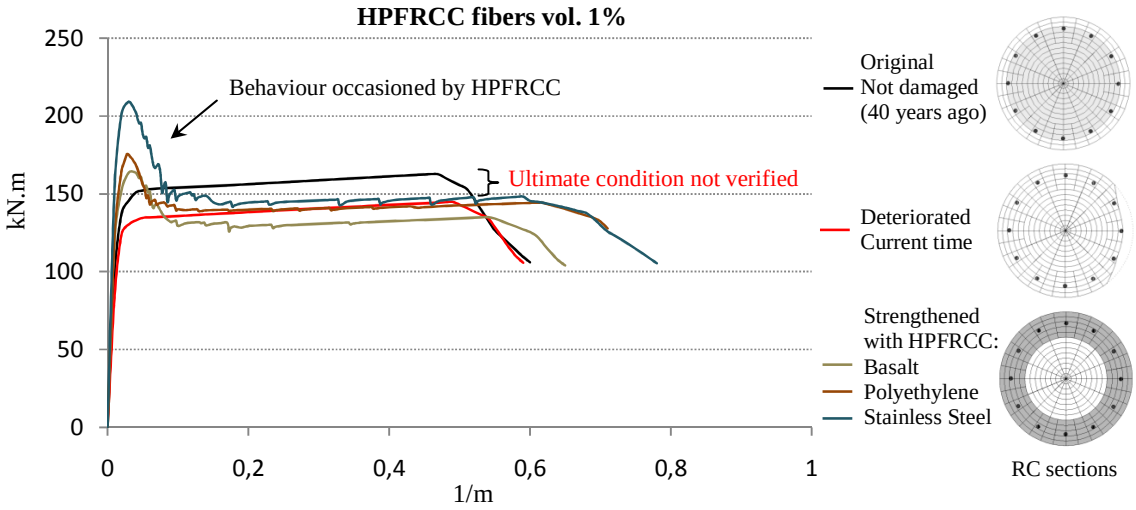

Figure 7.61 Moment-rotation capacity curves of the strengthened column section for assessment of the structural performance level (HPFRCC fiber vol. 1%)

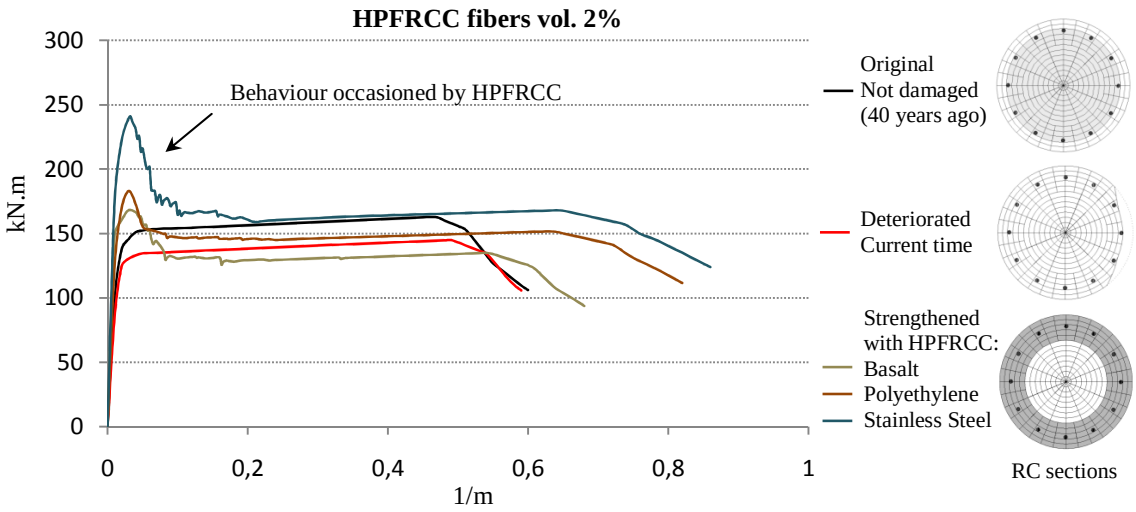

Figure 7.62 Moment-rotation capacity curves of the strengthened column section for assessment of the structural performance level (HPFRCC fiber vol. 2%)

Table 7.17: Comparison between moment-rotation of the column section

Column Section			M_{max} (kN.m)	F_p
Original condition Not damaged			163	1.00
Deteriorated Current time			145	0.89
Strengthened with HPFRCC	Basalt	(vol. 1%)	162	0.99
		(vol. 2%)	168	1.03
	Polyethylene	(vol. 1%)	176	1.08
		(vol. 2%)	183	1.12
	Stainless Steel	(vol. 1%)	209	1.28
		(vol. 2%)	241	1.48

Note: M_{max} = Maximum Moment; F_p = Performance Factor (in relation to the Maximum Moment of the original section – not damaged).

7.3.5.3.2 Cyclic analysis

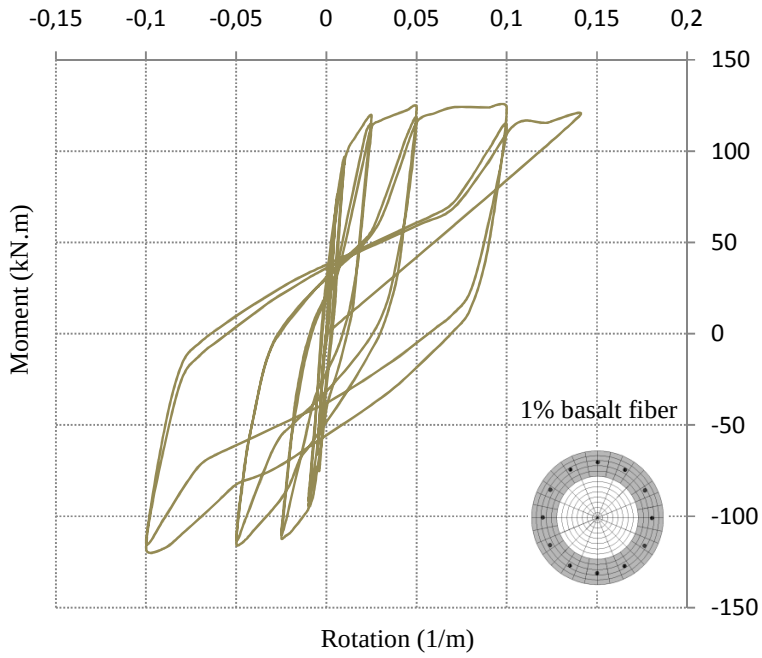

Figure 7.63 Cyclic analysis: strengthened column section with HPFRCC (1% basalt fiber)

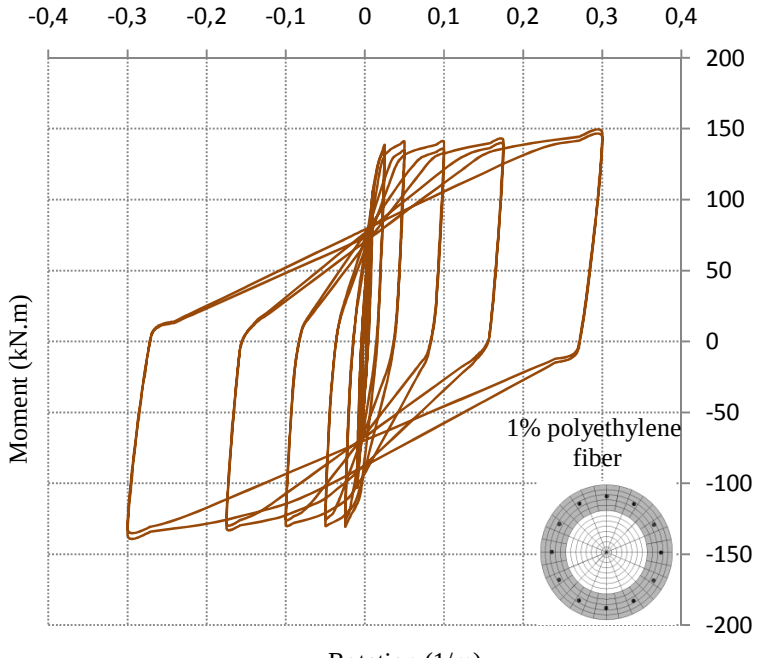

Figure 7.64 Cyclic analysis: strengthened column section with HPFRCC (1% polyethylene fiber)

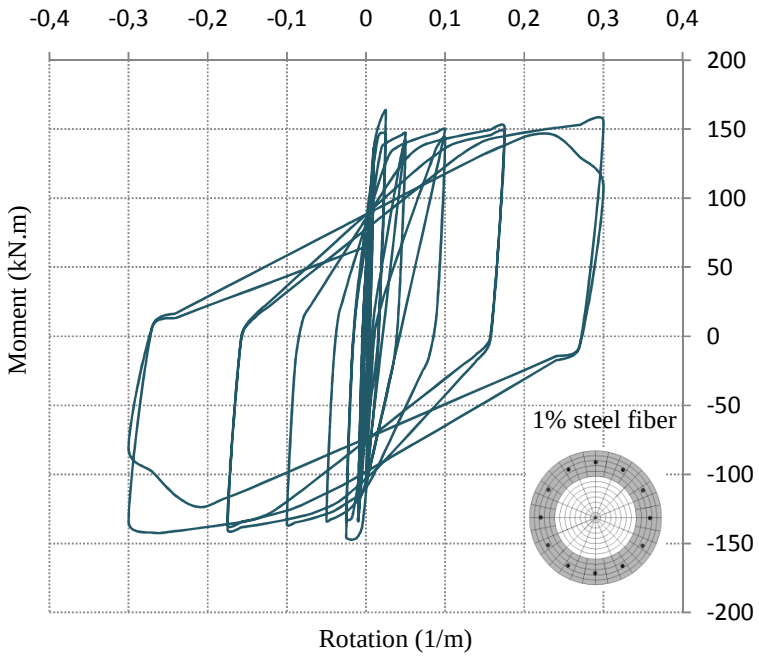

Figure 7.65 Cyclic analysis: strengthened column section with HPFRCC (1% stainless steel fiber)

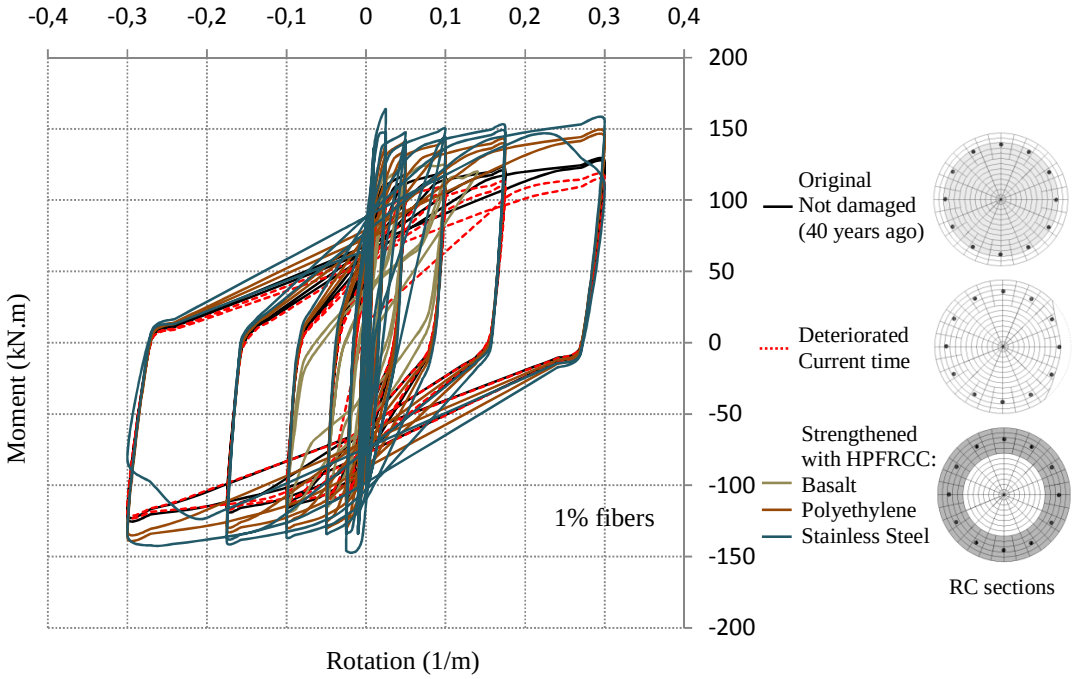

Figure 7.66 Cyclic analysis: strengthened column section with HPFRCC (1% basalt, polyethylene and steel fibers)

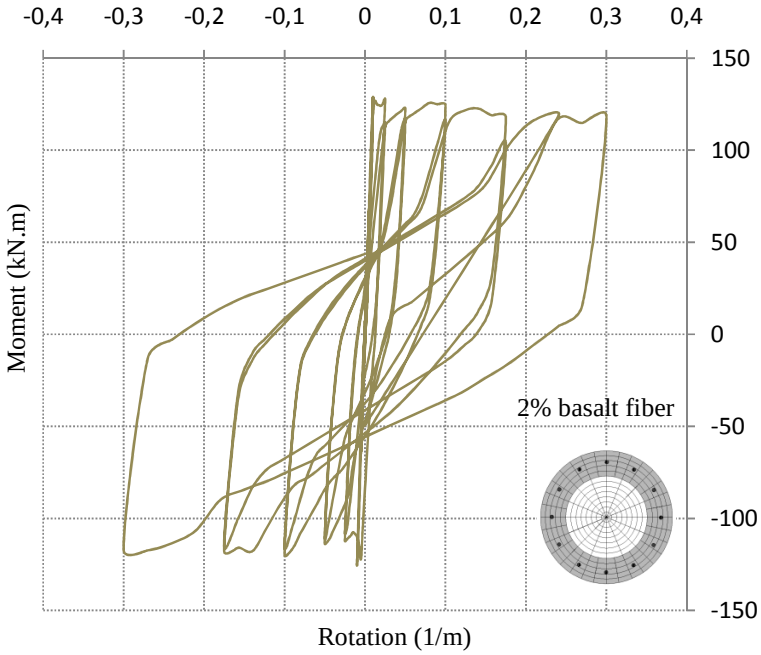

Figure 7.67 Cyclic analysis: strengthened column section with HPFRCC (2% basalt fiber)

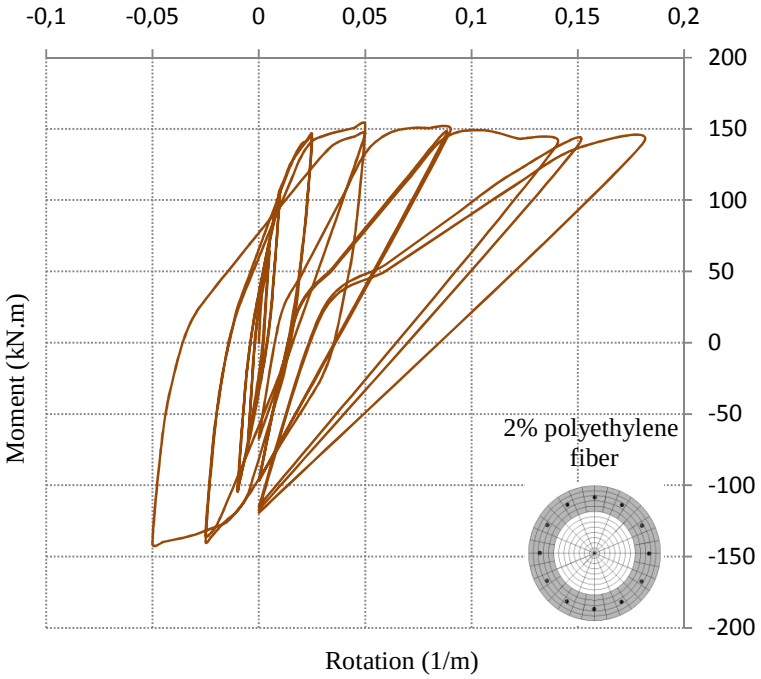

Figure 7.68 Cyclic analysis: strengthened column section with HPFRCC (2% polyethylene fiber)

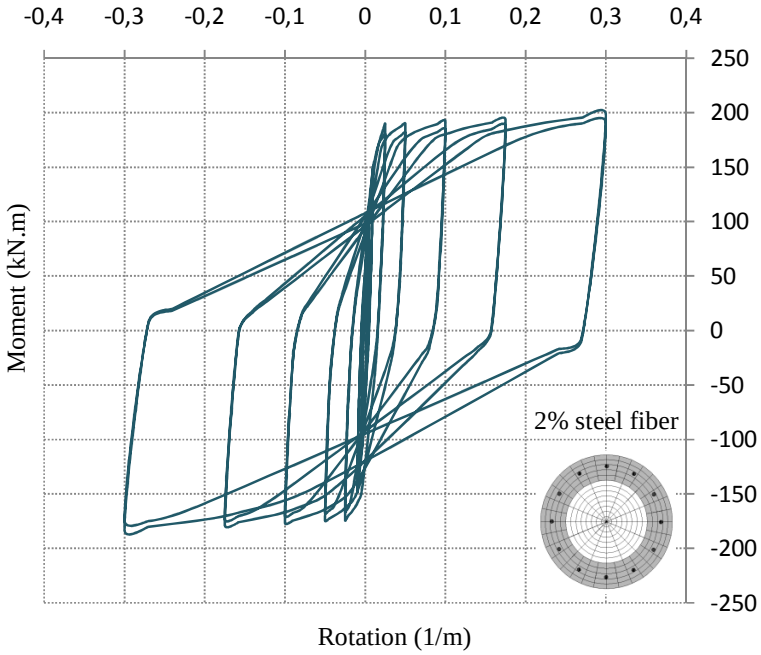

Figure 7.69 Cyclic analysis: strengthened column section with HPFRCC (2% stainless steel fiber)

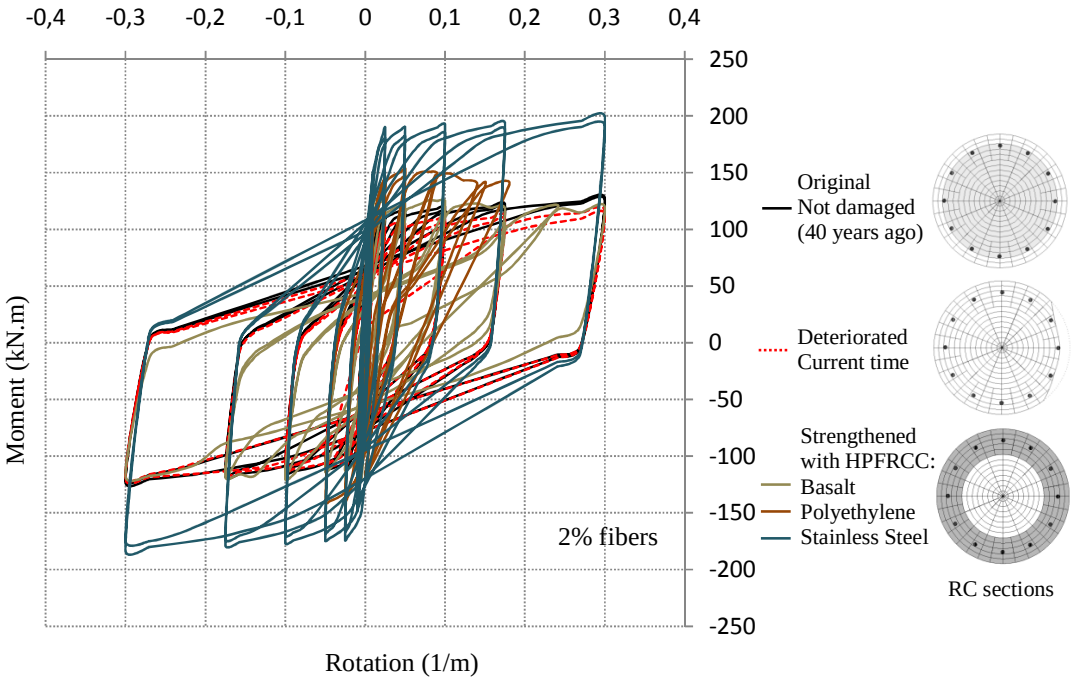

Figure 7.70 Cyclic analysis: strengthened column section with HPFRCC (2% basalt, polyethylene and steel fibers)

7.3.6 Rehabilitation with FRCM technique

7.3.6.1 Numerical model

To evaluate the flexo-compression strength increase of the damaged RC section analyzed, a series of numerical tests with application of internal FRCM by wet lay-up system (composed of cementitious matrix and a very thin mesh of fiber in carbon, stainless steel or glass) were performed. The analyses of structural strengthening of the RC column were carried out according to the current Italian standards, through *Opensees* software framework and using a calculator (Figure 7.71) for evaluation of RC elements strengthened with FRP and FRCM systems, which was developed during the PhD studies. The FRCM properties were assumed by commercial products specifications available in Italy (Table 7.07).

Figure 7.71 Calculator for evaluation of RC elements strengthened with FRP and FRCM systems (developed during the PhD studies)
Compression in RC Pillar (circular section)

For verification, Figures 7.73, 7.74 and 7.75 show input and output data on the calculator for FRCM confinement with meshes in carbon, stainless steel and glass fibers.

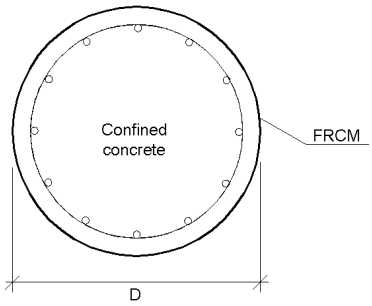

Figure 7.72 Representation of FRCM confinement
for strengthening of RC columns

Existing Materials Characteristics			
$f_{yk,m}$ (N/mm²)	574	$f_{ck,m}$ (N/mm²)	20
E_s	200000	f_{ctm}	2,21
γ_s	1,00	γ_c	1,00
FC	1,00	$\gamma_{Rd\ (SLU)}$	1,00

Data Column			
D (mm)	420	r_c (mm)	30
Num. rebar	12	Area rebar (mm²)	113
N_{Rd} (kN)	3550,43	N_{Sd} (kN)	266,00

Strengthening System Characteristics			
E_f (N/mm²)	240000	$t_{f,1}$ (mm)	0,167
f_{fk} (N/mm²)	4700	η_f	1
γ_f	1,10	η_a	0,85
$\gamma_{f,d}$	1,20	K_v	1
K_α	1	K_h	1
b_f	1	p_f	1

Results			
$N_{Rcc,d}$ (kN)	4367,17	f_{ccd} (N/mm²)	25,90
$f_{l,eff}$ (N/mm²)	0,76	ρ_f	0,0016
f_{cc} (N/mm²)	25,90	$\varepsilon_{fd,rid}$ (mm/mm)	0,0040

Exit

Figure 7.73 Input and output data from the calculator for evaluation
of RC elements strengthened with FRP and FRCM systems
(Confinement with Carbon FRCM)

Existing Materials Characteristics			
$f_{yk,m}$ (N/mm²)	574	$f_{ck,m}$ (N/mm²)	20
E_s	200000	f_{ctm}	2,21
γ_s	1,00	γ_c	1,00
FC	1,00	$\gamma_{Rd\ (SLU)}$	1,00

Data Column			
D (mm)	420	r_c (mm)	30
Num. rebar	12	Area rebar (mm²)	113
N_{Rd} (kN)	3550,43	N_{Sd} (kN)	266,00

Strengthening System Characteristics			
E_f (N/mm²)	190000	$t_{f,1}$ (mm)	0,167
f_{fk} (N/mm²)	2350	η_f	1
γ_f	1,10	η_a	0,85
$\gamma_{f,d}$	1,20	K_v	1
K_α	1	K_h	1
b_f	1	p_f	1

Results			
$N_{Rcc,d}$ (kN)	4249,38	f_{ccd} (N/mm²)	25,04
$f_{l,eff}$ (N/mm²)	0,60	ρ_f	0,0016
f_{cc} (N/mm²)	25,04	$\varepsilon_{fd,rid}$ (mm/mm)	0,0040

Exit

Figure 7.74 Input and output data from the calculator for evaluation
of RC elements strengthened with FRP and FRCM systems
(Confinement with Stainless Steel FRCM)

Existing Materials Characteristics			
$F_{yk,m}$ (N/mm²)	574	$F_{ck,m}$ (N/mm²)	20
E_s	200000	F_{ctm}	2,21
γ_s	1,00	γ_c	1,00
FC	1,00	γ_{Rd} (SLU)	1,00

Data Column			
D (mm)	420	r_c (mm)	30
Num. rebar	12	Area rebar (mm²)	113
N_{Rd} (kN)	3550,43	N_{Sd} (kN)	266,00

Strengthening System Characteristics			
E_f (N/mm²)	73000	$t_{f,1}$ (mm)	0,167
f_{fk} (N/mm²)	2600	η_f	1
γ_f	1,10	η_a	0,85
$\gamma_{f,d}$	1,20	K_v	1
K_α	1	K_h	1
b_f	1	p_f	1

Results			
$N_{Rcc,d}$ (kN)	3919,82	f_{ccd} (N/mm²)	22,67
$f_{l,eff}$ (N/mm²)	0,23	ρ_f	0,0016
f_{cc} (N/mm²)	22,67	$\varepsilon_{fd,rid}$ (mm/mm)	0,0040

Exit

Figure 7.75 Input and output data from the calculator for evaluation of RC elements strengthened with FRP and FRCM systems (Confinement with Glass FRCM)

7.3.6.1.1 Numerical modeling details

To predict the responses of the strengthened column with internal FRCM, in terms of flexo-compression strength, UniaxialMaterial Hysteretic model available in OpenSees on the parts of deteriorated section (Fig. 7.77) was used. The FRCM system was used considering the mechanical characteristics obtained from the commercial products specifications and for the RC section confinement model, the proposed equations from the Italian standard CNR-DT 200 R1/2013 (explained in Chapter VI) were used. Figure 7.76 shows the strain-strain hysteretic model used in OpenSees for confinement of the column section with FRCM System, in carbon, stainless steel and glass fibers.

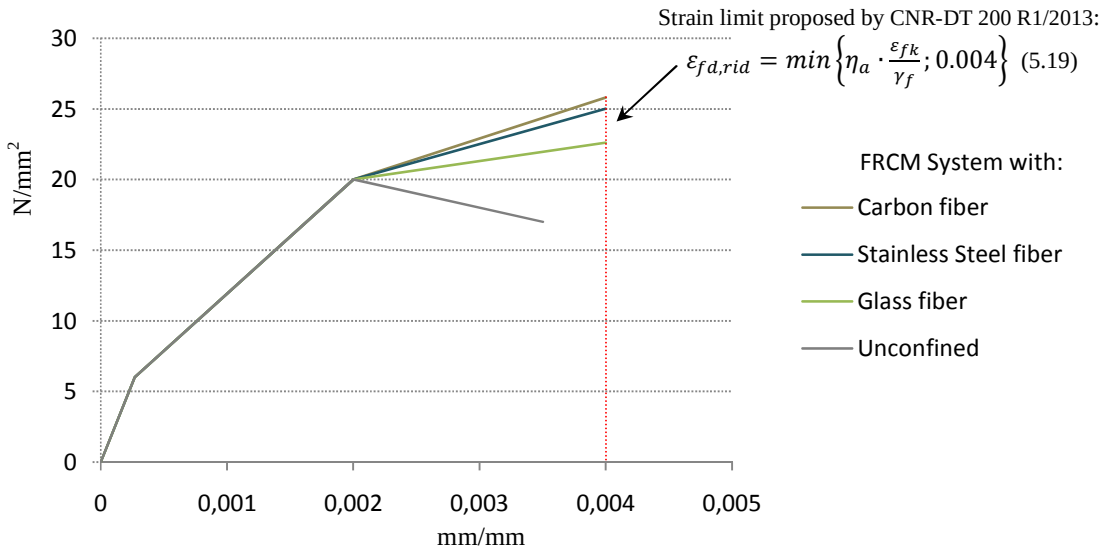

Figure 7.76 FRCM System Stress-Strain curves for confinement model in *OpenSees* Software (Hysteretic model for confined sections)

The values of mechanical characteristics of the confined sections are reported in Table 7.18.

Table 7.18: FRCM confinement mechanical characteristics for fiber model in OpenSees (1 and 2 layers)

FRCM System		FRCM confinement mechanical characteristics				
		f_{c0} (MPa)	f_{cc} (MPa)	ε_{c0} (%)	ε_{cc} (%)	k
Confinement with FRCM 1 layer	Carbon fiber	20.0	25.90	0.20	0.40	1.29
	S. Steel fiber	20.0	25.00	0.20	0.40	1.25
	Glass fiber	20.0	22.60	0.20	0.40	1.13
Confinement with FRCM 2 layers	Carbon fiber	20.0	29.36	0.20	0.40	1.47
	S. Steel fiber	20.0	28.00	0.20	0.40	1.40
	Glass fiber	20.0	24.23	0.20	0.40	1.21

Note: f_{c0} = strength of unconfined concrete; f_{cc} = strength of confined concrete; ε_{c0} = strain of unconfined concrete corresponding to the maximum compression strength; ε_{cc} = strain of confined concrete corresponding to the maximum compression strength; k = confinement coefficient.

7.3.6.2 Numerical tests

Pushover and cyclic analyses were conducted and the resistance moments, considering original condition, current condition (deteriorated) and rehabilitated, for the column cross-section were obtained.

For the analyses carried out (represented in Figure 7.78) one layer of fiber mesh was used and the regularization of the deteriorated column surface with plain concrete was performed.

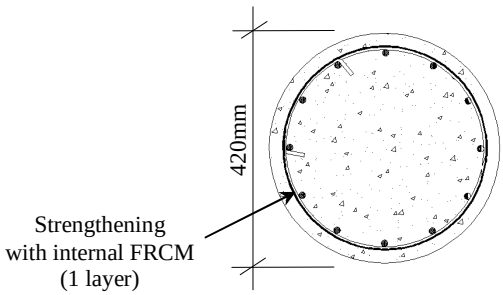

Figure 7.77 Strengthened cross section with internal FRCM (1 layer)

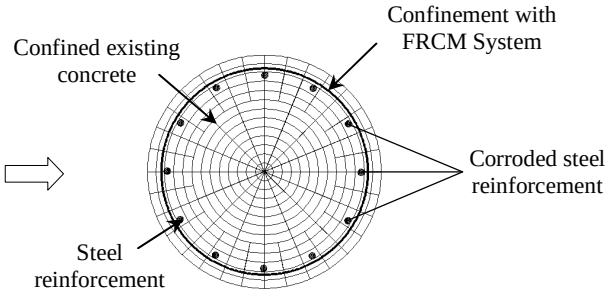

Figure 7.78 FEM model in OpenSees: fiber section model for steel-concrete (considering FRCM)

7.3.6.3 Tests results comparison

In order to assess the flexo-compression strength increase of the damaged reinforced concrete section analyzed, comparisons of moment-rotation behaviour are reported in the Figures below.

7.3.6.3.1 Pushover analysis for confined column

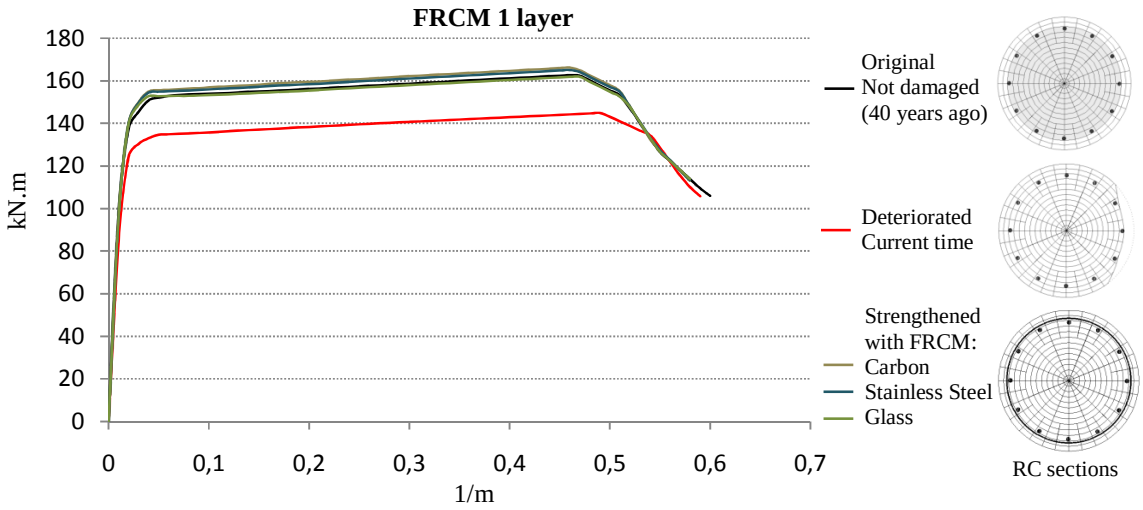

Figure 7.79 Moment-rotation capacity curves of the strengthened column section for assessment of the structural performance level (FRCM 1 layer - confinement)

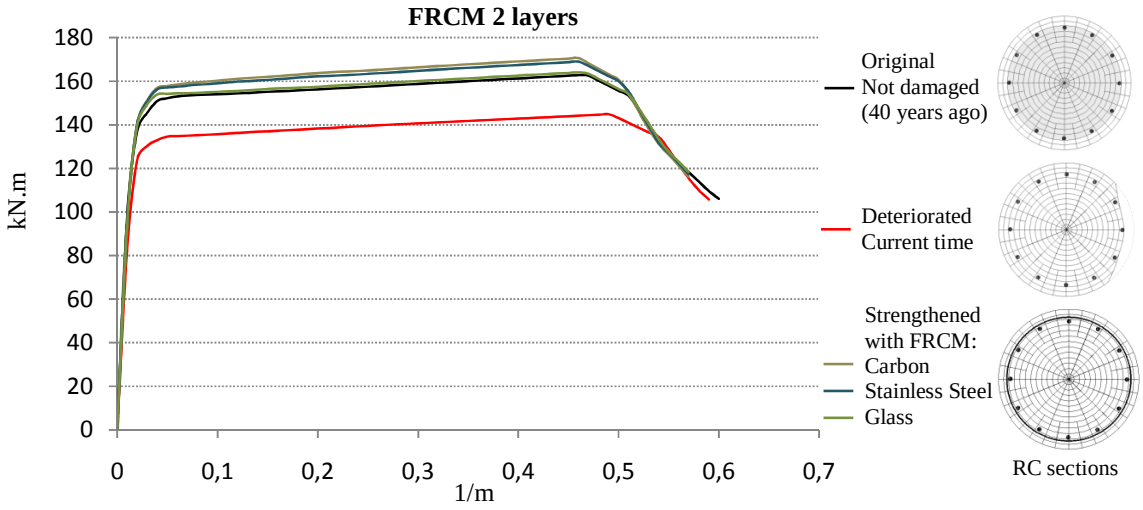

Figure 7.80 Moment-rotation capacity curves of the strengthened column section for assessment of the structural performance level (FRCM 2 layers - confinement)

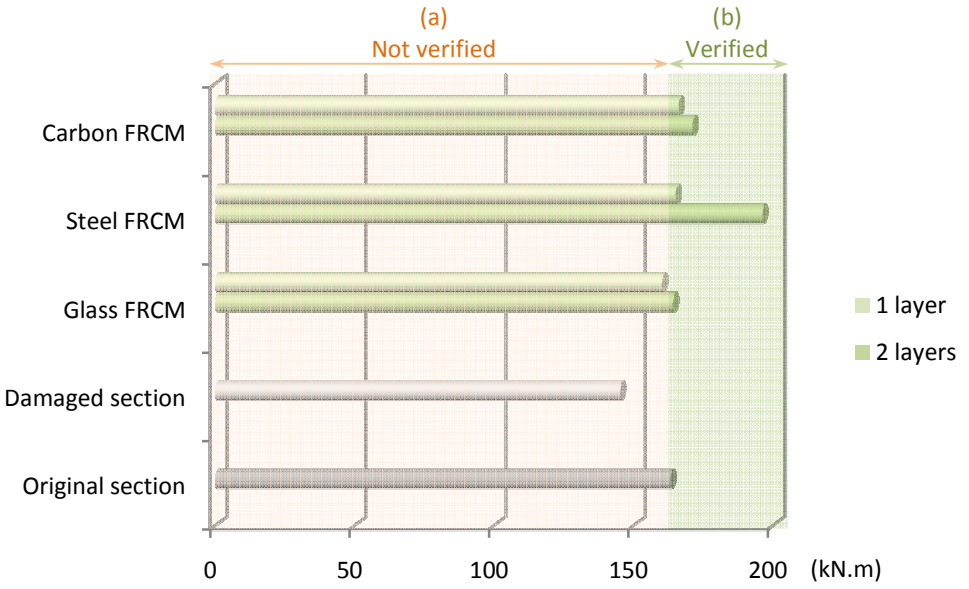

Figure 7.81 Comparison between moments of resistance of the
RC column section for assessment of the structural performance level

Table 7.19: Comparison between maximum moments and maximum axial capacity of the column section confined with 1 and 2 layers FRCM

Column Section		M_{max} (kN.m)	F_{pM}	N_{max} (kN)	F_{pN}
Original condition (Not damaged)		163	1.00	3550	1.00
Deteriorated (Current time)		145	0.89	3160	0.89
Confinement with FRCM (1 layer)	Carbon	166	1.02	4367	1.23
	Stainless Steel	165	1.01	4249	1.20
	Glass	162	0.99	3920	1.10
Confinement with FRCM (2 layer)	Carbon	171	1.05	4847	1.37
	Stainless Steel	169	1.04	4660	1.31
	Glass	164	1.01	4137	1.17

Note: M_{max} = Maximum Moment; F_{pM} = Moment Performance Factor (in relation to the Maximum Moment of the original section – not damaged); N_{max} = Maximum Axial Capacity; F_{pN} = Axial Capacity Performance Factor (in relation to the Axial Capacity of the original section – not damaged).

7.3.6.3.2 Pushover analysis for combined confinement and flexural strengthening

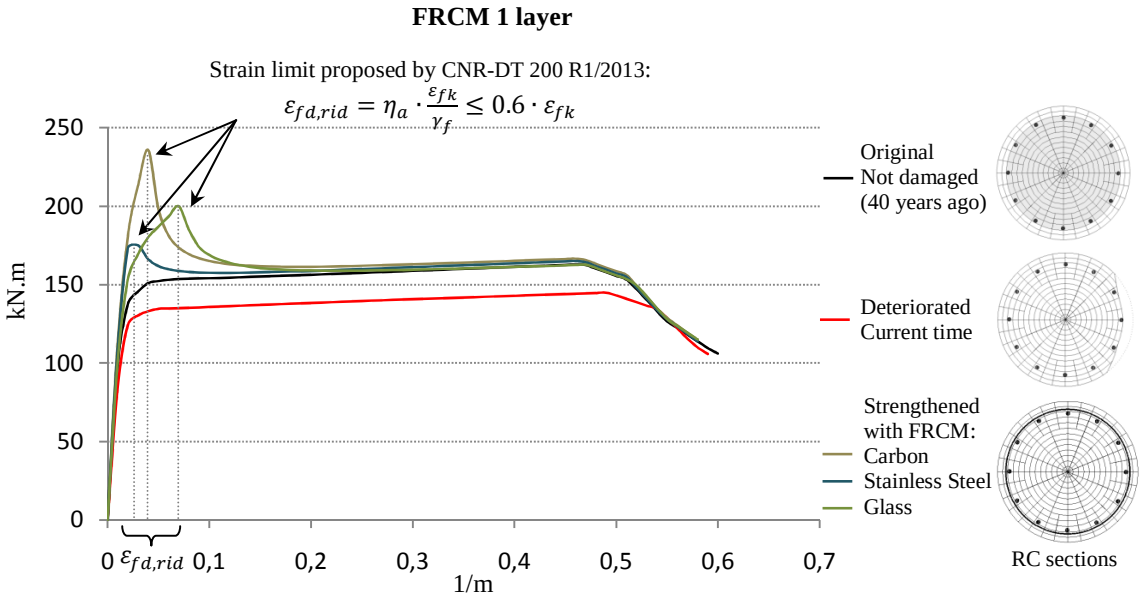

Figure 7.82 Moment-rotation capacity curves of the strengthened column section for assessment of the structural performance level (FRCM 1 layer – combined flexural and confinement)

Table 7.20: Comparison between maximum moments of the column section strengthened with combined flexural and confinement FRCM (1 layer)

Column Section		M_{max} (kN.m)	F_{pM}
Original condition (Not damaged)		163	1.00
Deteriorated (Current time)		145	0.89
Confinement FRCM (1 layer)	Carbon	166	1.02
	Stainless Steel	165	1.01
	Glass	162	0.99
Combined Flexural and Confinement FRCM (1 layer)	Carbon	236	1.45
	Stainless Steel	175	1.07
	Glass	200	1.23

Note: M_{max} = Maximum Moment; F_{pM} = Moment Performance Factor (in relation to the Maximum Moment of the original section – not damaged).

7.3.6.3.3 Cyclic analysis for combined confinement and flexural strengthening

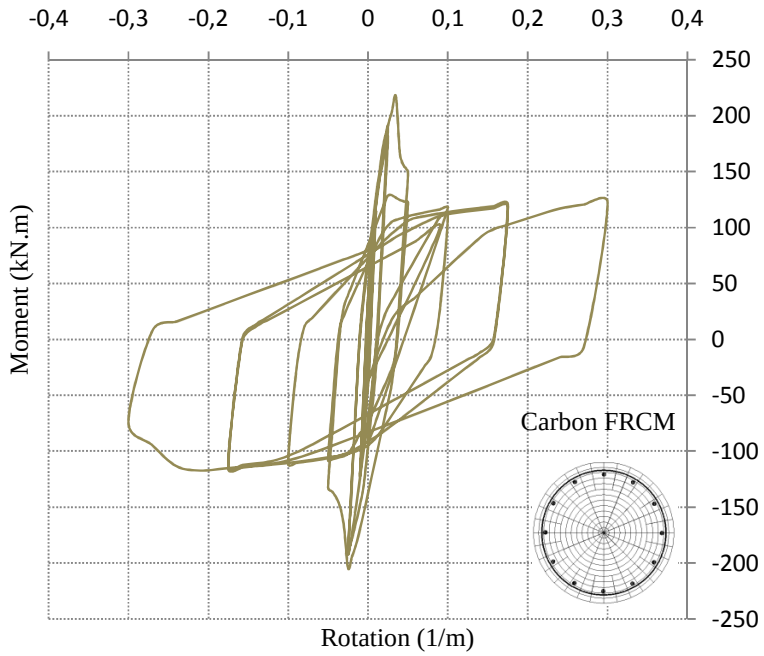

Figure 7.83 Cyclic analysis: strengthened column section with 1 layer of Carbon FRCM (Combined confinement and flexural strengthening)

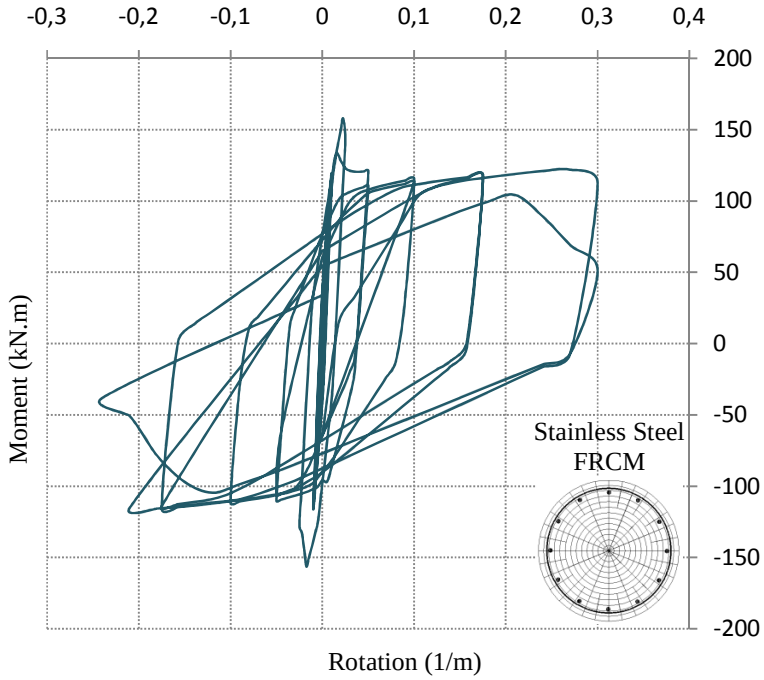

Figure 7.84 Cyclic analysis: strengthened column section with 1 layer of Stainless Steel FRCM (Combined confinement and flexural strengthening)

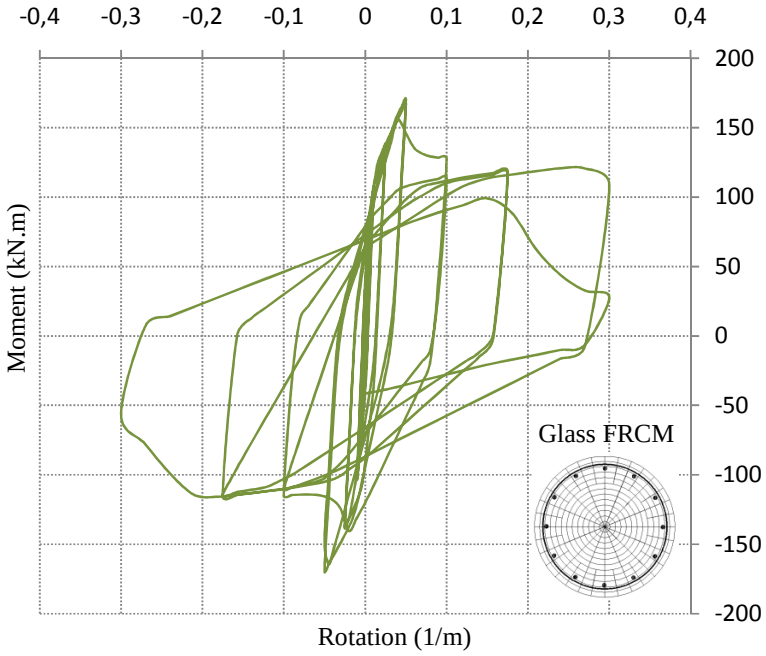

Figure 7.85 Cyclic analysis: strengthened column section with
1 layer of Glass FRCM (Combined confinement and flexural strengthening)

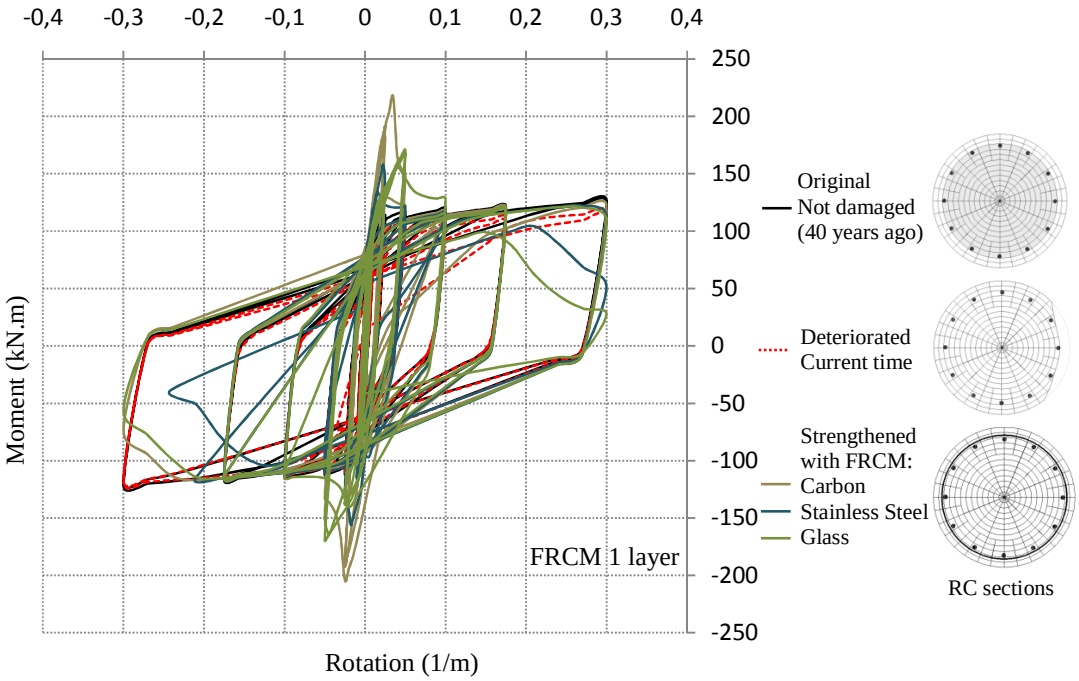

Figure 7.86 Cyclic analysis: strengthened column section with
1 layer of FRCM (Combined confinement and flexural strengthening)

7.3.7 Rehabilitation combining HPFRCC and FRCM techniques

7.3.7.1 Materials composition and numerical tests

A series of numerical tests for application of HPFRCC combined with internal FRCM system [1] through *Opensees* software framework were performed, to evaluate the flexural strength increase of the deteriorated section studied.

In order to assess the performance level of the rehabilitated column, four numerical models were built. Considering two types of HPFRCC with polyethylene and stainless steel fibers, vol. 2%, combined with two types of FRCM System (with 1 layer of stainless steel and glass fiber meshes). In the application of the two techniques, one layer of a very thin fiber mesh combined with a layer of 8.0 cm of HPFRCC was considered (Fig. 7.87).

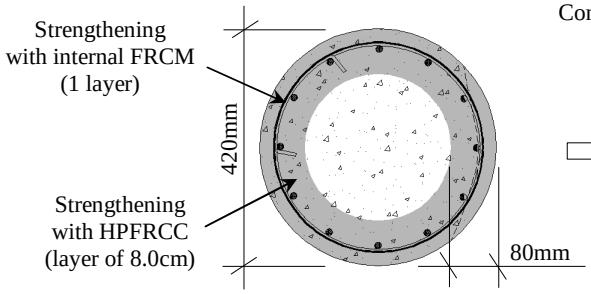

Figure 7.87 Combined HPFRCC and FRCM techniques for rehabilitation of RC section

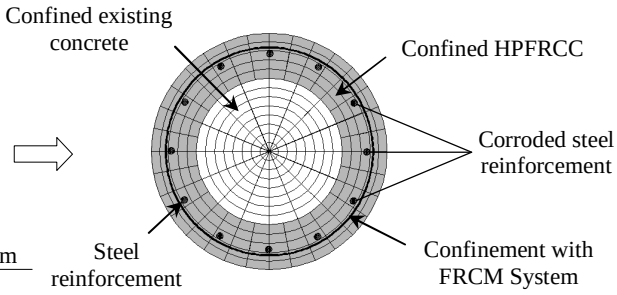

Figure 7.88 FEM model in OpenSees: fiber section model for steel-concrete (considering HPFRCC and FRCM)

7.3.7.2 Tests results comparison

To obtain the capacity curves of the cross-section, pushover and cyclic analyses were conducted. Considering original condition, current condition (deteriorated) and rehabilitated with Glass FRCM + Polyethylene HPFRCC and Glass FRCM + Steel HPFRCC; Steel FRCM + Polyethylene HPFRCC and Steel FRCM + Steel HPFRCC.

[1] Combined flexural and confinement strengthening for FRCM System in the fiber model of Opensees.

Comparisons to evaluate the moment-rotation behaviour are reported in the Figures and Table below.

7.3.7.3 Pushover analysis

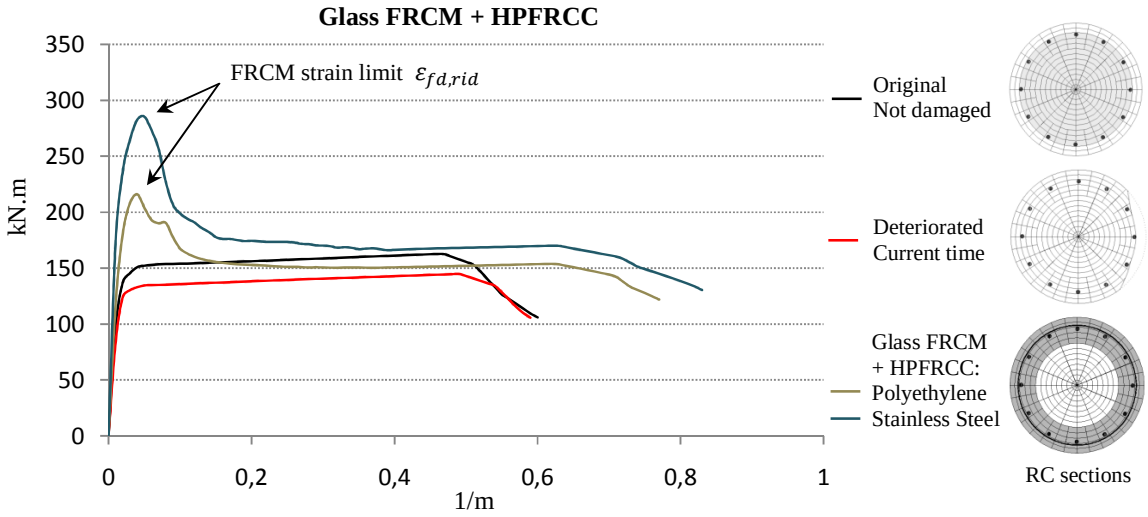

Figure 7.89 Moment-rotation capacity curves of the strengthened beam section for assessment of the structural performance level (Glass FRCM 1 layer + HPFRCC fibers vol. 2% layer 8.0cm)

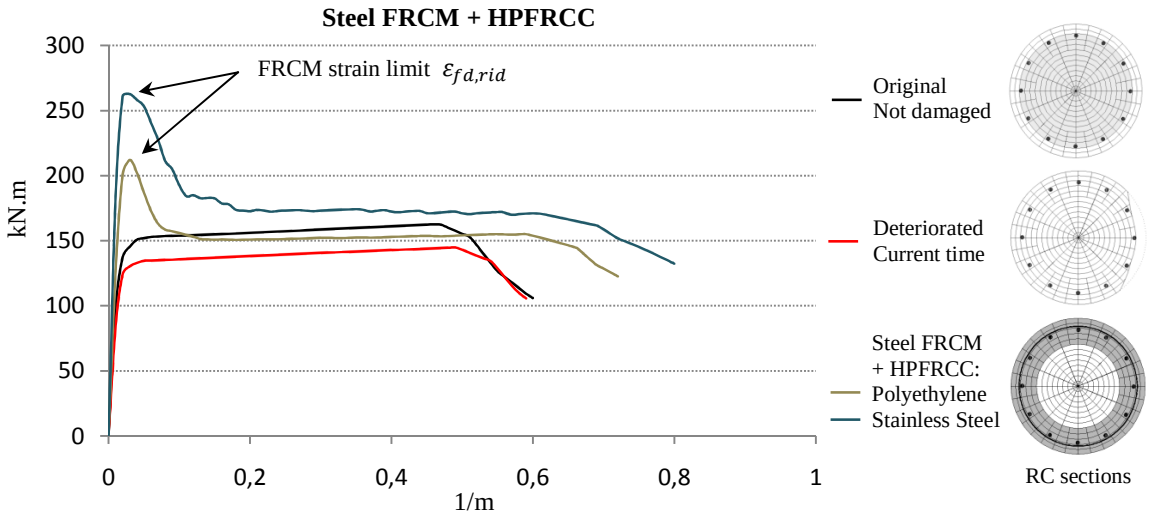

Figure 7.90 Moment-rotation capacity curves of the strengthened beam section for assessment of the structural performance level (Steel FRCM 1 layer + HPFRCC fibers vol. 2% layer 8.0cm)

Table 7.21: Comparison between maximum moments of the strengthened column section

Column Section		M_{max} (kN.m)	F_p
Original condition (Not damaged)		163	1.00
Deteriorated (Current time)		145	0.89
Strengthened with Glass FRCM (1 layer) +	Polyethylene HPFRCC	216	1.33
	Stainless Steel HPFRCC	285	1.75
Strengthened with Steel FRCM (1 layer) +	Polyethylene HPFRCC	212	1.30
	Stainless Steel HPFRCC	262	1.61

Note: M_{max} = Maximum Moment; F_p = Performance Factor (in relation to the Maximum Moment of the original section – not damaged).

7.3.7.4 Cyclic analysis

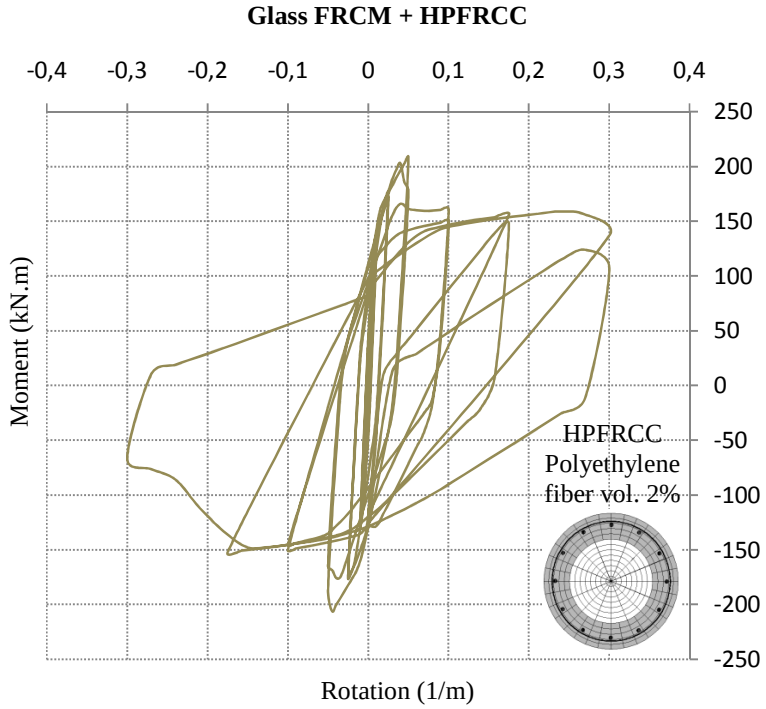

Figure 7.91 Cyclic analysis: strengthened column section with combined Glass FRCM 1 layer + HPFRCC Polyethylene fiber vol. 2% (8.0cm of layer)

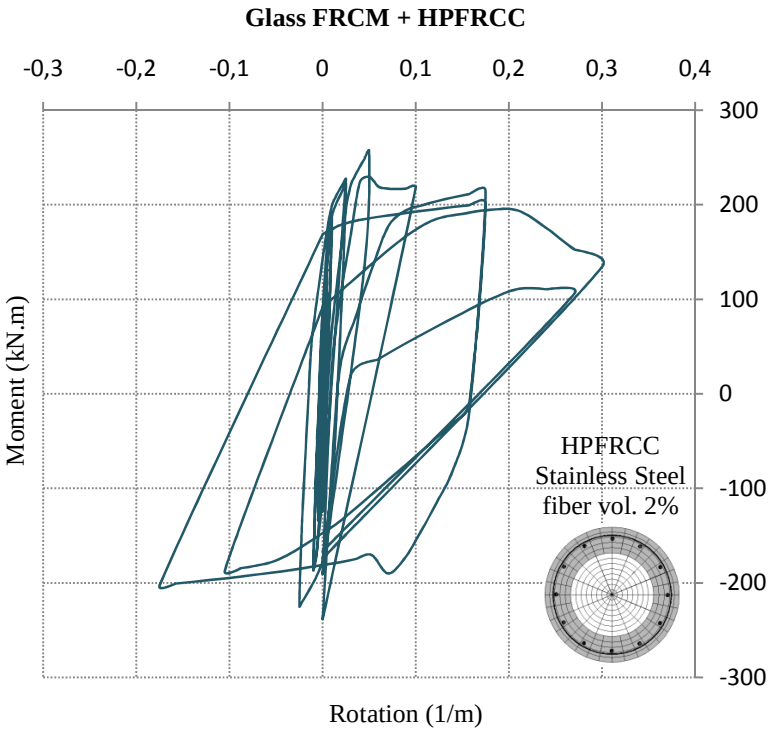

Figure 7.92 Cyclic analysis: strengthened column section with combined Glass FRCM 1 layer + HPFRCC Stainless Steel fiber vol. 2% (8.0cm of layer)

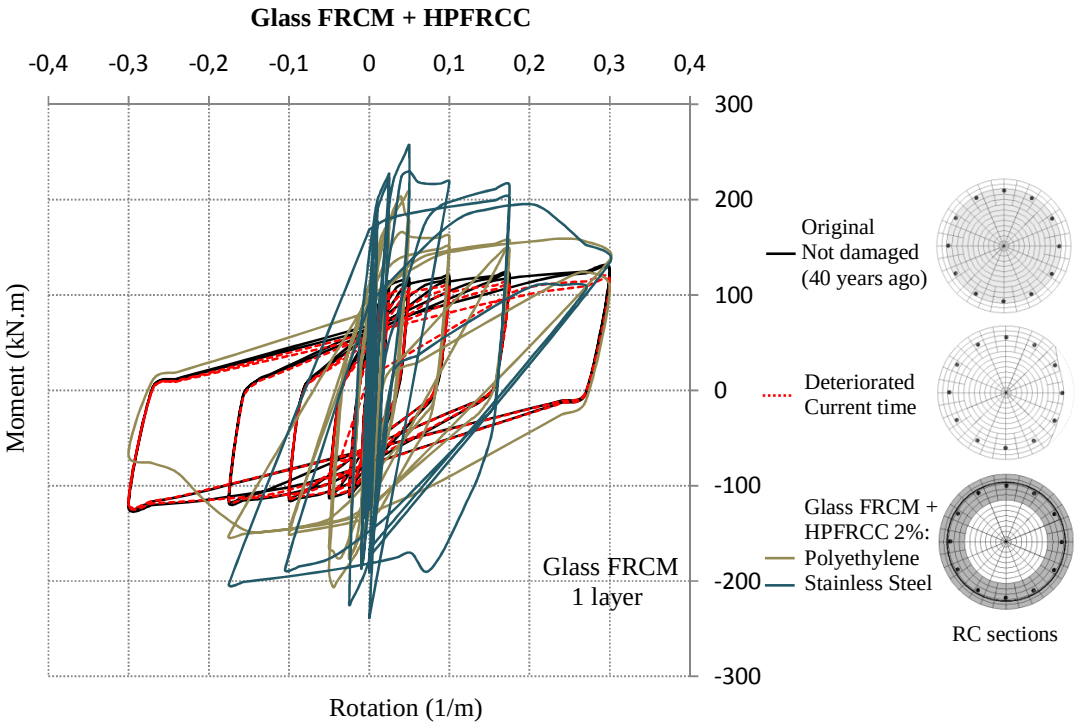

Figure 7.93 Cyclic analysis: strengthened column section with combined Glass FRCM 1 layer + HPFRCC fibers vol. 2% (8.0cm of layer)

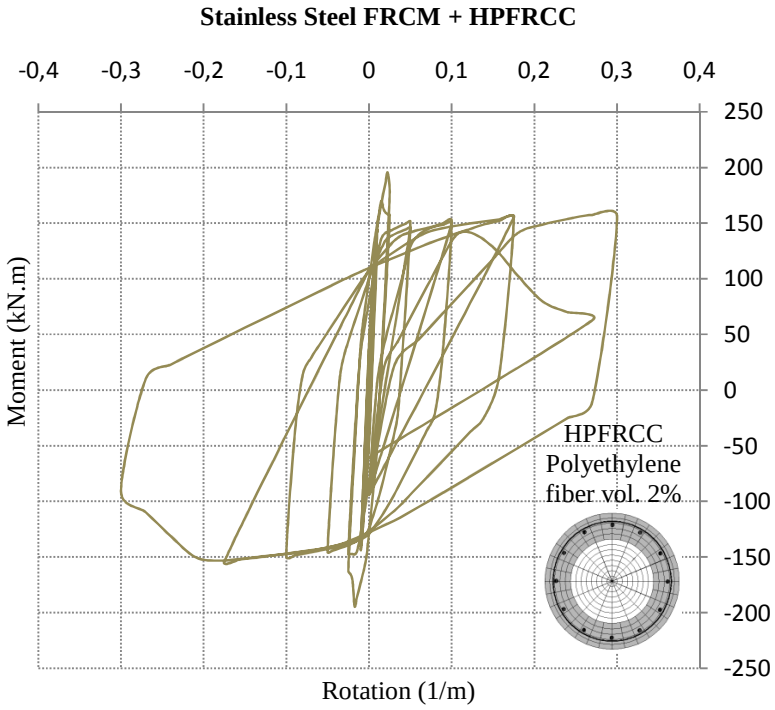

Figure 7.94 Cyclic analysis: strengthened column section with combined Stainless Steel FRCM 1 layer + HPFRCC Polyethylene fiber vol. 2% (8.0cm of layer)

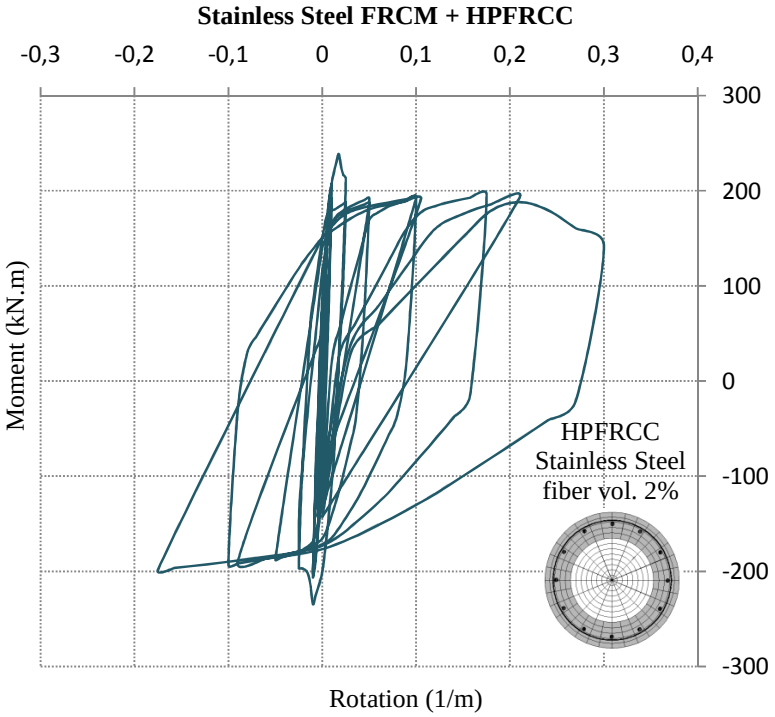

Figure 7.95 Cyclic analysis: strengthened column section with combined Stainless Steel FRCM 1 layer + HPFRCC Stainless Steel fiber vol. 2% (8.0cm of layer)

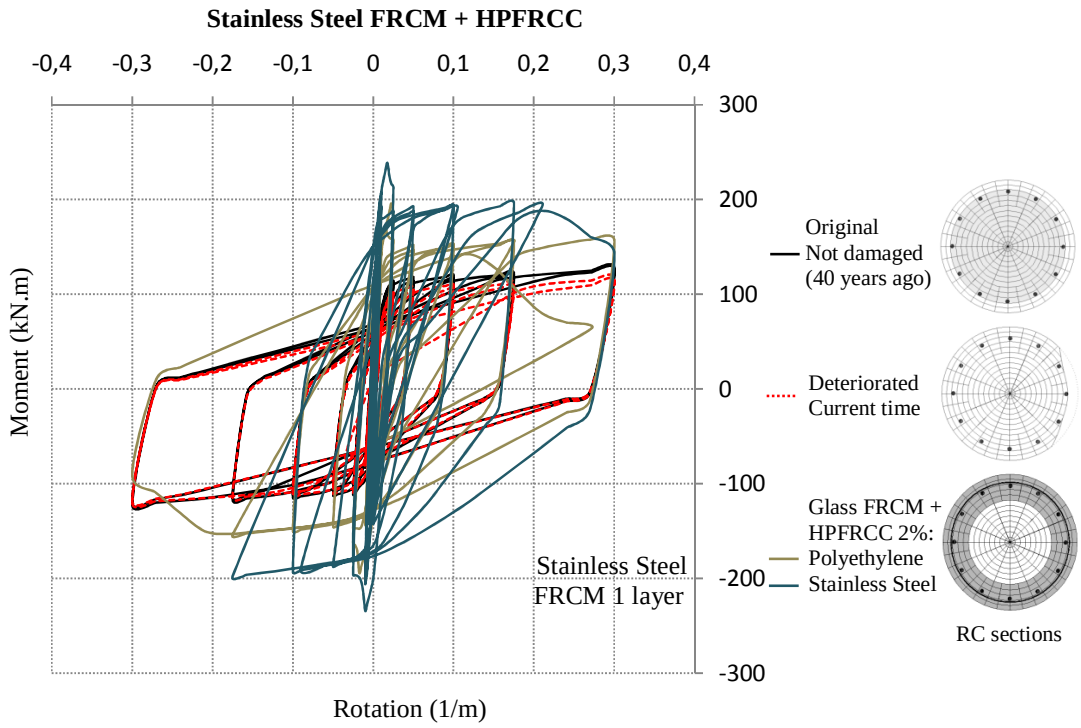

Figure 7.96 Cyclic analysis: strengthened column section with combined Stainless Steel FRCM 1 layer + HPFRCC fibers vol. 2% (8.0cm of layer)

7.4 References

1. Azeredo, Jeferson da R. Non-Linear Static Analysis (Push-Over) of an existing RC structure and Rehabilitation Intervention. University of *Roma Tre*. Master Thesis (Master in Reinforced Concrete – MICA). Rome, 2010.
2. Basic for Assessment of Existing Structures. Milan Holický, Klokner Institute et al., Czech Technical University in Prague, Czech Republic. 2013.
3. Bellomo M., D`Ambrosio V., Fibrorinforzati in Architettura. Le Tecnologie FRP e FRCM nel Recupero delle Strutture in C.A. Clean. Napoli, 2010.
4. Circolare 2 febbraio 2009, n. 617. Istruzioni per l'applicazione delle nuove Norme Tecniche per le Costruzioni (NTC), di cui al decreto ministeriale 14 gennaio 2008.

5. CNR-DT 200 R1/2013. Istruzioni per la Progettazione, l'Esecuzione ed il Controllo di Interventi di Consolidamento Statico mediante l'utilizzo di Compositi Fibrorinforzati. Consiglio Nazionale delle Ricerche. Roma, 2013.
6. Drakakaki Ar., Apostolopoulos Ch., Koulouris K. Mechanical Characteristics of dual-phase steel B500c after shot peening process. Proc. of the Third Intl. Conf. on Advances in Civil, Structural and Construction Engineering – CSCE, 2015.
7. Du Y.G., Clark L.A., Chan A.H.C. Residual capacity of corroded reinforcing bars. Magazine of Concrete Research, 2005;57(3):135–47.
8. Eurocode 8. 1998. "Design of structures for earthquake resistance, Part 2: Bridges. (Draft March 2005)".
9. Eurocode 8. 1998. "Design of structures of earthquake resistance, Part 3: Assessment and retrofitting of buildings" (Draft November 2004).
10. Fib Bulletin 14. Externally bonded FRP reinforcement for RC structures. Fib, Fédération internationale du béton / International Federation for Structural Concrete, 2001.
11. Fib Bulletin 24. Seismic assessment and retrofit of reinforced concrete buildings. *Fib, Fédération internationale du béton* / International Federation for Structural Concrete, 2001.
12. Fib Bulletin 34. Model code for service life design. *Fib, Fédération internationale du béton* / International Federation for Structural Concrete, 2006.
13. Fib Bulletin 59. Condition control and assessment of reinforced concrete structures. *Fib, Fédération internationale du béton* / International Federation for Structural Concrete, 2011.
14. Fib Model Code for Concrete Structures 2010. *Fib, Fédération internationale du béton* / International Federation for Structural Concrete, 2013.

15. Giuffrè, A., and Pinto, P. E. (1970). “Il comportamento del cemento armato per sollecitazioni cicliche di forte intensità.” Giornale del Genio Civile, 5(1), 391–408.
16. Hosotani J., Kawashima K. et al. Discussion by A. J. Kappos. Stress-strain model for confined reinforced concrete in bridge piers. J. Struct. Eng., 1998, 124(10): 1228-1230.
17. Hosotani J., Kawashima K. et al. Stress-strain model for confined reinforced concrete in bridge piers. Member, ASCE. J. Struct. Eng., 1997, 123(5): 624-633.
18. International standard ISO 13822:2010. Bases for design of structures - Assessment of existing structures. Published in Switzerland, 2010.
19. Kashani M.M., Crewe A.J., Alexander N.A.. Nonlinear stress–strain behaviour of corrosion-damaged reinforcing bars including inelastic buckling. Engineering Structures 48 (2013) 417–429.
20. Kashani, M. M., Lowes, L. N. et al. Phenomenological hysteretic model for corroded reinforcing bars including inelastic buckling and low-cycle fatigue degradation. Computers and Structures 156 (2015) 58–71.
21. Lavorato D., Nuti C. Pseudo-dynamic tests on reinforced concrete bridges repaired and retrofitted after seismic damage. Engineering Structures 94 (2015) 96–112.
22. Lavorato D., Nuti C. New Solutions for Rapid Repair and Retrofit of RC Bridge Piers. XII International Conference on Structural Repair and Rehabilitation (Cinpar 2016), 26-29 October, 2016, Porto, Portugal.
23. Lavorato D. Pseudo-dynamic tests on reinforced concrete bridge piers repaired and/or retrofitted by means of techniques based on innovative materials. PhD thesis. University of Roma Tre. Rome, 2009.
24. Mander, J. B., Priestley, M. J. N., and Park, R. Theoretical stress-strain model for confined concrete. Journal of structural engineering, ASCE 114, 8 (1988), 1804-1826.

25. Menegotto, M., and Pinto, P. (1973). “Method of analysis for cyclically loaded RC plane frames including changes in geometry and non-elastic behaviour of elements under combined normal force and bending.” Proc., IABSE Symp. on Resistance and Ultimate Deformability of Structures Acted on by Well Defined Repeated Loads, IABSE-AIPC-IVBH, ETH Zürich, Zürich, Switzerland, 15–22.
26. Ministry for Cultural Heritage and Activities, Italian Government. Guidelines for evaluating and mitigation of seismic risk to cultural heritage. Roma, 1997.
27. NTC 2008, Norme Tecniche per le Costruzioni, Decreto Ministeriale 14 gennaio 2008, Italia.
28. OpenSees [Computer software]. OpenSeesWiki, User Doc, Source Code. Berkeley, CA, Pacific Earthquake Engineering Research Center, Univ. of California (http://opensees.berkeley.edu/index.php).
29. Pedeferri P., Bertolini L. et al. “La corrosione nel calcestruzzo – Fenomenologia, prevenzione, diagnosi, rimedi”, AICAP, Roma - 2006.
30. Tuutti, K. Corrosion of steel in concrete. Swedish Cement and Concrete Research Institute. Stockholm, 1982.
31. Yassin, M. H. M. (1994). “Nonlinear analysis of prestressed concrete structures under monotonic and cyclic loads.” Ph.D. thesis, Univ. of California, Berkeley, CA.

Chapter VIII
Conclusions

Chapter II

In relation to Chapter II, it was possible to observe that every structure in reinforced concrete that has a cultural value could be protected. For this purpose there are the agencies of protection and safeguard of cultural goods, such as IPHAN in Brazil, and UNESCO and ICOMOS at the international level. The building needs to be well conserved so that its values are preserved, when in a state of degradation the structure could be recovered so that the building values are not erased.

A structural conservation design requires a work that involves several disciplines, including restoration and structural engineering (which could work simultaneously on the project). The principles and criteria to be adopted need to be aligned among all the parts involved in the design, therefore it is necessary to know what the real values of the building are, and then to know what is the most appropriate way to intervene in the recovery of the construction, in order to preserve these values.

In relation to the documental investigation of old reinforced concrete buildings in Brazil, there is a great difficulty in finding the original designs (especially the structural plans), even of the constructions that are considered important and representative, for example, those selected as case studies. In some cases, when the building does not belong to the records of goods protected by government agencies, the search may be even more laborious. For example, of the designs that were found during the study mission in Rio de Janeiro, most were incomplete or in poor condition. This could be considered as one of the first difficulties that

professionals who work with structures recovery find during the elaboration of intervention designs.

The agencies of the municipal, state and federal governments, such as the IPHAN and the municipal heritage offices, located in the city of Rio de Janeiro, have organized archives and are easily accessible to students, researchers and professionals in this area. Their professionals are trained and available to assist the researchers in their investigations. However, the collections could cover a larger number of buildings and a greater amount of data related to existing units (this issue could be related to Brazilian government incentives).

Considering the exposed scenario, the preservation culture of buildings with historical and cultural interest in Brazil could go beyond maintaining its physical structure in good aspect and service conditions, but essentially conserving its documentary composition (documents ranging from its initial design to the last maintenance interventions carried out). This would be a way of preserving the memories of the good's identity, which could also contribute fundamentally to the works of present and future interventions, both for those related to the discipline of restoration and for those related to the area of structural rehabilitation.

Chapter III

In Chapter III it was explained that Brazil is a country of great territorial extension which has varied climates among subtropical, tropical and equatorial, respectively distributed in regions from south to the north of the country. And, that the type of deterioration manifestation of the reinforced concrete structures varies according to the region. By comparing the data found in literature and in the latest research on structural pathologies in Brazil, it was possible to comprehend that the main causes of reinforced concrete degradation are related to the reinforcement corrosion, and that in most cases, this type of damage is a consequence of reinforcement electrochemical reactions, caused by the mechanisms of concrete carbonation or chlorides attack.

Regarding the durability of the structures, an important factor that has been identified during the research is related to the requirements for the concrete cover for reinforcements, which have increased substantially in the last decades in Brazil, following the evolution of the standards of procedures for structural design. This fact may be explained both in relation to environmental aggressiveness against structures and to protection against exceptional events, such as fire.

During the research it was observed that repair interventions of Brazilian heritage structures are common, however, only after the appearance of advanced signs of deterioration or when the structure presents damages that can compromise the safety of the users. Some examples are cited, such as the *São Francisco de Assis da Pampulha* Church in Belo Horizonte (one of the most important designs of Oscar Niemeyer) and the *A Noite* building in Rio de Janeiro (case study), among others. Many of these buildings have maintenance plans, but they are not always applied periodically. For this reason, it is understood that a more solid culture of conservation and periodic maintenance of reinforced concrete heritage structures could be implemented in Brazil, according to the criteria of preservation of the heritage goods discussed in this thesis.

Considering the current overview, it is recommended that the problem of the RC structures deterioration of historic buildings, especially those with architectural and cultural values, could be more frequently discussed in the area of Brazilian structural engineering. In particular, the issues related to the structural safety assessment criteria and existing models of analysis which are used in countries that already have tradition in the area of restoration and rehabilitation, as is the case of the Italy. With the purpose of creating guide documents or recommendations, with definition of specific criteria for interventions in heritage RC structures (these issues represent today an innovation to structural engineering in Brazil).

Italy is a country that has given important contributions to the scientific community in the area of intervention in existing structures and is open to carry out

collaborations and research at international level. Considering that inevitably this will be a broadly discussed subject in the future of the Brazilian structural engineering, it could represent an opportunity to initiate a research course in the area of heritage structures rehabilitation.

Chapter IV

In relation to Chapter IV, it was possible to observe that the evaluation criteria of heritage structures are, in many ways, different from those adopted in the evaluation of common structures. The evaluation of a heritage structure basically concerns its mechanical performance (familiar to structural engineers) and its value as a cultural resource. These two aspects could be taken into account in any decisions involving these types of interventions and could therefore be dealt together with the other disciplines. It is in this line of studies that the present thesis proposes the use of structural evaluation models that include the identification and preservation of the historic building values. These, which could be preserved by observing simple principles (known in the restoration area) such as the conservation of the shape and geometry of the elements, as well as the aesthetic aspect (especially when it comes to apparent concrete). Naturally, always considering that, according to the local culture, a structural rehabilitation design could also include the conservation of deterioration marks and / or their recovery interventions, as an integrative element, essential for the preservation of the history of the building.

In relation to the structural analysis, in particular the evaluation of the capacity loss of deteriorated structures, it was observed that if the reinforcement corrosion is not properly evaluated and treated in its initial phase, identifying its cause mechanisms and applying appropriate corrections, it can result in cross-section loss of the element (through spalling), loss of bond between concrete and reinforcement and cross-section loss of steel bars. Consequently, reducing the support capacity of the elements and compromising the safety of the structure.

According to the results of the numerical analysis performed to know the resistance capacity to flexural and flexo-compression of the damaged structural elements (case studies), it was possible to realize that the cross-section loss of steel bars, even in small proportions, may represent a considerable loss in the mechanical performance of the elements.

Some studies found in literature refer to the level of acceptance of steel cross-section losses (caused by corrosion), suggesting the use of this criterion to evaluate the residual capacity of degraded elements. Indeed, it was verified that this typology of simplified evaluation may be useful, when dealing only with a singular material (steel bar) and that could no longer be included in the latest models of evaluation of the resistance capacity of degraded RC elements[1].

In addition, it was verified that in the evaluation the performance level of a degraded element, it is possible to have more accurate results of the real condition of the structure through the use of structural analysis software with FEM numerical models (Finite Element Method) and fiber modeling, capable of analyzing the non-linear behaviour of the structure (in plastic field), considering its capacities and resistance limits (SLS and ULS). Therefore, damage models in materials such as corroded steel bars may be inserted into the structure original model.

Since it is feasible to perform more refined analyses in software that can produce results with greater precision in relation to structural performance, considering the mechanical and geometric characteristics of each material (degraded and non-degraded) integrated in a single model, a better understanding of the behaviour of the structure in order to provide a highest quality result, it is possible to obtain. This aspect could be essential to be taken into account in the rehabilitation design.

[1] Since there are finite element software with fiber modeling that are able to simulate the mechanical behaviour of the degraded material with greater precision and with more realistic and acceptable results.

Chapter V

The most important product of the research may have been in the observation that when it comes to recovering a heritage structure, the evaluation criteria commonly used for ordinary structures change substantially, both in relation to initial structural evaluations and analyses, and in choosing the most appropriate solutions for the intervention design (this issue, which today represents a novelty in the Brazilian structural engineering area, could begin to be part of procedures for structural rehabilitation design).

Among the conservation requirements of a historic building structure that present deterioration, there are those related by the need to recover the structure with the purpose of improve it from a performance point of view (including the need of changing the allocation of use, when applicable). In this case the employable technologies are diverse and the choices depend on several factors. Among them, are the intervention works that could be in reduced time, allowing the building to return the activities in short term, or that the structure could remain in operation during the interventions, with low disturbance in the construction site.

In addition to the need of preserving the original characteristics and the aesthetic aspect of the construction, the functional requirements related to the execution and its working methods could also be taken into account, limiting the interferences with building use as much as possible. Thereby, it is inevitable that the complexity of the construction site is transferred to the design phase.

In order to construct an analytical framework, current researches and the main existing technologies in the area of rehabilitation of reinforced concrete structures and their modalities of applications were studied. During the research, the knowledge about the characteristics of the technologies and materials, both the conventional and innovator, were acquired from different sources of the building process. Among these sources are Italian and European standards, data provided by the producing companies, designers of the area and technicians of construction

companies, as well as professors and researchers in the area of restoration and structural rehabilitation.

The main objective of the research was that this thesis could serve as an instrument of recommendations, defining the applicability of the existing solutions that contemplate the preservation of heritage values on the recovery of degraded reinforced concrete structures. Table 8.01 shows a comparison among characteristics of the main conventional and innovative techniques (including the HPFRCC technique, object of the experimental investigation), for structural rehabilitation, where some conservation criteria of the structures, considered important to be observed, are placed in accordance with the preservation principles of the heritage buildings, already discussed here.

Table 8.01: Comparison among characteristics of the main conventional and innovative techniques, with a view to the preservation principles and criteria to be observed in the structural rehabilitation design

Principles of Preservation of the heritage R C structures	Criteria to be observed in the intervention design[(a)]	Main conventional and innovative techniques of structural rehabilitation					
		Section increase in reinforced concrete	Insertion of metal structure	FRP system	CAM system	FRCM system	HPFRCC[(c)]
Invasiveness (architectural)	Preservation of the elements' geometry (hence the available building areas)	Excessive	High	Medium	Medium	Low	Null
Compatibility (with existing structure)	Use of materials with physical and chemical compatibility with the existing structure[(b)]	Total	Null	Null	Null	High	High
Architectural impact	Conservation of the architectural characteristics and aesthetic aspect of the structure	High	Excessive	Medium	High	Low	Null
Minimal intervention	Possibility of execution in reduced time and with low disturbance in the construction site	Low	Low	High	Medium	High	Medium
Tensile strength	Use of materials with high tensile strength	Low	High	High	High	High	Low/ Medium
Compressive strength	Use of materials with high compressive strength (without considering the effects of confinement)	High	High	Null	Null	Null	High
Compressive strength (confinement)	Use of materials with high compressive strength, considering the effects of confinement	Low	Medium	Medium	High	Medium	Low

Mechanical performance (stiffness)	Performance increase in terms of stiffness	High	Medium	Null	Medium	Null	Low
Mechanical performance (ductility)	Performance increase in terms of ductility	Low	High	High	High	High	Medium[(d)]
Lightness	Use of materials that do not represent a significant increase of weight in the structure	Low	Low	High	Medium	High	High
Versatility	Possibility of use in combination with other techniques or materials (flexibility of use)	High	Low	Medium	Low	High	High
Structural invasiveness	Conservation of the integrity of the existing materials (use of non-destructible techniques)	Low	Low	Low	Low	Low	Medium
Technological level	Use of innovative techniques and materials and specialized labor	Low	Medium	High	High	High	High
Durability	Possibility of using materials with high resistance to mechanical actions (such as impacts) and aggressive environmental agents	Low	Low	Medium	Medium	High[(e)]	High
Maintainability	Ease of maintenance of the recovered structure	Low	Low	High	Medium	High	High
Sustainability	Possibility of using materials with low energy consumption, considering the complete cycle (from the extraction of the raw material until the final recycling)	Low	Low	Medium	Medium	High	High
Final quality of intervention	Probability of elaboration of design and execution of works with high quality	Low	Low	High	High	High	High

Notes: (a) Design criteria that aim to preserve the original architectural characteristics, improve the mechanical performance and durability of the structure, and the minimal intervention (simplification of intervention works); (b) Materials with high bond strength to the support (existing structure) and with thermal expansion coefficients with approximate values to the existing materials; (c) At the stage of experimentation for structural rehabilitation; (d) Pseudo-ductility; (e) Especially when used in combination with the HPFRCC technique.

The question of the applicability of the main rehabilitation techniques to heritage structures could be evaluated considering not only the efficiency of the technology, that aims at the structural performance or the singular conservation of the building's architectural characteristics, but fundamentally the effectiveness of an intervention that includes the precepts related to the preservation of pre-existing cultural values in the construction.

The main conventional techniques can be considered unsuitable for structural rehabilitation, since they carry significant alterations in the geometry and

appearance of the recovered elements, modifying the original configuration of the structure. Thus, they could not be adapted, when an intervention is made in a heritage structure, and where the criteria related to the value conservation need to be taken into account. From this point of view, it would also have to be considered that judgments on patrimonial value and authenticity may differ from culture to culture and, therefore, there could be no fixed criteria for intervention. For example, in some regions, keeping the traditional practice of construction alive is privileged over the conservation of materials, with the same original features. This factor makes us understand that there is no better solution in absolute sense and that each case needs to be analyzed and evaluated singularly, considering the options of interventions that we have at disposal.

Chapter VI

In relation to the Chapter VI, which deals with the results of the experimental investigation, it was possible to observe that the geometry and the mechanical characteristics of the fibers and the composition of the cementitious matrix can influence considerably the behaviour of HPFRCC. For example, the results of uniaxial direct tensile tests with the use of polyethylene micro-fibers showed a non-linear behaviour, with an increase in tensile stress (retaining a deformation plateau) after the first cracking, known as strain-hardening. However, the results of the tests using hooked stainless-steel short fibers in the HPFRCC mixture presented a non-linear prevailing behaviour and a reduction in tensile stress after the first cracking, called strain-softening.

On the other hand, the same typology of test, using micro-fibers of basalt presented very different results from the first two mixtures of HPFRCC, with linear prevailing behaviour until the rupture and not presenting apparent history of crack opening. This characteristic could be considered similar to plain concrete.

In terms of tenacity, the HPFRCC mixtures which showed the best performance in the tensile tests were those with polyethylene micro-fibers, followed by mixtures

with hooked stainless-steel short fibers. The results of the tests with basalt fibers did not present a prevailing pseudo-ductile behaviour, as expected for the HPFRCC material, presenting characteristics of a brittle material and rupture in a single area.

The typology and the distribution of cracking of the specimens subjected to uniaxial direct tensile tests are important parameters for evaluating the performance of the HPFRCC material. For example, mixtures with polyethylene fibers showed a better pseudo-ductile behaviour compared to steel fibers, consequently a better distribution of finer cracks. This parameter could contribute to the use of this type of HPFRCC in the recovery of structural elements, where the factor "crack width" is important to increase the durability of the structure. On the contrary, it occurred with use of basalt fibers, which presented brittle rupture without apparent cracking. This behaviour does not correspond to the characteristic results of an HPFRCC material, and may interfere in the use of this type of fiber for its use in structural rehabilitation.

In terms of mechanical strength to axial direct tension, the types of mixtures that presented the best performance were those with steel fibers, with 2% and 1% volume of fibers, respectively, followed by basalt fibers, also with 2% and 1% volume. On the other hand, the mixtures with the polyethylene fibers, despite having a better performance in relation to the high deformation capacity of the HPFRCC, showed low tensile strength results, in an order of magnitude corresponding to half of the values obtained for the basalt and stainless steel fibers. It was also observed that, in most tensile tests, by increasing the fiber volume from 1% to 2%, the strength values increased by an order of 50%.

In terms of flexural strength, HPFRCC materials with polyethylene and basalt fibers presented similar values, but much lowers than the results with stainless steel fibers, in the order of 30% to 40% lower.

In terms of compressive strength, HPFRCC materials with polyethylene and basalt fibers presented low values, in some cases inferior to the same composite without

fiber addition. However, HPFRCCs with stainless steel fibers showed results with values in an order of magnitude of 25% higher. It was also observed that, in the results of the compressive strength tests, the parameter related to the percentage of fiber volume did not show significant gains of resistance, contrary to the results of the tensile and flexural strength tests.

Chapter VII

The conclusions related to Chapter VII present the main results of the numerical investigation with the application of HPFRCC and FRCM system[1], assuming different types and amounts of fibers, on the recovery of degraded reinforced concrete elements, and proposes the use of these two innovative techniques for interventions of rehabilitation of heritage structures, in order to observe as much as possible the principles of preservation of the structures. One aspect considered relevant is the possibility of applying these techniques without changing the geometry of the elements and improving the durability of the structure, due to the presence of micro-fibers (or short fibers) and the low porosity of the HPFRCC material.

In this final part of the research it was possible to gather and apply the theoretical studies developed so far and the results of the numerical analyses, in the recovery and strengthening of reinforced concrete elements damaged by corrosion (case studies), to evaluate the performance in terms of strength increase to flexural, compression and flexion-compression. In order to evaluate the loss (degraded element) and the increase (strengthened element) of resistance capacity, maximum moment-rotations were compared using a parameter based on the

[1] The combination of the two techniques (HPFRCC and FRCM) contributes to improve the mechanical properties of the strengthening (also in terms of impact resistance). In addition, the micro-fibers of the HPFRCC material may contribute to the minimization of the cracking effect after evaporation of water during thermo-hygrometric shrinkage of the conglomerate.

performance factor, taking as reference the model of the elements in its original state (not deteriorated).

The multilinear-hysteretic model, proposed for the application of HPFRCC on the recovery of case study elements, was numerically constructed using Opensees[1] software framework[2], in the Tcl programming language (Tool Command Language), through the simplification of the strain-stress curves of the experimental investigations' main results. Prior to its application, multilinear-hysteretic model was tested and compared with plain concrete models, already known and available in Opensees, showing satisfactory results so that it could be used in the numerical analysis.

The first results of the degraded beam section (belonging to the *A Noite* building) and reinforced to the flexural stresses with HPFRCC, showed that for a loss of 10% of steel area (caused by corrosion), in addition to loss of concrete through spalling, a 3.5cm layer of HPFRCC with basalt fibers (vol. 1% and 2%) and polyethylene fibers (vol. % 1) was not sufficient to recover the original load capacity of the beam. For the polyethylene (vol. 1%) and stainless steel (1% and 2%) fibers, acceptable values of resistance increase were observed.

On the other hand, the application of a 7.0cm HPFRCC reinforcing layer showed satisfactory results for the mixtures with polyethylene and stainless steel fibers (vol. 1% and 2%), especially the stainless steel fibers. However, the mixtures with basalt fibers did not reach representative values in the increase of resistance.

Regarding the use of the FRCM system in the rehabilitation of the studied beam section, the results were always close to those expected, since the theoretical bases and formulations used are related to the FRP system. Thus, all types of applied fibers (carbon, stainless steel and glass) reached representative values in

[1] OpenSees structural software [Computer software]. Berkeley, CA, Pacific Earthquake Engineering Research Center, Univ. of California.

[2] The use of finite element software with fiber modeling is indispensable for a better understanding of the nonlinear behaviour of the structure recovered with HPFRCC materials.

increasing the flexural strength of the beam. Particular attention should be given to the number of layers (meshes) applied, to meet the equilibrium conditions of the section and the relative deformations of the materials (fiber mesh, concrete and steel bar), and consequently the verification of the section according to the rupture mechanisms proposed by CNR-DT 200 R1 / 2013.

The results of the numerical analyses performed using the combination of the two investigated techniques were satisfactory, even in smaller layers of 3.5cm thick HPFRCC. This phenomenon may be explained by the high mechanical properties of the FRCM systems, in resisting tensile forces (and tensile on flexion).

The results of the degraded column section (belonging to a bridge located in seismic zone, in Italy) and reinforced to the flexo-compression efforts with HPFRCC showed that, for a 14% of area loss in three steel bars (caused by corrosion), in addition concrete loss through spalling, a 8.0cm layer of HPFRCC with basalt fibers applied at the perimeter of the section, was not sufficient to recover the original load capacity of the column. For polyethylene and stainless steel fibers, acceptable values of resistance increase were observed for both simple-compression and flexo-compression.

The use of FRCM system for the rehabilitation of the studied column presented satisfactory results to resist the load efforts, both compression by confinement and flexo-compression[1]. When a layer of fiber mesh is not sufficient to satisfy the equilibrium requirements of the confined column, it is possible to apply other layers until it reaches the values required for section verification, or to opt for a type of

[1] For the reinforcement to be effective, in relation to the stresses of compression and bending of the column, the mesh had to be arranged so that the fibers worked in both directions: longitudinal and transverse. For example, when considered only in the transverse direction, flexural reinforcement could not be considered in the numerical model.

fiber with a higher modulus of elasticity[1], provided that the limitations proposed by CNR-DT 200 R1 / 2013 are not exceeded.

Regarding the types of rupture mechanisms of the FRCM system applied in the column it was possible to observe that, for the increase of resistance to compression by confinement, the modulus of fiber elasticity presented an important function. Unlike the longitudinally arranged fibers which serve to increase the bending capacity of the column, where the tensile strength of the fiber had a more important function than the modulus of elasticity.

The combination of the two techniques, HPFRCC and FRCM, could be used for the rehabilitation of degraded columns. The analyses performed using HPFRCC with polyethylene and stainless steel fibers were representative for increasing column strength, both compression and flexo-compression. In addition, it was possible to observe that similar criteria to those used for the application of the unique FRCM system could be used in the application of the two combined techniques (HPFRCC and FRCM).

The results of the experimental and numerical investigations showed that the HPFRCC material could be used to recover the flexural and flexo-compression resistance capacity of elements in reinforced concrete deteriorated by reinforcement corrosion. However, due to the innumerable variables to be taken into account in the compositions of a HPFRCC during its production, application, curing and maintenance after intervention, and the degrees of uncertainties treated with probabilistic models, the use of the HPFRCC technique for structural rehabilitation would be recommended for relatively low values of flexural strength loss in an order of magnitude of up to 5% (Table 8.02). Above these values, the HPFRCC technique could be used in combination with the FRCM system (considering in particular the limitations provided by CNR-DT 200 R1 / 2013) for values in an order of magnitude of flexural strength loss up to a limit of 15%. For

[1] During the analysis it was observed that, contrary to the flexural reinforcement, the increase in the number of layers of fiber meshes contributed little to the increase of compressive strength by confinement of columns.

values higher than 15%, the use of other solutions could be recommended. One example would be the insertion of stainless steel bars (or replacement of deteriorated bars, when in extreme cases), combined with the use of HPFRCC (with micro-fibers) to recompose the original section of concrete.

According to the results obtained during the analysis, it was possible to conclude that the hooked stainless-steel fibers could be recommended to be used in structural rehabilitations that require a better resistance of the HPFRCC material to tension and flexion, and eventually to compression. It may be used to increase the resistance capacity of elements[1] subjected to flexural[2] and flexo-compression efforts. The polyethylene fibers could be recommended in HPFRCC for the structural rehabilitations that require a better distribution of finer cracks in the structure, consequently improving its resistance in relation to the entrance of aggressive agents and its performance relative to the structural durability. In this case, for a better increment of mechanical performance, it would be precisely advisable to combine it with the FRCM systems. In addition, according to the observed results, better results of the application of HPFRCC may be achieved using a 2% fiber volume, mainly in relation to tensile and flexural stresses.

Considering dealing with the recovery of heritage structures, whose interest is to preserve and conserve, the concern with the durability of the materials and consequently the extension of the service life of the structure becomes a fundamental aspect to be considered in the rehabilitation design. This is a particularly important factor in the use of HPFRCC materials, which could be effectively designed and applied according to the best and most efficient modalities

[1] Always considering that any intervention of local structural recovery or strengthening, in elements that contribute to the stability of the structure and that could cause a behavioural change in the structural performance, partially or for the overall structure, analyses and verifications of the resistance capacity of the structure concerned, in addition to structural safety assessment, need to be carried out.

[2] Considering that small layers of HPFRCC, for example, corresponding to the concrete cover, may be insufficient to have a significant increase of flexural strength.

provided by the designer, under an appropriate knowledge of this innovative technology.

Table 8.02: Recommendations for rehabilitation solutions to degraded heritage structures

Loss of capacity of the element[(a)]	Typology of Rehabilitation	
	Recommendations[(b)]	Observation
Up to 5%	Use of HPFRCC with hooked stainless-steel fibers (vol. 2%).	Layer with minimum thickness = concrete cover + diameter of steel bars.
Up to 15%	Use of HPFRCC with polyethylene fibers (vol. 2%) combined with FRCM system[(c)]. In this case it would not be necessary to meet a minimum thickness of HPFRCC, in relation to the bending efforts.	For better physical-chemical compatibility with the existing structure, steel fibers could be used in both systems. For example, HPFRCC with stainless steel micro-fiber (vol. 2%) and FRCM with stainless-steel fiber mesh.
Above 15%	In this case it would be recommended to use other solutions, such as the insertion of stainless steel bars (or replacement of deteriorated bars, when in extreme cases), combined with use of HPFRCC in polyethylene or stainless steel micro-fibers (vol. 2%).	In this case, use of HPFRCC with micro-fibers is recommended to contribute to the durability of the structure.

Notes: (a) Loss of bending strength (in order of magnitude); (b) The above recommendations aim to contribute to the conservation of the geometry of the structure and, therefore, do not contemplate an increase of section of the elements. However, fire protection requirements must be met in accordance with local standards; (c) The use of FRP systems could also be recommended, if it were not for its limitations as low resistance to heat and humidity. In addition of the issues regarding to the number of layers of different products that need to be used in the application of an FRP system.

List of Tables

Table	Description	Page
	Chapter II	
2.01	Minimum thickness of reinforcement cover	31
2.02	Comparison of general characteristics of the buildings	56
	Chapter III	
3.01	Classes environmental aggressiveness (ABNT NBR 6118:2014 - Brazilian standard)	70
3.02	Correspondence between the class of aggression and the quality of concrete (ABNT NBR 6118:2014 - Brazilian standard)	71
3.03	Correspondence between the class of aggression and the nominal concrete cover (ABNT NBR 6118:2014 - Brazilian standard)	71
3.04	Exposure classes (UNI 11104:2004 - Italian standard. Harmonized with the European standard EN 206)	72
3.05	Exposure classes (UNI 11104:2004 - Italian standard. Harmonized with the European standard EN 206)	77
3.06	Service life (nominal life) for various types of structures (NTC 2008 – Italian standard)	79
3.07	Service life for the corresponding performance levels (ABNT NBR 15575:2013 – Brazilian standard)	80
	Chapter V	
5.01	Comparison between the properties (average values) of the various types of reinforcing matrix	133
5.02	Comparison between the properties (average values) of the various types of reinforcing fiber	134
5.03	Comparison between the main characteristics of the existing fibers in the market	135
	Chapter VI	
6.01	Comparison of mechanical properties of various classes of composites	153
6.02	Typical mechanical properties of fibers	154
6.03	List of materials and specific gravity	156

6.04	Geometry and mechanical properties of the fibers	156
6.05	Mixture proportions of binder for HPFRCC (main parameters)	158
6.06	Mixture proportions of HPFRCC (main parameters)	159
6.07	Tests results: mechanical characteristics of HPFRCCs	163
6.08	Characteristics of HPFRCC under uniaxial direct tensile test	171
	Chapter VII	
7.01	Key Information of the beam section and materials	180
7.02	Concrete mechanics characteristics	183
7.03	Steel mechanical characteristics for longitudinal bars	183
7.04	Comparison between the three sections	186
7.05	HPFRCC mechanics characteristics	189
7.06	Comparison between moment-rotation of the beam section	193
7.07	FRCM properties used on the numerical tests	194
7.08	Comparison between maximum moments of the beam section, using OpenSees and FRCM Calculator	199
7.09	Comparison between maximum moments of the strengthened beam section	204
7.10	Key Information of the section and materials	206
7.11	Current condition and remaining service life assessment - General framework	211
7.12	Comparison between the confinement models applied in the case study	221
7.13	Confined and unconfined concrete mechanical characteristics	222
7.14	Steel mechanical characteristics for uncorroded reinforcement	222
7.15	Steel mechanical characteristics for corroded longitudinal bars	223
7.16	Comparison between the three sections	226
7.17	Comparison between moment-rotation of the column section	233
7.18	FRCM confinement mechanical characteristics for fiber model in OpenSees (1 and 2 layers)	241
7.19	Comparison between maximum moments and maximum axial capacity of the column section confined with 1 and 2 layers FRCM	244
7.20	Comparison between maximum moments of the column section strengthened with combined flexural and confinement FRCM (1 layer)	245
7.21	Comparison between maximum moments of the strengthened column section	250
	Chapter VIII	
8.01	Comparison between the characteristics of the main conventional and innovative techniques, with a view to the preservation principles and criteria to be observed in the structural rehabilitation design	263
8.02	Recommendations for solutions of rehabilitation of degraded heritage structures	272

List of Figures

Fig.	Description	Page
	Chapter II	
2.01	*Copacabana, Rio de Janeiro,* 1906	27
2.02	Water reservoir of the *Engenho de Dentro* (built in reinforced concrete, circa 1908)	28
2.03	Eng. Emílio Henrique Baumgart	29
2.04	Standard ABCP for execution and calculation of reinforced concrete in 1937	31
2.05	Evolution of construction in Rio de Janeiro. View of the port zone (*Mauá* square)	32
2.06	Gloria Hotel, built in 1922	34
2.07	Copacabana Palace Hotel, built in 1923	34
2.08	Brazilian newspapers called *A Noite* of July 18, 1928, with some photos of the construction of the *A Noite* building	36
2.09	Building construction in 1928	36
2.10	*Mauá* square in the 20s, before the construction of the building *A Noite*	36
2.11	Aerial view of the port area of Rio, in 1920	37
2.12	Copy of the original structural plans made by Baumgart	38
2.13	Beam section detail made by Baumgart	38
2.14	Reproduction of the beam section (dimensions in cm)	38
2.15	Internal building photo showing a beam with corbels. Photograph taken in July 2014	38
2.16	View of the pergola after completion of the structural reinforcement works. [Concreto Magazine n. 75 June 1945]:183	39
2.17	Current photo of the building's roof, taken in July 2014	39
2.18	Reproduction of bending moment diagram of the reinforced slab. The strongest line represents the unreinforced slab moments. The crosshatch diagram represents the final moments. [Concreto Magazine n. 75 June 1945]:186	40
2.19	Representative section of the new structure (pergola). [Concreto	40

	Magazine n. 75 June 1945]:185	
2.20	Aerial view of the *Mauá* square, in 1930	41
2.21	Headline in the *O Globo* newspaper, about the supposed demolition of the building on September 27, 1978	42
2.22	Building photograph taken in July 2014	42
2.23	ABI Building (Brazilian Press Association), built between 1936 and 1938. Photograph taken in the 40s, after the inauguration of the building	44
2.24	ABI Building during construction	45
2.25	View of the building. Photograph taken in the 40s	45
2.26	Reproduction of the original architecture plans (facades and 7th floor)	45
2.27	Reproduction of the original structural plans	46
2.28	Photographs taken in July 2014, during the restoration works of the facades	47
2.29	Structure in initial deterioration process. Photographs taken in July 2014	48
2.30	MES (Ministry of Education and Health), inaugurated in 1943. Photograph taken in the 40s, after its inauguration	49
2.31	*Pilotis*. Photograph taken in July 2014	49
2.32	Glass facade. Photograph taken in July 2014	49
2.33	Le Corbusier and Oscar Niemeyer with the committee responsible for building construction, in 1936	50
3.34	Second trip of Le Corbusier in Rio de Janeiro, in 1936 (in the background the hill *Pão de Açucar*)	50
2.35	Corbusier on the ship returning from Brazil to France, in 1929 (his first trip in Brazil)	50
2.36	Preliminary studies made by Le Corbusier	50
2.37	Photographic reproduction of the letter from Le Corbusier to engineer Marques Porto. Rio de Janeiro, July 31, 1936	51
2.38	Photographic reproduction of the front page of Le Corbusier report about the MES design, Rio de Janeiro, August 10, 1936	51
2.39	Photographic reproduction of the original design of Le Corbusier for the MES, Rio de Janeiro, 1936	51
2.40	Photographic reproduction of the original volumetric design made by Le Corbusier, Rio de Janeiro, 1936	51
2.41	Photographic reproduction of the original architecture plans (2nd and 3rd floors) Rio de Janeiro, 1936	52
2.42	Photographic reproduction of the original structural plans made by Baumgart Rio de Janeiro, 1937	53
2.43	Quantitative of materials for the building structure made by Baumgart in 1937	53
2.44	Photographs of the slab reinforcements, taken in 1939. To the right,	53

	reinforcement of the capitals and on the left, the reinforcement of the merged beams in the slab	
2.45	To the left, the structure of the building under construction and over a reinforcement cage of a beam. Photographs taken in 1939	53
2.46	Deterioration of the structure of the second floor. Photographs taken in July 2014	54
2.47	Restoration works on the facades. Photographs taken in July 2014	55
2.48	Center of Rio de Janeiro: 1. *A Noite* building; 2. *ABI* building; 3. *MES* building	55
2.49	The main values of heritage RC buildings	59
	Chapter III	
3.01	Brazilian coast: considered aggressive environment for reinforced concrete structures	67
3.02	Studies on the incidence of reinforcement corrosion in buildings with the presence of structural deterioration in Brazil	68
3.03	Deterioration mechanisms and consequences for reinforced concrete structures	82
3.04	Main causes of damage to reinforced structures in the State of Pernambuco	83
3.05	Main causes of damage to reinforced structures in the city of Rio de Janeiro	84
3.06	Deterioration of the slab of the 1st floor. Reinforcement corrosion and concrete spalling likely caused by chloride attack. Building of the *Faculdade de São Bento*, located in the marine environment, in the center of Rio de Janeiro (photographs taken in July 2014)	85
3.07	Deterioration of the columns of the *Rua do Passeio* building, built in the 30s in the center of Rio de Janeiro. Concrete spalling and reinforcement corrosion likely caused by carbonation of concrete. Extreme case of deterioration with breaking of longitudinal and transverse bars of the external columns (photographs taken in July 2014)	85
3.08	Steel corrosion and concrete spalling of columns and beams likely caused by carbonation of concrete (most likely occasioned by having a small layer of concrete cover for reinforcement). *Rua Nilo Peçanha* building, built in the 50s in the center of Rio de Janeiro (photographs taken in July 2014)	85
3.09	Structural deterioration of the ground floor and roof, concrete spalling and steel corrosion with cross-section loss of the transverse and longitudinal reinforcement, likely caused by chloride attack. *A Noite* building, built in 1929, located in the marine environment, in the center of Rio de Janeiro (photographs taken in July 2014)	86
3.10	Extreme case of deterioration of the *Ouro Branco* building, built in 1935, in the center of São Paulo. Steel corrosion and concrete	87

	spalling caused by carbonation of concrete, with cross-section loss of reinforcement (photographs taken in January 2014)	
3.11	Structure in terminal state of deterioration caused by chloride attack. Extreme case of steel corrosion and concrete disintegration. Building located in the marine environment in Fortaleza city (photographs taken in May 2015)	88
3.12	General representation of corrosion effects in reinforced concrete structures	89
3.13	Representation of reinforcement corrosion in concrete (adapted from *fib* Bulletin 59)	90
3.14	Representation of the concrete carbonation process. Carbon dioxide diffuses through the pore system of the concrete and finally forms calcium carbonate (Tuutti model, adapted from *fib* Bulletin 59)	91
	Chapter IV	
4.01	Assessment hierarchy model for heritage structure with deterioration	97
4.02	Deterioration model of reinforced concrete structure due to corrosion	101
4.03	Initiation period and propagation period of corrosion in RC structure (adapted from Tuutti model)	102
4.04	Damage of a reinforced concrete structure due to corrosion (adapted from *fib* Bulletin 59)	103
4.05	Depassivation due to carbonation [$X_c(t) \geq X_{cover}$] (adapted from *fib* Bulletin 59)	105
4.06	Depth of carbonation as a function of time and K	106
4.07	Initiation time at different depths in the concrete for several values of diffusion coefficient in the hypothesis of critical chloride content (C_{crit}) equal to 1% and surface concentration of 5% (adapted from *Corrosion in concrete, AICAP*)	109
4.08	Depassivation due to chloride ingress [$C_{crit} \geq C(x_{cover},t)$] (adapted from *fib* Bulletin 59)	110
4.09	Correlation between corrosion rate and degradation of reinforcement cross section (adapted from *fib* Bulletin 59)	112
4.10	Local attack penetration and stress concentrations of corroded reinforcement	114
	Chapter V	
5.01	Column strengthening details: (a) Original RC column; (b) Reinforcement assembly; (c) Concreting of the new section	125
5.02	Column strengthening details: (a) Original RC column; (b) Fixing of steel profiles; (c) Welding of steel plates	126
5.03	Column strengthening details: (a) Original RC column; (b) Fixing of steel profiles; (c) Prestressed steel strips	128
5.04	Stress-strain relationship of fibers, matrix and FRP System (adapted from *fib* Bulletin 14)	132

5.05	Failure mechanism. Debonding between FRP and concrete (adapted from *fib* Bulletin 14)	137
5.06	Failure mode of a RC member strengthened with FRP (source CNR-DT 200 R1/2013)	138
5.07	Flexural strengthening with laminate FRP	139
5.08	Strengthening configurations in lateral view of FRP (source CNR-DT 200 R1/2013)	140
5.09	Cross section of FRP strengthened members	141
5.10	Notation for shear strengthening using FRP strips (source CNR-DT 200 R1/2013)	142
5.11	Shear strengthening with laminate FRP	142
5.12	Confining pressure exerted by the FRP (adapted from *fib* Bulletin 14)	143
5.13	Comparison of confinement actions of steel and FRP materials (adapted from *fib* Bulletin 14)	144
5.14	Column strengthening details: (a) Original RC column; (b) Confinement with discontinuous FRP strips; (c) Finishing	146
5.15	Effectively confined core for non-circular sections (adapted from *fib* Bulletin 14)	147
	Chapter VI	
6.01	(a) Basalt micro-fiber, (b) Polyethylene micro-fiber and (c) Hooked Stainless Steel fiber	151
6.02	Typical stress-strain curve for comparison between conventional FRCC and high performance FRCC behaviour	152
6.03	(a) Basalt, (b) Polyethylene and (c) Stainless Steel fibers	156
6.04	General composition of HPFRCC	157
6.05	Preparing of HPFRCC: (a) Composite consistency test; (b) e (c) Molding of the test specimens	158
6.06	Flexural test specimen	160
6.07	Uniaxial tensile test on dog-bone specimen	160
6.08	Compression test specimen	160
6.09	Universal Testing Machine MTS	161
6.10	Support apparatus for uniaxial tensile test	162
6.11	Longitudinal elastic modulus test	163
6.12	Compressive strength test	164
6.13	Compressive strength results	164
6.14	Flexural strength results	165
6.15	Flexural test on HPFRCC with 2 vol.% of polyethylene fiber. Pseudo ductile failure mode	166
6.16	Uniaxial direct tensile strength results	167
6.17	Cracks opening and force-displacement graph from tests on dog-bone specimen	168
6.18	Dog-bone specimen after tests and force-displacement graphs from	169

	universal testing machine MTS (a) Basalt micro-fiber; (b) Polyethylene micro-fiber; (c) Hooked Stainless Steel fiber	
6.19	Force-displacement curves from uniaxial direct tensile test, for comparison between HPFRCCs behaviour (fibers vol. 1%)	170
	Chapter VII	
7.01	Front façade of the building (photo taken in July 2014)	175
7.02	Lateral façade of the building (photo taken in July 2014)	175
7.03	Wall-pillars in the most requested direction for wind actions (copy of the original structural design)	177
7.04 (a)	Roof floor: damaged RC beam in advanced state of reinforcement corrosion (with loss of bars cross-section) and concrete spalling	178
7.04 (b)	Ground floor: damaged RC beam and slab by reinforcement corrosion and concrete spalling	178
7.05	Main facade design	178
7.06	Damaged RC beam in advanced state of reinforcement corrosion. With loss of longitudinal bars cross-section, transverse reinforcement broken and loss of concrete cross-section	179
7.07	Damaged RC section beam by reinforcement corrosion	180
7.08	FEM model in OpenSees: fiber section model for steel-concrete	182
7.09	Current cross section of the deteriorated beam	184
7.10	FEM model in OpenSees: fiber section model for steel-concrete (considering RC deterioration)	184
7.11	Stress-Strain behaviour of the materials under a Push-Over analysis	185
7.12	Moment-rotation capacity curves of the beam section to assessment of the structural performance level	186
7.13	Simplified multilinear-hysteretic model for tensile strength of HPFRCC with basalt fiber	187
7.14	Simplified multilinear-hysteretic model for tensile strength of HPFRCC with polyethylene fiber	188
7.15	Simplified multilinear-hysteretic model for tensile strength of HPFRCC with stainless steel fiber	188
7.16	Strengthened cross section with 3.5 cm of HPFRCC	190
7.17	FEM model in OpenSees: fiber section model for steel-concrete (considering HPFRCC)	190
7.18	Moment-rotation capacity curves of the strengthened beam section for assessment of the structural performance level (HPFRCC fiber vol. 1% - layer 3.5cm)	190
7.19	Moment-rotation capacity curves of the strengthened beam section for assessment of the structural performance level (HPFRCC fiber vol. 2% - layer 3.5cm)	191
7.20	Strengthened cross section with 7.0 cm of HPFRCC	191
7.21	FEM model in OpenSees: fiber section model for steel-concrete	191

	(considering HPFRCC)	
7.22	Moment-rotation capacity curves of the strengthened beam section for assessment of the structural performance level (HPFRCC fiber vol. 1% - layer 7.0cm)	192
7.23	Moment-rotation capacity curves of the strengthened beam section for assessment of the structural performance level (HPFRCC fiber vol. 2% - layer 7.0cm)	192
7.24	Calculator for evaluation of RC elements strengthened with FRP and FRCM systems (developed during the PhD studies) Bending in RC Beam (ULS)	194
7.25	FRCM System Stress-Strain curves for analyses with fiber model in *OpenSees* Software (elastic-linear tensile behaviour)	195
7.26	Strengthened cross section with FRCM System and plain concrete	196
7.27	FEM model in OpenSees: fiber section model for steel-concrete (considering FRCM)	196
7.28	Moment-rotation capacity curves of the strengthened beam section for assessment of the structural performance level (FRCM System with fiber mesh)	197
7.29	Representation of FRCM strengthening for flexural strength in RC beams	197
7.30	Input and output data from the calculator for evaluation of RC elements strengthened with FRP and FRCM systems (Strengthening with Carbon FRCM)	198
7.31	Input and output data from the calculator for evaluation of RC elements strengthened with FRP and FRCM systems (Strengthening with Stainless Steel FRCM)	198
7.32	Input and output data from the calculator for evaluation of RC elements strengthened with FRP and FRCM systems (Strengthening with Glass FRCM)	199
7.33	Comparison between moments of resistance of the RC beam section for assessment of the structural performance level	200
7.34	Failure mode of a RC member strengthened with FRCM (source CNR-DT 200 R1/2013)	201
7.35	Strengthened cross section with FRCM System and 3.5 cm of HPFRCC	202
7.36	FEM model in OpenSees: fiber section model for steel-concrete (considering FRCM + HPFRCC)	202
7.37	Moment-rotation capacity curves of the strengthened beam section for assessment of the structural performance level (Glass FRCM 1 layer + HPFRCC fibers vol. 2% layer 3.5cm)	203
7.38	Moment-rotation capacity curves of the strengthened beam section for assessment of the structural performance level (Steel FRCM 1 layer + HPFRCC fibers vol. 2% layer 3.5cm)	203

7.39	Bridge prototype configurations. Case study for numerical example (adapted from Lavorato D. et al., 2015, *University of Roma Tre*)	205
7.40	Pier reference element (from Lavorato D. and Nuti C., 2015)	207
7.41	Carbonation-induced corrosion effects in the reinforced concrete pier (damaged RC section)	207
7.42	Section subdivision: moist zone and not moist zone	208
7.43	Historic of the structure and remaining service time	212
7.44	FEM model in OpenSees: fiber section model for steel-concrete	215
7.45	Graphic representation of the Mander et al.´s stress-strain model for steel-confined concrete	217
7.46	Original cross section of the non-deteriorated column	223
7.47	FEM model in OpenSees: fiber section model for steel-concrete	223
7.48	Current cross section of the deteriorated column	224
7.49	FEM model in OpenSees: fiber section model for steel-concrete (considering RC deterioration)	224
7.50	Stress-Strain behaviour of the materials under a Push-Over analysis	225
7.51	Moment-rotation capacity curves of the column section to assessment of the structural performance level	226
7.51 (a)	Comparison between the Performance curves corresponding to the service time of the structure	226
7.52	Cyclic behaviour (stress-strain) of the Uncorroded Steel	228
7.53	Cyclic behaviour (stress-strain) of the Corroded Steel (14%)	228
7.54	Cyclic behaviour (stress-strain) of the Corroded Steel (14%) and Uncorroded Steel	228
7.55	Cyclic analysis: Original RC section (no damaged)	229
7.56	Cyclic analysis: Damaged RC section (current time)	229
7.57	Cyclic analysis: Damaged RC section (in 25 years)	230
7.58	Cyclic analysis: Comparison between the three sections	230
7.59	Strengthened cross section with 8.0 cm of HPFRCC	232
7.60	FEM model in OpenSees: fiber section model for steel-concrete (considering HPFRCC)	232
7.61	Moment-rotation capacity curves of the strengthened column section for assessment of the structural performance level (HPFRCC fiber vol. 1%)	232
7.62	Moment-rotation capacity curves of the strengthened column section for assessment of the structural performance level (HPFRCC fiber vol. 2%)	233
7.63	Cyclic analysis: strengthened column section with HPFRCC (1% basalt fiber)	234
7.64	Cyclic analysis: strengthened column section with HPFRCC (1% polyethylene fiber)	234

7.65	Cyclic analysis: strengthened column section with HPFRCC (1% stainless steel fiber)	235
7.66	Cyclic analysis: strengthened column section with HPFRCC (1% basalt, polyethylene and steel fibers)	235
7.67	Cyclic analysis: strengthened column section with HPFRCC (2% basalt fiber)	236
7.68	Cyclic analysis: strengthened column section with HPFRCC (2% polyethylene fiber)	236
7.69	Cyclic analysis: strengthened column section with HPFRCC (2% stainless steel fiber)	237
7.70	Cyclic analysis: strengthened column section with HPFRCC (2% basalt, polyethylene and steel fibers)	237
7.71	Calculator for evaluation of RC elements strengthened with FRP and FRCM systems (developed during the PhD studies) Compression in RC Pillar (circular section)	238
7.72	Representation of FRCM confinement for strengthening of RC column	239
7.73	Input and output data from the calculator for evaluation of RC elements strengthened with FRP and FRCM systems (Confinement with Carbon FRCM)	239
7.74	Input and output data from the calculator for evaluation of RC elements strengthened with FRP and FRCM systems (Confinement with Stainless Steel FRCM)	239
7.75	Input and output data from the calculator for evaluation of RC elements strengthened with FRP and FRCM systems (Confinement with Glass FRCM)	240
7.76	FRCM System Stress-Strain curves for confinement model in *OpenSees* Software (Hysteretic model for confined sections)	241
7.77	Strengthened cross section with FRCM (1 layer)	242
7.78	FEM model in OpenSees: fiber section model for steel-concrete (considering FRCM)	242
7.79	Moment-rotation capacity curves of the strengthened column section for assessment of the structural performance level (FRCM 1 layer - confinement)	243
7.80	Moment-rotation capacity curves of the strengthened column section for assessment of the structural performance level (FRCM 2 layers - confinement)	243
7.81	Comparison between moments of resistance of the RC column section for assessment of the structural performance level	244
7.82	Moment-rotation capacity curves of the strengthened column section for assessment of the structural performance level (FRCM 1 layer – combined flexural and confinement)	245
7.83	Cyclic analysis: strengthened column section with 1 layer of Carbon	246

	FRCM (Combined confinement and flexural strengthening)	
7.84	Cyclic analysis: strengthened column section with 1 layer of Stainless Steel FRCM (Combined confinement and flexural strengthening)	246
7.85	Cyclic analysis: strengthened column section with 1 layer of Glass FRCM (Combined confinement and flexural strengthening)	247
7.86	Cyclic analysis: strengthened column section with 1 layer of FRCM (Combined confinement and flexural strengthening)	247
7.87	Combined HPFRCC and FRCM techniques for rehabilitation of RC section	248
7.88	FEM model in OpenSees: fiber section model for steel-concrete (considering HPFRCC and FRCM)	248
7.89	Moment-rotation capacity curves of the strengthened beam section for assessment of the structural performance level (Glass FRCM 1 layer + HPFRCC fibers vol. 2% layer 8.0cm)	249
7.90	Moment-rotation capacity curves of the strengthened beam section for assessment of the structural performance level (Steel FRCM 1 layer + HPFRCC fibers vol. 2% layer 8.0cm)	249
7.91	Cyclic analysis: strengthened column section with combined Glass FRCM 1 layer + HPFRCC Polyethylene fiber vol. 2% (8.0cm of layer)	250
7.92	Cyclic analysis: strengthened column section with combined Glass FRCM 1 layer + HPFRCC Stainless Steel fiber vol. 2% (8.0cm of layer)	251
7.93	Cyclic analysis: strengthened column section with combined Glass FRCM 1 layer + HPFRCC fibers vol. 2% (8.0cm of layer)	251
7.94	Cyclic analysis: strengthened column section with combined Stainless Steel FRCM 1 layer + HPFRCC Polyethylene fiber vol. 2% (8.0cm of layer)	252
7.95	Cyclic analysis: strengthened column section with combined Stainless Steel FRCM 1 layer + HPFRCC Stainless Steel fiber vol. 2% (8.0cm of layer)	252
7.96	Cyclic analysis: strengthened column section with combined Stainless Steel FRCM 1 layer + HPFRCC fibers vol. 2% (8.0cm of layer)	253

Appendices

Numerical modeling

```
# ------------------------------------------------------------------------------------------
# build original beam section
# Jeferson Azeredo da Rosa, 2016
#
# SET UP ---------------------------------------------------------------------------
wipe;                                   # clear memory of all past model definitions
model BasicBuilder -ndm 2 -ndf 3;       # Define the model builder, ndm=#dimension, ndf=#dofs
set dataDir Data;                       # set up name of data directory -- simple
file mkdir $dataDir;                    # create data directory
source LibUnits.tcl;                    # define units

# MATERIAL parameters --------------------------------------------------------------
set IDconcCore 1;                       # material ID tag -- concrete core
set IDconcCover 2;                      # material ID tag -- concrete cover
set IDreinf 3;                          # material ID tag -- reinforcement
set IDdamagedConc 4;                    # material ID tag -- damaged concrete

# Concrete -------------------------------------------------------------------------
uniaxialMaterial Hysteretic $IDconcCore [expr 2.21*$MPa] 0.0001 0.0 0.0003 0.0 0.0005 [expr -6.00*$MPa] -0.00027 [expr -20.00*$MPa] -0.002 [expr -17.00*$MPa] -0.0035 1 1 0.0 0.0 0.0;
uniaxialMaterial Hysteretic $IDconcCover [expr 2.21*$MPa] 0.0001 0.0 0.0003 0.0 0.0005 [expr -6.00*$MPa] -0.00027 [expr -20.00*$MPa] -0.002 [expr -17.00*$MPa] -0.0035 1 1 0.0 0.0 0.0;
uniaxialMaterial Hysteretic $IDdamagedConc [expr 2.21*$MPa] 0.0001 0.0 0.0003 0.0 0.0005 [expr -6.00*$MPa] -0.00027 [expr -20.00*$MPa] -0.002 [expr -17.00*$MPa] -0.0035 1 1 0.0 0.0 0.0;

# Reinforcement --------------------------------------------------------------------
set Fy [expr 500*$MPa];
set e1p [expr $Fy/(200000.*$MPa)];
set Fyu [expr 550*$MPa];
set e2p 0.1;
set F3  0.0;
set e3p 0.12;
```

```
uniaxialMaterial Hysteretic $IDreinf $Fy $e1p $Fyu $e2p $F3 $e3p -$Fy -$e1p -$Fyu -$e2p -$F3 -$e3p 1 1 0.0 0.0 0.0;

# Define ELEMENTS & SECTIONS -------------------------------------------------------
set HBeam [expr 350*$mm];                    # beam Depth
set BBeam [expr 150*$mm];                    # beam Width
set coverBeam [expr 15*$mm];                 # beam cover to reinforcing steel NA.
set numBarsBeam 2;                           # number of longitudinal-reinforcement bars in beam.
set diamBarsBeam [expr 12*$mm];              # diameter of longitudinal-reinforcement bottom bars of Beam section.
set barAreaBeam [expr 113.0976*$mm2];        # area of longitudinal-reinforcement bars
set SecTag 1;                                # assign a tag number to the beam section

# section GEOMETRY -----------------------------------------------------------------------
# FIBER SECTION properties ---------------------------------------------------------------
# Beam section:
# RC section:
set coverY [expr $HBeam/2.0];                                  # The distance from the section z-axis to the edge of the
cover concrete -- outer edge of cover concrete
set coverZ [expr $BBeam/2.0];                                  # The distance from the section y-axis to the edge of the
cover concrete -- outer edge of cover concrete
set coreY [expr $coverY-$coverBeam];
set coreZ [expr $coverZ-$coverBeam];
set core2Y [expr $coverY-($coverBeam+55*$mm)];
set bottomBarsY [expr $coverY-($coverBeam+5*$mm+$diamBarsBeam/2.0)];   # Bottom layer reinforcement in Y-axis
set bottomBarsZ [expr $coverZ-($coverBeam+5*$mm+$diamBarsBeam/2.0)];   # Bottom layer reinforcement in Z-axis
#Core
set nfYCore 11;                                                # number of fibers for confined concrete in y-direction
set nfZCore 4;                                                 # number of fibers for confined concrete in z-direction
#Cover
set nfYCoverHor 3;                                             # number of fibers for unconfined concrete in y-direction
set nfZCoverHor 6;                                             # number of fibers for unconfined concrete in z-direction
set nfYCoverVer 11;                                            # number of fibers for unconfined concrete in y-direction
set nfZCoverVer 1;                                             # number of fibers for unconfined concrete in z-direction

# Define the fiber section
section fiberSec $SecTag   {;                                  # Define the fiber section
patch quadr $IDconcCore $nfYCore $nfZCore -$core2Y $coreZ -$core2Y -$coreZ $coverY -$coreZ $coverY $coreZ;
# Define the concrete core patch
patch quadr $IDdamagedConc $nfYCoverHor $nfZCoverHor -$coverY $coverZ -$coverY -$coverZ -$core2Y -$coverZ -
$core2Y $coverZ; # Define the concrete (cover) patch
patch quadr $IDconcCover $nfYCoverVer $nfZCoverVer -$core2Y -$coreZ -$core2Y -$coverZ $coverY -$coverZ $coverY -
$coreZ;    # Define the concrete (cover) patch
patch quadr $IDconcCover $nfYCoverVer $nfZCoverVer -$core2Y $coverZ -$core2Y $coreZ $coverY $coreZ $coverY
$coverZ;      # Define the concrete (cover) patch
```

```
layer straight $IDreinf $numBarsBeam $barAreaBeam -$bottomBarsY -$bottomBarsZ -$bottomBarsY $bottomBarsZ;
# Bottom layer reinforcement
};                                                                    # end of fibersection definition
# Define RECORDERS ----------------------------------------------------------
recorder Element -file data/Str_Core(174).out -time -ele 2001 section fiber 0.174 0 $IDconcCore stressStrain;
# ConcCore fiber stress-strain, node i
recorder Element -file data/Str_Cover(-174).out -time -ele 2001 section fiber -0.174 0 $IDconcCover stressStrain;
# ConcCover fiber stress-strain, node i
recorder Element -file data/Str_Steel(-149).out -time -ele 2001 section fiber -0.149 0.049 $IDreinf stressStrain;
# Steel fiber stress-strain, node i
recorder Element -file $dataDir/ForceBeamSec.out -time -ele 2001 section force;
# section forces, axial and moment, node i
recorder Element -file $dataDir/DefoBeamSec.out -time -ele 2001 section deformation;
# section deformations, axial and curvature, node i
recorder Node -file $dataDir/R1.out -time -node 1001 -dof 1 reaction;
# support reaction, node i


# ------------------------------------------------------------------------------------
# build damaged beam section
# Jeferson Azeredo da Rosa, 2016
#
# SET UP ---------------------------------------------------------------------------
wipe;                                   # clear memory of all past model definitions
model BasicBuilder -ndm 2 -ndf 3;       # Define the model builder, ndm=#dimension, ndf=#dofs
set dataDir Data;                       # set up name of data directory -- simple
file mkdir $dataDir;                    # create data directory
source LibUnits.tcl;                    # define units

# MATERIAL parameters --------------------------------------------------------
set IDconcCore 1;                       # material ID tag -- concrete core
set IDconcCover 2;                      # material ID tag -- concrete cover
set IDreinf 3;                          # material ID tag -- reinforcement
set IDdamagedConc 4;                    # material ID tag -- damaged concrete

# Concrete -------------------------------------------------------------------------
uniaxialMaterial Hysteretic $IDconcCore [expr 2.21*$MPa] 0.0001 0.0 0.0003 0.0 0.0005 [expr -6.00*$MPa] -0.00027 [expr -
20.00*$MPa] -0.002 [expr -17.00*$MPa] -0.0035 1 1 0.0 0.0 0.0;
uniaxialMaterial Hysteretic $IDconcCover [expr 2.21*$MPa] 0.0001 0.0 0.0003 0.0 0.0005 [expr -6.00*$MPa] -0.00027 [expr
-20.00*$MPa] -0.002 [expr -17.00*$MPa] -0.0035 1 1 0.0 0.0 0.0;
uniaxialMaterial Hysteretic $IDdamagedConc [expr 0.01*$MPa] 0.0001 0.0 0.0003 0.0 0.00032 [expr -0.01*$MPa] -0.0001
[expr -0.02*$MPa] -0.0002 [expr -0.01*$MPa] -0.00035 1 1 0.0 0.0 0.0;
```

```
# Corroded Reinforcement 10% ------------------------------------------------------
set Fy [expr 452.5*$MPa];
set e1p [expr $Fy/(200000.*$MPa)];
set Fyu [expr 497.75*$MPa];
set e2p 0.1;
set F3  0.0;
set e3p 0.12;
uniaxialMaterial Hysteretic $IDreinf $Fy $e1p $Fyu $e2p $F3 $e3p -$Fy -$e1p -$Fyu -$e2p -$F3 -$e3p 1 1 0.0 0.0 0.0;

# Define ELEMENTS & SECTIONS ------------------------------------------------------
set HBeam [expr 350*$mm];                       # beam Depth
set BBeam [expr 150*$mm];                       # beam Width
set coverBeam [expr 15*$mm];                    # beam cover to reinforcing steel NA.
set numBarsBeam 2;                              # number of longitudinal-reinforcement bars in beam.
set diamBarsBeam [expr 12*$mm];                 # diameter of longitudinal-reinforcement bottom bars of Beam section.
set barAreaBeam [expr 113.0976*$mm2];           # area of longitudinal-reinforcement bars
set SecTag 1;                                   # assign a tag number to the beam section

# section GEOMETRY -------------------------------------------------------------------
# FIBER SECTION properties -------------------------------------------------------------
# Beam section:
# RC section:
set coverY [expr $HBeam/2.0];                   # The distance from the section z-axis to the edge of the cover
concrete -- outer edge of cover concrete
set coverZ [expr $BBeam/2.0];                   # The distance from the section y-axis to the edge of the cover
concrete -- outer edge of cover concrete
set coreY [expr $coverY-$coverBeam];
set coreZ [expr $coverZ-$coverBeam];
set core2Y [expr $coverY-($coverBeam+55*$mm)];
set bottomBarsY [expr $coverY-($coverBeam+5*$mm+$diamBarsBeam/2.0)];   # Bottom layer reinforcement in Y-axis
set bottomBarsZ [expr $coverZ-($coverBeam+5*$mm+$diamBarsBeam/2.0)];   # Bottom layer reinforcement in Z-axis
#Core
set nfYCore 11;                                 # number of fibers for confined concrete in y-direction
set nfZCore 4;                                  # number of fibers for confined concrete in z-direction
#Cover
set nfYCoverHor 3;                              # number of fibers for unconfined concrete in y-direction
set nfZCoverHor 6;                              # number of fibers for unconfined concrete in z-direction
set nfYCoverVer 11;                             # number of fibers for unconfined concrete in y-direction
set nfZCoverVer 1;                              # number of fibers for unconfined concrete in z-direction

# Define the fiber section
section fiberSec $SecTag   {;                   # Define the fiber section
patch quadr $IDconcCore $nfYCore $nfZCore -$core2Y $coreZ -$core2Y -$coreZ $coverY -$coreZ $coverY $coreZ;
# Define the concrete core patch
```

```
patch quadr $IDdamagedConc $nfYCoverHor $nfZCoverHor -$coverY $coverZ -$coverY -$coverZ -$core2Y -$coverZ -$core2Y $coverZ; # Define the concrete (cover) patch
patch quadr $IDconcCover $nfYCoverVer $nfZCoverVer -$core2Y -$coreZ -$core2Y -$coverZ $coverY -$coverZ $coverY -$coreZ;    # Define the concrete (cover) patch
patch quadr $IDconcCover $nfYCoverVer $nfZCoverVer -$core2Y $coverZ -$core2Y $coreZ $coverY $coreZ $coverY $coverZ;      # Define the concrete (cover) patch
layer straight $IDreinf $numBarsBeam $barAreaBeam -$bottomBarsY -$bottomBarsZ -$bottomBarsY $bottomBarsZ;
# Bottom layer reinforcement
};                                                                  # end of fibersection definition
# Define RECORDERS ----------------------------------------------------------------------------------------------------------------------------
recorder Element -file data/Str_Core(174).out -time -ele 2001 section fiber 0.174 0 $IDconcCore stressStrain;
# ConcCore fiber stress-strain, node i
recorder Element -file data/Str_Cover(-174).out -time -ele 2001 section fiber -0.174 0 $IDdamagedConc stressStrain;
# ConcCover fiber stress-strain, node i
recorder Element -file data/Str_Steel(-149).out -time -ele 2001 section fiber -0.149 0.049 $IDreinf stressStrain;
# Steel fiber stress-strain, node i
recorder Element -file $dataDir/ForceBeamSec.out -time -ele 2001 section force;
# section forces, axial and moment, node i
recorder Element -file $dataDir/DefoBeamSec.out -time -ele 2001 section deformation;
# section deformations, axial and curvature, node i
recorder Node -file $dataDir/R1.out -time -node 1001 -dof 1 reaction;
# support reaction, node i


# ------------------------------------------------------------------------------------------
# build rehabilitated beam section
# Jeferson Azeredo da Rosa, 2016
#
# SET UP ---------------------------------------------------------------------------
wipe;                                   # clear memory of all past model definitions
model BasicBuilder -ndm 2 -ndf 3;       # Define the model builder, ndm=#dimension, ndf=#dofs
set dataDir Data;                       # set up name of data directory -- simple
file mkdir $dataDir;                    # create data directory
source LibUnits.tcl;                    # define units

# MATERIAL parameters --------------------------------------------------------------
set IDconcCore 1;                       # material ID tag -- concrete core
set IDconcCover 2;                      # material ID tag -- concrete cover
set IDreinf 3;                          # material ID tag -- reinforcement
set IDhpfrccS2 4;                       # material ID tag -- HPFRCC Steel Fiber 2%

# Concrete -------------------------------------------------------------------------
uniaxialMaterial Hysteretic $IDconcCore [expr 2.21*$MPa] 0.0001 0.0 0.0003 0.0 0.0005 [expr -6.00*$MPa] -0.00027 [expr -20.00*$MPa] -0.002 [expr -17.00*$MPa] -0.0035 1 1 0.0 0.0 0.0;
```

```
uniaxialMaterial Hysteretic $IDconcCover [expr 2.21*$MPa] 0.0001 0.0 0.0003 0.0 0.0005 [expr -6.00*$MPa] -0.00027 [expr -20.00*$MPa] -0.002 [expr -17.00*$MPa] -0.0035 1 1 0.0 0.0 0.0;
uniaxialMaterial Hysteretic $IDhpfrccS2 [expr 4.40*$MPa] 0.000078 [expr 7.26*$MPa] 0.0012 [expr 5.84*$MPa] 0.0014 [expr -21.95*$MPa] -0.00084 [expr -73.16*$MPa] -0.0034 [expr -5*$MPa] -0.0035 1 1 0.0 0.0 0.0;

# Corroded Reinforcement 10% ----------
set Fy [expr 452.5*$MPa];
set e1p [expr $Fy/(200000.*$MPa)];
set Fyu [expr 497.75*$MPa];
set e2p 0.1;
set F3  0.0;
set e3p 0.12;
uniaxialMaterial Hysteretic $IDreinf $Fy $e1p $Fyu $e2p $F3 $e3p -$Fy -$e1p -$Fyu -$e2p -$F3 -$e3p 1 1 0.0 0.0 0.0;

# Define ELEMENTS & SECTIONS ----------
set HBeam [expr 350*$mm];                    # beam Depth
set BBeam [expr 150*$mm];                    # beam Width
set coverBeam [expr 15*$mm];                 # beam cover to reinforcing steel NA.
set numBarsBeam 2;                           # number of longitudinal-reinforcement bars in beam.
set diamBarsBeam [expr 12*$mm];              # diameter of longitudinal-reinforcement bottom bars of Beam section.
set barAreaBeam [expr 113.0976*$mm2];        # area of longitudinal-reinforcement bars
set SecTag 1;                                # assign a tag number to the beam section

# section GEOMETRY ----------
# FIBER SECTION properties ----------
#
# Beam section:
# RC section:
set coverY [expr $HBeam/2.0];                # The distance from the section z-axis to the edge of the cover concrete -- outer edge of cover concrete
set coverZ [expr $BBeam/2.0];                # The distance from the section y-axis to the edge of the cover concrete -- outer edge of cover concrete
set coreY [expr $coverY-$coverBeam];
set coreZ [expr $coverZ-$coverBeam];
set core2Y [expr $coverY-($coverBeam+55*$mm)];
set bottomBarsY [expr $coverY-($coverBeam+5*$mm+$diamBarsBeam/2.0)];   # Bottom layer reinforcement in Y-axis
set bottomBarsZ [expr $coverZ-($coverBeam+5*$mm+$diamBarsBeam/2.0)];   # Bottom layer reinforcement in Z-axis
#Core
set nfYCore 11;                              # number of fibers for confined concrete in y-direction
set nfZCore 4;                               # number of fibers for confined concrete in z-direction
#Cover
set nfYCoverHor 3;                           # number of fibers for unconfined concrete in y-direction
set nfZCoverHor 6;                           # number of fibers for unconfined concrete in z-direction
set nfYCoverVer 11;                          # number of fibers for unconfined concrete in y-direction
```

```
set nfZCoverVer 1;                                  # number of fibers for unconfined concrete in z-direction

# Define the fiber section
section fiberSec $SecTag   {;                       # Define the fiber section
patch quadr $IDconcCore $nfYCore $nfZCore -$core2Y $coreZ -$core2Y -$coreZ $coverY -$coreZ $coverY $coreZ;
# Define the concrete core patch
patch quadr $IDhpfrccS2 $nfYCoverHor $nfZCoverHor -$coverY $coverZ -$coverY -$coverZ -$core2Y -$coverZ -$core2Y
$coverZ;    # Define the concrete (cover) patch
patch quadr $IDconcCover $nfYCoverVer $nfZCoverVer -$core2Y -$coreZ -$core2Y -$coverZ $coverY -$coverZ $coverY -
$coreZ;    # Define the concrete (cover) patch
patch quadr $IDconcCover $nfYCoverVer $nfZCoverVer -$core2Y $coverZ -$core2Y $coreZ $coverY $coreZ $coverY
$coverZ;      # Define the concrete (cover) patch
layer straight $IDreinf $numBarsBeam $barAreaBeam -$bottomBarsY -$bottomBarsZ -$bottomBarsY $bottomBarsZ;
# Bottom layer reinforcement
};                                                  # end of fibersection definition
# Define RECORDERS ----------
recorder Element -file data/Str_Core(174).out -time -ele 2001 section fiber 0.174 0 $IDconcCore stressStrain;
# ConcCore fiber stress-strain, node i
recorder Element -file data/Str_Cover(-174).out -time -ele 2001 section fiber -0.174 0 $IDhpfrccS2 stressStrain;
# ConcCover fiber stress-strain, node i
recorder Element -file data/Str_Steel(-149).out -time -ele 2001 section fiber -0.149 0.049 $IDreinf stressStrain;
# Steel fiber stress-strain, node i
recorder Element -file $dataDir/ForceBeamSec.out -time -ele 2001 section force;
# section forces, axial and moment, node i
recorder Element -file $dataDir/DefoBeamSec.out -time -ele 2001 section deformation;
# section deformations, axial and curvature, node i
recorder Node -file $dataDir/R1.out -time -node 1001 -dof 1 reaction;
# support reaction, node i

# ------------------------------------------------------------------------------
# build original column section
# Jeferson Azeredo da Rosa, 2016
#
# SET UP ---------------------------------------------------------------------
wipe;                                               # clear memory of all past model definitions
model BasicBuilder -ndm 2 -ndf 3;                   # Define the model builder, ndm=#dimension, ndf=#dofs
set dataDir Data;                                   # set up name of data directory -- simple
file mkdir $dataDir;                                # create data directory
source LibUnits.tcl;                                # define units

# MATERIAL parameters ------------------------------------------------------------
set IDconcCore1 1;                                  # material ID tag -- confined core1 concrete
set IDconcCore2 2;                                  # material ID tag -- confined core2 concrete
set IDconcCover 3;                                  # material ID tag -- unconfined cover concrete
```

```
set IDreinf 4;                                  # material ID tag -- longitudinal reinforcement

# Concrete ---------------------------------------------------------------------
uniaxialMaterial Hysteretic $IDconcCore1 [expr 2.51*$MPa] 0.0001 0.0 0.0003 0.0 0.0005 [expr -7.28*$MPa] -0.0003 [expr -24.26*$MPa] -0.0039 [expr -19.88*$MPa] -0.0069 1 1 0.0 0.0 0.0;
uniaxialMaterial Hysteretic $IDconcCore2 [expr 2.51*$MPa] 0.0001 0.0 0.0003 0.0 0.0005 [expr -7.28*$MPa] -0.0003 [expr -24.26*$MPa] -0.0039 [expr -19.88*$MPa] -0.0069 1 1 0.0 0.0 0.0;
uniaxialMaterial Hysteretic $IDconcCover [expr 2.21*$MPa] 0.0001 0.0 0.0003 0.0 0.0005 [expr -6.00*$MPa] -0.00027 [expr -20.00*$MPa] -0.002 [expr -17.00*$MPa] -0.0035 1 1 0.0 0.0 0.0;

# Reinforcement ----------------------------------------------------------------
set Fy [expr 574.37*$MPa];
set e1p [expr $Fy/(200000.*$MPa)];
set Fyu [expr 666.24*$MPa];
set e2p 0.127;
set F3  0.0;
set e3p 0.15;
uniaxialMaterial Hysteretic $IDreinf $Fy $e1p $Fyu $e2p $F3 $e3p -$Fy -$e1p -$Fyu -$e2p -$F3 -$e3p 1 1 0.0 0.0 0.0;

# section GEOMETRY -------------------------------------------------------------
set DSec [expr 420*$mm];                        # Column Diameter
set newSec [expr 50*$mm];                       # Column concrete core2
set coverSec [expr 30*$mm];                     # Column cover to reinforcing steel NA.
set numBarsSec 12;                              # number of uniformly-distributed longitudinal-reinforcement bars
set barAreaSec [expr 113.0976*$mm2];            # area of longitudinal-reinforcement bars
set SecTag 1;                                   # set tag for symmetric section

# Generate a circular reinforced concrete section
# with one layer of steel evenly distributed around the perimeter and a confined core.
# confined core.
#
# Notes
#
#    The center of the reinforcing bars are placed at the inner radius
#    The core concrete ends at the inner radius (same as reinforcing bars)
#    The reinforcing bars are all the same size
#    The center of the section is at (0,0) in the local axis system
#    Zero degrees is along section y-axis
#
set ri 0.0;                     # inner radius of the section, only for hollow sections
set ro [expr $DSec/2];          # overall (outer) radius of the section
set nfCoreR 8;                  # number of radial divisions in the core (number of "rings")
set nfCoreT 16;                 # number of theta divisions in the core (number of "wedges")
set nfNewR 3;                   # number of radial divisions in the new concrete (number of "rings")
```

```
set nfNewT 32;                  # number of theta divisions in the new concrete (number of "wedges")
set nfCoverR 2;                 # number of radial divisions in the cover
set nfCoverT 32;                # number of theta divisions in the cover

# Define the fiber section
section fiberSec $SecTag  {
set rn [expr $ro-$coverSec-$newSec];                                    # New concrete radius
set rc [expr $ro-$coverSec];                                            # Core radius
patch circ $IDconcCore1 $nfCoreT $nfCoreR 0 0 $ri $rn 0 360;            # Define the core patch
patch circ $IDconcCore2 $nfNewT $nfNewR 0 0 $rn $rc 0 360;              # Define the new concrete patch
patch circ $IDconcCover $nfCoverT $nfCoverR 0 0 $rc $ro 0 360;          # Define the cover patch
set theta [expr 360.0/$numBarsSec];                                     # Determine angle increment between bars
layer circ $IDreinf $numBarsSec $barAreaSec 0 0 $rc $theta 360;         # Define the reinforcing layer
}
recorder Element -file data/Str_Core(100).out -time -ele 2001 section fiber 0.100 0 $IDconcCore1 stressStrain;
#ConcCore fiber stress-strain, node i
recorder Element -file data/Str_Core(-100).out -time -ele 2001 section fiber -0.100 0 $IDconcCore1 stressStrain;
#ConcCore fiber stress-strain, node i
recorder Element -file data/Str_New(155).out -time -ele 2001 section fiber 0.155 0 $IDconcCore2 stressStrain;
#New fiber stress-strain, node i
recorder Element -file data/Str_New(-155).out -time -ele 2001 section fiber -0.155 0 $IDconcCore2 stressStrain;
#New fiber stress-strain, node i
recorder Element -file data/Str_Cover(195).out -time -ele 2001 section fiber 0.195 0 $IDconcCover stressStrain;
#ConcCover fiber stress-strain, node i
recorder Element -file data/Str_Cover(-195).out -time -ele 2001 section fiber -0.195 0 $IDconcCover stressStrain;
#ConcCover fiber stress-strain, node i
recorder Element -file data/Str_Steel(180).out -time -ele 2001 section fiber 0.180 0 $IDreinf stressStrain;
#Steel fiber stress-strain, node i
recorder Element -file data/Str_Steel(-180).out -time -ele 2001 section fiber -0.180 0 $IDreinf stressStrain;
#Steel fiber stress-strain, node i


# ----------------------------------------------------------------------------------
# build damaged column section
# Jeferson Azeredo da Rosa, 2016
#
# SET UP ---------------------------------------------------------------------------
wipe;                                   # clear memory of all past model definitions
model BasicBuilder -ndm 2 -ndf 3;       # Define the model builder, ndm=#dimension, ndf=#dofs
set dataDir Data;                       # set up name of data directory -- simple
file mkdir $dataDir;                    # create data directory
source LibUnits.tcl;                    # define units

# MATERIAL parameters --------------------------------------------------------
```

```
set IDconcCore1 1;                          # material ID tag -- confined core1 concrete
set IDconcCore2 2;                          # material ID tag -- confined core2 concrete
set IDconcCover 3;                          # material ID tag -- unconfined cover concrete
set IDreinf 4;                              # material ID tag -- longitudinal reinforcement
set IDnoConcCover 5;                        # material ID tag -- damaged concrete cover
set IDcorroReinf 6;                         # material ID tag -- corroded longitudinal bars

# Concrete ----------------------------------------------------------------------
uniaxialMaterial Hysteretic $IDconcCore1 [expr 2.21*$MPa] 0.0001 0.0 0.0003 0.0 0.0005 [expr -6.00*$MPa] -0.00027 [expr
-20.00*$MPa] -0.002 [expr -17.00*$MPa] -0.0035 1 1 0.0 0.0 0.0;
uniaxialMaterial Hysteretic $IDconcCore2 [expr 2.21*$MPa] 0.0001 0.0 0.0003 0.0 0.0005 [expr -6.00*$MPa] -0.00027 [expr
-20.00*$MPa] -0.002 [expr -17.00*$MPa] -0.0035 1 1 0.0 0.0 0.0;
uniaxialMaterial Hysteretic $IDconcCover [expr 2.21*$MPa] 0.0001 0.0 0.0003 0.0 0.0005 [expr -6.00*$MPa] -0.00027 [expr
-20.00*$MPa] -0.002 [expr -17.00*$MPa] -0.0035 1 1 0.0 0.0 0.0;
uniaxialMaterial Hysteretic $IDnoConcCover [expr 0.01*$MPa] 0.0001 0.0 0.0003 0.0 0.00032 [expr -0.01*$MPa] -0.0001
[expr -0.02*$MPa] -0.0002 [expr -0.01*$MPa] -0.00035 1 1 0.0 0.0 0.0;

# Reinforcement -----------------------------------------------------------------
set Fy [expr 574.37*$MPa];
set e1p [expr $Fy/(200000.*$MPa)];
set Fyu [expr 666.24*$MPa];
set e2p 0.127;
set F3  0.0;
set e3p 0.15;
uniaxialMaterial Hysteretic $IDreinf $Fy $e1p $Fyu $e2p $F3 $e3p -$Fy -$e1p -$Fyu -$e2p -$F3 -$e3p 1 1 0.0 0.0 0.0;

# Corroded Reinforcement cross section loss of 14%
set Fy [expr 498.76*$MPa];
set e1p [expr $Fy/(200000.*$MPa)];
set Fyu [expr 578.54*$MPa];
set e2p 0.127;
set F3  0.0;
set e3p 0.15;
uniaxialMaterial Hysteretic $IDcorroReinf $Fy $e1p $Fyu $e2p $F3 $e3p -$Fy -$e1p -$Fyu -$e2p -$F3 -$e3p 1 1 0.0 0.0 0.0;

# section GEOMETRY --------------------------------------------------------------
set DSec [expr 420*$mm];                    # Column Diameter
set newSec [expr 50*$mm];                   # Column concrete core2
set coverSec [expr 30*$mm];                 # Column cover to reinforcing steel NA.
set numBarsSec 12;                          # number of uniformly-distributed longitudinal-reinforcement bars
set barAreaSec [expr 113.0976*$mm2];        # area of longitudinal-reinforcement bars
set SecTag 1;                               # set tag for symmetric section

# Generate a circular reinforced concrete section
```

```
# with one layer of steel evenly distributed around the perimeter and a unconfined core.
#
# Notes
#
#    Broken reinforcing hoops --> no confinement
#    The center of the reinforcing bars are placed at the inner radius
#    The core concrete ends at the inner radius (same as reinforcing bars)
#    The reinforcing bars are all the same size
#    The center of the section is at (0,0) in the local axis system
#    Zero degrees is along section y-axis
#
set ri 0.0;                    # inner radius of the section, only for hollow sections
set ro [expr $DSec/2];         # overall (outer) radius of the section
set nfCoreR 8;                 # number of radial divisions in the core (number of "rings")
set nfCoreT 16;                # number of theta divisions in the core (number of "wedges")
set nfNewR 3;                  # number of radial divisions in the new concrete (number of "rings")
set nfNewT 32;                 # number of theta divisions in the new concrete (number of "wedges")
set nfCoverR 2;                # number of radial divisions in the cover
set nfCoverT 32;               # number of theta divisions in the cover

# Define the fiber section
section fiberSec $SecTag  {
set rn [expr $ro-$coverSec-$newSec];                                 # New concrete radius
set rc [expr $ro-$coverSec];                                         # Core radius
patch circ $IDconcCore1 $nfCoreT $nfCoreR 0 0 $ri $rn 0 360;         # Define the core1 patch
patch circ $IDconcCore2 $nfNewT $nfNewR 0 0 $rn $rc 0 360;           # Define the core2 patch
patch circ $IDconcCover $nfCoverT $nfCoverR 0 0 $rc $ro 45 315;      # Define the cover patch
patch circ $IDnoConcCover $nfCoverT $nfCoverR 0 0 $rc $ro 315 45;    # Define the damage cover patch
#set theta [expr 360.0/$numBarsSec];                                 # Determine angle increment between bars
#layer circ $IDreinf $numBarsSec $barAreaSec 0 0 $rc $theta 360;     # Define the reinforcing layer

set yLoc1 0.180;
set yLoc2 0.155;
set yLoc3 0.090;
set yLoc4 0;
set yLoc5 -0.090;
set yLoc6 -0.155;
set yLoc7 -0.180;
set yLoc8 -0.155;
set yLoc9 -0.090;
set yLoc10 0;
set yLoc11 0.090;
set yLoc12 0.155;
set zLoc1 0;
```

```
set zLoc2 0.090;
set zLoc3 0.155;
set zLoc4 0.180;
set zLoc5 0.155;
set zLoc6 0.090;
set zLoc7 0;
set zLoc8 -0.090;
set zLoc9 -0.155;
set zLoc10 -0.180;
set zLoc11 -0.155;
set zLoc12 -0.090;
fiber $yLoc1 $zLoc1 $barAreaSec $IDcorroReinf;     # Corroded bar Cross-section loss 14%
fiber $yLoc2 $zLoc2 $barAreaSec $IDcorroReinf;     # Corroded bar Cross-section loss 14%
fiber $yLoc3 $zLoc3 $barAreaSec $IDreinf;          # uncorroded bar
fiber $yLoc4 $zLoc4 $barAreaSec $IDreinf;          # uncorroded bar
fiber $yLoc5 $zLoc5 $barAreaSec $IDreinf;          # uncorroded bar
fiber $yLoc6 $zLoc6 $barAreaSec $IDreinf;          # uncorroded bar
fiber $yLoc7 $zLoc7 $barAreaSec $IDreinf;          # uncorroded bar
fiber $yLoc8 $zLoc8 $barAreaSec $IDreinf;          # uncorroded bar
fiber $yLoc9 $zLoc9 $barAreaSec $IDreinf;          # uncorroded bar
fiber $yLoc10 $zLoc10 $barAreaSec $IDreinf;        # uncorroded bar
fiber $yLoc11 $zLoc11 $barAreaSec $IDreinf;        # uncorroded bar
fiber $yLoc12 $zLoc12 $barAreaSec $IDcorroReinf;# Corroded bar Cross-section loss 14%
}
recorder Element -file data/Str_Core(100).out -time -ele 2001 section fiber 0.100 0 $IDconcCore1 stressStrain;
#ConcCore1 fiber stress-strain, node i
recorder Element -file data/Str_Core(-100).out -time -ele 2001 section fiber -0.100 0 $IDconcCore1 stressStrain;
#ConcCore1 fiber stress-strain, node i
recorder Element -file data/Str_New(155).out -time -ele 2001 section fiber 0.155 0 $IDconcCore2 stressStrain;
#ConcCore2 stress-strain, node i
recorder Element -file data/Str_New(-155).out -time -ele 2001 section fiber -0.155 0 $IDconcCore2 stressStrain;
#ConcCore2 stress-strain, node i
recorder Element -file data/Str_Cover(195).out -time -ele 2001 section fiber 0.195 0 $IDnoConcCover stressStrain;
#No Concrete Cover fiber stress-strain, node i
recorder Element -file data/Str_Cover(-195).out -time -ele 2001 section fiber -0.195 0 $IDconcCover stressStrain;
#Concrete Cover fiber stress-strain, node i
recorder Element -file data/Str_Steel(180).out -time -ele 2001 section fiber 0.180 0 $IDcorroReinf stressStrain;
#Corroded Steel fiber stress-strain, node i
recorder Element -file data/Str_Steel(-180).out -time -ele 2001 section fiber -0.180 0 $IDreinf stressStrain;
#Steel fiber stress-strain, node i
```

```
# ------------------------------------------------------------------------------
# build rehabilitated column section
# Jeferson Azeredo da Rosa, 2016
#
# SET UP ---------------------------------------------------------------------
wipe;                                   # clear memory of all past model definitions
model BasicBuilder -ndm 2 -ndf 3;       # Define the model builder, ndm=#dimension, ndf=#dofs
set dataDir Data;                       # set up name of data directory -- simple
file mkdir $dataDir;                    # create data directory
source LibUnits.tcl;                    # define units

# MATERIAL parameters --------------------------------------------------------
set IDconcCore1 1;                       # material ID tag -- confined core1 concrete
set IDhpfrccS2 2;                       # material ID tag -- confined core2 concrete HPFRCC (Stainless Steel
Fiber 2%)
#set IDconcCover 3;                     # material ID tag -- unconfined cover concrete
set IDreinf 4;                          # material ID tag -- longitudinal reinforcement
#set IDnoConcCover 5;                   # material ID tag -- damaged concrete cover
set IDcorroReinf 6;                     # material ID tag -- corroded longitudinal bars

# Concrete -------------------------------------------------------------------
uniaxialMaterial Hysteretic $IDconcCore1 [expr 2.21*$MPa] 0.0001 0.0 0.0003 0.0 0.0005 [expr -6.00*$MPa] -0.00027 [expr
-20.00*$MPa] -0.002 [expr -17.00*$MPa] -0.0035 1 1 0.0 0.0 0.0;
uniaxialMaterial Hysteretic $IDhpfrccS2 [expr 4.40*$MPa] 0.000078 [expr 7.26*$MPa] 0.0012 [expr 5.84*$MPa] 0.0014 [expr
-21.95*$MPa] -0.00084 [expr -73.16*$MPa] -0.0034 [expr -5*$MPa] -0.0035 1 1 0.0 0.0 0.0;
#uniaxialMaterial Hysteretic $IDconcCover [expr 2.21*$MPa] 0.0001 0.0 0.0003 0.0 0.0005 [expr -6.00*$MPa] -0.00027
[expr -20.00*$MPa] -0.002 [expr -17.00*$MPa] -0.0035 1 1 0.0 0.0 0.0;
#uniaxialMaterial Hysteretic $IDnoConcCover [expr 0.01*$MPa] 0.0001 0.0 0.0003 0.0 0.00032 [expr -0.01*$MPa] -0.0001
[expr -0.02*$MPa] -0.0002 [expr -0.01*$MPa] -0.00035 1 1 0.0 0.0 0.0;

# Reinforcement --------------------------------------------------------------
set Fy [expr 574.37*$MPa];
set e1p [expr $Fy/(200000.*$MPa)];
set Fyu [expr 666.24*$MPa];
set e2p 0.127;
set F3  0.0;
set e3p 0.15;
uniaxialMaterial Hysteretic $IDreinf $Fy $e1p $Fyu $e2p $F3 $e3p -$Fy -$e1p -$Fyu -$e2p -$F3 -$e3p 1 1 0.0 0.0 0.0;

# Corroded Reinforcement cross section loss of 14%
set Fy [expr 498.76*$MPa];
set e1p [expr $Fy/(200000.*$MPa)];
```

```
set Fyu [expr 578.54*$MPa];
set e2p 0.127;
set F3  0.0;
set e3p 0.15;
uniaxialMaterial Hysteretic $IDcorroReinf $Fy $e1p $Fyu $e2p $F3 $e3p -$Fy -$e1p -$Fyu -$e2p -$F3 -$e3p 1 1 0.0 0.0 0.0;

# section GEOMETRY -------------------------------------------------------------------
set DSec [expr 420*$mm];                    # Column Diameter
set newSec [expr 50*$mm];                   # Column concrete core2
set coverSec [expr 30*$mm];                 # Column cover to reinforcing steel NA.
set numBarsSec 12;                          # number of uniformly-distributed longitudinal-reinforcement bars
set barAreaSec [expr 113.0976*$mm2];        # area of longitudinal-reinforcement bars
set SecTag 1;                               # set tag for symmetric section

# Generate a circular reinforced concrete section
# with one layer of steel evenly distributed around the perimeter and a unconfined core.
#
# Notes
#
#    Broken reiforcing hoops --> no confinement
#    The center of the reinforcing bars are placed at the inner radius
#    The core concrete ends at the inner radius (same as reinforcing bars)
#    The reinforcing bars are all the same size
#    The center of the section is at (0,0) in the local axis system
#    Zero degrees is along section y-axis
#
set ri 0.0;                 # inner radius of the section, only for hollow sections
set ro [expr $DSec/2];      # overall (outer) radius of the section
set nfCoreR 8;              # number of radial divisions in the core (number of "rings")
set nfCoreT 16;             # number of theta divisions in the core (number of "wedges")
set nfNewR 3;               # number of radial divisions in the new concrete (number of "rings")
set nfNewT 32;              # number of theta divisions in the new concrete (number of "wedges")
set nfCoverR 2;             # number of radial divisions in the cover
set nfCoverT 32;            # number of theta divisions in the cover

# Define the fiber section
section fiberSec $SecTag  {
set rn [expr $ro-$coverSec-$newSec];                    # New concrete radius
set rc [expr $ro-$coverSec];                            # Core radius
patch circ $IDconcCore1 $nfCoreT $nfCoreR 0 0 $ri $rn 0 360;        # Define the core1 patch
patch circ $IDhpfrccS2 $nfNewT $nfNewR 0 0 $rn $rc 0 360;           # Define the core2 patch (HPFRCC)
patch circ $IDhpfrccS2 $nfCoverT $nfCoverR 0 0 $rc $ro 0 360;       # Define the cover patch (HPFRCC)
#patch circ $IDnoConcCover $nfCoverT $nfCoverR 0 0 $rc $ro 315 45;  # Define the damage cover patch
#set theta [expr 360.0/$numBarsSec];                     # Determine angle increment between bars
```

```
#layer circ $IDreinf $numBarsSec $barAreaSec 0 0 $rc $theta 360;            # Define the reinforcing layer

set yLoc1 0.180;
set yLoc2 0.155;
set yLoc3 0.090;
set yLoc4 0;
set yLoc5 -0.090;
set yLoc6 -0.155;
set yLoc7 -0.180;
set yLoc8 -0.155;
set yLoc9 -0.090;
set yLoc10 0;
set yLoc11 0.090;
set yLoc12 0.155;
set zLoc1 0;
set zLoc2 0.090;
set zLoc3 0.155;
set zLoc4 0.180;
set zLoc5 0.155;
set zLoc6 0.090;
set zLoc7 0;
set zLoc8 -0.090;
set zLoc9 -0.155;
set zLoc10 -0.180;
set zLoc11 -0.155;
set zLoc12 -0.090;
fiber $yLoc1 $zLoc1 $barAreaSec $IDcorroReinf;     # Corroded bar Cross-section loss 14%
fiber $yLoc2 $zLoc2 $barAreaSec $IDcorroReinf;     # Corroded bar Cross-section loss 14%
fiber $yLoc3 $zLoc3 $barAreaSec $IDreinf;          # uncorroded bar
fiber $yLoc4 $zLoc4 $barAreaSec $IDreinf;          # uncorroded bar
fiber $yLoc5 $zLoc5 $barAreaSec $IDreinf;          # uncorroded bar
fiber $yLoc6 $zLoc6 $barAreaSec $IDreinf;          # uncorroded bar
fiber $yLoc7 $zLoc7 $barAreaSec $IDreinf;          # uncorroded bar
fiber $yLoc8 $zLoc8 $barAreaSec $IDreinf;          # uncorroded bar
fiber $yLoc9 $zLoc9 $barAreaSec $IDreinf;          # uncorroded bar
fiber $yLoc10 $zLoc10 $barAreaSec $IDreinf;        # uncorroded bar
fiber $yLoc11 $zLoc11 $barAreaSec $IDreinf;        # uncorroded bar
fiber $yLoc12 $zLoc12 $barAreaSec $IDcorroReinf;# Corroded bar Cross-section loss 14%
}
recorder Element -file data/Str_Core(100).out -time -ele 2001 section fiber 0.100 0 $IDconcCore1 stressStrain;
#ConcCore1 fiber stress-strain, node i
recorder Element -file data/Str_Core(-100).out -time -ele 2001 section fiber -0.100 0 $IDconcCore1 stressStrain;
#ConcCore1 fiber stress-strain, node i
```

```
recorder Element -file data/Str_New(155).out -time -ele 2001 section fiber 0.155 0 $IDhpfrccS2 stressStrain;
#ConcCore2 stress-strain, node i
recorder Element -file data/Str_New(-155).out -time -ele 2001 section fiber -0.155 0 $IDhpfrccS2 stressStrain;
#ConcCore2 stress-strain, node i
recorder Element -file data/Str_Cover(195).out -time -ele 2001 section fiber 0.195 0 $IDhpfrccS2 stressStrain;
#HPFRCC fiber stress-strain, node i
recorder Element -file data/Str_Cover(-195).out -time -ele 2001 section fiber -0.195 0 $IDhpfrccS2 stressStrain;
#HPFRCC fiber stress-strain, node i
recorder Element -file data/Str_Steel(180).out -time -ele 2001 section fiber 0.180 0 $IDcorroReinf stressStrain;
#Corroded Steel fiber stress-strain, node i
recorder Element -file data/Str_Steel(-180).out -time -ele 2001 section fiber -0.180 0 $IDreinf stressStrain;
#Steel fiber stress-strain, node i
```

“Il costruire è, senza confronti, la più antica ed importante delle attività umane.
È la sintesi più espressiva delle capacità di un popolo.”
Pier Luigi Nervi